AN ALTERNATIVE AGENT TO INDUCE CARDIAC ARREST FOR NORMOTHERMIC CARDIAC SURGERY

By

Mauricio Ede

A Thesis
Submitted to the Faculty of Graduate Studies
In Partial Fulfillment of the Requirements
For the Degree of

Doctor of Philosophy

Department of Physiology,
Faculty of Medicine
University of Manitoba
Winnipeg, Manitoba

THE UNIVERSITY OF MANITOBA

FACULTY OF GRADUATE STUDIES

*****

COPYRIGHT PERMISSION PAGE

AN ALTERNATIVE AGENT TO INDUCE CARDIAC ARREST

FOR NORMOTHERMIC CARDIAC SURGERY

BY

MAURICIO EDE

A Thesis/Practicum submitted to the Faculty of Graduate Studies of The University of Manitoba in partial fulfillment of the requirements of the degree

of

DOCTOR OF PHILOSOPHY

Foreword

The work described in this Thesis was initially motivated by the observation of the too often occurrence of systemic hyperkalemia at the end of cardiac operations which employed cardiopulmonary bypass and hyperkalemic cardioplegic arrest. These observations were gathered mainly during five years of training as a Cardiovascular Surgeon, however I have witnessed its appearance in other Centres I had the opportunity to visit.

Esmolol, (Brevibloc®, Zeneca Pharma Canada, Inc.) was the alternative drug chosen to be tested simply because it is the only drug available commercially that possesses the required effects and has a ultra-short acting period. Esmolol, in commercial presentation vials, was the only gift from Zeneca Pharma Canada Inc., and this study was not the result of a contractual research agreement.

The following pages will describe, after a dissertative background on aspects of Cardiac Physiology pertinent to the work pursued, the results of three consecutive studies designed to investigate whether Esmolol has cardioplegic property, if this effect is toxic and what mechanism(s) may underlie its action.

Acknowledgements

This thesis is the result of a multidisciplinary team effort. I am indebted to several individuals who graciously have provided, directly or indirectly, help and support in the forms of technical skills, teachings and constructive criticism; and on a more personal basis, friendship. These individuals, outstanding scientists, technicians and clinicians, I wish to acknowledge and express my deepest gratitude.

To all the surgical team of the Hôpital Européen de Paris, Service de Chirurgie Cardiovasculaire, especially Drs. Arrigo Lessana, Mauro Romano, Daniel LeHouerou, Shirish Pargaonkar and Ajoy Singh, with whom initial discussions helped concretize the main hypothesis of this work.

To Dr. Tomás Antonio Salerno, who first recognized the potential of this work and was the responsible for my coming to Canada. Dr. Salerno has been since, my mentor and established my contact with who was to become my supervisor, Dr. Roxanne Deslauriers, at the Department of Physiology, University of Manitoba and at the Institute for Biodiagnostics, National Research Council of Canada.

To my supervisor, Dr. Roxanne Deslauriers, who provided all the conditions for me to pursue this research and always welcomed my many (and sometimes naïve) questions and concerns. Dr. Deslauriers outstanding scientific conduct and reasoning has become to me a model, which I will uphold and cherish during my scientific career.

To all the exceptional staff of Research and Technical Officers of the Biosystems Group at the IBD, including Drs. Valery Kupryianov, Hong Tian, Ursula Tuor, John Rendell and John Docherty, always available for discussions, advice and constructive criticism. To Mss. Bo Xiang, Bozena Kuzio, and Dr. Luojia Yang for their patience,

cooperation and invaluable help during the NMR and fluorescence experiments and histological analyses.

To all staff at the Animal Resources and Care Group, Dr. John Copps, Catherine Kellar, Denis Olynick and Allan Turner, for taking such an excellent care of all my "raties and piggies".

To my surgical "pals", Research Council Officer Dr. Jian Ye, and Technical Officers Monique St.-Jean, Lori Gregorash, Shelley Germsheid and Rachelle Perchaluk, for their priceless friendship and help during the never-ending pig experiments.

To Rene Leiva, Lori Shoemaker at the Biochemistry Lab, and to Dr. Dorothea Blandford, for the invaluable help with the gas chromatography analyses and data processing.

To Dr. Christian Schultz at the IBD Spectroscopy Group for his friendship and collaboration in the infrared measurement experiments and data analysis.

For shedding light in my murky universe of Biostatistics, I wish to acknowledge Mr. Randy Summers, outstanding mathematician, the only man I know capable of mastering the art of mixing statistical analyses of biomedical data and Jazz and make beautiful sense of it all.

To all staff of the MR Technology Group, especially Dr. Piotr Kozlowsky, for his fraternal friendship and informal lessons on Physics and basics of NMR in between sets of tennis.

To Dr. David O. Foster, Senior Research Officer and former Chairman of the Animal Care Committee at IBD for his invaluable teachings on scientific excellence, scientific conduct, and Ethics. Also for his friendship, patience and obstination to

transform what were mere sparse ideas into strong scientific rationales and comprehensive scientific protocols. Dave's teachings have produced a permanent effect in my career and they are the reason I might call myself a scientist one day.

To my advisory committee at the Departments of Physiology and Surgery, Faculty of Medicine, University of Manitoba, Drs. Ian Dixon, Anton Lukas and William Lindsay, always available for discussions, support, and constructive suggestions.

To the National Research Council and the Heart & Stroke Foundation of Manitoba for allowing me the opportunity and the financial support to conduct this research.

Finally, I wish to thank all individuals who indirectly provided help and support, including librarians David Colborne and Pauline Kulbalba, secretary Nancy Anderson, and the people who actually run the IBD building, facilities managers, administration staff, Commissionaires and the man at the helm, IBD Director General, Dr. Ian C. P. Smith.

Mauricio Ede
September 1998

List of Figures

List of Tables

CHAPTER 1 - INTRODUCTION

1.1 Statement of the clinical problem

1.2 Hypotheses

1.3 General description of the work

1.1 Statement of the Clinical Problem

Conventional coronary artery bypass grafting (CABG) surgery, although relatively safe, can result in complications, including myocardial infarction, stroke, renal failure, neurovascular and aortic injury, respiratory failure and coagulation abnormalities. Many of these are associated with the use of classical cardiopulmonary bypass (CPB), including surgical trauma (sternotomy, sternal retraction, cannulation of the aorta and atria, and aortic cross-clamping), apulsatility, heparinization and exposure of blood components to non-endothelized surfaces. Cardiopulmonary bypass is associated with a variety of responses that include leukocyte-mediated inflammation, coagulopathy due to trauma to blood elements, deleterious effects of hemodilution, and embolisms caused by air and atherosclerotic debris, with the potential risk of post-operative stroke and/or cognitive dysfunction[1, 2, 3, 4, 5].

Hyperkalemic cardioplegia has been associated with post-operative contractile dysfunction especially when it is associated with hypothermia[6, 7, 8]. At the subcellular level, hyperkalemic cardioplegic solutions alter the affinity of myofibrils for calcium, thus compromising cardiac output immediately after removal of the aortic crossclamp in procedures involving CPB[9, 10]. In patients with any degree of renal insufficiency, clearance of potassium from the circulation may be difficult and the patient may require longer periods of bypass and/or inotropic support, either pharmacological or mechanical or additional procedures, such as hemofiltration[11, 12].

In a desire to improve patient outcome while enhancing cost-effectiveness, surgeons and clinical investigators became interested in new strategies for performing coronary artery bypass surgery[13] (and more recently, valve operations[14]). Coronary

bypass grafting operations without CPB were first performed by Kolessov[15] in the Soviet Union (1967) and by Favaloro[16] (1968) and Garret[17]. Trapp and Bisarya[18] in Canada and Ankeney[19] in the United States reported on the technique but it was later abandoned as the use of CPB and cardioplegic arrest became routine. Surgeons are now reassessing the risks/benefits of extracorporeal circulation. One of the most extensive studies to date on CABG without CPB[20], has identified the clinical indications for use of the technique (high-risk patients with renal failure, respiratory problems, advanced age, previous cerebrovascular accidents, neoplasias and other major systemic diseases--an estimated 25% of the total number of patients undergoing CABG) and established a low (2.5%) mortality rate in these selected patients. According to the report, the incidence of complications such as arrhythmias, pulmonary and neurologic sequelae was significantly lower relative to patients who underwent extracorporeal circulation. The study also showed a significant reduction in cost (up to US$3,000) per case due to the decrease in use of oxygenators, cardioplegic sets and reduced length-of-stay in the Intensive Care Unit and in the hospital[20].

The technique is indicated mainly for patients undergoing revascularization of the anterior walls of the left and right ventricles (namely, grafting the left-anterior descending coronary artery (LAD, and its diagonal branches) and proximal portions of the right main coronary artery). Grafting of the posterior and lateral walls of the heart requires a greater amount of traction and displacement of the heart, which may compromise the function of the aortic valve, leading to impaired cardiac output and potential arrhythmias. In order to increase the safety of the procedure, some surgeons are now using a centrifugal pump (bi- or left-ventricular assistance devices, LVAD's) for circulatory support and ensure

minimal myocardial contraction using ultra-short acting beta-blockers. Minimal Myocardial Contraction (MMC) is a concept introduced by Frazier[21] that has been used by others experimentally[22] and clinically in adult and pediatric cardiac surgery patients[23,24]. The goal is to reduce motion of the heart while avoiding aortic crossclamping and cardioplegic arrest. To achieve this, it is important that the effects of the agent be continuously monitored and titrated in each patient[25]. The use of circulatory support and reduction in heart motion is advantageous relative to classic techniques proposed without extracorporeal circulation, in that it allows better manipulation of the heart, thus access to the posterior coronary vessels and intracardiac structures. It has also been reported that MMC during CPB or bi-ventricular assistance allows maintenance of lymphatic function resulting in minimal myocardial edema and restoration of full cardiac function after circulatory support[26]. We propose the use of an ultra-short acting β–blocker as a new concept in myocardial preservation. In our initial approach, we proposed esmolol as an alternative to potassium and as an arrest-inducing agent in the classical bypass setting[12]. However, esmolol is already being used to reduce heart rate and motion during minimally invasive operations (MIDCAB) and its dose titrated to a level at which the surgeon is comfortable with. On the other hand, for more complex cases using classical bypass techniques (longer crossclamp times, reoperations, multiple grafts, associated procedures), the strategy of a "one-drug-blood-solution" has the potential of becoming easier and safer to use. We recognize that the overall mortality of routine myocardial revascularization is already very low; and that if potassium has been used for the last 40 years, its safety is already established. We propose, however, to

provide practicing surgeons with a wider choice of modalities and the possibility of tailoring the myocardial preservation strategy to individual patients.

In an effort to understand the effects of alternative 'cardioplegic' agents and optimize the conditions for their use, we proposed to test an ultra-short acting beta-blocker (esmolol, Brevibloc®, Zeneca Pharma Canada, Inc.) as an alternative to potassium for use during normothermic cardiac surgery. In our initial experiments, we tested the ability of esmolol to induce and maintain safe and promptly reversible cardiac arrest. A second series of experiments focused on the metabolism of esmolol and the monitoring of its metabolites using Infrared spectroscopy. At a subcellular level, the mechanisms of action of esmolol have not yet been established, but we hypothesize effects on sodium, calcium, and potassium channels. In order to assess transmembrane ionic fluxes of these ions prior to arrest, during arrest and reperfusion we performed magnetic resonance spectroscopic studies (MRS) on isolated rat hearts to observe Li^+ (a congener for Na^+ [27, 28]) Rb^+ (a congener for K^+ [28]) and Ca^{++} (using fluorescent microscopy in isolated cells). The levels of high-energy phosphates were also monitored with ^{31}P MRS[29].

Magnetic resonance spectroscopy (MRS) is the analytical tool of choice for these experiments because of its non-invasive nature[28]. The purpose of the work was to observe and compare the changes caused by esmolol and potassium when used as cardioplegic agents over a period of one hour of arrest followed by 30 minutes of reperfusion. The peaks (their position and intensity) in the spectra yielded information on the relative intra- and extracellular levels of ions when the heart was perfused with

esmolol or potassium. These values were compared with those obtained initially when no drug was added to the perfusate.

The work was divided in three parts:

- Functional analyses of the effects of esmolol in the isolated rat, rabbit and pig hearts;
- Study of the metabolism of esmolol and its detection using infrared spectroscopy;
- Study of the mechanisms of action of esmolol in the isolated heart model using Magnetic Resonance Spectroscopy.

1.2 General Hypotheses

1. Esmolol is capable of producing and maintaining a promptly reversible cardiac arrest after interrupting its infusion in the isolated heart model.

2. Esmolol has cardioprotective effects when given before and/or after an ischemic insult.

3. Esmolol can be used at high concentrations to induce cardioplegic arrest without the accumulation of toxic levels of methanol.

4. The concentrations of esmolol and methanol can be monitored in blood in a continuous fashion using infrared spectroscopy.

5. Esmolol acts as a cardioplegic agent by mechanism(s) other than beta-blockade. Effects on sodium, potassium and calcium channels may also take place during induction and maintenance of cardiac arrest.

6. Esmolol-induced cardiac arrest is not associated with disturbances in high-energy phosphate levels in the heart.

1.3 General Description of the Work

All the experimental work was carried out at the Institute for Biodiagnostics, National Research Council of Canada. The protocols were subjected to review for scientific merit and ethics approval was obtained from the IBD Animal Care Committee.

1.3.1 Functional Evaluation

Hypothesis:

Esmolol is capable of producing and maintaining cardiac arrest. The arrest can be promptly reversed by interrupting infusion of the drug. Esmolol may also have cardioprotective effects when given before and/or after an ischemic insult.

Experiments:

- Initial assessment of effects

Using the isolated buffer-perfused rat heart, esmolol arrest was induced with a bolus injection and the dose further titrated for the maintenance of mechanical arrest. Arrest periods were maintained for 30, 60, 90 and 120 minutes. Functional recovery values (± dP/dt, ventricular pressures, and heart rate) of 20 minutes post-interruption of infusion were compared against pre-arrest values.

- Dose-response curves

The effects of esmolol on function and ECG were evaluated at different concentrations. A Starling curve (stepwise increase in end-diastolic pressure) was performed for each concentration. These experiments were carried out using isolated rat and rabbit hearts (Langendorff preparation).

- Effects of a ischemic insult prior to and after esmolol arrest

An ischemic insult (global no-flow ischemia at 37°C for 20 minutes) was given prior to (group B) and after (group A) esmolol arrest and compared to high K^+ (25mM) arrested hearts. The effects on function and ECG activity were compared among the groups.

- Suitability of esmolol (as a one-drug-blood-solution) as a cardioplegic agent in the pig under extra-corporeal circulation

The suitability of esmolol as a cardioplegic agent was tested in a more clinically relevant model and compared to high K^+ arrest. Pigs were subjected to extra-corporeal circulation and continuous, undiluted normothermic blood cardioplegic arrest during normothermic cardiopulmonary bypass for a period of one hour. Hemodynamics and ability to wean the animal off bypass was compared against initial controls and to the high K^+ group.

1.3.2 Study of the Metabolism of Esmolol and its Monitoring via Infrared Spectroscopy

Hypotheses

Esmolol can be used at high concentrations to induce cardioplegic arrest without producing toxic levels of methanol accumulation. The concentrations of esmolol and methanol can be monitored in blood in a continuous fashion using infrared spectroscopy.

Experiments

Pigs were subjected to normothermic extracorporeal circulation and continuous, undiluted antegradely delivered normothermic blood cardioplegia. The animals were divided in esmolol and potassium groups. Cardiopulmonary bypass was established and the heart was arrested for a period of one hour. Infrared spectrometers (two) were placed (i) in the venous return line and (ii) in gas exhaust line of the pump oxygenator for continuous monitoring of esmolol and methanol levels. In addition, blood samples were collected for measurements of methanol using gas chromatography.

1.3.3 Mechanism(s) of Action of Esmolol at the Subcellular Level - Effects on Transmembrane Ionic Homeostasis Using Multi-nuclear Magnetic Resonance Spectroscopy (MRS) and Ca^{++} Fluorescence Microscopy Techniques.

Hypothesis

We hypothesize that esmolol acts as a cardioplegic agent by mechanism(s) other than beta-blockade. Effects on sodium, potassium and calcium channels take place during induction and maintenance of cardiac arrest. Esmolol arrest does not perturb high-energy phosphate levels in the heart during the arrest or recovery periods.

Experiments

An isolated rat heart model buffer perfused inside the bore of a 360 MHz magnet (8.7T) was used to assess:

- the kinetics of Na^+ (via its congener, lithium - ^7Li MRS);
- the kinetics of K^+ (via its congener, rubidium - ^{87}Rb MRS);
- the levels of high-energy phosphates as well as intracellular pH - ^{31}P MRS.
- changes in intracellular concentrations of Ca^{++} (using fluorescence spectroscopy) in isolated rat myocytes.

CHAPTER - II BACKGROUND

- ***2.1 - Pertinent Aspects of Cardiac Physiology***
  - 2.1.1 The Action Potential in the Heart
  - 2.1.2 Excitation-Contraction Coupling
  - 2.1.3 Important Functional and Structural Aspects of Ion Channels.
  - 2.1.4 Adrenergic and Cholinergic Regulation of the Heart

- ***2.2 - Beta-adrenergic Receptor Blocking Drugs***
  - 2.2.1 Classification of β–adrenergic blocking agents
  - 2.2.2 Cardiovascular Effects of β–blockade
  - 2.2.3 Non β–adrenoceptor properties of β–blockers
  - 2.2.4 Metabolism

- ***2.3 - Cardiac Surgery***
  - 2.3.1 Extracorporeal Circulation
  - 2.3.2 Hypothermia
  - 2.3.3 Hyperkalemic Arrest
  - 2.3.4 Warm Heart Surgery
  - 2.3.5. Most Recent developments in Myocardial Protection Techniques and Future Trends

- ***2.4 - Magnetic Resonance Spectroscopy (MRS) as a Tool for Studying Biological Systems***
  - 2.4.1 The Nuclear Magnetic Resonance Phenomenon
  - 2.4.2 The NMR spectrum
  - 2.4.3 Limitations and Sample Requirements - Signal-to-Noise Ratio (SNR)
  - 2.4.4 Observable Nuclei and its Biological Applications

- ***2.5 - Infrared spectroscopy***
  - 2.5.1 Basic principles
  - 2.5.2 Instrumentation and Spectral Analyses
  - 2.5.3 Biomedical applications

- ***2.6 - Pertinent Characteristics of Esmolol***
  - 2.6.1 Pharmacological & Pharmacokinetics Peculiarities of Esmolol
  - 2.6.2 Chemistry
  - 2.6.3 Details of Metabolism of Esmolol

❑ *2.1 - Pertinent Aspects of Cardiac Physiology*

2.1.1 The Action Potential in the Heart

The myocardium is an example of tissue in which bioelectrogenecity is mandatory to its function. In tissue, electrical charges exist predominantly as positively or negatively charged ions. The movement of charges generates current, which in tissue, flows across the cell membrane. It is assumed that the flow of charge crosses the membrane at a 90° angle relative to the membrane plane, and electric currents can occur by either positively charged ions moving in one direction or negatively charged ions moving in the opposite direction. The potential causing electric charges to move or the force developed by charge movement is expressed as voltage.

In tissues such as the heart, an important electrical property of the cell membrane is its insulating capacity. Because of its components (molecular bilayer of phospholipids) which form a barrier limiting the movement of ions in and out of the cell, the cell membrane makes a good insulator, and therefore a good capacitor. Ions and water move poorly through the bilayer, but intrinsic proteins spanning the bilayer create an environment favorable for ion and water movement (Figure 2.1). This combination of capacitance and selective ability to allow ionic flow through the cell membrane (with however a certain resistance) form the basis of the electrical behavior of heart tissue and generation of the action potential (Figure 2.2). All living cells have an electrical potential difference across their surface membranes. This is due to different ionic compositions of the cytoplasm relative to the extracellular medium and the relative permeability of the membrane to these different ions, principally potassium (K^+) and sodium (Na^+). Under

physiological conditions, the intracellular concentration of K^+ is approximately 140 mM while in the extracellular medium [K^+] is 4.5 mM. The inverse occurs with sodium, where the intracellular concentration is low and [Na^+] in the extracellular fluid is 135 mM. This difference in ionic concentrations is maintained mainly by the enzyme Na^+/K^+ ATPase at the cost of energy (ATP). This delicate balance reflects the resting potential of the cell. The transmembrane potential (E_m) in resting atrial and ventricular myocardial cells is about -80 mV, whereas the resting E_m in Purkinje fibers is somewhat greater (-90 mV) and in the nodal cells the resting potential is -60 mV. Thus, the myocardial cells under physiological conditions maintain an internal ionic concentration markedly different from the outside medium, which underlies the resting potential and excitability. When this balance is disturbed the result is the action potential (AP)[30,31].

2.1.1.1 Action-potential Generation

The AP is a sudden depolarization of the potential across the membrane resulting in a positive potential inside the cell. Briefly, the sequence of events that follow depolarization and generation of an action potential are: after a large increase in the permeability to sodium, Na^+ enter the cell (and Ca^{++}) along its transmembrane electrochemical gradient. Repolarization begins with a decrease in the membrane permeability to sodium (because of the change in the membrane potential) and an increase in the permeability to potassium. This K^+ however, will tend to exit the cell down its electric and concentration gradients. Action potentials are classified as fast or slow action potentials. The fast response AP is found mainly in atrial, ventricular and Purkinje cells, whereas in the sino-atrial (SA) node and in the atrio-ventricular (AV) node

a slow response AP is observed. The major difference between these two types of AP is the current that mediates them. The typical, fast-response cardiac action potential is composed of five phases[1, 2]. (Figure 2.2)

(i) *Phase 0*: the upstroke or rapid depolarization. In atrial, ventricular and Purkinje fibres the phase 0 is due to a sudden increase in membrane conductance to Na^+. When the membrane voltage reaches a given threshold (~ -75 mV in most cells), Na^+ rushes into the cell, down its electrochemical gradient via ion-specific, voltage-sensitive channels. The transient increase in Na^+ conductance is quickly inactivated, lasting only 0.5 to 2 msec, but the inward current is intense at that moment. In cardiac Purkinje fibres and possibly in ventricular muscle, two different modes of operation (or two different types of Na^+ channels) have been hypothesized[32]. One is responsible for the brief Na^+ current while the other, longer lasting, participates in the plateau (phase 2, see below). A hypothetical model of activation and inactivation of the Na^+ channel has been proposed consisting of gates (*m* gates and *h* gates) which have integrated activity between activated, inactivated and resting states.

(ii) *Phase 1*: early rapid repolarization. This phase follows the phase 0 and is characterized by a rapid and transient repolarization of the membrane to near 0 mV, partly due to inactivation of the Na^+ current (I_{Na}) and the activation of a transient outward current (I_{to}) mediated mostly by K^+ ions. Two components of this current have been described in human atrial cells[33]: a long-lasting and a brief outward currents which overlap the inward calcium current and will modulate the amplitude of the following plateau phase and therefore the amount of calcium entering the cell through calcium

channels. This is of paramount importance in the excitation contraction-coupling mechanism, since this modulation can alter contractility of the cardiac cell.

(iii) *Phase 2*: the plateau phase. This phase may last several hundreds of milliseconds. In contrast to the nerve tissue, in the heart this is functionally desirable, as it provides adequate Ca^{++} entry to trigger contraction and prevents very rapid heart rates. There are several mechanisms acting in concert during the plateau phase. K^+ channels show inward-rectification so that the repolarizing currents carried by K^+ decrease. This means that the membrane at this instance passes inward current more easily than it passes outward current, and therefore, despite a strong electrochemical gradient, potassium conductance (g_K) is low and few K^+ ions leave the cell. The cell also is held at plateau voltage due to the entry of Na^+ and Ca^{++} ions. Na^+ current is mediated by a small component of I_{Na}, which has slow inactivation. The slow calcium current (I_{si} or $I_{Ca\text{-}L}$) is triggered by voltage-sensitive calcium channels and is a major contributor to the maintenance of the plateau phase. Other minor contributors consist of a small chloride inflow (Cl^-) through a Cl^- channel, and the activity of the Na^+/K^+ pump that restores the ionic gradient over time[34]. Beta-adrenoceptor stimulation via cyclic AMP-dependent protein kinase, activation of adenylate cyclase[35] and histamine[36] increase the chloride current. All these different currents work in synchrony and the result is an almost perfect balance of charges, such that the membrane potential (E_m) changes little for 200-400 ms, the duration of the plateau phase.

(iv) *Phase 3*: rapid repolarization. During this phase, the rapid repolarization is due mainly to the inactivation of $I_{Ca\text{-}L}$ and the activation of an outward K^+ current (I_K)[37]. The net membrane current becomes more outward and the membrane potential shifts in a

negative direction. The channel responsible for I_K activates at an E_m of about -50 mV and is fully activated at about +20 mV. Its time constant is such that the current reaches its peak about 300 msec after phase 0. It has been shown that inactivation of $I_{Ca\text{-}L}$ alone is insufficient to induce repolarization in the absence of I_K[8, 38]. Evidence based on the reversal potential (of -70 mV) of these channels suggests that it may not be strictly selective for K^+ ions[8]. As I_K carries the membrane potential to a negative direction, inward rectification of other K^+ channels decreases and other outward K^+ currents (repolarizing) may be recruited. The accumulation of K^+ ions in narrow extracellular clefts may play a role in repolarization and further complicates the study of these different currents[8, 9].

(v) *Phase 4*: diastolic depolarization. Under normal conditions, atrial and ventricular myocytes have steady membrane potentials during diastole. In other fibres, such as the P cells in the SA, AV nodes as well as the His-Purkinje system and cells in the muscle of mitral and tricuspid valves[39, 40], the resting membrane potential is not constant during diastole but gradually depolarizes. If a propagating impulse does not depolarize the cell or group of cells, it may reach the threshold by itself and produce a spontaneous action potential. This spontaneous discharging property of some cells (and typical of phase 4 of the AP) is called Automaticity. The discharge rate of cells in the SA node normally exceeds the discharge rate of other potentially automatic pacemaker sites and thus dominates the cardiac rhythm ("overdrive suppression" phenomenon)[41]. Because of this, the SA node cells are subject to strict neural modulation mediated via norepinephrine and acetylcholine.

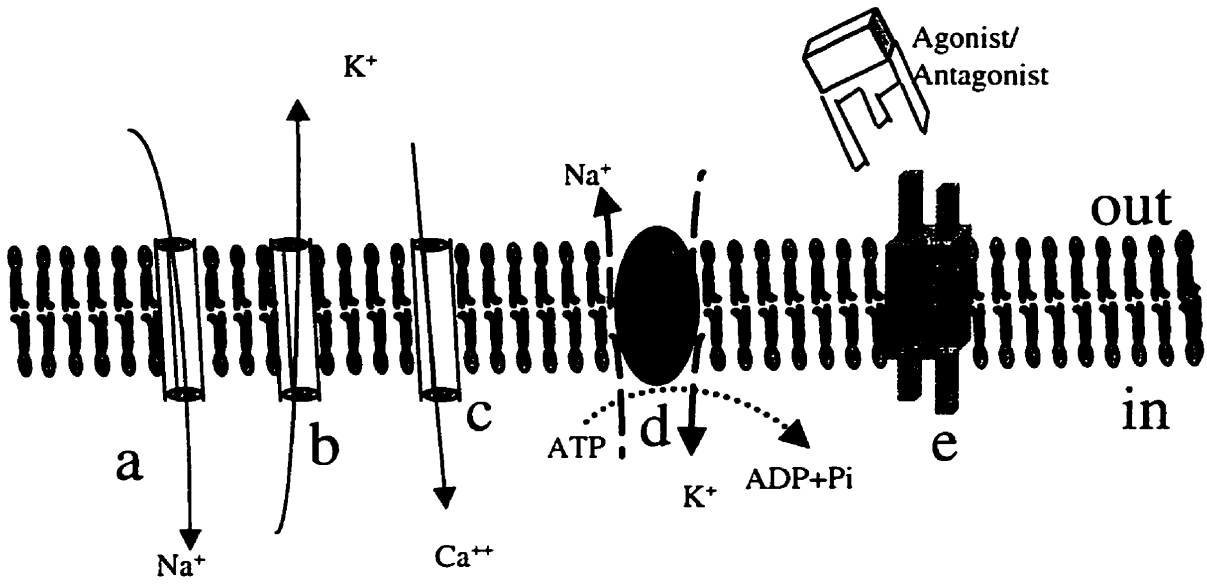

Figure 2.1 - Representation of the cellular membrane with some of its electrophysiologically important components: **(a)** Sodium channel; **(b)** Potassium channel; **(c)** Calcium channel; **(d)** Na^+/K^+ pump; **(e)** membrane receptor embedded in the phospholipid bilayer.

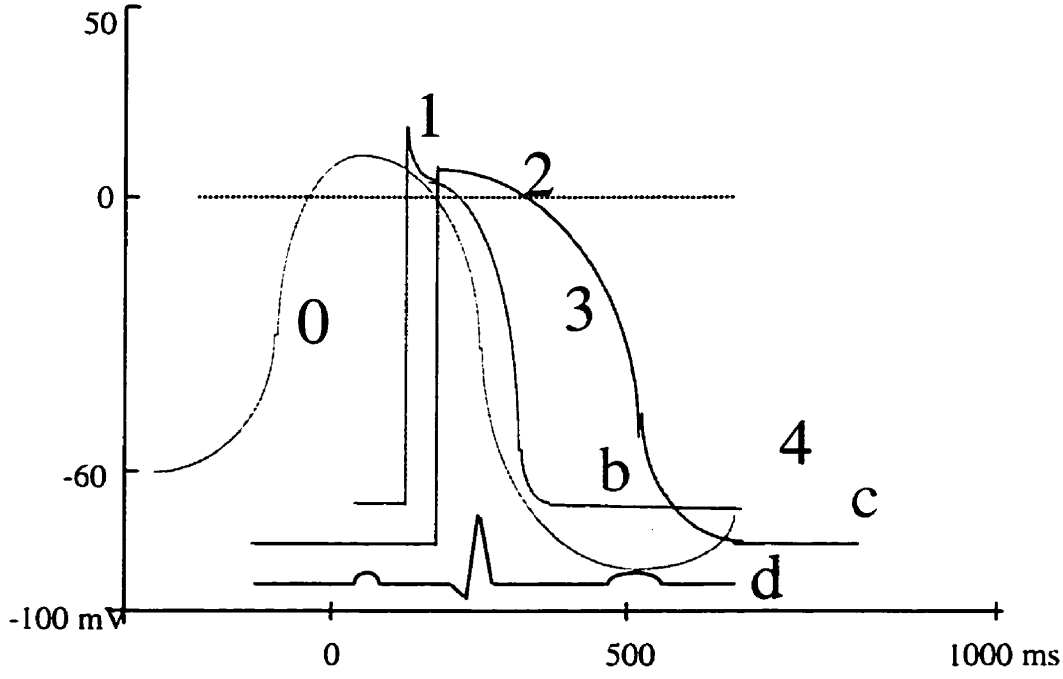

Figure 2.2 - Schematic representation of the action potential (AP) in the different regions of the conduction system: **(a)** SA node slow AP; **(b)** Purkinje fibres; **(c)** ventricular myocardium; **(d)** ECG. Phase 0 corresponds to AP upstroke, phase 1 early depolarization; phase 2 plateau; phase 3 repolarization and phase 4, full repolarization and resting potential.

2.1.1.2 Action-potential Automaticity

The heartbeat is governed by a specialized system, the main characteristic of which is to spontaneously generate and distribute each impulse in a coordinated way to achieve efficient myocardial contraction and pump function. Since myocardial cells are linked by low-resistance junctions (gap junctions and intercalated disks), cardiomyocytes behave as a functional and electrical syncytium. Therefore, an AP that occurs in one cell rapidly spreads to the adjacent cells of the structure. In normal sinus rhythm, the AP usually begins in the cells of the sino-atrial (SA) node and is propagated rapidly to the atria (right atrium activates before the left), which corresponds to the P wave seen in electrocardiogram (ECG) traces (Figure 2.2 (d)). This type of AP is called the slow type, and is believed to be mediated by Ca^{++} and Na^{+} ions. The AP arrives at the atrioventricular node (AV node) almost simultaneously with the right atrial activation. The interval from the onset of the P wave to the onset of the QRS complex is an approximation of the total time for conduction in the AV node and Purkinje system, and can be measured in ECG traces. The QRS complex reflects activation of the ventricles. This activation can be divided in thirds, with the first third corresponding to septal activation, the middle third to the apex, and the final third to the base of the heart. Any alteration in conduction prolongs the duration of the QRS phase, which will enlarge the complex seen in an ECG trace. The T wave is the result of repolarization of the ventricles, and its vector is directionally opposite to that of the second phase of depolarization. During the second phase of depolarization the apical and free walls depolarize from endocardium to epicardium, while the repolarization follows from epicardium to endocardium. During the latter half of the T wave, part of the ventricle is

repolarized, a period (relative refractory period) in which a sufficiently strong stimulus may generate a disorganized activation leading to arrhythmia and/or fibrillation ("R-on-T" phenomenon).

Normally, the sinus node initiates the cardiac impulse while the His-Purkinje system serves as a backup in case sinus node pacemaking fails or an AV block occurs. Impulse generation in the sinus node is much faster (60-100 beats/min) than in the His-Purkinje system (35-50/min), thereby allowing the sinus node to control cardiac rhythm. The cardiac impulse is generated in a small cluster of cells (P cells) that constitute the primary pacemaker of the heart and then spreads slowly through the sinus node and perinodal fibres to reach specialized atrial tracts and ordinary atrial muscle[42]. The specialized atrial tracts transmit the cardiac impulse rapidly (fast conducting fibres) from the SA node to the AV node via the anterior, middle, and posterior internodal tracts and to the left atrium via the Bachman's bundle[43,44]. Despite physiological evidence, the concept of specialized conducting fibres in the atrial myocardium is still questioned by anatomists who often cannot find any histological structure that could correspond to such a function.

The only normal conduction pathway from the atria to the ventricles is via the AV node. As the impulse enters the AV node, it slows dramatically, accounting for most of the P- R interval in the ECG. The explanation for this phenomenon is to allow ventricular filling during the cardiac cycle. When the impulse emerges from the AV node into the His bundle, conduction speeds dramatically and the spread of excitation through the bundle branches and peripheral Purkinje fiber network occurs with great rapidity in the normal heart. The action potential duration (APD) and refractoriness in the Purkinje

system increases as a function of distance from the AV node to reach a maximum value about 2 to 3 mm from the Purkinje fibre-ventricular muscle junction. The ventricular muscle is activated almost simultaneously over much of its endocardial surface via the extensive subendocardial Purkinje fibre network.

2.1.1.2.1 Ionic Basis for Automaticity

Early studies showed that K^+ conductance was slower as Purkinje fibres spontaneously depolarized[45]. Further experiments with high $[K^+]_o$ and voltage-clamp techniques applied at the end of phase 4 showed a decrease in the net inward current as a function of time[46] and therefore it was postulated that cardiac Purkinje fibres experienced a decrease in an outward K^+ current (called I_{K2}) during a relatively constant background inward Na^+ current that caused pacemaker activity[47]. It is now thought that all cardiac pacemaker cells exhibit a voltage-dependent channel that is activated by potentials of -50 to -60 mV, passing the so-called *hyperpolarization-activated inward pacemaker current*[48]. At this potential, an inward current becomes activated and is carried by a channel that is relatively nonselective for monovalent cations. Hyperpolarization increases its rate of activation and at -70 mV, the time constant ranges from 2 to 4 s. This pacemaker current (I_f) would then underlie the slow diastolic depolarization that occurs between -90 and -60 mV in Purkinje fibres. Although it is thought that I_f is carried by Na^+ ions, its channel does not seem to have voltage-dependent properties and its reversal potential is -20 mV, far from E_{Na}, and is not blocked by tetrodotoxin. All this may suggest the presence of an additional type of Na^+ channel that would be responsible for I_f, since reduction in K^+ conductance (with barium or amantidine) could at least theoretically unmask I_f and

produce automaticity at normal membrane potentials[49]. As a general concept, the ionic basis of automaticity can be explained as a net gain in intracellular positive charges during diastole, which slowly brings the E_m close to threshold and generates the subsequent action potential.

2.1.1.2.2 Autonomic Modulation of the SA Node

Stimulation of the sympathetic nervous system and/or adrenal release of catecholamines cause an increase in the rate of firing of the SA node, which is associated with an increase in the rate of depolarization of the pacemaker potential. Timing of changes in the membrane potential during diastole is also an important factor on the rate of automaticity. Cathecolamines increase $I_{Ca\text{-}L}$ ($I_{Ca\text{-}T}$ current in the SA node) primarily by increasing cyclic AMP and activating the protein kinase A system and also increase I_K which shortens the AP and triggers the pacemaker potential earlier in the cycle[50]. It has also been shown that catecholamines increase I_f in Purkinje and SA node cells[51,52,53]. The overall result is an increase in diastolic depolarization rate secondary to a faster development of inward current.

Vagal stimulation slows the SA node pacemaker rate through its mediator acetylcholine (ACh). Binding to a surface muscarinic receptor activates a G protein that inhibits adenylate cyclase (G_i) thereby reducing cAMP levels. Reduction in cAMP results in reduction in all three currents ($I_{Ca\text{-}L}$, I_K, and I_f)[54]. Recent work suggests that the ACh receptor may be coupled directly to Ca^{++} channels and to I_f [24] and to another type of K^+ channel the ACh-dependent K^+ channels or $K_{(ACh)}$. It has also been suggested that there is a difference in the dose dependency of the different ACh effects[55], in which low

doses of ACh (and/or low frequency stimulation of the vagal nerve) appear to slow the rate of diastolic depolarization with little or no effect on the action potential. This mechanism seems at least in part independent of I_f, nevertheless physiological modulation of pacemaker activity seems to require only subtle alterations in membrane currents[56]. It should be taken into account the technical difficulties and the controversy in the literature since these small effects are difficult to measure unambiguously under physiological conditions[57].

2.1.1.3 Action Potential Propagation

The movement of ionic current through the membrane, within the cells, and back through the extracellular space completes a circuit. The speed of propagation of the cardiac impulse in tissues composed of cells with fast action potentials varies, but a mutual dependent relationship exists between the active and passive cellular properties and the excitability properties of the cell. This relationship is exemplified by the liminal length concept, which was developed from the cable theory of analysis. The classic cable theory and its equation was initially developed by Hodgkin and Rushton[58] using nerve axons and later Weidmann[59] extrapolated its use to cardiac tissue using cable-like strands of the specialized conduction system, the Purkinje fibres. The One-dimensional Cable Theory has been used as the basis of experimental cable analysis in several nerve and heart preparations. Additional mathematical and analytical models have been developed suitable for considering experimental results in two or three dimensions[60]. *The liminal length concept* in a uni-dimensional cable is that length of tissue required to be raised above threshold such that the inward depolarizing current from that region is greater than

the repolarizing influences of adjacent tissues. If the local circuit currents fulfill the liminal length requirements of the next unit membrane, an AP will result. Propagation, then, depends on one unit membrane fulfilling the liminal length requirements of its neighbor, which, in turn, must do the same for the next unit[61]. Cable-like structures without extensive branches, such as the His bundle, bundle branches, or Purkinje fibres, conduct faster and with a greater safety factor than tissues with extensive three-dimensional branching, such as ordinary ventricular muscle[62]. In addition, spread of excitation is faster along the long axis of myocardial fiber bundles than transversely[63].

If the local circuit currents are of sufficient strength to excite its neighbor unit a regenerative AP will result, otherwise only local electrotonic effects will take place. When sodium channels open and Na^+ enters the cell down its electrochemical gradient, these positive charges displace the negative charges stored inside the membrane and result in depolarization. The membrane potential in that localized region becomes more positive than in neighboring parts of the cell, and a driving force for longitudinal current in the myoplasm is established. The potassium ion is the major carrier of the longitudinal current within and between cells, and its flow is regulated primarily by the resistance and capacitance at the gap junctions and to a lesser extent, by impedances in the myoplasm. The longitudinal current displaces negative charge located on the inner surface of the membrane, depolarizes adjacent elements toward threshold, and thereby brings the membrane to the potential required to trigger the membrane conductance to Na^+ and trigger depolarization. The circuit is completed by a capacitative current flow across the membrane and, finally, by current flow in the extracellular space. If local electrotonic currents established by these events in one unit of membrane are sufficient to bring the

next unit above the threshold, the next unit opens its Na^+ channels and propagation of the AP results. In the normal tissue, discontinuities are negligible in the Purkinje cell cable but become important when several bundles run together, when there is change in fiber size, when the transverse and longitudinal communications differ, when there is damage to the membrane or individual cells, branches or in any morbid process that alter the microstructure of the myocardial cells, including ischemia, hypertrophy, remodeling and dilatation[64].

2.1.2 Excitation-Contraction Coupling

Once threshold potential is reached, Na^+ ions will rush into the cell and depolarize the membrane. With what purpose? The sequence of events that follow membrane depolarization represents one of the most sophisticated mechanisms in the heart to perform its pumping function.

The essential event in initiation of contraction is believed to be the rise in cytoplasmic calcium concentration[65,66,67,68]. Since the late 1800's with the work of Ringer, it has been thought that cardiac contraction depends on Ca^{++} levels. Despite an average concentration of calcium in the heart of approximately 2.5 mM, in the relaxed cell Ca^{++} is not directly available to initiate contraction, but is mostly stored in the sarcoplasmatic reticulum (SR). Calcium triggers the contraction process by binding to the subunit C of Troponin and producing a conformational change in tropomyosin ("roll-over" of tropomyosin) thereby exposing the actin binding site for myosin. The immediate source of the myofilament-activating Ca^{++} varies depending on the cell type. In frog

hearts the activating Ca^{++} flows from extracellular sources, whereas in skeletal muscle it comes almost exclusively from the SR. In the mammalian heart, calcium flows from the SR and extracellular sources in such a way that the initial Ca^{++} inflow (from extracellular space) triggers the release of a much larger quantities of Ca^{++} from the SR which will then activate the contractile machinery. This concept has been described by Fabiato and others as the ***Calcium-Induced-Calcium-Release*** phenomenon[69, 70, 71, 72, 73, 74, 75, 76].

Following depolarization of the cell membrane, Ca^{++} ions flow through highly specific channels in cardiac cell membranes. Generally, there are two types of Ca^{++} channels, the L-type[77, 78, 79] and the T-type[80, 81, 82]. Both channels are three to four orders of magnitude more selective for Ca^{++} than Na^{+} or K^{+} ions, and can transfer over 100 Ca^{++} ions per second. Both currents ($I_{Ca\text{-}L}$ and $I_{Ca\text{-}T}$) are activated by cell membrane depolarization and are inactivated in a time- and voltage-dependent manner when the depolarization is maintained. Although both currents are fully activated upon depolarizations from -90 mV, $I_{Ca\text{-}T}$ is inactivated when cells are steadily depolarized to -50 mV, whereas $I_{Ca\text{-}L}$ remains still available at this voltage[83, 84].

In the mammalian heart, calcium ions that have entered the cell do not directly activate the contractile apparatus. Rather, they trigger the release into the cytoplasm of much larger quantities of Ca^{++} from SR stores (from the terminal cisternae of the SR, increasing $[Ca^{++}]_i$ from 10^{-7} during diastole to 10^{-5} M during systole)[85]. The amount of Ca^{++} released is graded according to the rate of rise and magnitude of the inward Ca^{++} current: larger and faster transients release more Ca^{++} from the SR. Studies performed in skinned fibres (after removing its sarcolemma) have shown that the fast, initial component of the Ca^{++} current triggers the release of Ca^{++}, whereas the slow and

sustained component (during the plateau phase) loads the SR with Ca^{++} that becomes available for subsequent beats [43]. Contractile grading can also be altered by voltage[86], the degree of channel availability[87, 88], endogenous and exogenous pharmacological agents (cathecolamines, isoproterenol[89, 90], digitalis[91, 92]), force-frequency relation (where there is an increase in $[Ca^{++}]_i$ accumulation over time)[93] and the activity of the Na^+/Ca^{++} exchanger[94, 95, 96].

The structure responsible for the release of calcium from the sarcoplasmatic reticulum is a protein called the SR Ca^{++} release channel or ryanodine receptor (RyR). This protein has been purified[97, 98] and cloned[99]. It is a homotetramer, with monomers of 4969 aminoacids and a molecular weight of about 565,000 kDa. It is a complex structure with six membrane-spanning domains, with pores originating in the SR lumen and ending at the cytosol, where the channel is surrounded by structures of fourfold symmetry from which four radial branches protrude into the cytosol. No Ca^{++} binding site has been identified in the protein, however there have been reports that Ca^{++}, ATP and calmodulin may bind near residues 3600-4500 and also a potential site for phosphorylation by cAMP-dependent protein kinase has been proposed[100, 101].

Several studies have been undertaken using preparations of purified RyRs inserted in planar phospholipid bilayers, with promising but inconclusive results regarding modulation of release, single channels analysis and ionic selectivity, probably due to technical difficulties in the preparation of the experiments. Up to now, in vitro activation of the RyR channel has required milimolar concentrations of ATP and magnesium, and micromolar concentrations of Ca^{++}. However inhibition of Ca^{++} efflux with Mg^{++}, H^+ and calmodulin has been reported, but no evidence of time-dependent inactivation has been

proposed[102, 103]. The single channel analysis (and the calculation of the probability (P_o) of channel opening under different conditions) has indicated that its opening is not dependent on membrane potential (being a ligand-gated channel per excellence) without evidence of inactivation and refractoriness (even with major increases in $[Ca^{++}]_i$ and frequency of stimulation)[104]. Ion selectively studies[105] have shown the RyR receptor about 6 times more selective to Ca^{++} than to K^+ ions but little selectivity was seen when compared to Mg^{++} ions ($P_{Ca++}/P_{Mg++} = 2.3$).

Relaxation is brought about through different processes, which include the combination of the active uptake of Ca^{++} by the SR and Ca^{++} extrusion via the Na^+/Ca^{++} exchanger. These are quite capable of returning Ca^{++} concentrations to diastolic levels and promote the detachment of Ca^{++} from troponin C within the appropriate time frame[106]. Contributions from the sarcolemmal Ca^{++} ATPase and mitochondrial uptake are negligible under physiological conditions and it has been demonstrated that inactivation of the SR uptake and activity of the Na^+/Ca^{++} exchanger dramatically slow relaxation[107]. The voltage-dependent action of the electrogenic Na^+/Ca^{++} exchanger may be responsible for the enhanced rate of relaxation at more negative potentials (favoring Ca^{++} extrusion)[108].

Several factors can modulate Ca^{++} movements in the myocyte. The most physiologically important is probably the activity of the beta-receptor agonist. When bound to an agonist, the β–adrenoceptor leads to activation (in the presence of ATP and Ca^{++}) of the membrane bound enzyme adenylyl cyclase the activity of which is modulated by the guanine-nucleotide bound regulatory protein (G proteins)[109]. The activated stimulatory dimer (G_s) interacts with adenylyl cyclase and increases its activity. The

resulting increase in the levels of cAMP will activate the so-called cAMP-dependent protein kinases, which phosphorylate at least 3 different intracellular proteins to promote an increase in contractility. These include (i) phosphorylation of a protein located near the Ca^{++} channel and enhancing its open state (receptor-operated channels); (ii) phosphorylation of phospholamban and subsequent stimulation of calcium uptake by the SR (and therefore accelerate relaxation)[110]; and (iii) some evidence exists of reduction of the sensitivity of the myofibrils to Ca^{++} via phosphorylation of the subunit I of Troponin[111]. Beta-adrenergic stimulation will then increase Ca^{++} influx through the sarcolemma (by recruiting additional channels rather than affecting the rate of opening of the channels)[112]; enhance relaxation by increasing the rate of Ca^{++} active uptake by the SR and reduce the sensitivity of the myofibrils to Ca^{++}.

2.1.3 Important Functional and Structural Aspects of Ion Channels

Ion channels are complex membrane-spanning proteins upon which depend the ion conductance activity of the cardiac sarcolemma and other excitable tissues. In the heart, voltage-gated ion channels mediate changes in ion permeability during the action potential and are characterized by high ion selectivity. In recent years, mainly due to the development of techniques of molecular biology in identification and purification of protein components of ion channels, associated with refinements in electrophysiology techniques, an overwhelming amount of information on function and diversity of ion channels has been uncovered. It is beyond the scope of this manuscript to give a detailed description of the molecular structures and variety of these proteins. Important general

aspects of function however, and their correlation to channel structure, are required for a better understanding of the proposed effects of esmolol in different types of ion channels.

The ion conductance activity of voltage-sensitive ion channels is controlled on the millisecond time scale by voltage-gated activation and inactivation. Activation is related to time and voltage-dependence of opening in response to changes in membrane potential, whereas inactivation controls rate and extent of ion channel closure[113]. These two processes provide a transient control of ion conductance in response to changes in the membrane potential. A longer and more sustained form of regulation is mediated by phosphorylation and interaction with other membrane-bound proteins, especially the regulatory G proteins. These processes play an essential role in the regulation of cardiac function mediated by hormones and neurotransmitters.

2.1.3.1 General Structural Organization

The determination of subunits of the voltage-sensitive ion channels has provided insights on transmembrane organization of the ion channel structure and function at a higher level of resolution previously impossible. On the same basis, analyses of the hydrophobicity, secondary structure and amino acid sequence of the α subunit of the Na^+ channel and of the $\alpha 1$ subunit of the Ca^{++} channel have led to a proposed model which postulates a structure composed of six membrane-spanning segments per homologous domain interconnected by hydrophilic segments. A substantial level of similarity between the Ca^{++} channel $\alpha 1$ subunit and the Na^+ channel α subunit led to the proposal that Na^+ and Ca^{++} channels have analogous transmembrane structure. Purified preparations of voltage-sensitive Na^+ and Ca^{++} channels have revealed that the resulting cDNA sequences encode

for a large polypeptide of 1,832 amino acids containing four repeated domains of 300 to 400 amino acids with approximately 50% homology between Na^+ and Ca^{++} channels[114]. For potassium channels, analysis of hydrophobicity reveals six or seven possible membrane-spanning segments. The fourth of these segments has striking homology with the S4 segments of the Na^+ channel, and the overall arrangement of the proposed transmembrane segments is similar to that within each of the four homologous domains of the Na^+ channel.

The Na^+ channel from the mammalian brain consists of heterotrimetric complex of α– (260 kDa), β–1 (36 kDa) and β–2 (33 kDa) subunits. The β–2 subunit is attached to the α– subunit by disulfide bonds. The Na^+ channel from mammalian skeletal muscle contains subunits of 260 kDa and a 38 kDa analogous to the brain Na^+ channels α and β–1 subunits, whereas the Na^+ channel from the eel electroplax contains only a single 260 kDa subunit. In pharmacological binding studies, α subunits contain the binding site for tetrodotoxin and saxitoxin and this may indicate that these subunits are the main functional component of Na^+ channels[115]. In the heart, specific antibodies against the Na^+ channel subunits recognize α and β–1, but not β–2 subunits. The α and β–1 subunits bind neurotoxins that act from outside the cell, and all three subunits are heavily glycosylated with up to 30% of their apparent mass due to carbohydrate, indicating exposure to extracellular surface. The α subunit is phosphorylated by cyclic AMP (adenosine 3', 5'-monophosphate, cAMP)-dependent protein kinase *in vitro*. The β–1 and β–2 subunits are also intrinsic membrane proteins and can be extracted by hydrophobic detergent phases[116].

There have been several classes of Ca^{++} channels identified in most excitable cells[117]. In cardiac physiology, the majority of molecular studies have concentrated on the L-type channel that mediates the long lasting calcium current ($I_{Ca\text{-}L}$) during the plateau phase of the AP. These channels are inhibited by three distinct classes of organic Ca^{++} channels antagonists which act on separate receptor sites. Dihydropyridines (such as nifedipine) produce activity inhibition, phenylalkylamines (verapamil) produce channel blockade, and benzothiazepines (diltiazem) also inhibit channel activity. The purified Ca^{++} channel is a complex of five polypeptide chains, with the central component appearing to be the $\alpha 1$ subunit with an apparent mass of 175 kDa[118]. The central $\alpha 1$ subunit is associated with a disulfide-linked complex $\alpha 2$ (143 kDa) and δ (27 kDa) subunits that are heavily glycosylated. The β subunits (54 kDa) are neither glycosylated nor hydrophobic and the γ subunits (30 kDa) present substantial hydrophobic domains and carbohydrate moieties. The $\alpha 1$ and β subunits are sites of phosphorylation by cAMP-dependent protein kinase. The overall structure of both Na^+ and Ca^{++} channels consist of a single principal subunit expressed in association with a variable number of other polypeptides. The β–1 subunit of the Na^+ channels and the γ subunits of the Ca^{++} channels are similar in size, hydrophobicity, and extent of glycosylation[119].

The purification of the K^+ channel has revealed a complex of subunits of 35 to 40 kDa in addition to the main glycoprotein subunits[120]. The primary structures of these principal subunits and their presence in a complex, suggest that they form a tetramer that is functionally analogous to the α subunit of the sodium channel and the $\alpha 1$ subunit of the calcium channel. The K^+ channel corresponds, in structure, to one single domain of the principal subunits of the Na^+ or Ca^{++} channel. Because K^+ channels are commonly found

in yeast, while Ca^{++} channels are found in protozoa and Na^{+} channels are present only in multicellular organisms, an evolutionary relationship among the voltage-sensitive ion channels has been proposed[121].

2.1.3.2 Ion Pore

The presence of four homologous domains in the primary structures of the Na^{+} and Ca^{++} channels led to the proposal that the transmembrane pore is formed in the centre of a square array of the four transmembrane domains. All models of voltage-gated ion channels structure have incorporated this basic architecture which relies on conservation of the corresponding aminoacids sequences in Na^{+}, Ca^{++} and K^{+} channels. Based on hydrophobicity analysis, the membrane-spanning domains are believed to form α–helical secondary structures that correspond to the "walls" of the transmembrane pore. Based on studies of permeability of organic cations of different sizes, the Na^{+} channel pore limiting size has been estimated to be 3 by 5 Å in dimension. Further pharmacological analyses and mutation-deletion of aminoacids resulting in the analyses of function of mutant channels identified sites within the S5-S6 linker aminoacids (called the SS1-SS2 region or P region for 'pocket') which is believed to dip into and out of the membrane, forming the narrow pore of the channel[122,123].

2.1.3.3 Ion Selectivity

Glutamic acid residues have been identified in the pore region that appear to be important for ion conduction and toxin block in sodium channels. The sodium channels have two negatively charged residues which, in association with a positive amino acid in repeat III

and a neutral amino acid in repeat IV, seem to regulate pore selectivity. Specific alterations of the sequences of these amino acids have generated mutant channels with altered or completely abolished selectivity[124]. Thus, the initial indication for a structure-based selectivity filter has been proposed. Although the exact mechanisms of selectivity are yet to be elucidated, site-directed mutagenesis of sodium, potassium and calcium channels have clearly identified the transmembrane segments S5 and S6 with ion-selectivity properties. Aminoacids within the P-region are the ones believed to play key roles in permeation of ions in the different channels[125,126].

2.1.3.4 Activation and Gating Mechanisms

A central and most physiologically relevant characteristic of the sodium channel is its voltage-dependent gating, and it represents Nature's most sophisticated way to transduce voltage changes at the cell membrane. Understanding of the Na^+ channel gating mechanism has relied on the Hodking-Huxley model derived from voltage-clamp studies of macroscopic currents in the squid giant axon[127,128]. In their classical study, Hodgkin and Huxley demonstrated the biphasic time course of I_{Na} after a step depolarization. They hypothesized that the Na^+ channel exists in three states: closed (C), open (O) and inactivated (I) and assumed that activation and inactivation were independent processes. According to this model, at the normal resting potential, channels are mostly in the C state and able to provoke Na^+ current upon depolarization; after an overthreshold stimulus the channels open. Because of the multistep assumption of activation, Hodgkin and Huxley postulated the probability (m) of the channel opening as m^3, and voltage dependence as the cube root of the peak conductance. The inactivation process was

represented by the decay of I_{Na} which reflected the increasing number of channels becoming inactivated and was described as a single transition with the probability of $1-h$. I_{Na} would then be proportional to m^3h. Recovery would be represented by the return of channels from the inactivated to the closed conformation and occurred only at potentials negative to the threshold potential (hyperpolarization). Although the relationship of the charge and conductance curves support the Hodgkin-Huxley model, other aspects of gating current measurements do not. In single channel conductance studies, it became evident that decay current does not follow a single time-constant. Rather three voltage-dependent gating transitions occur, instead of the current disappearing when the first open-closed transition occurs. Differences between the predictions derived from the model and experimental data, especially of the rate of decay of currents during depolarization[129] and upon hyperpolarization[130] led to the idea that the activation rate constants are not mere multiples of each other, and that the voltage dependence of activation is concentrated closer to the open state. Overall, the gating currents suggest that although the Hodgkin-Huxley model of multistep activation was correct, experimental data did not fit the model predictions. These data may be better modeled by a set of sequential closed channel steps, each of which has a characteristic voltage dependence. In cardiac cells, the voltage dependence of activation is concentrated to the open state, however the closed conformations of the channel appear to have more rapid rate constants than the closed-open state but with less voltage-dependence[131,132].

In a practical sense, the current hypothetical model describes function of the Na^+ channel in a manner similar to the Hodgkin-Huxley model (taking into account the above considerations): the three *m* gates (activation) and the three *h* gates (inactivation) are lined

up in series along the membrane with *m* gate on the extracellular side and the *h* gate towards the intracellular side of the membrane. When the membrane is at resting potential (polarized), the *m* gates are virtually all closed and the *h* gates are all open, and almost no Na^+ can cross the membrane. Depolarization opens the *m* gates and closes the *h* gate, however the closure of the *h* gate happens much slower than the opening of the *m* gates. Activation then occurs much faster than inactivation can occur and Na^+ ions flow through the channels for about 1 msec while both gates are simultaneously open. When the membrane repolarizes and its potential drops to values lower than -60 mV, the *h* gates open slowly (reactivation occurs) and the membrane is ready for another depolarization. Until this happens the cell remains refractory (in the inactivated state) and will not respond to any magnitude stimulus[1].

Applying the Hodgkin-Huxley framework to calcium channels, the steady state activation variable ranges from 0 at threshold to near 1 at +10 mV. The threshold for activation of L-type Ca^{++} channels in cardiac myocytes is around -40 mV at $[Ca^{++}]_o$ = 2.0 mM[133] and the activation curve is sigmoidal[134,135]. The voltage dependence of T-type Ca^{++} channel opening is similar, except that it is displaced by 10 to 25 mV in the negative direction, and the threshold occurs at -65 to -50 mV[136]. The study of Ca^{++} agonists and antagonists have led Hess and colleagues to develop a kinetic model for the Ca^{++} channel[137]. This model describes the Ca^{++} channel shifting between three discrete gating patterns or modes. These modes are distinguished by different rates of channel opening and closing with (a) brief openings that occur in bursts--mode 1; (b) much longer openings interrupted by very brief closings--mode 2; and (c) no openings at all--mode 0. Under control conditions, mode 1 is the predominant mode of gating, and transitions into

mode 2 are rare and can be mediated by β–adrenergic stimulation[138]. This channel gating behaviour has been described as a kinetic model with two C1-C2-0 reaction schemes with reactions rates of transitions between the states of different values depending on the mode. One of the major assumptions is that the transitions between modes have to be much slower than the gating reactions within modes. A different kinetic model has been put forward by Cavalié et al. which consists of two subsets of channel states[139]. Subset B (for bursting) is formed by channels with fast transition rates (C1-C2-0) and are characterized by closely spaced bursts of single-channel openings. This behaviour is related to the opening pathway of the L-type channel and generated $I_{Ca\text{-}L}$ upon depolarization. Subset Q (for quiescence) is characterized by long periods of inactivity interrupted by brief periods of activity (bursts or clusters of bursts). Channels on Q states remain so for seconds and they present low $I_{Ca\text{-}L}$ and moderate pulsing rates. Under equilibrium conditions, the gating transitions between subsets B and Q are responsible for slow consecutive cycles of L-type Ca^{++} channel availability and unavailability and perhaps their modulation by β–adrenergic agonists and specific antagonists[140,141].

Several authors have attempted to describe the behaviour of T-type calcium channels by state models. The models that have accounted best for single-channel data are consisted of one resting, one closed, one open, and one inactivated state which could be reached by any one of the other states[142].

2.1.3.5 Voltage Sensing and Inactivation

A unique characteristic of voltage-sensitive ion channels is its capability of "sensing" an electric field and its intrinsic ability to alter its conformation in response to changes in the surrounding field. This requires charged aminoacid residues or strongly oriented dipoles within the membrane bilayer. The movement of these gating charges across the membrane causes a measurable capacitative gating current that can be detected in voltage-clamp experiments in Na^+ channels. This movement of gating charge begins immediately upon depolarization of the membrane, is largely completed before any current is detected through the open channel and is blocked if the Na^+ channel is first inactivated before depolarization. It has been proposed that the segment S4 has a transmembrane orientation and are the gating charges or voltage sensors of the Na^+ channel. This has had experimental support by site-directed mutagenesis experiments on Na^+ channels and has provided the basis of the "sliding helix" model of voltage-dependent gating[143]. According to this model, S4 helices are proposed to initiate sequential conformational changes in the four domains of the Na^+ channel, resulting in transfer of gating charges across the membrane and finally, in activation of the ion channel. *Inactivation* is intrinsically a voltage-independent process coupled to the voltage-dependent changes that lead to channel activation. The lack of intrinsic voltage dependence and the complete removal of inactivation by internally applied proteolytic enzymes has led to the development of a model of inactivation in which a protein component on the intracellular surface of the channel occludes the intracellular opening of the activated transmembrane pore leading to inactivation.

2.1.3.6 Receptor Sites

Most of the initial work was pharmacologically-based studies in which compounds (mainly neurotoxins in the case of the sodium channel–the first to be studied) were used as molecular probes to identify and isolate the protein components of the ion channels. A number of special neurotoxins have identified at least five different receptor sites in the sodium channel: Tetrodotoxin (site 1) which inhibits ion conductance; Veratridine which induces persistent activation (acting at site 2); α–scorpion and sea anemone toxins that act at site 3 and inhibit inactivation and/or enhance persistent activation; β–scorpion toxins which act at site 4 and shift the voltage-dependent activation, as well as brevetoxins which act at site 5 and also induce repetitive firing. Binding to yet unidentified sites are insecticides, the Gonoipora toxin, local anesthetics, antiarrhythmics, beta-adrenergic blockers and anticonvulsivants, which induce frequency and voltage-dependent inhibition[144].

2.1.3.7 Modulation of Ion Channels

2.1.3.7.1 Phosphorylation

Many Ca^{++} and K^{+} channels are regulated by pathways involving protein phosphorylation, suggesting that long-term modulation of ion channel function by phosphorylation is a wide-spread regulatory mechanism[145,146]. Purified and reconstituted Ca^{++} channels are activated by phosphorylation of their α1 and β subunits by cyclic AMP-dependent protein kinase, and it is consensus that this is the mechanism of Ca^{++} channel regulation by β–adrenergic agonists in the heart and possibly in other tissues. However, the physiologically significant sites of phosphorylation of Ca^{++} and K^{+} remain poorly defined.

Evidence for in vitro phosphorylation of the Na^+ and K^+ channels by protein kinase C and A has been gathered showing effects on channel kinetics and amplitude[147,148].

2.1.3.7.2 Reduction-oxidation (redox) potential.

Redox potential is tightly controlled in the cytoplasm and is affected by metabolic changes. Specific K^+ channels, such as Kv1.4 and Raw3 are regulated by the redox potential. When at reduced form, the currents mediated by these channels are fast inactivating. In the heart, this current forms part of I_{to}. This current has been shown to affect the shape of the action potential and the firing rate during repetitive firing. This fast inactivation of Kv1.4 is rapidly removed if the cytoplasmic side of the membrane is oxidized and the site of the redox process has been suggested as the cysteine residue in the amino terminal of Kv1.4. Kv1.4 is abundant in brain tissue but it has also been identified in the heart[149].

2.1.3.7.3 Extracellular K^+ concentration

The effects of extracellular K^+ concentration on modulation of some types of K^+ channels is important when considering the effects of hyperkalemic cardioplegia. The amount of current through Kv1.4 is proportional to $[K^+]_o$ in such a way that it overcomes the effect of changing the equilibrium potential for K^+ to more positive values[150]. Since local $[K^+]_o$ is dependent on the magnitude of I_{to} and therefore dependent on previous activity, the current through Kv1.4 may play a role in modulating the activity of pacemaker cells, specially at high firing rates. In pathological situations (such as ischemia) or any other situation where $[K^+]_o$ increases (possibly high K^+ cardioplegic infusion), this will not only

alter the electrical properties of the cells, but also increase the fraction of I_{to} flowing through Kv1.4 channels. These combined actions may alter the shape of the action potential and repolarization properties of the myocyte, leading to potential rhythm disturbances.

Suspension of heart work can be achieved by any type of pharmacologic or electophysiologic intervention that inactivates the electrical and mechanical functions of the heart and leads to diastolic arrest. A number of different cardioplegic strategies have failed either due to irreversible toxicity, accumulation in the myocardium or narrow therapeutic range. Hyperkalemic cardioplegia, and in some instances, hypothermic arrest, are still the most popular methods of inducing cardiac arrest. The reason for the success of strategies such as electrolyte manipulation is probably because they are inexpensive, simple, promptly washed away upon intermittent perfusion, and effective. Increasing $[K^+]_o$ alters the E_m and slowly deactivates Na^+ channels at 25-30 mM in the human heart thereby inducing diastolic arrest. It has been shown that high $[K^+]_o$ when associated with Mg^{++}, low calcium and sodium and hypothermia allows the use of lower concentrations of potassium. Magnesium by itself may induce cardiac arrest at $[Mg^{++}]_o$ = 20-25 mM[151] by inactivating the Na^+ channel, and competitive inhibition of Ca^{++} flow and displacing Ca^{++} at intracellular binding sites[152]. Reduction of $[Na^+]_o$ and $[Ca^{++}]_o$ has been advocated by Bretschneider et al. as a cardioplegic strategy[153]. However, reducing only $[Na^+]_o$ produces an increase in myocardial tonus, and intracellular calcium overload through the Na^+/Ca^{++} exchanger[154].

2.1.4 Adrenergic and Cholinergic Regulation of the Heart

The autonomic nervous system is the main extrinsic modulator of cardiac function. It is divided functionally and anatomically in sympathetic and parasympathetic nervous systems. In general, sympathetic stimulation increases heart rate, conduction velocity and contractility, while augmentation of parasympathetic activity is inhibitory. The neurotransmitter released in preganglionic fibres in both systems is acetylcholine, whereas in post-ganglionic fibres of the sympathetic system norepinephrine is released, and in vagal (parasympathetic) innervation of the myocardium, acetylcholine is the mediator. Both neurotransmitters exert their actions through terminal nerve endings and have local effects (mainly on pacemaker cells and conduction fibres). Epinephrine is a cathecolamine released by the adrenal medulla, which will act as a hormone, directly on myocytes through the circulation.

For sympathetic and parasympathetic stimuli to exert their actions, their mediators must interact with receptors located in the sarcolemma of cardiac cells. Sympathetic receptors have been broadly divided in α and β and further subdivided into subclasses designated as $\alpha 1$ and $\alpha 2$; $\beta-1$ and $\beta-2$. Acetylcholine is released by parasympathetic nerve endings and interacts with muscarinic receptors.

The sympathetic and parasympathetic nervous systems interact in a dynamic and coordinated manner to regulate cardiac function. This interaction occurs centrally (through vasomotors regulatory centres in the brain medulla) and locally, at the level of the nerve terminals, pre- and post-junctionally[155]. In this section, the mechanisms and structures involved in autonomic regulation of the cardiac function relevant to the scope of this manuscript will be discussed. The focus will be on specific molecular structures of

the myocyte, mainly membrane receptors and important intracellular compounds which interact with these receptors when exerting modulation of cardiac function.

2.1.4.1. Adrenergic Receptors

Adrenergic receptors (AR - α-1, α-2, β-1, β-2) are membrane-bound proteins involved in many aspects of humoral and neural regulation of cardiovascular function. Myocardial rate and contractility, systemic and pulmonary vascular tone, blood pressure, platelet aggregation, and myocardial blood flow are all modulated by interaction of ARs with catecholamines or several classes of drugs. When occupied by agonists, these receptors couple to specific effector molecules via specific intermediary G proteins. Beta-1 and β–2 receptors couple to the stimulatory G protein (G_s), that activates the enzyme adenylyl cyclase, resulting in increases in intracellular cAMP. The α_2–AR inhibits adenylyl cyclase through coupling to the inhibitory G protein (Gi). The signal transduction pathway utilized by an occupied α_1–AR is mediated by a yet poorly characterized G protein and phospholipase C, which causes hydrolysis of inositol phospholipids and increases free cytosolic Ca^{++} inducing a metabolic or functional response in the cell.

Structurally, adrenergic receptors are integral membrane proteins that contain seven transmembrane domains that likely associate to form a "bundle" with a central "pocket" very similar to an ion channel[156]. Unlike an ion channel however, the pocket forms the binding site for the ligand and determines the ligand specificity for each receptor. Three extracellular and three intracellular loops followed by two carboxyl tails intra and extracellularly connect the transmembrane domains. All adrenergic receptors are single-subunit proteins and each of the seven transmembrane domains contain 20 to

28 hydrophobic amino acids. These domains are likely arranged as an α helix. The extracellular and intracellular loops contain more hydrophilic amino acids that can interact with the aqueous environment. The function of the extracellular domains is still unclear, however it is established that the second extracellular loop and the amino terminus tail are the sites for glycosylation, but their function in the receptor has yet to be established[157]. The cytoplasmic regions, especially loop III and the carboxyl tail, are important for receptor coupling to its G protein and contain sites important for regulation of receptor function.

2.1.4.1.1 Beta-adrenergic Receptors

Radio-ligand binding studies have revealed that the heart contains both types of receptors, β–1 and β–2. A third type of β receptor, β–3 has been identified but does not appear to exist in the human heart[158]. There are important interspecies differences relative to the distribution of β–receptors in the heart. In most mammalian hearts, left-ventricular β–receptors are predominantly (human, dog, rabbit, cat) or almost exclusively (rat, guinea pig) of the β–1 subtype. The β–1/β–2 ratio also varies topographically within the heart among different species[159]. These facts should be taken into account in the design of experiments and data interpretation. Studies using selective β–1 and β–2 agonists have suggested that the β–2 receptor exert more of a chronotropic effect whereas β–1 receptors would be related to inotropy[160]. Based on competitive agonist/antagonist binding studies, it has been postulated that the β–receptor cycles between high- and low-affinity states, these changes resulting in activation of adenylate cyclase[161]. The high-affinity state receptor-agonist complex would then bind a third component, a coupling regulatory

protein and then activate adenylyl cyclase, which at the same time would return the receptor to the low-affinity state and produce dissociation of the agonist-receptor complex.

Beta-adrenergic receptors are not static, but dynamic entities whose properties can change in response to physiologic stress, pathological states and drug administration. One of the easiest ways to assess this dynamic property is through membrane receptor-density studies. In a general way, receptor-density increases when stimulation is low (upregulation) and decreases when stimulation is high (downregulation).

2.1.4.1.1.1 Regulation of Beta-adrenergic Receptors

All adrenergic receptors are subject to dynamic regulation by a variety of mechanisms. The one that received the most attention from researchers is desensitization especially of the β-AR because of its clinical applications in congestive heart failure.

2.1.4.1.1.1.1 Desensitization

Desensitization is the general term given to the phenomenon whereby the intensity of response weakens over time despite the continued presence of a stimulus[162]. Two distinct patterns of hormone-induced desensitization have been described: homologous and heterologous desensitization. Homologous, also termed agonist-specific, desensitization occurs when the response is diminished to a specific agonist of the β–AR only. The functions of other receptors also coupled to the stimulation of adenylyl cyclase remain intact. Heterologous desensitization, or agonist non-specific desensitization, occurs when exposure to a β–AR agonist attenuates responsiveness to a number of agonists operating

through different receptors. Three distinct but interrelated mechanisms of desensitization have been described: receptor uncoupling, sequestration and down-regulation. Receptor uncoupling occurs within seconds to minutes of agonist exposure and results from modification of receptor protein by phosphorylation. Different protein kinases, specifically protein kinase A, protein kinase C and β–ARK have been proposed to play distinct roles in β–AR regulation and desensitization.

Protein kinase A (PKA). Phosphorylation by PKA has been implicated as a possible mechanism for heterologous desensitization because PKA inhibitors prevent heterologous desensitization activated via the β–AR system. Moreover, cyclic AMP analogues can induce both phosphorylation and heterologous desensitization. Substitution mutation of the β–AR that eliminates PKA phosphorylation sites results in a mutant receptor with impaired desensitization, suggesting that PKA-mediated phosphorylation plays an important physiological role in rapid agonist-induced desensitization in intact cells.

Protein kinase C, contrary to PKA, is cyclic-AMP independent. Phosphorylation of α_1–AR and β_2–AR may occur via both PKC and PKA. The site for PKA phosphorylation is present in the third cytoplasmatic loop of the α_1–AR. However, the site of PKC phosphorylation has not been identified in the α_1–AR. Phosphopeptide maps of trypsinized α_1–AR phosphorylated by each kinase differ significantly, suggesting that distinct regions of the receptor are phosphorylated by each kinase. Norepinephrine stimulation of the α_1–AR is capable of increasing the rate of phosphorylation of the receptor by PKC but not PKA. In contrast, isoproterenol agonist occupancy of β–AR

increases the rate of phosphorylation by PKA but not PKC. On the other hand, phosphopeptide maps of trypsinized β–AR phosphorylated by either PKA or PKC have similar profiles, suggesting the sites of phosphorylation are similar (if not the same) for these two kinases in the β–AR. However, the significance of PKC phosphorylation of β–AR is unclear.

The *β–adrenergic receptor kinase (β–ARK)*, described in 1986, is a cyclic AMP-independent kinase capable of phosphorylating the agonist occupied form of the β–AR. Initial reports suggested that β–ARK only phosphorylated the β–AR, but subsequent studies revealed that it may also phosphorylate α_2–ARs but not α_1-ARs. Phosphorylation by β–ARK leads to uncoupling of the β–AR from G_s. It has been suggested that β–ARK-mediated phosphorylation has an important physiological role in rapid agonist-induced desensitization in intact cells. The fact that β–ARK activity increases during the process of desensitization opens a potential pharmacological strategy for developing inhibitors or preventing transcription of β–AR. However, this approach may make an individual more susceptible to angina, ventricular arrhythmias and even sudden death due to the increased level of sympathetic activity in the CHF patient.

The possibility that ***β-arrestin*** may be important in desensitization of β–AR was first indicated by enhancement of β–ARK inactivation of the β–AR by the addition of its retinal cousin, arrestin in the cellular medium. In the eye, light dependent phosphorylation of serine and thereonine residues in the receptor carboxyl terminus by rhodopsin kinase enables rhodopsin to bind arrestin, thus preventing the interaction of rhodopsin with transducin. Recently, β–arrestin has been cloned and shown to be a 418-

amino-acid protein present mainly in the brain, heart and lung that appears to inhibit β–AR signal transduction significantly in an agonist-dependent fashion.

During congestive heart disease the levels of noradrenaline are high and the number and responsiveness of β–AR are reduced. However, the exact physiological roles of each of the receptor kinases involved in this process have yet to be established. Agonist-specific phosphorylation by β–ARK is important in homologous desensitization, whereas non-agonist-specific phosphorylation by PKA seems important in heterologous desensitization. In the non-failing heart, at low agonist concentrations such as might occur in the physiological response to catecholamines during exercise or stress, sufficient activation of adenylyl cyclase occurs to produce increased levels of cyclic AMP and thus phosphorylation of all β–ARs via PKA. At high agonist concentrations, such as in congestive heart failure, a larger proportion of the receptors is occupied, each being phosphorylated by β–ARK as well as by PKA. It is tempting to speculate that PKA may be involved in the desensitization process in peripheral regions of the body where relatively small concentrations of noradrenaline are present and that, along the same lines, β–ARK may be involved in the desensitization process at nerve synapses, where relatively high concentrations of noradrenaline abound in the cleft.

2.1.4.1.1.1.2 Sequestration

One of the fates of the β–AR during the process of desensitization is to be internalized, moved away from the cell surface into membrane compartments. Strong suggestions have come from reports of loss of receptors from the plasma membrane and association with an increase in binding activity in the cell cytosol. Further localization of these

cytosolic β–AR and evidence that these particles were devoid of adenylyl cyclase activity and G_s, in addition to the development of a more hydrophobic β–AR antagonists that would penetrate into the cell and label internalized receptors, provided evidence for sequestration. The mechanism(s) through which the β–AR is sequestered from the plasma membrane is not known. Two key questions that have been asked and await definite response are whether phosphorylation and/or G_s-protein-uncoupling (or both) are processes required for sequestration. Inhibitors of sequestration and inhibitors of β–ARK and PKA phosphorylation were tested in the presence of high agonist concentration, and the two kinase inhibitors did not substantially inhibit sequestration either alone or in combination. The technique of substitution mutation of phosphorylating sites in the β–AR also did not affect sequestration. Taken together, these studies suggest that at least the early phase of homologous desensitization and sequestration are entirely different processes and that phosphorylation is not required for sequestration. The other important issue is if uncoupling (physical removal of the receptor from its G protein) is part of the sequestration process. Studies with a line of cells lacking functional G_s (*cyc*$^-$ cells, a variant line of S49 lymphoma cells) and deletion and substitution of a portion of the β–AR have resulted in mutant β–ARs that sequester normally suggesting that G_s is not required for sequestration[133]. Despite the intense controversy, the process of sequestration has been considered well-described and there appears to be a consensus that G-protein uncoupling is not required for sequestration. However, a great deal of research has been dedicated to this area, mainly to shed some light on the role of sequestration in the overall process of desensitization, which remains unclear.

2.1.4.1.1.1.3 Down-regulation

When receptors cannot be detected in any cell portion by any radioligand, the process is defined as down-regulation and reflects actual loss of receptors. In this intriguing process, some β–AR appear to be proteolytically degraded and resynthesized, whereas others remain undetected for a period of time and then return to control levels, suggesting that down-regulated receptors can regain their binding activity with time. Initially it was thought that activation of adenylyl cyclase was required for down-regulation, but this was proven not true once down-regulation was demonstrated in cells lacking adenylyl cyclase or cells lacking the ability to couple to adenylyl cyclase (*cyc*$^-$ cells). Instead, it has been suggested that mechanisms such as reduced levels of β–2–mRNA are present, indicating decreased β–2–AR synthesis and/or increased β–2–AR degradation. Recent data involving measurements of β–mRNA transcription rates and mutant β_2 –ARs which lack the PKA sites have found that decreased levels of β–mRNA as well as phosphorylation of the β–AR are involved in the process of down-regulation. Receptor degradation may also play a potentially important role and seems to be enhanced by receptor phosphorylation by PKA because β–AR may also be phosphorylated in a cyclic AMP- independent manner. The logical sequence of events would then be that after exposure to an agonist, simultaneous disappearance of the receptor (from either sequestration or degradation) offsets synthesis of a new β–AR. Questions such as whether PKA is also involved in the reduction of β–mRNA levels remain unanswered.

2.1.4.1.2 Effects via Adenylyl Cyclase

Adenylate cyclase is an integral part of the hormone-regulated complex located in the sarcolemma of myocardial cells and acts as a catalytic unit for the conversion of ATP to cyclic AMP[163]. This complex is comprised of 3 major units: the beta-receptor, the catalytic enzyme adenylyl cyclase and a guanine nucleotide binding protein (G protein), which couples the receptor to the catalytic unit. It has been established that adenylyl cyclase can be regulated both in a stimulatory and in an inhibitory manner. Beta- and α1–adrenergic stimulation will increase adenylyl cyclase activity whereas α2– and muscarinic stimulation will inhibit this activity[164]. Experimental evidence has been accumulated in recent years indicating that these effects are mediated by the G proteins[165].

2.1.4.1.3 Guanine Nucleotide Binding Protein (G proteins)

Many types of heterotrimeric G proteins (over 20) have been described[166]. At least 3 major classes have been identified in the myocardium[167]. G_s (stimulatory) mediates the effects of stimulatory receptors, whereas G_i mediates inhibitory stimuli and G_o (for other or unknown function) may be involved in mediating receptor modulation of inositol-containing phospholipid hydrolysis.

Structurally, all G proteins seem to be heterotrimetric proteins composed of 3 subunits, α, β and γ. Differences between the three types of G proteins seem to reside in the α subunit of each type. The α subunit of G_s ($G_s\alpha$) has a molecular weight of 45 kDa whereas $G_i\alpha$ is a 41 kDa protein and $G_o\alpha$ has a molecular weight of 35 kDa. The β and γ subunits have molecular weights of 35 kDa and 8-10 kDa, respectively and appear tightly coupled together in a so-called $\beta\gamma$ complex. Toxins such as the cholera toxin and

the pertussis toxin act (via ADP rybosylation) on different but specific sites on these proteins, which may also serve as a criterion of differentiation. The $G_s\alpha$ subunit in the presence of the cholera toxin is rybosylated at a specific arginine residue, whereas the $G_i\alpha$ and the $G_o\alpha$ are ribosylated at asparagine residues by one of the pertussis toxins. ADP rybosylation of $G_s\alpha$ by cholera toxin results in inhibition of the GTPase activity and a reduction in the affinity of α_s for $\beta\gamma$, thus resulting in persistent activation of adenylate cyclase activity. The effect of ADP ribosylation of G_i via the pertussis toxin is an increased affinity of α_i for $\beta\gamma$ promoting their reassociation, and the consequential abolition of the effects of inhibitory receptor stimulation on adenylate cyclase[168].

A hypothetical cyclical mechanism has been proposed for the functional aspect of the G proteins[169]. The beta-agonist receptor complex binds to α_s and is associated with displacement of GDP by GTP from the guanine nucleotide binding site. The binding of GTP to α_s promotes the dissociation of α_s from $\beta\gamma$. This activation results in the stimulation of the catalytic activity of adenylate cyclase. The nucleotide binding site possesses intrinsic GTPase activity, which in the presence of the agonist-receptor complex results in the hydrolysis of the bound GTP to GDP and a reduction of the stimulatory effect of α_s on the catalyst. The complex α_s-GDP has a higher affinity for $\beta\gamma$, resulting in the reassociation of the heterotrimer. In a similar manner, binding of an appropriate agonist on inhibitory receptors results in the dissociation of α_i from $\beta\gamma$. The complex appears to mediate inhibition of andenylate cyclase activity, presumably by association with α_s to form the inactive heterotrimer[170]. It is yet unknown if direct interaction occurs of α_i with adenylyl cyclase.

In cardiac membranes, guanine nucleotides have intrinsic enzyme activity, and can stimulate or inhibit activity of adenyl cyclase in both ways. Cathecolamines do not stimulate the enzyme unless guanine nucleotides are present. Muscarinic stimulation takes place only in presence of GTP and if non-hydrolizable analogues are used, muscarinic inhibition of the enzyme does not occur. In the cardiac muscle sarcolemma then, both stimulatory (β–adrenergic) and inhibitory (muscarinic) mechanisms co-exist, activated by their specific agonist, and resulting in increased or reduced activity of adenylyl cyclase which in turn results in higher or lower levels of one of the main so-called second messengers, cAMP. Increase in cAMP will produce and augment activation of cAMP-dependent protein kinases, which will phosphorylate a number of intracellular proteins, including pumps, ion channels and contractile proteins. Intracellular cAMP levels are controlled by the activity of two enzymes: adenylate cyclase and phosphodiesterase. Phosphodiesterase transform cAMP in 5'-AMP, but there has been experimental evidence that autonomic stimulation may alter phosphodiesterase activity directly. The new non-catecholamine positive inotropic agent (amrinone) produces at least part of its positive inotropic effect via inhibition of phosphodiesterase and thereby increasing the levels of cAMP.

2.1.4.1.4 c-AMP mediated Protein Phosphorylation

Various cytosolic and intrinsic membrane proteins in cardiac muscle have been shown *in vitro* to serve as substrates for cAMP-dependent protein kinase. The specific functional responses are determined by the proteins phosphorylated and their intracellular location. Three broad classes of intracellular proteins are thought to be subjected to the actions of

phosphorylation and, via this process, play a major role in regulation of cardiac contractility. These include the regulatory contractile subunit I of troponin (TnI) and protein C. The other classes are membrane-bound sarcolemmal and sarcoplasmatic proteins, such as Ca^{++} channels, Ca^{++} pumps and phospholamban.

2.1.4.1.4.1 Contractile proteins

In vitro studies have shown that cAMP-dependent phosphorylation of TnI results in reduced Ca^{++} sensitivity of actomyosin ATPase activity[171], which is mediated by an increase in the rate of Ca^{++} dissociation from the Ca^{++} specific binding site of troponin C (TnC). It appears that phosphorylation of TnI may be thus involved in relaxation of the sarcomere, but the presence or the extent to which TnI phosphorylation is involved in interactions with the other regulatory mechanisms of relaxation remains to be established.

Protein C is a 155-165 kDa protein that is associated with the thick filament of striated muscle. Its exact function has not been fully defined, however it has been demonstrated that the protein C undergoes phosphorylation upon beta-adrenergic stimulation in the mammalian myocardium, which was correlated to the positive inotropic effect of catecholamines[172]. Protein C is a substrate for cAMP-dependent protein kinase as well as calcium-calmodulin dependent protein kinase and it has been shown that phosphorylation by cAMP-dependent protein kinase attenuates the stimulation of actin-activated myosin ATPase activity by C protein[173]. Some controversy remains regarding the physiological role of phosphorylation of protein C since it had been speculated that it might affect relaxation by altering the interaction between actin and myosin, however it

has been shown recently that beta-adrenergic stimulation results in increased activity of actin-activated ATPase in intact myocardial preparations[174].

2.1.4.1.4.2 Sarcoplasmic Reticulum Proteins

A major substrate for cAMP-dependent protein kinase has been shown to be the 22 KDa protein phospholamban in *in vitro* studies; it also has been demonstrated that it regulates Ca^{++} transport activity of the sarcoplasmatic reticulum. Studies have shown that addition of cAMP to SR membranes in the presence or absence of cAMP-dependent protein kinase resulted in increased activation of Ca^{++} ATPase[175]. Phospholamban is a homopentameric protein, composed of five identical monomers, each containing specific phosphorylation sites for cAMP-dependent and Ca^{++}/calmodulin-dependent protein kinase activities[176]. It has been shown that monoclonal antibodies to phospholamban inhibit cAMP-dependent stimulation of Ca^{++} transport *in vitro*, and that the purified phospholamban forms Ca^{++} channels in planar (reconstituted) lipid bilayers[177]. Phosphorylation of phospholamban can rapidly occur in intact hearts and is a highly sensitive mechanism requiring minute amounts of β–adrenergic agonist[178]. Phospholamban is target to cAMP-dependent protein kinase as well as to calcium-calmodulin protein kinase. Beta-adrenergic stimulation promotes phosphorylation by both protein kinases in their specific sites in the phospholamban molecule and in a sequential manner (cAMP-dependent protein kinase first), suggesting and interdependence of site phosphorylation by the two enzymes[179].

The activity of the SR Ca^{++} release channels (or ryanodine receptors, RyR) is modulated by calmodulin and Ca^{++}/calmodulin protein kinase[180]. Millimolar

concentrations of calmodulin inhibit Ca^{++} release from the SR of cardiac and skeletal muscle and it partially reduces single-channel open-time without affecting conductance[181]. Recent reports have suggested however that the role of calmodulin is more complex, and is concentration dependent. At concentrations prevalent in relaxed muscle, calmodulin increases the open probability of the RyR channel and SR Ca^{++} release by several fold, whereas at higher Ca^{++} concentrations (i.e., during systole), it has the opposite effect[182]. In addition to its direct effect, calmodulin can also alter function of the RyR via Ca^{++}/calmodulin protein kinase. Conflicting data have been reported[183,184,185], which may be related to the site of phosphorylation and/or to the ionic concentrations used in the experiments[186]

2.1.4.1.4.3 Sarcolemmal proteins

Beta-adrenergic stimulation modulates several sarcolemmal ionic currents (including Ca^{++}, Na^+, K^+, and Cl^-), through $G_s\alpha$ proteins acting directly on the channel or indirectly, through cAMP-dependent protein phosphorylation. The most direct evidence of cAMP-dependent protein phosphorylation in mediating beta-adrenergic stimulation was obtained from studies measuring increases in I_{Ca} in ventricular myocytes following β–stimulation[187]. *In vitro* studies, using purified sarcolemmal preparations have revealed a number of substrates for cAMP-dependent protein kinase. Which of these substrates is activated during beta-stimulation has not been established. The predominant sarcolemmal substrate has been shown to be a 15 kDa peptide called *phospholemman* which has not been identified in L-type Ca^{++} channels[188]. Inoculation of phospholemman

mRNA in *Xenopus oocytes* results in expression of a Cl^- selective current that differs from other reported cardiac Cl^- currents and is insensitive to Ca^{++}[189].

2.1.4.1.5 States in disease

The β–receptor is a dynamic structure and its pharmacological and molecular characteristics are altered in pathological situations. As a result of the complexity and variety of regulatory mechanisms, species differences, lack of accurate experimental models, technical difficulties, (...) , and also due to the fact that the understanding of all these processes is far from complete, the literature is full of conflicting data. Some facts where there seems to be agreement, and speculative considerations on the underlying mechanisms will be outlined regarding the major changes that occur in β–receptor activity during cardiac failure, ischemia and hypertension.

2.1.4.1.5.1 Cardiac failure

Many investigators have reported that the number and/or affinity of beta receptors to agonists in the failing heart is decreased or reduced through a variety of mechanisms, some of which were described above. Plasma norepinephrine levels are used as an index of sympathetic activity and are often inversely correlated with the severity of heart failure. Clinically, high levels of norepinephrine tend to be interpreted as poor prognosis[190,191,192]. It is assumed that the increase of cathecolamines in plasma is due to norepinephrine spillover from organs subjected to a high sympathetic drive and/or to a decrease in neuronal uptake of norepinephrine[193]. It is accepted that cardiac stores of norepinephrine

are depleted at least partly, whereas plasma norepinephrine levels are elevated. Although this type of determination may be useful as an indicator, interpretation should be cautious since the levels of norepinephrine in mixed venous blood may not accurately reflect neuronal cathecolamine release [164]. Thus an enhanced local release of endogenous norepinephrine from the heart and a simultaneous decrease in cardiac neuronal uptake of norepinephrine may lead to increases in synaptic cleft norepinephrine concentrations that will produce down-regulation of cardiac β–receptors.

Beta–1 and β–2 receptors change in different manners in different forms of heart failure. These changes vary not only according to the subtype of receptor, but also differ topographically in the heart. The literature reveals a great deal of controversy regarding many aspects of receptor distribution during CHF. The pathophysiological mechanisms underlying the differential changes are not understood and a general rule or consensus has not yet been achieved. Studies have shown that in end-stage dilated cardiomyopathy β–1 receptors are down-regulated whereas β–2 receptors are only marginally affected[194]. In a recent study using a canine model of tachypacing failure the authors report positive inotropic responses mediated by functional β–2 receptors that are not mediated by increases in cAMP or cAMP-dependent phosphorylation of phospholamban[195]. Regarding etiology of the cardiomyopathy, conflicting results have been reported. Some studies describe a decrease in β–1 receptor levels and no change in β–2 receptors in patients with aortic valve disease [164]. A recent study in patients with aortic disease but preserved LV systolic function and normal plasma cathecolamine levels, showed that chronic LV overload induces a selective down-regulation of β–1 AR that is compensated by an increase in β–2 receptors[196]. These data were acquired in hypertrophic patients

prior to deterioration of LV function and vary according to volume or pressure overload (i.e., valvular stenosis or insufficiency). In patients with mitral valve disease, tetralogy of Fallot and in patients with end-stage ischemic cardiomyopathy a decrease is reported in β–1 and β–2 receptors [164].

There seems to a be a consensus that β–1 receptor function decreases in all types of heart failure. There is also evidence suggesting that β–2 AR function decreases or remains unchanged depending on the etiology of the heart failure. A recent report evaluated the response to isoproterenol and forskolin in adult spontaneous hypertensive rats (SHR) and in Wistar rats, and did not associate the depressed inotropic responsiveness to β-adrenergic stimulation with down-regulation of β-receptors. Instead, the impaired inotropic and intact lusitropic responses were attributed to "downstream" events found in this SHR model with chronic left ventricular hypertrophy and failure. The authors describe "downstream" events as cellular defects distal to cAMP production such as abnormalities in calcium handling or sensitivity of the contractile proteins to calcium or even diminished calcium release from the sarcoplasmatic reticulum[197].

2.1.4.1.5.2 Ischemia

The data on β–receptor changes during ischemia have been gained almost exclusively from experimental studies and the results bear the bias of species differences, technical difficulties and assumptions. From experiments on dogs, evidence gathered suggests an increase in the number of β–receptors in the ischemic zone following 1 to 8 hours of acute ischemia[198]. Evidence indicates that progressive damage to the sarcolemma and organelle membranes is a key factor in the evolution of irreversible injury[199]. The

functional consequences of altered membrane function involve (a) altered flux of sodium, potassium, chloride and water, leading to cell swelling; and (b) net influx of calcium, leading to toxic effects of this ion. Several mechanisms are involved in the pathogenesis of membrane injury[200]. Progressive membrane phospholipid degradation occurs as a result of activation of phospholipase(s) and leads to accumulation of free fatty acids and arachidonic acid, which is fueled by impaired mitochondrial oxidation, further altering membrane fluidity and permeability[201,202]. Damage to the cytoskeleton, peroxidation of membrane lipids by free radicals produced by myocytes, endothelium and invading leukocytes, further destabilizes the membrane and predisposes it to rupture as the final event[203,204]. This progression is influenced at least in part by the adrenergic nervous system. Acute coronary occlusion is followed by an increase in the population of membrane-associated beta- and alpha-adrenergic receptors and also results in an increase in the release of norepinephrine from nerve endings[205]. These processes in association with the previously described electrolytes alterations can contribute to the progression of ischemic injury and the genesis of ventricular arrhythmias[206].

2.1.4.1.5.3 Hypertension

The data on β–receptor changes in the myocardium of hypertensive patients are conflicting and differ according to the model of hypertension studied. Reports of no change, increases and decreases in numbers and/or ligand affinity or response have been published[207]. Simpson and colleagues in earlier studies have advocated that the major changes occur with α–adrenergic receptors and reported α1–mediated hypertrophy in rat isolated myocytes[208,209,210].

2.1.4.1.6 Alpha-adrenergic Receptors

The presence of α–adrenergic receptors in the myocardium has been demonstrated in many laboratories, mainly by radioligand binding studies from which it is now evident that α–stimulation can result in significant effects on the myocardium[211,212]. However, the magnitude of contractile response is small relative to those produced by beta-stimulation. In the myocardium, there is a predominance of the α–1 subtype although studies in other tissues have revealed a large variety of α–1 receptors, including $\alpha 1_a$, $\alpha 1_b$, $\alpha 1_c$ and $\alpha 1_d$ subtypes. There is also evidence that receptors are linked to G proteins, however different subtypes are not linked to the same effector mechanisms[213].

The positive inotropic effects elicited by alpha-adrenergic stimulation are associated with increases in transarcolemmal Ca^{++} influx, however an increase in I_{Ca} has not been documented in isolated myocytes by patch-clamp or whole cell recording[214]. Nevertheless, specific Ca^{++} channel blockers antagonize the positive inotropic effects without altering α-agonist binding, suggesting that alpha-stimulation enhances voltage-dependent Ca^{++} influx via mechanisms other than a direct effect on Ca^{++} channels, possibly mobilizing Ca^{++} from intracellular stores[215].

Alpha-adrenergic stimulation has been shown to alter several K^+ currents. It inhibits I_{to} (and therefore prolongs the action-potential duration and causes an increase in Ca^{++} transient), reduces I_{K1}[216], and stimulates the Na^+/K^+ pump current[217].

2.1.4.1.6.1 Effects Via G Proteins

The predominant physiological effect of α–adrenergic receptors are attenuated or abolished by pretreatment with pertussin toxin, suggesting that the receptor binds G proteins. Reports on guanine nucleotide effects have suggested this receptor is coupled to adenylate cyclase via G_i, and therefore inhibiting the catalytic activity of the enzyme. Thus, there are two ways by which α–stimulation can reduce cAMP levels: via inhibition of adenylate cyclase and also by enhancing phosphodiesterase activation[218]. The negative chronotropic effects of α–stimulation in canine Purkinje fibres and neonatal ventricular rat myocytes are associated with a 41 kDa pertussis toxin substrate, and absence of this substrate or pretreatment with pertussis toxin results in a positive inotropic response to α–stimulation, similar to muscarinic cholinergic stimulation[219]. On the other hand, other actions elicited via the α–adrenergic receptor such as activation of phosphoinositol hydrolysis, are not altered by pertussin toxin[220]. This variability of response suggests that multiple G proteins may be involved in mediating these effects and that different G proteins may be linked to specific alpha-receptor subtypes[221].

2.1.4.1.6.2 Effects Via Phosphoinositol Hydrolysis

There has been evidence from a number of cell types that alpha-adrenergic effects are mediated by hydrolysis of inositol-containing phospholipids. It has been proposed that α–agonist binding stimulates phosphodiesteric (via phospholipase C) hydrolysis of phosphatidylinositol 4,5-biphosphate, resulting in the formation of 1,2-diacylglycerol (DAG) and inositol 1,4,5-triphosphate (IP_3), compounds which have been shown to function as second messengers. DAG stimulates the activity of protein kinase C, which will result in several protein phosphorylations and IP_3 results in mobilization of

intracellular Ca^{++}[222]. Recent studies have suggested that the rapid formation of IP_3 is associated with the transient positive inotropic effect of α stimulation in papillary muscle, which is not affected by nifedipine, suggesting that IP_3 mobilizes Ca^{++} from intracellular stores. It seems that IP_3 can stimulate Ca^{++} release from the SR; however this effect seems to be rather small, it is not known if it is sufficient to mediate the functional effects of alpha-stimulation[223].

2.1.4.1.6.3 Changes in Pathological States

There is relatively less information about the behavior of α–receptors in the diseased heart, than there is on β–receptors. Early studies have revealed an increase in the number of α–receptors in the ischemic or hypoxic myocardium; and more recently, these findings have been reported in rats following coronary artery occlusion at moderate and severe stages of congestive heart failure[182]. Other reports describe unchanged or reduced response following agonist stimulation[164].

A recent report studied α_2–receptors located in the presynaptic nerve terminals in the heart rather than focusing on the α–receptors located in the myocytes. These receptors are known to inhibit the release of norepinephrine (NE) from these terminals. The study demonstrated that not only is NE elevated in congestive heart failure patients, but when an α–blocker is given, the levels of NE increase further, resulting in a significant positive inotropic effect not seen in patients with normal ventricular function. The authors used a non-specific α–receptor blocker, phentolamine, injected into the

coronary vessels of patients undergoing routine diagnostic coronary angiography. Phentolamine not only produced increased contractility in patients with congestive heart failure, but also induced an increase in coronary sinus NE concentration without any change in arterial NE levels. It was proposed that NE released by neurons stimulates inhibitory presynaptic α_2–adrenergic receptors, resulting in a local feedback mechanism, that limits further release of norepinephrine. Phentolamine, by blocking presynaptic α_2–adrenergic receptors, interrupts this mechanism, producing a further increase in cardiac neuronal release of NE, which was measured as an increase in the concentration of norepinephrine in the coronary sinus blood. This study has raised important questions regarding the mechanism proposed, e.g., how the increase in NE levels acts in a desensitized β–receptor-adenylyl cyclase system, as well as the long term risks of a high adrenergic drive treatment in these patients[224].

2.1.4.2 Cholinergic Receptors

Parasympathetic regulation differs from sympathetic in that there is much more variability in response of different cardiac tissue to parasympathetic than to sympathetic stimulation. All tissues of the heart seem to have similar responses to beta-stimulation whereas ventricular tissue is much less responsive to cholinergic stimulation than atrial tissue. Choline esters are potent in reducing heart rate and exert powerful negative inotropism in atrial tissue, whereas they produce minimal inotropic and electrophysiologic effects on isolated ventricular tissues, in the absence of sympathetic stimulation. Because of the relatively small effects of muscarinic agonists in ventricular tissues, the muscarinic antiadrenergic effect is pronounced relative to the effect seen with muscarinic agonists

alone. This magnification of muscarinic effect during simultaneous sympathetic stimulation is termed *accentuated antagonism.* These differences in responses suggest that multiple subcellular mechanisms mediate the cardiac effects of muscarinic stimulation, and only some of these subcellular mechanisms are shared by atrial and ventricular tissues.

2.1.4.2.1 Muscarinic Receptors

The differences in atrial and ventricular responses cannot be explained by topographical distribution differences among the different regions of the heart. Radioligand binding assays have demonstrated that muscarinic receptors exist in both atria and ventricles, with ventricular density at least similar to atria density. It also appears that in most species, the majority of these receptors are M2 receptors with exception of the chick heart, which are M1[225].

Binding assays have also revealed that the interaction of agonists with muscarinic receptors is much more complex than that of antagonists, suggesting that the receptors exist in multiple states in terms of their interaction with agonists. The analysis of the curves relating the occupancy of muscarinic receptors with agonist concentration suggest that the same binding sites that interact with antagonists in a uniform manner interact with agonists heterogeneously, and differ markedly from the simple mass-action relationship. At least two binding sites (high and low affinity) have been described in several organs, including heart, and they seem interconvertible.

The interaction of guanine nucieotides, presumably via G proteins, with muscarinic receptors might be a mechanism for coupling the receptor to intracellular effectors. In recent studies, muscarinic receptors purified from brain have been reconstituted with G_o or G_i in phospholipid vesicles[226].

2.1.4.2.1.1 Effects on Ion Channels

The electrophysiologic and inotropic effects of muscarinic activation in mammalian atrial myocytes appear to be mediated predominantly by alterations in the outward K^+ current (I_K) and the inward Ca^{++} current (I_{Ca}). In atrial tissues, increases in I_K result in earlier repolarization of the membrane, shortening of the action potential duration and decreases in contractility. Parallel effects on I_K and I_{Ca} have been noted (increase in I_K and decrease in I_{Ca}) with increasing concentrations of acetylcholine, but the effect on I_{Ca} was not reproducible in isolated ventricular myocytes. Thus, these effects on I_{Ca} and I_K appear to be concentration dependent, at least in atrial myocytes[227].

Studies using the pertussis toxin as a marker of G protein binding have brought several lines of evidence suggesting that G proteins (presumably G_i) can directly activate K^+ channels or act through its subunits. This activation did not require ATP or free GTP, suggesting that intracellular second messengers or protein phosphorylation do not mediate these effects. These studies provide strong evidence for direct activation of myocardial K^+ channels (K_{Ach}) by activated G proteins or its subunits[228,229].

2.1.4.2.1.2 Effects via Cyclic GMP

It was first shown that cyclic-GMP (cGMP) levels in cardiac tissue could be elevated by activation of muscarinic receptors[230]. This original observation of muscarinic-induced increases in cGMP levels in cardiac tissues was confirmed and extended by subsequent studies in hearts from a variety of species; whether this muscarinic-induced elevation of cGMP has any physiologic role remained controversial[231]. It was concluded that cGMP seems to mimic the effect of acetylcholine on action potential configuration and alters contractility in rat atrial myocytes; it was also suggested that it was capable of antagonizing the electrophysiologic, inotropic and metabolic actions of beta agonists[232]. Nevertheless, if cGMP is involved in mediating some of the effects of muscarinic-receptor stimulation in the heart, the biochemical mechanism(s) by which this occurs remains unknown. It is hypothesized that, analogous to the cAMP-dependent protein kinase system, cGMP interacts with a specific protein kinase, which in turn phosphorylates substrates and alters protein function. There are only a few possible mechanisms: either cGMP, after alteration of its level due to muscarinic stimulation, could modify protein function and physiology of the heart; or cGMP and its intracellular effectors could be compartmentalized; or yet cGMP does not mimic choline esters.

Two enzymes regulate cyclic GMP: guanylate cyclase and cGMP phosphodiesterase. Guanylate cyclase occurs in two forms: as membrane-bound and cytoplasmic enzymes in cardiac tissues. Sodium nitroprusside is known to stimulate only the soluble enzyme, providing support for the notion of different cellular pools of cGMP that can be selectively modified by certain agents. It has also been suggested that Ca^{++} may play a role as an intermediary between the muscarinic receptor and cGMP, however other studies have shown Ca^{++} inhibition of guanylate cyclase. Although Ca^{++} is required

for muscarinic-induced increases in cGMP levels, the physiological response to muscarinic stimulation is either no change or a decrease in contractile state, without a generalized increase in intracellular Ca^{++} concentration. If activation of muscarinic receptors leads to Ca^{++} mobilization, this must happen in localized pools, because contractile proteins do not appear to be affected[233].

2.1.4.2.1.3 Effects via Phosphatidyl-inositol Hydrolysis

The administration of muscarinic agonists to intact myocardial preparations results in stimulation of phosphatidyl-inositol hydrolysis[120,166]. Several studies have linked muscarinic stimulation and phosphatidyl-inositol hydrolysis either via radioactive (^{32}P and $[^3H]$-inositol) or quantification of accumulation of inositol phosphates. However, oxotremorine, a complete muscarinic agonist (as per inhibition of adenylyl cyclase and negative chronotropic effects) produces only submaximal formation of inositol phosphates[234]. The functional significance of phosphatidyl-inositol hydrolysis remains to be established.

2.1.4.2.1.4 Muscarinic Inhibition of Adenylyl Cyclase and cAMP

Muscarinic inhibition of adenylyl cyclase was first shown in preparations of canine myocardium in which carbachol inhibited both basal and epinephrine-stimulated adenylyl cyclase activity[235]. Evidence now exists that muscarinic receptors are coupled to adenylyl cyclase via a G_i regulatory protein. An additional potential mechanism for a muscarinic decrease in cAMP levels is stimulation of cAMP phosphodiesterase activity, but limited

data are available and studies examining this possibility in intact cells have yielded conflicting results[236].

Acetylcholine reverses epinephrine-induced phosphorylation of TnI[237]. Acetylcholine also attenuated the incorporation of ^{32}P into phospholamban induced by isoproterenol while antagonizing the intropic effects of the catecholamines[238]. Thus, muscarinic agonists can antagonize catecholamine-induced phosphorylation of myocardial cell proteins, which may be involved in mediating the positive inotropic effects of catecholamines. It is not likely that this attenuation in protein phosphorylation (and therefore in cAMP levels), can be entirely the result of muscarinic stimulation only. The hypothesis of phosphatase activation seems plausible but no study has addressed this question specifically.

2.2 Beta-adrenergic Receptor Blocking Drugs

Beta-blockers have several clinical indications in a variety of specialties, presumably due to the widespread distribution of β–receptors in the human body. In cardiology, beta-adrenergic antagonism is used mainly in the management of angina pectoris, hypertension, myocardial infarction, arrhythmia, and also has a potential role in the treatment of congestive heart failure. Since the introduction of propranolol, almost 30 years ago, beta-blockers have demonstrated the most consistent beneficial effect on sudden death and cardiac mortality in a wide range of cardiovascular diseases. New agents still continue to be studied and introduced into clinical practice.

There are several beta-blockers and a pharmacological discussion on all types of agents available today is beyond the scope of this manuscript. Instead, a dissertation on

general pharmacological characteristics common to all beta-blockers with focus on their applications in cardiology will be given. The characteristics and use of esmolol will be emphasized in separate section.

2.2.1 Classification of β–adrenergic Blocking Agents

In 1948 Ahlquist first suggested that there were two "distinct types of adrenotropic receptors" based on physiological parameters which defined their relative responsiveness to a series of sympathomimetic amines. The α–adrenergic receptor was characterized by its preferences to epinephrine relatively to norepinephrine and isoproterenol. The β–receptor, in its turn, was more selective for isoproterenol than for epinephrine and norepinephrine[239]. In 1967 evidence based on the relative affinity of β–receptors to epinephrine and norepinephrine produced a further subclassification into β–1 and β–2 subtypes[240]. The β–1 receptors that were found in mammalian cardiac and adipose tissue displayed approximately equal affinities for epinephrine and norepinephrine, whereas the β–2 subtype, found in trachea and vascular smooth muscle, had considerably higher affinity for epinephrine than for norepinephrine. The implicit concept of receptor subtype homogeneity within organs subsisted until 1972, when pharmacological evidence of the existence of functional β–1 and β–2 receptors was presented in experiments performed in the cat heart[241]. The β–3 subtype has now been identified, isolated and expressed in Chinese hamster ovary cell line[242]. Norepinephrine is still the most potent agonist, however propranolol seems to have little antagonistic effect. It has been suggested that the β–3 receptors can mediate vasodilation in dogs, but the human β–3–receptor seems to

respond differently than other species studied (rats, mice, dogs and cats), and its function in the heart has not been established[243].

Blocking agents have then been classified as "β–1–selective" or "β–inespecific" (a slightly inappropriate use of the term, since specificity implies mainly that the β–blocking agent does not interfere with the actions of other agonists such as histamine or acetylcholine). Most of the antagonism mediated by β–blockers is through competitive binding and the concept of selectivity towards one subtype or the other became popular in clinical practice. Agents with higher affinity for β–1–receptors became 'cardiac-specific', and this selectivity is still expressed as β–1/β–2 ratios, as it became clear that 'β–1–selectivity' was dose-dependent. Beta-1 blocking agents can produce bronchospasm in clinical practice, but the relative lack of β–2 activity allows reversal by selective β–2–agonism. Esmolol is considered a highly selective β–1–blocking agent with a β–1/β–2 ratio of 35.

Great effort has been directed towards the development of beta-blockers with less effect on heart rate and cardiac output (which can be achieved by a property described as *partial agonism (PA) or intrinsic sympathomimetic activity*); and drugs that can produce vascular smooth muscle relaxation (either via β–2–induced relaxation, α–blockade or some non-adrenoceptor mediated inhibition of vascular smooth muscle tone). Beta-blockers then began being classified according to potency, tolerability, and hypotensive effects somewhat apart from pure specificity, affinity or selectivity. Esmolol and acebutolol are examples of β–1–selective β–blockers that act as partial agonists, whereas pindolol, carteolol and penbutolol also present PA but are non-selective. Nadolol, timolol

and propranolol are non-selective agents that lack PA and labetalol and carvedilol are examples of non-selective agents with vasodilating properties[244].

2.2.2 Cardiovascular Effects of β–blockade

The main determinants of the net hemodynamic effects of beta-blockers can be summarized as (i) the level of sympathetic stimulation prior to β–blockade; (ii) the speed of onset of β–blockade; (iii) the underlying type and degree of cardiac disorder; (iv) and the pharmacologic profile of the β–blocking agent, such as PA, β–1–selectivity or vasorelaxant effects. Classically, the reference agent Propranolol in normal subjects at rest at doses in 0.17mg/kg i.v. will produce a 20% reduction in heart rate and cardiac output, a reduction of mean arterial pressure of 15% a 34% reduction in the LV stroke minute work. A 6% decrease in oxygen consumption, a 12% increase in A-V O_2 difference and a small rise in venous pressure[215] may also accompany these effects. Clinically, these are much more remarkable when measured as reversal of the effects of sympathomimetic drugs or exercise, due to the competitive antagonistic mechanism of action of the beta-blockers.

2.2.2.1 Effects on Heart Rate

Small bolus i.v. administration of β–blockers can reduce the average resting heart rate by 10-12 beats/minute, however heart rate is a misleading parameter by which to assess beta-blockade in chronic therapy, since the net effect on the heart rate is, during beta-blockade, much more dependent of the amount of endogenous resting vagal tone. Beta-blockers (propranolol) affect not only the discharge rate of the SA node but also reduce the

conduction speed of the impulse. Agents such as pindolol or xamoterol which possess PA, produce no prolongation of the SA node recovery time or A-V conduction. Sotalol is unique in that it has class III effects in addition to class II electrophysiological actions mainly due to its effects on K^+ channels resulting in prolongation of the refractory period which may lead to arrhythmias such as long-QT syndrome and the serious "torsade de pointes".

2.2.2.2 Effects on Contractility of Acute and Chronic β-blockade

A remarkable reduction in cardiac output follows acute administration of beta-blockers, mainly due to their effects on heart rate and contractililty. The physiological mechanism of acute blockade has been described above. From a clinical perspective, subsequent chronic levels of β–blockade, will be dependent upon: the prior degree of catecholamine stimulation; the presence or not of previous ventricular dysfunction; proportion and distribution of adrenoceptors in the heart, and the pharmacological properties of the β–blocker being used. Animal experiments, where cardiac work was increased by exercise of volume loading, have showed that acute β–blockade may induce increases in cardiac output, via an increase in the end-diastolic volume and stroke work, a response explained by the Frank-Starling mechanism. Similar effects have been observed in hypertensive humans treated with atenolol, in which the cardiac index was reduced approx. 15% but the stroke index increased up to 30% [245].

Echocardiography provides an additional assessment of ventricular function by measuring the movement of the LV wall. In patients who responded to exercise with increased LV ejection-fraction, atenolol reduced this increase at a dose of 100 mg/day.

The same dose administered to patients with severe impairment of LV function (minimal increase of ejection-fraction to exercise) produced an incremental effect on ejection-fraction upon exercise. In patients with normal systolic contraction, propranolol reduced systolic wall motion with little diastolic effects; in patients with ischemic heart disease and diastolic dysynergy, it prolonged the isovolumic relaxation period and aggravated the uncoordinated relaxation. Prolonged treatment of essentially hypertensive patients with atenolol produced significant reduction in cardiac mass and improved LV ejection-fraction, reduced wall stress and increased circumferential fibre shortening[215]. In patients with idiopathic cardiomyopathy acute β–blockade results in an early rise in left-atrium pressures secondary to reduction in cardiac output, however chronic therapy (1 month to 1 year) leads to a gradual improvement in the reduced ejection fraction[246].

2.2.2.3 Effects on the Vasculature

Beta-adrenoceptors are found predominantly in resistance vessels of skeletal musculature, coronary arteries and in splanchnic circulation vessels. Their activation causes relaxation of vascular smooth muscle. Assessment of the effects of beta-blockade on the vasculature are less difficult to measure because the net vascular tone results from the interaction of several control mechanisms, which include: (i) post-synaptic α–1– and α–2–mediated vasoconstriction; (ii) presynaptic activity of α–2–mediated inhibition of norepinephrine release; (iii) circulating levels of epinephrine and norepinephrine; (iv) effects of other substances such as prostaglandins, thromboxane, endotheline, NO, adenosine; and (v) local metabolic activity and metabolites which can produce significant local effects. Moreover, the effects of β–blockade will depend on the prevailing

conditions at the time of drug administration and on the intrinsic pharmacologic properties of the β–blocker.

2.2.2.3.1 Skeletal Muscle Vasculature

Skeletal muscle vasculature contain mainly β–2–receptors that mediate vasodilation which is can be counteracted by propranolol during neural stimulation or epinephrine infusion. In exercising subjects, propranolol given systemically reduces muscle blood flow. When given directly into the blood vessel supplying the exercising muscle, it does not alter flow, whereas a small neurogenic effect on small resistance vessels could be demonstrated experimentally[215]. In general, it seems that in humans β–blockers have less effects on vessels that supply voluntary muscle. An effect on smooth muscle may be present depending on the class of agent. Selective β–1-blockers and those with partial-agonism or α– and β– blocking properties cause a moderate increase in arterial compliance, whereas non-selective agents have minimal effects[247].

2.2.2.3.2 Coronary Vasculature

The adventitia of the coronary tree contains many nerves distributed throughout the circumference of the large arteries. The nerve plexus appears to come directly in contact with the media only in smaller arteries. In the distal arteries, the plexus forms two nerve strands, which seem characteristic of small coronary arteries and terminate in close apposition to the media. Cardiac veins, however, seem to have little adrenergic

innervation[248]. Beta-1 and β–2 receptors exist in the coronary vasculature of cats, dogs, pigs and humans. The primary effect of β–blockade on coronary flow is a reduction proportional to the β– effect on heart rate and contractility. A question remains if β–1–stimulation produces or enhances α–mediated coronary vasoconstriction. A study on ischemic patients (whose angina was triggered by the cold-pressor test) has concluded that propranolol increases coronary vascular resistance. On the other hand, coronary dynamic studies showed an overall lack of effect of both propranolol and atenolol with no significant coronary vasoconstriction [215]. On the basis of current evidence, it appears that the major effect of β–blockade on coronary vasculature occurs secondary to (and proportional to) the reduction in myocardial work.

2.2.2.3.3 Splanchnic Circulation

It seems that the β–2 subtype dominates the widespread population of β–receptors found in visceral vessels. Administration of isoproterenol in a canine experimental model caused an increase in blood flow in the gastro-intestinal tract mainly in the stomach, and to a lesser extent in caudal portions of the mesenterium. In humans, propranolol reduces splanchnic circulation and potentates epinephrine-mediated vasoconstriction. Beta-1 antagonism with atenolol and metoprolol have lesser effects, but propranolol administration has been shown to elevate portal pressure up to 25% in cirrhotic patients participating in a study evaluating reduction of bleeding from esophageal varicosities [215].

2.2.2.3.4 Cerebral Circulation

Autoregulatory mechanisms dominate the control of cerebral blood flow and propranolol has no clinically important effects. Studies carried out with systematic administration of propranolol in monkeys have documented a reduction of cerebral blood flow of 5% despite a 25% reduction of cardiac output[249]. In another study Propranolol did not impair autoregulatory mechanisms in patients surviving stroke but intracarotideal injection has been shown to produce a small reduction of blood flow [215].

2.2.2.3.5 Effects on Blood Volume and Na^+ Homeostasis

The proximal and distal renal tubes have sympathetic innervation mediated by β–receptors, which results in sodium excretion and increased urine flow. In dogs, the acute administration of propranolol significantly reduced sodium excretion, cardiac output and increased renal vascular resistance. In humans, it has been shown that propranolol does not alter the maximal rate of sodium excretion but reverses its pattern of excretion. Although alterations in sodium handling, reductions in renin release in hypertensive patients, and reductions of circulating levels of aldosterone could be demonstrated, prolonged administration of propranolol has produced no consistent alterations in circulating volume in humans [215].

2.2.2.4 Effects on the Respiratory System

Activation of alpha-adrenoceptors mediate bronchial constriction whereas β–stimulation results in relaxation. The presence of β–1–receptors has been demonstrated by radioligand binding studies but β–2–receptors are said predominant in the respiratory tract. In asthmatic subjects, β–1–selective antagonists induce less bronchoconstriction

than do nonselective antagonists in adequate cardiac β–blocking doses. Comparing propranolol, practolol, and bevantolol, Mackay observed that the β–1–selective agents reduced heart rate as much as did propranolol but did not alter the salbutamolol dose ratio for airways conductance[250]. Clinically, however, the current unequivocal advice is that hypertensive patients with reversible airway disease should be managed with alternative therapy first, because β–1–antagonism is capable of producing bronchospasm in an unpredictable fashion, with possible death due to *status asmaticus*, in susceptible patients. This spasm is likely to be less severe (and reversible with β–2–agonists administration) than that caused by propranolol, but still in such patients β–blocking are not considered first line agents for the treatment of hypertension[215].

2.2.2.5 Effects on Metabolism

Adrenotropic receptors are also involved in the metabolism of lipids, carbohydrates, and proteins either directly or indirectly via modulation of the release of hormones such as insulin, glucagon, gastrin, growth hormone, adrenocorticotrophic hormone, and thyroxine. The nonselective blocker propranolol blocks the increase of circulating levels of glucose, free fatty acids, insulin and glucagon[213,214]. The classic effect of isoproterenol in adipose tissue is lipolysis, mediated by β3–receptors, even though β–1– and β–2–receptors are found in adipose cells in the omentun and subcutaneous tissue[215]. Selective β–1–antagonism are less effective in blocking isoproterenol-induced lipolysis than blocking heart rate response in isolated atria[251,252].

Propranolol acts on plasma lipoproteins by blocking the epinephrine-mediated reduction on VLDL (very low density lipoprotein), either directly on the hepatocyte or via suppression of pancreatic insulin release, or reduction of clearance of triglycerides via its hemodynamic effects. In chronic non-selective β–blocking therapy, the ratio total cholesterol/HDL is raised, there is a mean increase of 20% in total VLDL and triglycerides levels and 11% reduction of HDL cholesterol. Beta-1 selective agents may produce lesser effects but with the same characteristics [253]. The clinical importance of these data is not established. The β–blocker heart attack trial (BHAT) confirmed that propranolol caused a 6% reduction in HDL levels and a 17% increase in plasma triglyceride levels, but this has had little effect in modifying the 20% reduction in morbidity and mortality in the cohort of patients[254].

Prolonged administration of propranolol does not alter fasting levels of insulin, but may alter fasting plasma glucose levels and glucose tolerance, especially under conditions of extreme stress, prolonged (> 24h) fasting and severe sustained exercise[215]. Propranolol may cause a delay in the return of the plasma glucose level due to an enhanced glucose uptake without an increase in glucose mobilization, because of its suppressive effect on counterregulatory mechanisms, which are epinephrine-mediated. These effects are also less important with β–1–selective blockade. In diabetic patients, the incidence of adverse metabolic reaction to β–blocking agents is low, however the warning tachycardia and palpitations of hypoglycemia are abolished[215].

Non-selective β–blocking therapy can also alter hormonal release either by blocking β–receptor mediated effects or indirectly by enhancing α–mediated effects. Beta-receptor activation increases the release of thyrotropin-releasing hormone and

parathyroid hormone but suppresses growth hormone release. The antral release of gastrin is also decreased by β–blocker therapy, however there is no evidence that prolonged β–1–blocker therapy can adversely affect the role of hormones in controlling homeostasis [215].

2.2.2.6 Effects on Central Nervous System

Chronic administration of propranolol has been associated with higher incidence of dreams, insomnia, occasional hallucinations, and depression[255]. The specific central β–adrenoceptor involved in such disturbances in unknown, however the alterations in the sleeping patterns are typically associated with suppression of REM (rapid-eye movement) periods of sleep. It has also been suggested that atenolol may interfere with recent memory[256] but this has not been confirmed. The acute administration of different β–blockers can also slow the central nervous system reaction-time, but this appears to diminish during prolonged therapy. The degree of lethargy also seems dependent on the hydrophobicity of the agent. Hydrophilic agents such as sotalol, nadolol, and atenolol are associated with significant fewer effects[257].

2.2.3 Non β–adrenoceptor Properties of β–Blockers

Many are the possible structures capable of interacting with the β–receptor and therefore achieve some level of β–blockade, with or without selectivity. It is therefore plausible that these structures may have additional pharmacological properties. This in fact, is true for many of the compounds available today. Initially, the clinical differentiation that mattered was the selectivity issue. With an increasing number of agents becoming

available, the ancillary or additional pharmacological properties of β–blockers have also been exploited clinically. Characteristics such as "membrane stabilizing" effects and vasorelaxant properties which are common to many compounds will be discussed.

2.2.3.1 Membrane-stabilizing Properties

The term "quinidine-like" properties was first coined by Vaughn Williams[258] who observed that propranolol depressed the rate of rise and overshoot of the transmembrane action potential in rabbit atria, an effect analogous to that of quinidine. Propranolol requires a concentration of 10^{-5} M to depress phase 0 of the action potential in the frog nerve and leads to slowing of conduction. At these concentrations, propranolol is even more potent than procaine as a local anesthetic, and when applied at the conjuntival sac, causes a dose-dependent inhibition of the corneal reflex [215]. This phenomenon has also been termed as "lidocaine-like", alluding to the local anesthetic characteristics observed.

In general, β–blockers differ markedly in their actions on the action-potential, and this has been correlated with their liposolubility. The positive and negative isomers of propranolol show a 100-fold difference in receptor affinity, however their lipophilicity and thus their effects on the action-potential are similar. In contrast, hydrophilic β–blockers do not present such an effect [215]. Until today, the clinical importance of lipophilicity has relied on absorption, distribution, and metabolism of the different agents mainly with interest to the posology of different agents. The secondary effects under these conditions lose their importance, vis à vis the high doses required for these effects to become apparent. Lipophilic agents tend to have higher rates of intestinal absorption, extensive hepatic first-pass metabolism, and are highly bound to plasma proteins.

Because of this, and in the absence of active metabolites, they also tend to have shorter serum half-lives relative to hydrophilic β-blockers. These characteristics are typical of propranolol, alprenolol, and metoprolol. On the other hand, hydrophilic agents such as sotolol, atenolol, and nadolol may present lower absorption rates, minimal protein binding ratios and minimal hepatic metabolism. Further, reduced lipophilicity also results in lesser potential accumulation in the central nervous system and fewer neurological side-effects[259].

2.2.3.2 Vasorelaxant Properties

The pre- and post-synaptic mediated regulation of α and β receptors exerted by the afferent sympathetic system keeps the neuronal release of norepinephrine under tight control. Beta-blockers can alter this balance in a variety of ways either via β–receptor selectivity or via intrinsic properties of the agent, such as additional α–stimulation or blocking effect or even selective β–2 partial agonism. Non-selective agents can enhance α–mediated vasoconstriction, block β–2–mediated vasodilation, and block β–2–mediated bronchodilation. Beta-1 selective agents will have, in a dose-dependent fashion, fewer effects on these mechanisms. Agents like delevalol and celiprolol can cause vascular smooth muscle relaxation due to their selective β–2–agonism effect, whereas agents such as labetalol, carvedilol and amosulol may produce similar results by blocking α–mediated vasoconstriction, due to their intrinsic α–mediated blocking capabilities. Carvedilol has been subject of special attention because of in addition to its α–blocking characteristics, it also seems to have antioxidant properties, making it a

potential agent for long-term therapy[260,261,262]. Beta-blockers can produce ancillary effects not mediated through β–receptors. Nipradilol can mediate vasorelaxation through a nitrodilatory mechanism, in a manner similar to prizidolol and mindolol[215].

2.2.4 Metabolism

Apart from being classified by their pharmacological properties of specificity, selectivity, potency and biophysical characteristics such hydro/lipophilicity, beta-blocking agents can also be classified by their metabolic fate. A variety of metabolic clearances occurs for different compounds (including either hepatic or renal metabolism and/or excretion) in association with differing degrees of first-pass metabolism in the liver and active renal excretion. The majority of compounds available today have extensive or moderate (above 50%) hepatic metabolism. Examples of this group are propranolol, metoprolol, betaxolol, acebutolol, labetalol, bevantolol, bucindolol, and carvedilol. Each of these have characteristics that must be judged and weighed by the prescribing physician as being more or less applicable for the patient receiving the therapy. For example, the products of propranolol degradation include more than 15 metabolites (which in general, do not have significant clinical repercussions). Acebutolol, a β–1-selective with intrinsic partial agonism however, produces an active metabolite, diacetalol, which has a half-life of 8-12 h. Most products of labetalol metabolization are conjugates and are excreted in the bilis, only 5% will have renal excretion. Atenolol is excreted almost exclusively by the kidney and 90% in an unchanged form. The fate of esmolol is independent of liver or kidney metabolism, because blood estearases transform it into a clinically inactive

metabolite excreted unchanged in the urine[215]. The details of the metabolism of esmolol will be discussed in a separate section (section 2.6).

2.3 Cardiac Surgery

Operations on the heart are among the most complicated surgical procedures. The surgical repair of cardiac structures and the process of revascularization of the myocardium is complex and difficult, not mainly due to the surgical technique per se, but rather to all the apparatus and infra-structure that has to be in place and available to perform cardiac surgery safely and successfully. Not taking into account all the efforts undertaken during investigation, diagnosis and clinical indication of surgery preoperatively, the intra- and post-operative care periods are fundamental to the outcome of the patient undergoing cardiac interventions. In this section, we will discuss intra-operative aspects of cardiac surgery, mainly related to extra-corporeal circulation, cardioplegia and anesthetic management of the patient during surgery, which are pertinent to the work developed in this thesis.

The history of cardiac surgery blends into the history of hypothermia and extracorporeal circulation. Before the advent of these strategies, very little could be done in terms of surgery on the beating heart. Cardiac surgery as we know today was born in the early 50's with the initial work of Bigelow on extracorporeal circulation and hypothermia. Further, Melrose introduced the concept of elective cardiac arrest and coined the term 'cardioplegia' or 'cardioplegic solutions' for solutions that can arrest the heart and allow better exposure and the access to the internal structures. Since then, cardiac surgery has expanded in all industrialized countries and has continued to evolve at a very rapid pace. A great deal of research has been done and some of the most relevant aspects of extracorporeal circulation, cardioplegia and myocardial protection will be discussed in the paragraphs that follow.

2.3.1. Extracorporeal Circulation

The early historical aspects of cardiopulmonary bypass for cardiac surgery are not easily described, and it is almost impossible to know who first had the idea of diverting the circulation to an oxygenator outside the body and pump it back to the patient's arterial system in order to allow surgery within the heart. The patient whose arterial blood flow is temporarily provided by means of a pump-oxygenator is in an abnormal state that affects most, if not all, the body's physiologic processes. Throughout evolution, blood has passed only through channels lined with endothelial cells, but during cardiopulmonary bypass (CPB) it passes across non-endothelial foreign surfaces. As a result of this and other factors, virtually all the humoral and cellular components of the inflammatory response are activated acutely, and probably some of the more slowly reacting specific immune responses are also activated, at least initially. Other damaging effects, such as the general stress response often seen after surgery and trauma may occur to a major degree.

References to extracorporeal gas exchange date back to the late nineteenth century, when in 1885 Frey and Gruber worked in an "oxygenator device"[263]. Serious consideration, however, to the use of pump-oxygenators for cardiac surgery had to await the development of modern anesthesia and modern surgical methods. Particularly scientific developments, such as the discovery and use of heparin, and modern structural materials in instrumentation. Gibbon (Massachusetts General Hospital, Boston) was a major contributor to the development of CPB and its first appearance in clinical practice in the late 1930s. In 1953, he performed the first successful operation in which the patient was totally supported by CPB when he repaired an atrial septal defect in a young

woman[264]. His four subsequent patients did not survive the operation for a variety of problems and he did not pursue. At the University of Minnesota, in the late 1940s Dennis and Varco were also developing a pump-oxygenator for clinical use. In the early 1950s, apparently at the same time as Gibbon, they performed the correction of what was thought to be an atrial septal defect with the patient completely supported by CPB. The patient, however, did not survive the operation. The autopsy found that the primary disease was in fact a partial atrioventricular canal defect and misinterpretation of the anatomy was the primary factor of the patient's death. In Stockholm, Bjork[265] and Senning[266] were also working on a pump-oxygenator system. Their work allowed Crafoord's early use of this method for a successful removal of an atrial myxoma[267]. After Dennis unsuccessful effort, Lillehei and colleagues at the University of Minnesota developed the "azygos flow principle"[268] and began working in the laboratory with cross-circulation using another intact subject as the "oxygenator" [269]. In April 1954 he started a series of operations of congenital heart disease using "controlled cross-circulation" and the mother or the father as the "oxygenator". Kirklin and Barrat-Boyes began experimental work at the Mayo Clinic in Rochester, Minnesota, also during the early 1950s. In 1955 they successfully repaired a ventricular septal defect and started the world's first series of intracardiac operations using a pump-oxygenator for CPB[270]. Quickly, the field began to expand and today approximately 1 million cardiac operations with CPB are performed per year, worldwide.

During total CPB, a number of physiological variables are under direct external control, in contrast to the situation in intact humans. These include total systemic blood flow ("cardiac output"), input pressure waveform, systemic venous pressure, pulmonary

venous pressure, hematocrit of the initial perfusate and its chemical composition, arterial oxygen, carbon dioxide, and nitrogen levels; temperature of the perfusate and of the patient. A second group of partly controllable variables is determined by the patient and includes systemic vascular resistance, total body oxygen consumption, mixed venous oxygen levels, lactic acidemia and pH, regional and organ blood flow and regional and organ function. A third group of largely uncontrolled variables includes, to a certain extent, all processes of inflammation and immunological response. All these factors make the patient undergoing extracorporeal circulation a unique organism that requires close monitoring and detailed knowledge of the pathophysiology of the post-CPB state during intense post-operative care.

2.3.2. Hypothermia

Interest in the clinical effects of hypothermia dates back to the end of the eighteenth century when Currie described the use of body immersion in water at 7° C for the treatment of fever[271] .

Hypothermia has played a major role in myocardial preservation for cardiac operations since Bigelow first proposed its value in this regard[272] . Prior to the advent of cardiopulmonary bypass, some cardiac operations were conducted with total body immersion hypothermia which allowed brief intervals of total circulatory arrest. Following the advent of cardiopulmonary bypass, hypothermia played a major role in cardiac operations with use of a heat exchanger in the cardiopulmonary bypass circuit so the body could be initially cooled and then rewarmed at the conclusion of the procedure. Additional topical cooling of the heart was achieved with irrigation of the pericardial wall

with saline at 4° C which was then discarded from the operative field by a separate suction system with care taken to keep the heart covered with wet gauze sponges except at the site needed to conduct the operation[273,274]. Subsequently, the technique was modified by the addition of a single bolus of cold crystalloid cardioplegia administered at the time of aortic crossclamping[275]. Intermittent ischemic arrest is a variation on this procedure that is generally combined with systemic and topical hypothermia with intervals of aortic crossclamping of 10 to 20 minutes followed by intervals of reperfusion of 3 to 5 minutes. Ideally, the heartbeat resumes during the intervals of reperfusion. This technique was common in the 1960s and into the 70s when it was generally replaced by cold crystalloid cardioplegia although it is still being used by some surgeons[276]. According to a survey of clinical practice performed in 1977, 87% of respondents used intermittent ischemic arrest for distal coronary anastomoses[277]. When the survey was repeated in 1981, 91% of those responding were using cold cardioplegia[278].

Another technique is that of hypothermic fibrillation where the myocardium and the body temperature of the patient are maintained at 25° to 28° C [279]. When this technique is employed, it is imperative that a left ventricular vent be placed to prevent distention of the left ventricle which would otherwise result in impaired distribution of blood flow to the inner layers of the myocardium. Elevation or displacement of the heart will frequently render the aortic valve incompetent and result in cardiac distention if a vent is not used. This technique is not appropriate in hypertrophied hearts because ventricular fibrillation in these hearts is associated with impaired coronary flow and relative endocardial ischemia. This technique cannot be used in procedures requiring opening of the aorta.

The optimal myocardial temperature for myocardial preservation remains controversial. Using the isolated perfused rat heart, hypothermia to 0.5° C in the absence of ischemia does not appear to be harmful to the heart[280]. Hearse could find no significant increase in protection when the myocardial temperature was lowered below 25° C although there was some incremental advantage at 12° C[281,282]. Tyers and associates found that myocardial recovery was best when the myocardium was kept at 10° to 15° C[283]. Flaherty and co-workers found that a temperature of 27° C was as good as temperatures of 20° C or 10° C for preservation of ventricular function during 60 minutes of ischemia[284]. Although myocardial temperature can be maintained at 5° to 10° C in experimental studies, this is not practical clinically. Clinically, temperatures of 12° to 20° C can realistically be attained and are used by many surgeons. Despite this common usage, it is still not clear whether this practice provides optimal protection.

2.3.3 Hyperkalemic Arrest

The use of hyperkalemia to arrest the heart and facilitate cardiac operation was reported in 1955[285] following experimental studies in dogs using a Melrose heart-lung machine or using a Langendorff apparatus for perfusion of hearts isolated from rabbits and other species. Potassium citrate was used initially because potassium chloride was not readily available commercially. Melrose concluded from these early experiments that the dose of potassium citrate needed to be greater than 3 mM, that there was no upper limit to the safe concentration of potassium and that cardiac arrest continued for as long as potassium citrate was present in the coronary circulation. He found a normal beat was established after simple reperfusion and stimuli such as calcium chloride or adrenaline were

unnecessary. He concluded that "this method may offer an opportunity for careful surgery on the motionless heart without the danger of air embolism". Thus, the focus was on avoiding the dreaded complication of air embolism and myocardial preservation was not considered an important component of the cardiac operation. In his series of studies on dogs, Melrose added 77 mM potassium citrate to 20 mL of dog blood and infused the solution into the crossclamped aorta. Clinical application of this technique of cardiac arrest was adopted by a number of surgeons. However, reports of myocardial necrosis resulted in abandonment of the original method[286,287,288].

Hoelscher, using the newly available electron microscope for ultrastructural studies, found that ten minutes of ischemia at 37° C produced ultrastructural changes while 40 minutes at 20° C produced no change and that 770 mM potassium or sodium citrate produced marked changes that were different from those of ischemia alone[289]. A smaller dose (77 mM) of sodium or potassium citrate produced less marked changes and he concluded that citrate was damaging the myocardium, not potassium. Hoelscher later reported the effects of magnesium chloride-procaine amine or potassium citrate on the myocardium in induced cardiac arrest. He used a bolus of 1 mg/kg and 30 minutes of ischemia and found that hearts arrested with potassium citrate showed poor function and ultrastructural damage whereas the use of magnesium/procaine resulted in no apparent myocardial injury[290].

Bretscheneider also became interested in myocardial preservation in the early 1960s and formulated a major principle of myocardial preservation with his understanding that the energy pool of adenosine triphosphate (ATP) and creatine phosphate (PCr) could be preserved by arresting the heart. He chose to do this using a so-

called "intracellular" type of electrolyte solution which induced cardiac arrest by reducing transmembrane gradients. He reduced the sodium to leave the membrane polarized, reduced calcium to decrease energy consumption and added procaine to accelerate asystole and stabilize the cell membrane. He measured myocardial ATP and PCr during ischemia and showed that 120 minutes of ischemia was tolerated at a myocardial temperature of 27° C[291,292]. Sondergaard was struck by the logic of Bretschneider's work and began using his technique clinically. In 1975 he reported 100 aortic valve procedures involving ischemia of 80 to 120 minutes with 6% mortality[293] . There were only two cardiac deaths with none of the other deaths showing myocardial injury at autopsy. Sondergaard used Bretschneider No. 3 solution which contained 12 mM sodium chloride, 10 mM potassium, 2 mM magnesium, 7 mM procaine and mannitol 43.5 g/L. The heart was precooled with a cold glucose solution and then infused with Bretschneider's solution slowly by gravity over eight to ten minutes at 4° C to allow the solution to equilibrate with the tissues and abolish the transmembrane gradients.

Another principle which Bretschneider provided was that of buffering the cardioplegic solution[294,295]. He used the amino acid histidine in combination with histidine-HCl and demonstrated that several cardioplegic methods reduced the decay of the high-energy phosphates by decreasing the energy demand of the myocardium relative to pure ischemia. He demonstrated that the critical ATP content of left ventricular myocardium was 4 mM/g wet weight which was associated with reversibility of function and a post -ischemic recovery period of 20 to 30 minutes, which could be prolonged by 60 to 80% using Bretschneider's solution buffered with 180 mM histidine plus 18 mM histidine-HCl. This buffering effectively delayed the development of myocardial acidosis

and significantly improved the generation of ATP via the enhanced degradation of glycogen to lactate during ischemia. The use of histidine as a buffer has not been adopted by others in formulating cardioplegic solutions, however is now recognized that one of the advantages of blood-based cardioplegia is the presence of histidine which is highly prevalent in hemoglobin and one of the main blood buffers.

In 1972 Kirsch and Rodewald, reported a cardioplegia technique that used a solution containing no sodium and no calcium, but large amounts of magnesium and procaine[296]. In 161 patients undergoing repair of valve lesions or septal defects, the mortality was 17% and the cardiac death rate was 10%. This was higher than reported using other techniques and his methodology was not adopted clinically. Subsequent work demonstrated that use of calcium-free solutions created the potential for "calcium paradox" which, it was later learned, could be avoided by even trace amounts of calcium or by the use of hypothermia[297]. Bleeze and Rodewald modified Kirsch's solution and then infused 800 mL of "Hamburg solution" which was a highly complex mixture of hydroxyl starch, magnesium aspartate, procaine, calcium, potassium, sodium bicarbonate, glucose, mannitol, methylprednisolone and gentamycin (because the solution was oxygenated overnight). This approach resulted in an acceptable surgical mortality[298].

Gay and Ebert in 1973 reported on laboratory experience with a crystalloid solution of extracellular composition using potassium chloride as the arresting agent[299]. The following year Hearse and associates reported on crystalloid cardioplegia using potassium chloride as the arresting agent[300], and in 1976 a second report expanded on the initial work[301]. These three reports from 1973 to 1976 produced widespread interest in the extracellular type of solution for hypothermic cardioplegic myocardial preservation.

Hearse's laboratory, using the isolated perfused rat heart and a systematic approach to evaluating the various components and their concentrations in crystalloid cardioplegia motivated many surgeons to pursue cardioplegia as clinical means for myocardial protection following the 1976 report[302,303]. Hearse working with Braimbridge and others developed what became known as St. Thomas's cardioplegic solution which was first used clinically in 1975. Optimal concentrations were determined from dose-response curves and similar stepwise studies of temperature, volume and duration of cardioplegic infusion were undertaken. They subsequently developed the second St. Thomas's Hospital formulation which was marketed commercially under the name of Plegisol®. Hearse's laboratory screened with dose-response curves many potential additives to crystalloid cardioplegia (glucose, lactate, ATP, PCr, mannitol verapamil, adenosine, lidocaine, diltiazem, nifedipine and insulin), but St. Thomas's Hospital cardioplegic solution No. 2 differed from the St. Thomas's solution No. 1 only by the amount of calcium being halved, procaine being omitted, sodium bicarbonate added as a buffer and with a final pH of 7.8 versus 5.5-7.0[304].

The formulation standard for cardioplegia was laid by the development of intracellular solutions for inducing cardioplegic arrest, in Europe by Hearse and Braimbridge and by Gay and Ebert in North America with both groups utilizing crystalloid solutions of extracellular composition. The use of blood as a vehicle for cardioplegia, although originally practiced by Melrose, was specifically studied in the laboratory by Buckberg and Barner and their associates and introduced into clinical usage in 1977. Blood cardioplegia provided the advantages of rapid cardiac arrest in an oxygenated environment; intermittent reoxygenation with reinfusion of cardioplegia,

intermittent reoxygenation to promote aerobic metabolism; the presence of oncotic constituents contained in blood, and buffering capacity inherent in the red cell; the free radical scavenging activity of blood and plasma and the better capillary flow distribution provided by the red cell[305,306,307,308].

Buckberg's laboratory at the University of California at Los Angeles has contributed to the understanding and implementation of many facets of cardioplegia in general and blood based cardioplegia in particular. Warm induction of blood cardioplegia was proposed to replenish the high energy phosphates of chronically energy depleted hearts prior to an interval of cold cardioplegic arrest[309]. Warm induction is also appropriate for the acutely energy depleted or injured myocardium such as the patient suffering from acute ischemia.

A second innovation is that of terminal warm blood cardioplegia which is administered after an interval of cardioplegic arrest, again to facilitate metabolic restoration while the heart remains immobile so that energy is not needlessly wasted on contractile activity[310]. This terminal warm cardioplegia ("hot shot") has been assessed in a clinical randomized study and was found to be beneficial[311].

A third component of the warm cardioplegia strategy is that of substrate enhancement with the addition of the Krebs cycle intermediates glutamate and aspartate to warm cardioplegia[312]. Experimental demonstration of the benefit of these additives to warm induction and warm reperfusion blood cardioplegia has been confirmed in the clinical setting with recovery of ventricular function and reduced requirements for postoperative inotropic and left ventricular mechanical support[313]. A recent study, however, using Magnetic Resonance Spectroscopy of the nucleus of phosphorus (^{31}P

MRS) investigated the effects of an enriched exogenous source of aspartate/glutamate on normal, isolated blood perfused pig hearts subjected to a period of normothermic ischemia. The results showed no beneficial effects of these amino acids on myocardial energy levels or intracellular pH before, during or after ischemia. There were no effects on myocardial function nor on oxygen consumption at anytime during the experimental protocol. According to this study, the applicability of this approach to the clinical setting merits further investigation[314].

2.3.4 Warm Heart Surgery

"Warm Heart Surgery" evolved from concepts that were first used during the early days of modern cardiac surgery[315,316]. Like many "new" developments in medicine, the technique of continuous normothermic blood cardioplegia arose as a result of the discovery and adaptation of ideas which for various reasons had been forgotten or discarded. The principle for its development was extremely simple: to avoid myocardial ischemia during cardiac surgery.

The concept of affecting the heart beat by manipulating ionic fluxes in the heart dates back to the pioneering work of Sydney Ringer in the last century[317,318]. During the late 19th century physiologists were studying the control of cardiac function largely in terms of myogenic versus neurogenic theories of control. It was amidst this controversy that Ringer performed experiments on the effects of various ions on the heartbeat in frogs[319]. This basic research showed that the ionic composition of the extracellular fluid profoundly affects the heartbeat. Ringer described ways to affect cardiac activity long before much was known about membrane physiology.

Ringer's work was not widely appreciated in Europe, but was noticed by American physiologists who confirmed Ringer's observations and extended them[320,321,322]. The ionic theory of cardiac contraction was slowly developed and came to be accepted during the first years of the twentieth century. Zwikster and Boyd described the reversible arrest of the heart using potassium in 1935[323]. However, this research was largely confined to the physiology literature and had no immediate clinical applications.

After the historical events previously described regarding the development of cold hyperkalemic cardioplegic solutions in the early 1950s, interest in warm blood cardioplegia increased as a result of the development by Buckberg's group of the already described "hot shot". Buckberg and associates also demonstrated that the normothermic non-working vented heart (beating empty) consumes 6-8 mL O_2/100 g wt weight/ min myocardium versus 0.6-1.5 mL O_2/100 g wt weight/ min in the normothermic arrested heart[324,325]. With antegrade delivery, a flow rate of at least 80 mL/min with a hemoglobin concentration of at least 8.0 g/L was found to preserve perioperative myocardial metabolism[326,327].

The re-introduction of continuous normothermic blood cardioplegia was done by Salerno and associates in 1990[328,329]. This created a great deal of interest among cardiac surgeons. This group while reviewing the idea of cardioplegia, began to question the necessity of hypothermia in myocardial protection. As described previously by Bernhard (1961)[330] and Buckberg (1977), the major reduction (~ 90%) in energy demand of the heart with hypothermic cardioplegia results from electromechanical arrest, and cooling contributes only slightly to this end. In fact, myocardial oxygen consumption when expressed *per beat* actually increases at lower temperatures because hypothermia

enhances contractility via calcium dependent subcellular processes. It is the concomitant bradycardia that leads to an overall decrease in myocardial oxygen consumption. Cooling causes bradycardia, then ventricular fibrillation (approx. at 28° C) and eventually, diastolic arrest. It is this cessation of electromechanical activity with hypothermia which accounts for the significant decrease in energy demand of the heart. The levels of myocardial hypothermia employed (at that time but still today, by many) during cold cardioplegia (10°-15° C) could result in several undesirable side effects including impaired mitochondrial and cell volume control[331] , membrane instability[332] and poor sarcoplasmatic reticulum calcium handling[333]. Clinical studies showed that hypothermic cardioplegia results in myocardial energy depletion and a delay in the metabolic and functional recovery of the heart[334,335,336]. On the other hand, blood cardioplegia delivery at 37° C optimizes the biochemical and biophysical properties of blood for organ perfusion. Unloading of oxygen from hemoglobin is optimal at 37° C as is the capacity of the myocardium to utilize oxygen. Delivery of normothermic oxygenated blood to the electromechanically arrested heart may allow myocardial resuscitation and repair to occur during the period of aortic clamping.

The main drawback of normothermic blood cardioplegia is that because it is normothermic, it must be continuous. When delivered antegradely and in a normal heart, sufficient experimental and clinical data have emerged that justifies its use. However, this approach has been criticized in terms of the homogeneity of distribution of flow in the different areas and layers of the myocardium, the practicality of having a perfused heart rather than a flaccid asanguineous field, and the difficulty in visualization during coronary bypass surgery and neurologic outcome. The problems of overdilution,

hyperglycemia, hyponatremia and hyperkalemia have been, at least in part, dealt with the introduction of the "Miniplegia"[337] and this will be the object of further discussion.

Regarding the homogeneity of flow distribution, a great deal of clinical and experimental research has been done. Clinically, retrograde normothermic perfusion has received a lot of attention and seems effective in the diseased myocardium[338]. In the hypertrophied myocardium, the data seem conflicting. It has been reported that the retrograde delivery of cardioplegia at normothermia results in similar distribution as that of cold cardioplegia[339,340]. Depending on the species examined, much of the cardioplegia delivered retrogradely distributes in a "non-nutritive" fashion, bypassing the microcirculation and emptying directly into the right or the left ventricle via the Thebesian system. Quantitative studies have shown minimal perfusion with retrograde cardioplegia[341]. With the heart at normothermia, retrograde warm delivery raises the real potential for inadequate right ventricular preservation[342]. In dogs, retrograde perfusion appears to provide inadequate protection to the right ventricle[343]. Clinically, however, a series of studies have suggested that in humans retroperfusion is capable of metabolic and functional preservation of the right ventricle[344,345]. In our experimental setting in pigs, retrograde perfusion with warm blood seems quite ineffective in preserving the myocardium especially with an acute occlusion of the left anterior descending artery (LAD)[346]. A number of variations and uses of retrograde cardioplegia have been proposed, including a technique that employs both antegrade and retrograde perfusion in an alternate but also in a simultaneous fashion[347]. This last trend is now under experimental and clinical investigation. The search for a device or method to verify the

viability of different areas of the myocardium is under development and will probably contribute significantly to identifying areas of higher sensitivity within the heart.

Problems related to visualization and practicality are subjective and vary from one surgeon to another. Visualization is critical especially during coronary bypass operations, but again some surgeons seem to adapt to the use of a CO_2 blower to clear blood from the site during the quick moment of passing a stitch in a coronary vessel. This requires an extra hand while grafting most coronary vessels but it does not seem to represent a major surgical obstacle.

An important problem facing the proponents of warm cardioplegia however, is not related to myocardial protection. Rather, there is concern regarding cerebral perfusion during bypass surgery. An increasing rate of neurologic events (stroke or even intermittent ischemic events without rough neurologic repercussion, such as cognitive dysfunction) has been reported in recent years[348,349]. The exact origin of this remains obscure and a great deal of research is now being directed to this problem. The argument that the brain at 37° C is more sensitive to the side-effects of extracorporeal circulation and the lack of pulsatility has become popular among many surgeons. These now tend to allow the temperature drift to 31°-32° C instead of actively maintaining the systemic temperature at 37° C. This practice has not yet received much experimental or clinical support.

2.3.4.1 Selective Retroperfusion of the Heart and of the Brain During Surgery

Also termed as retrograde cardioplegia and retrograde cerebroplegia, these two types of perfusion strategies have received a great deal of attention in recent years. These procedures have found applications in clinical practice and many surgeons rely on them despite the polemics generated and the deficiency of definitive scientific documentation of its advantages.

2.3.4.1.1 Selective Retroperfusion of the Heart During Surgery (Retrograde Cardioplegia)

The goal of any cardioplegic solution is preservation of the myocardium during surgery. An examination of the venous drainage system of the myocardium reveals a system that drains myocardial capillaries into the middle and great cardiac veins and a second system of smaller magnitude, which consists of arteriosinusoidal and Thebesian vessels draining directly into the left and right ventricular chambers. In addition, these two systems communicate with each other, forming a vast non-capillary vasculature. As a result, retrograde coronary sinus perfusion is divided in "nutritive" and "non-nutritive" flow systems. The former enters the capillaries and eventually exits the coronary ostia. The latter is shunted through a plethora of venovenous connections into the Thebesian vessels and into the ventricles. The ratio of nutritive to non nutritive flow appears to be species dependent and is the subject of considerable debate [350,351,352].

Experimental studies utilizing techniques of collecting effluent from the aortic root, radioactive microspheres, contrast echocardiography, resin casting, angiography and staining as well as electron microscopy have been undertaken to clarify the fate of perfusate directed through the coronary sinus. Overall, a considerable fraction of

retrograde cardioplegia is distributed via the non nutritive pathway exiting directly into the ventricles via the Thebesian system. Experimental and clinical evidence show that retrograde perfusion provides protection to the left ventricle, apex and septum. The efficacy of retrograde cardioplegia to protect the right ventricle remains controversial[353,354,355,356,357,358,359].

It appears that retrograde continuous normothermic blood cardioplegia (RCNBC) has gained world-wide acceptance and the interest in this method continues to grow, as illustrated by the increasing number of publications and meetings concerning this topic. Above all, there has been a rethinking of accepted principles, such as hypothermia, which have remained unquestioned over the years. It seems evident that RCNBC is an important addition to the armamentarium of myocardial protective techniques currently available. While the technique may, in fact, slightly increase the complexity of surgery, its obvious advantages cannot be overlooked. Moreover, there should be no adversarial positions regarding the various myocardial protective techniques. The surgeon should utilize the best techniques for the particular situation minimizing the period of ischemia and, if possible, preventing ischemia altogether[360]. The advent of RCNBC has provided surgeons with an important tool to the search for the "ideal" method of myocardial protection[361,362].

2.3.4.1.2 Selective Perfusion of the Brain During Surgery (Cerebroplegia)

The brain is the organ most sensitive to ischemia[363]. Under normothermic conditions, obstruction of the cerebral circulation produces irreversible lesions in 5 minutes. Hypothermia is the most effective method of brain protection available to use[364]. It

decreases metabolism and preserves intracellular high-energy phosphates[365]. The brain can be preserved up to 45 minutes with deep hypothermic circulatory arrest[366,367]. During the last two decades, clinical and experimental efforts have aimed at improving brain protection for the surgical treatment of aortic arch aneurysms and complex congenital heart diseases by the use of deep hypothermia[368]. Antegrade and retrograde brain perfusion performed in conjunction with circulatory arrest have improved brain protection and increased the safe time of circulatory arrest[369,370]. Deep hypothermia, although effective in reducing metabolism, is associated with several disadvantages[371,372,373,374,375], and consequently, the mortality and morbidity remain high for these procedures.

Moderate hypothermia provides less protection than deep hypothermia when retrograde brain perfusion is used in conjunction with circulatory arrest. This suggests that low brain temperature, rather than the supply of oxygen to the brain, is the major determinant of the brain protection during retrograde cerebral perfusion. Hypothermia may protect the brain by attenuating the generation of reactive oxygen species[331]. Removal of toxic metabolites and the provision of metabolic substrates may also contribute to brain protection during retrograde cerebral perfusion. Antegrade brain perfusion associated with circulatory arrest at 28° C provides excellent protection of brain ATP and intracellular pH, as does antegrade brain perfusion during hypothermic circulatory arrest at 15° C. It was also demonstrated[332] that during hypothermic circulatory arrest antegrade cerebral perfusion offered better brain protection than retrograde cerebral perfusion in sheep.

2.3.4.2 The French Experience - Undiluted Cardioplegia (the Miniplegia)

The need for a new warm blood cardioplegia delivery system derived from work developed by Dr. Arrigo Lessana's group in Paris, France. After a year and 660 operations using the so-called Toronto technique, first proposed by Salerno and associates, Lessana's group identified pitfalls in the technique (mainly hyponatremia, hyperkalemia, hyperglycemia and excessive hemodilution), leading in some cases to a vasoplegic syndrome[302,376].

The Initial Toronto Technique

Briefly, myocardial perfusion is instituted by employing a 4:1 mixture of blood and crystalloid solution. Oxygenated blood is withdrawn from an arterial blood line and is mixed with Fremes' solution through double tubing passing through a roller pump. The blood cardioplegic solution is rewarmed to 37° C with a heat exchanger. The Fremes' solution is used in two presentations: High K^+ with 100 mEq/L of KCl, intended for induction of arrest, and the Low K^+, containing 30 mEq/L KCl for maintenance of arrest.

High KCl Fremes solution is injected, in the absence of aortic insufficiency, into the aortic root at flow rates of 250 to 300 mL/min during 1 to 3 minutes. Cardiac arrest is achieved within a minute and myocardial retroperfusion is thereafter continued with Low-KCl Fremes solution via the coronary sinus throughout the aortic cross clamping period. The cardioplegic flow in the coronary sinus varies from 100 to 300 mL/min as a function of myocardial mass and volume induced pressure not exceeding 50 to 60 mmHg. This

pressure is continuously monitored since it represents a fundamental element for controlling coronary perfusion.

To avoid the complications mentioned above and improve the efficacy of normothermic cardioplegia, five modifications were proposed:

a) Dissociation between injecting the cardioplegic components and coronary blood volume.

The basic principle of myocardial protection is dictated by two separate elements: The cardioplegic solution and myocardial oxygenation. It is not possible to dissociate the injection of cardioplegic components from the blood with the double tubing system. This is a major drawback for several reasons:

(i) The amount of KCl injected is not controllable;

(ii) the K^+ levels used for arrest the heart are neither constant nor controllable during aortic crossclamping, and their levels may differ from patient to patient. The constant addition of doses of either high or low KCl solution into the cardioplegic line increases the systemic levels of K^+ during aortic cross clamping. Moreover, cardioplegic K^+ levels will increase progressively to a peak at the end of coronary perfusion just prior to removal of the aortic clamp, which might potentially delay the onset of electromechanical activity; and

(iii) interruption of the injection of crystalloid solution is possible only in association with that of the blood perfusate, whereas on occasion, one may need to stop crystalloid infusion but continue blood perfusion, so as to avoid compromising

myocardial oxygenation. Cardiac activity during the period of aortic clamping, e.g., rippling movements, are most likely related to excessive intracellular K^+ concentrations. It is therefore preferable to be able to interrupt or reduce the flow of KCl to abolish these movements and to facilitate electromechanical reactivation of the myocardium.

b) Increase myocardial O_2 delivery

The factors that influence myocardial oxygenation are as follows[377]:

(i) cardioplegic flow and its distribution in the capillary bed. The coronary flow should always be at its maximum with respect to the pressure values and ensure homogeneous perfusion;

(ii) the diffusion parameters existing between the capillary bed and mitochondria; and

(iii) the quality of blood used as the O_2 carrier[378]. Myocardial oxygen delivery (MVO_2) is the volume of O_2 delivered to the myocardium per minute and is the product of the oxygen content in the arterial blood (O_2 cont) multiplied by the coronary flow. The O_2 content should always be at its maximum since the MVO_2 of a heart is variable and cannot easily be determined. Since coronary flow is optimized during the aortic cross clamping period, the only tool to augment the O_2 content is to increase the concentration of hemoglobin. Thus, the higher the level of hemoglobin in the cardioplegic perfusion, the better the myocardial oxygenation.

c) Reduce hemodilution

Another major pitfall of the original technique is systemic hemodilution. The detrimental effects of this phenomenon are two-fold. Continuous cardioplegic inflow leads to progressive systemic dilution which may be important during long periods of aortic cross clamping. The onset of hemodilution reduces blood viscosity and thus systemic resistance, requiring further infusions of supplementary crystalloid solutions and the use of vasopressive drugs to maintain perfusion pressure above 65 mmHg. It may also be necessary to induce diuresis and/or utilize hemofiltration. On the other hand, 20% (4:1 ratio) reduction in hemoglobin level in blood cardioplegia may potentially affect myocardial oxygenation through reduced O_2 delivery.

d) Increase oncotic pressure

Continuous coronary perfusion with 4:1 blood and crystalloid solution, progressively reduces the oncotic pressure of blood cardioplegia, thereby increasing the risk of myocardial edema[379]. Moreover, priming of the CPB circuit is performed with an asanguineous solution that further reduces the oncotic pressure. To prevent or mitigate the development of myocardial edema, it is necessary to reduce hemodilution.

e) Reduce the secondary effects correlated to continuous perfusion of Fremes solution

It was noted that continuous infusion of Fremes solution without sodium chloride (NaCl) and containing 250 mmol/L dextrose would induce dilution-related hyponatremia as well as hyperglycemia, mainly during long aortic cross clamping periods. Different teams have reported increased neurological accidents after normothermic cardiac surgery

and have postulated that both hyperglycemia and hyponatremia may be risk factors[380]. It is well known that dextrose and insulin concentrations are increased in normothermic, relative to hypothermic, bypass but continuous cardioplegic infusion containing 5% dextrose will only amplify hyperglycemia.

The proposed technique: Continuous non-diluted myocardial perfusion

To enhance the efficacy of this new concept, a different system for cardioplegia delivery was developed that should reduce or avoid the above mentioned drawbacks[381]. The potassium and magnesium concentrations were maintained as initially described by Salerno et al., but modifications were made to the mode of administration. These modifications are:

(i) Use of blood directly from the oxygenator for myocardial perfusion;

(ii) use of a syringe pump for infusion of potassium chloride solution directly into the cardioplegic line; and

(iii) avoidance of a heat exchanger in the cardioplegic circuit.

Description of the cardioplegia delivery system

The system of double tubing and heat exchanger is eliminated and replaced with tubing that withdraws oxygenated blood from an arterial line via a calibrated roller pump. The cardioplegic components are distributed in two syringes: one contains 20% KCl and the other 10% magnesium sulfate ($MgSO_4$). The syringes are mounted on two electronic syringe infusion pumps which allow the injection of the cardioplegic components into the

cardioplegia line at controlled flows. This separation is dictated by the fact that serum potassium is the most important element in cardioplegia and its injection needs to be modulated, while the concentration of $MgSO_4$ is identical in both Fremes solutions. The systematic utilization of citrate-phosphate dextrose (CPD) has been abandoned and is employed only in emergent surgery for acute myocardial ischemia to reduce the concentration of ionized calcium, as described by Allen et al.[382].

a) Potassium (S1)

The control of cardioplegic K^+ depends on several elements. First, two different K^+ concentrations, e.g., "high" (25 mM) for cardiac arrest and "low" (12 mM) for maintenance of arrest. Secondly, the K^+ concentration should be easily and rapidly adjustable. Thirdly, the K^+ concentration should be adjusted according to the serum potassium level. By applying the Lavoisier Principle of Conservation of Mass for the K^+ pump, the infusion rate at a given cardioplegic roller pump output was obtained using the following formula:

$$q_1 = \frac{60 . Q . (p - k)}{K - p} \qquad \text{(i)}$$

Where:

q_1 represents the estimated rate of infusion of undiluted KCl into the blood cardioplegia line in mL/h;

60 the conversion factor of mL/min to mL/h;

Q the oxygenated blood output from the cardioplegia pump in mL/min.;

p the desired concentration of K^+ in the blood cardioplegia ($p_1 = 25$; $p_2 = 12$);

k the patient's serum K^+ expressed in mmol/L;

K the concentration of K^+ in the undiluted KCl solution.

Based on this formula, nomograms were calculated to determine the infusion rate of potassium as a function of these different parameters. This allows modifications or even stopping the infusion rate, to take into account systemic potassium (monitored regularly during the cross clamp period), to select the cardioplegic K^+ concentration, and to choose the amount of K^+ that needs to be injected. If cardiac activity resumes during maintenance cardioplegia, the infusion rate of p_2 is enhanced to 16 mmol/L by augmenting the infusion rate of KCl (q_1) within a few seconds. By using this modality of injection, Lessana et al. reduced the dose of KCl injected, systemic potassium overload, administration of hypokalemic drugs and the time of circulatory assistance and hemofiltration. Cardioplegic potassium was thus maintained almost constant during aortic cross clamping, could be adapted to various patients, and readjusted in the event of electromechanical activity or snaky movements of the heart, and could be progressively reduced before declamping to facilitate the reappearance of myocardial contractility.

b) Magnesium (S2)

The output of S_2 (q_2, mL/h) containing $MgSO_4$ at 10% is correlated to the oxygenated blood output from the cardioplegia pump (Q, mL/min) according to the following formula:

$$q_2 = 0.48 \cdot Q \qquad \text{(ii)}$$

Where 0.48 represents the factor which permits a Mg concentration of 6 mmol/L in the blood cardioplegia. The major advantages are:

(i) it increases the cardioplegic activity of potassium;

(ii) reduces the dose of KCl and the intracellular uptake of calcium[383];

(iii) eliminates the need for CPD; and

(iv) corrects for hypomagnesemia, almost always present in cardiac surgery and responsible for significant post-op morbidity[384].

For acute ischemia cases, the composition of S_2 is modified to obtain a reduction in ionized Ca^{++} by adding CPD to a 10% solution of $MgSO_4$ in a 3:1 ratio.

Aerobic, normothermic cardiac arrest approximates physiological conditions more closely than traditional methods employing hypothermia. The method proposed by Salerno et al. offers greater tolerance for prolonged aortic cross clamping and allows for longer and complex operations[385,386] on compromised myocardium by eliminating ischemia, post ischemic reperfusion injuries and their related sequelae. This new delivery system further improves and enhances the advantages of the warm technique reducing hemodilution, hyperglycemia, and hyponatremia. It also offers a better control over

serum potassium and optimizes myocardial oxygenation during the aortic cross clamp period.

The Miniplegia technique was used in our experiments described later in pigs under extra-corporeal circulation. The use of esmolol as a cardioplegic agent evolved from the same concept of undiluted cardioplegia or Miniplegia. The only difference between the two techniques is the replacement of potassium by esmolol.

2.3.5. Most Recent developments in Myocardial Protection Techniques and Future Trends

Cardiac surgery as a whole has been changing at a very rapid pace. New conduits, grafting techniques, access incisions, and myocardial protection strategies have been proposed, including alternative cardioplegic agents. Esmolol as a cardioplegic agent is one of these new strategies that has already found its way into clinical use. One of the initial reports was that of Sweeney and Frazier who introduced the concept of Minimal Myocardial Contraction (MMC) and reported the use of esmolol injected systemically to reduce heart rate and motion under partial bypass[387]. Melhorn et al. have shown that MMC also helps lymphatic drainage of the heart during the period of arrest, and reduces myocardial edema and contractile dysfunction upon separation from bypass[388, 389]. Our first contribution was reported in 1995[390]. Promising results led to the work performed in the large animal model (pig)[12] that are detailed further in this manuscript. The idea of

minimal myocardial contraction has also led surgeons to use left-ventricular assistance devices (using femoral artery and vein cannulation) rather than the full-circuit setup, thus avoiding the use of oxygenators and the side effects thereof [391,392].

The MIDCAB technique is another surgical technique in which myocardial revascularization is accomplished through a small anterior thoracotomy and esmolol is titrated to reduce heart rate and motion without compromising cardiac output[393, 394, 395]. A more recent technique that is still in its infancy is the video-thoracoscopic technique in which only 3 small ports are made in the thoracic wall and the operation is performed from the outside of the body via telescopic instruments. This however is yet to become more popular mainly due to the technical challenges involved in performing delicate anastomoses on a beating heart and using telescopic instruments.

Esmolol may prove useful with virtually all these techniques that require an easily tritrable agent to reduce, for short periods of time, motion of the heart for surgical utility, facilitating the completion of delicate sutures.

2.4 Magnetic Resonance Spectroscopy (MRS) as a Tool for Studying Biological Systems

The major MRS characteristic that makes it attractive as a tool for studying biological systems is its non-destructive nature. The use of MRS allows *in vivo* observations, avoids loss of information associated to the disruption of cellular integrity (required for most other analyses) and allows the time course of a metabolic process to be followed within a single preparation. In addition, the refinement of several experimental techniques available today has made MRS a quantitative method of analysis able to measure many biomedically important metabolites and assess changes in their content under different conditions, within the same experiment. Magnetic resonance spectroscopy can also be used to measure steady-state levels, rates or fluxes through specific biochemical reactions, and is suited to many experimental models, such as bodily fluids and intact organs *in vitro* (such as the isolated heart preparation) and *in vivo*. Despite great improvements in hardware, software, data acquisition/processing methods and experimental techniques, the most important limitations of MRS are its sensitivity and resolution.

In this section, the basis of the NMR phenomenon will be described briefly followed by a discussion of the most biomedically important MR sensitive nuclei and the biochemical parameters they can measure. Emphasis will be placed on the nuclei used in this work (phosphorus, rubidium, and lithium) and a background on how information can be extracted from these strategies will be provided.

2.4.1. The Nuclear Magnetic Resonance Phenomenon

2.4.1.1 Historical Note

The phenomenon of magnetism was known in antiquity, its first mention occurred in the Greek literature dating back to 800 BC, its name probably being derived from that of the province of Magnesia where it was first observed. The earliest European reference dates from the 13th century, but the explanation of how and why a compass would resolutely keep its North-South alignment independent of any other conditions started to emerge only in the last century, with the observations of Romagnosi (1802) and Ørsted (1820), who made the first link between electricity and magnetism. After the publication of Ørsted's work, a bustle of research was started with fundamental contributions from Ampère, Weber, Faraday, Maxwell, Hertz, Curie, and others. From a spectroscopic standpoint, the work of Sir Isaac Newton on the prism, which separated light in different colours, started what is now known as Spectroscopy and deals with the interaction of eletromagnetic radiation and matter.

Einstein's special theory of relativity with the aid of the quantum theory set the grounds for elucidating the magnetic properties of materials. Many important contributions regarding electronic and protonic angular moment (spin) were made by Compton (1921), Goudsmit and Uhlenbeck (1925), Pauli (1924) and Dirac (1928). The detection of nuclear magnetism in solid hydrogen was accomplished in 1937 by Lazarew and Schubnikow and electronic magnetism was confirmed by Zavoisky in 1944 with the aid of resonance techniques. In 1946, in the United States, Bloch and Purcell independently announced the first observations of nuclear magnetic resonance in bulk material for which they were awarded the Nobel Prize in 1952[396,397].

Physicists were interested in the NMR phenomenon mainly as a physical phenomenon. Chemists and physico-chemists raised the level of interest in using high resolution MR techniques for studies of biological problems. In 1973, Moon and Richards[398] measured intracellular pH of red blood cells and Hoult et al.[399] Demonstrated that MR spectra could be obtained from isolated skeletal muscle. Magnetic resonance spectroscopy is still a very useful tool today for structural molecular analysis and protein conformation.

2.4.1.2 The Basis of the NMR Phenomenon

The NMR phenomenon is specific to certain atoms, more specifically, certain nuclei. The fundamental requirement for the NMR phenomenon to be observed in a certain type of material or compound is that the atomic nuclei must have an angular momentum, in other words, spin. Many are the species that fulfill this requirement, including the most popular and abundant, hydrogen (other important nuclei are ^{7}Li, ^{13}C, ^{14}N, ^{15}N, ^{17}O, ^{23}Na, ^{31}P, ^{39}K, ^{87}Rb). The nucleus of hydrogen spins about its own axis (the z axis) and according to quantic determinations its spin = 1/2. In nature, Hydrogen atoms have their nuclei spinning in random directions. When a magnetic field is applied to a sample containing these nuclei (for example, water) they will align with or against the lines of force of the magnetic field (B_0). These two orientations have slightly different energies, the energy difference is proportional to the magnitude of the applied magnetic field. The Boltzmann's Law describes the spin population ratio between the energy levels:

$$N_1/N_2 = e^{-\Delta E / RT}$$

Where: N_1 and N_2 are the different energy levels,

ΔE is proportional to the strength of the magnetic field,

R is the universal constant of Planck and

T represents temperature.

The time constant which characterizes the return of magnetization to the equilibrium after excitation is represented by T_1. Because T_1 involves a loss in the energy status of the nucleus it is also known as the *spin-lattice relaxation time*. Each atomic species (or each nucleus) has its own spinning frequency. Larmor described in 1897 that the application of any aligning force to a spinning object causes this object to move in a circular motion known as *precession* equivalent of that of a child's top when it slows down. In the case of the top, the aligning force being applied is gravity. The concept of *Larmor Frequency* is then particular to each and every nucleus and is directly proportional to the intensity of the magnetic field applied to the sample. This constitutes the most important relationship in MR and is described mathematically by the expression:

$$\omega = \gamma . B_0$$

Where ω is the Larmor Frequency;

γ is a proportionality constant known as the magnetogyric ratio of each nucleus;

B_0 is the strength of the magnetic field.

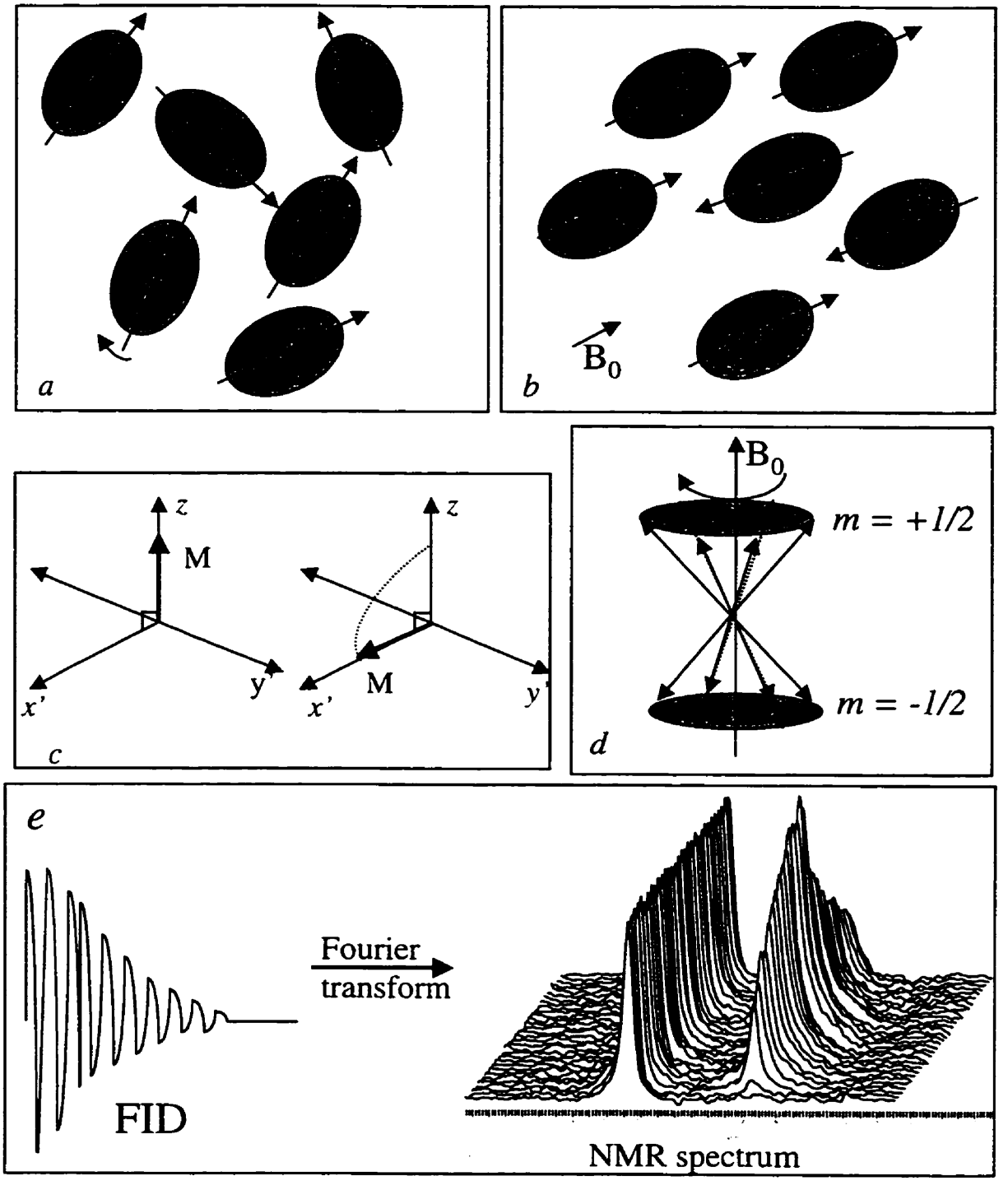

Figure 2.3 - The MR phenomenon in a nutshell (see text for a more detailed explanation). a), spinning (NMR sensitive) nuclei existent in nature; (b), these nuclei placed under a magnetic field B_0 where they align in a parallel or anti-parallel orientation to the lines of force of the field; (c) the bulk magnetization vector M is tipped with an rf pulse and (d) the movement of precession along the Z axis in a nucleus of spin 1/2; (e) the NMR signal is captured by the coil, accumulated, filtered and amplified, and is received as an FID (free induction decay). The application of Fourier transformation transforms the signal from the time domain to frequency domain and the result is an NMR spectrum.

The Larmor frequency is typical of each species and will vary according to the strength of the magnetic field used. For example, the ω for hydrogen (proton) at 8.7T is 360 MHz; at 11.7 T it is 500 MHz. It is possible to apply another magnetic field that is perpendicular to and rotates about the z axis with equal frequency to the Larmor frequency, defined as B_1[369]. The rotating field B_1 may be generated by an oscillating field, such as an oscillating electromagnetic frequency or radio frequency (rf), along the z axis and at the Larmor frequency. A pulse applied from a nearby transmitter/receptor at the nucleus' Larmor frequency will cause the spinning nuclei to precess and to tip the bulk magnetization vector M towards the x-y plane, about B_0 at ω_0 and causes an electromotive force (e.m.f.) to be induced in the coil of the probe that surrounds the sample. The return of the nucleus to its initial position induces voltage in the receiving coil and is the basis of the NMR signal. This signal is captured by the antenna (transmitter/receiver coil) and fed to a computer. A coil is, in essence, a loop of wire that encompasses or is attached to the sample with its axis perpendicular to the axis of B_0. Typical coils consist of a number of wrappings of wire and may incorporate capacitors for tuning and optimizing the field homogeneity.

The electromotive force that is generated induces current in the coil and oscillates at ω_0. According to Faraday's law of magnetic induction, its magnitude depends on the amount of net magnetization, which is proportional to the concentration of the nuclei of interest in the sample. As soon as nuclei start precessing in the x-y plane, there is a natural decay representing the transverse relaxation, caused by spin-spin interaction. This period of time can be measured and is called the *transverse relaxation time constant* or T_2, and is specific to each nucleus. The signal detected by the coil is amplified and

digitized in the spectrometer. This signal is called *free-induction decay* (FID) and represents the initial e.m.f. induced by the magnetization precessing in the *x-y* plane with a decay approximately equal to T_2. The FID is an exponential function in which T_2 is the time constant. In order to separate the different components of the FID, a mathematical conversion process known as Fourier transformation is performed. The Fourier transformation is a set of equations that allows the mathematical transfer of data from the time domain signal (FID) to the frequency domain (spectrum).

Because the resonance frequency (or Larmor frequency) is also proportional to the local magnetic field experienced by the nucleus and is also affected by the electrons, nuclei in different chemical environments will give rise to signals at slightly different frequencies. This separation of different resonance frequencies is called the *chemical shift*, and is expressed in dimensionless units of parts per million (p.p.m.) that do not vary with the intensity of the magnetic field.

2.4.2 The NMR spectrum

Each line of the NMR spectrum has a shape and amplitude determined mainly by two factors: field homogeneity (instrumental factor) and properties of the sample (molecular factor). Some nuclei will normally present broader lines in the solid state than in the liquid state. This is due to the restricted molecular mobility in the solid state. Small molecules, such as metabolites and ions, are better observed in the NMR spectrum in solution or in the cytoplasm than if they are bound to macromolecules or cellular structures.

In a general manner, the areas or intensities of the signals within a spectrum are proportional to the number of nuclei that contribute towards them. Other factors may affect these measurements such as saturation effects, the nuclear Overhauser effect (important in low magnetogyric ratio nuclei such as ^{15}N and ^{13}C and represents a change in the relative population of spin states), pulse widths and other factors related to the electronics of the spectrometer. Under optimal conditions these factors have negligible effects. The peak heights and areas beneath the peaks in an NMR spectrum are commonly measured by integration of a Lorentzian lineshape which better models the NMR signal. Alternative methods may include plotting the spectrum on graph paper and counting the number of squares underneath the peaks or cutting out the peaks and weighing them. Nowadays with processing software available in personal computers, data processing and analyses have become faster and easier. However, estimating the area of a Lorentzian lineshape still causes problems in practice, mainly due to imperfections caused by inhomogeneities in the magnetic field and other spin interactions, noise, and sloping baselines. Several mathematical approaches have been developed to 'correct or compensate' for these imperfections, but because of many uncertainities, a margin of ± 10% in the accuracy of measurements of peaks areas/heights is generally accepted. If the intent is to compare changes in the intensity signals, a reference substance (the signal of which will not vary over time) is normally used and data are expressed as a percentage of the initial values relative to the reference. These techniques allow identification of substances and/or its functional groups, and establish measurements of amounts or relative concentrations, but do not provide absolute measurement values.

To obtain absolute concentrations of a compound it is necessary to adopt a calibration procedure whereby the signal intensity is compared to that of a known quantity of a reference compound. In living systems, however this calibration is much more complicated because of the difficulties in estimating volume of cells and tissue that contribute to the NMR signal.

2.4.3 Limitations and Sample Requirements - Signal-to-Noise Ratio (SNR)

The principal advantage of MR spectroscopy as a technique for biomedical studies is its non-destructive nature. Samples may be examined repeatedly and each sample can serve as its own control. However, compared to most techniques used in biochemistry or molecular biology, the quantities of material required for MR studies are very large. Studies carried out in living systems are normally performed on solutions where molecules are mobile (metabolites in biological tissue) under conditions known as high resolution. For this, MR spectroscopic studies are easier at high magnetic fields (as high as 11.7 T) whereas MR imaging techniques may be performed easily at 1.5 T of field strength. This is due to the fact that the water signal used in MR imaging is so intense. Because biological molecules are present at low concentrations in tissue, they produce weak signals, and so it is usually necessary to improve the quality of the signal by accumulating a number of observations (known as scans).

A major disadvantage of NMR is its inherent lack of sensitivity, which can be expressed in terms of the signal-to-noise ratio of the spectral lines and is described by:

signal-to-noise ratio = signal height / peak-to-peak noise

The signal-to-noise ratio depends upon a wide range of factors including:

- (i) the nucleus that is being studied and its relative sensitivity;
- (ii) the volume of the sample;
- (iii) the magnetic field strength, B_0 of the spectrometer;
- (iv) the design of the spectrometer, particularly of the radiofrequency coil;
- (v) the time over which the spectra are accumulated;
- (vi) the width of the spectral lines;
- (vii) the relaxation times T_1 and T_2;
- (viii) the extent of isotopic enrichment (in the case of ^{13}C, ^{15}N and ^{17}O MR spectroscopy);
- (ix) the concentration of nuclei under investigation.

To improve the signal-to-noise ratio of the spectral lines, one can simply increase the number of observations. The accumulation of N responses leads to improvement of the signal because it increases by a factor of N whereas the noise, being random, increases by $\sqrt{N}$. Thus the process is repeated a number of times at intervals that depend on the relaxation times of nuclei of interest. For nuclei known to have broader spectral lines (for example, rubidium ^{87}Rb MRS), a very large number of scans may be required to obtain a good SNR, whereas for narrower linewidths (such as ^{1}H MRS) a lesser number of repetitions may be required.

Other disadvantages of the use of MR in biological systems include the requirement for large samples (and length of time for data accumulation), the technique is

limited to MR active nuclei and it is relatively expensive. MR spectrometers and scanners are typically large instruments in order to house the superconducting coils that generate the strong magnetic field. Moreover, to maintain the coils superconductive and not have the magnetic field decay, large tanks filled with liquid helium and liquid nitrogen are placed surrounding the superconductive coils to maintain the cold temperatures required for superconduction. These tanks have to be kept constantly filled and regular maintenance of the magnet is crucial for its functioning, which also increases costs.

2.4.4 Observable Nuclei and Their Biological Applications

Table 2.1 lists the nuclei most commonly used for MR spectroscopy in living systems along with their NMR properties and what they can measure.

Magnetic resonance spectroscopy allows continuous monitoring of transmembrane ionic flow and cellular energetics under a variety of conditions including ischemia, in response to work, stress and drugs. Moreover, based on comparisons of control and experimental situations, one can infer mechanisms of actions of pharmaceuticals and upon removal of the drug, monitor the return to the initial (control) situation. Metabolites such as ATP, phosphocreatine (PCr) and lactate will have their levels altered as a consequence of ischemic oxygen deprivation. The measurement of one or more of these compounds can provide an almost instantaneous picture of the metabolic state of the cell, tissue or organ.

- ^{1}H MRS

Despite its abundance in biological systems, ^{1}H MRS spectra of biological samples are difficult to obtain due to the strong resonance arising from water that hides the weaker signal arising from metabolites and other hydrogen-containing compounds in solution. This problem may be alleviated by saturation of the water resonance. While proton MRS has shown a great potential for diagnosis of cancerous cells in tissue or tissue extracts obtained from prostate, cervix and colon[400,401,402], its most important application has been in studies of the brain.

- ^{2}H and ^{3}H MRS

Deuterium has an extremely low natural abundance and low detection sensitivity, but has been useful in studies of fluid flow, where D_2O is substituted for H_2O, as well as to measure concentration and metabolism of drugs in vivo[403,404]. Tritium with an extremely low natural abundance but high detection sensitivity has been used in studies of metabolism, but its applications has been complicated by difficulties in synthesizing ^{3}H-labelled compounds and in handling of radioactive compounds[405].

- ^{14}N and ^{15}N

These nuclei have not been extensively used in biomedical NMR mainly due to their low natural abundance (^{15}N) and large linewidths (^{14}N). They can however be used in tracer studies by means of enriched compounds[406]. Recently, they have been used to measure ammonium production in tumours[407].

- ^{19}F MRS

Despite its excellent detection sensitivity, fluorine does not occur in any significant number of natural compounds nor is it present at high concentrations in biological tissues. Its principal use has been as an intracellular calcium indicator[408] and for detection of fluorine-containing pharmaceuticals. It has also been used to measure intracellular pH *in vivo* and for assessing tumour vascularity[409,410].

- ^{13}C MRS

Due to its wide range of chemical shifts, ^{13}C offers a great potential for studies of specific compounds *in vivo*. In combination with specifically labeled compounds, ^{13}C MRS is a useful technique for evaluation of intermediary metabolic pathways[411]. Carbon-13 MRS can also be used to study glycogen metabolism in human liver, in which the rates of synthesis and utilization of glycogen can be continuously monitored[412].

- ^{35}Cl MRS

The ^{35}Cl nucleus has a large quadrupole moment which leads to very broad spectral lines. In addition, it also suffers from low detection sensitivity despite its natural abundance. Although it has been little used so far, it has the potential for the study of chloride ions or extracellular volumes[413].

- ^{31}P MRS

Phosphorus MR spectra of living tissues generally show resonances for ATP, phosphocreatine (PCr), and inorganic phosphate (Pi); resonances arising from NAD(H), phosphomonoesters (PME) and phosphodiesters (PDE) may also be observed. These characteristics have made ^{31}P the most popular nucleous for metabolic studies using MR spectroscopy. The chemical shift of Pi is also a reliable indicator of intracellular pH. In the absence of a reference compound, this shift can be measured with respect to the resonance of PCr in tissues such as the brain, heart and skeletal muscle. In living tissue, inorganic phosphate predominantly exists as either HPO_4^{2-} or $H_2PO_4^-$. In solution, these two forms give rise to one resonance (because they exist in rapid exchange between the two forms) which is sensitive to pH. From a standard titration curve the chemical shift may be compared and the pH calculated. The pH-sensitive range for the chemical shift of the Pi peak lies within that of greatest interest for biological species, between pH values of 6.0 to 8.0 [371]. The magnitude of the 3 peaks of ATP (representing each of the phosphorus nuclei in the α, β and γ positions in the ATP molecule) and PCr provide a measurement of the energetic status of the sample, and are sensitive to pathological and pharmacological stress[414]. All three ATP phosphates have unique chemical environments resulting in clear separation of their chemical shifts. In addition, two resonances of ADP merge with both γ– and α–ATP resonances. The NAD resonance appears as a shoulder on the α–ATP resonance. Thus, the γ–ATP peak is comprised of γ–ATP and β–ADP, whereas the α–ATP peak consists of α–ATP, α–ADP and NAD. The β–ATP peak is considered the most "pure" with less than 5% contribution from other nucleotide triphosphates and for this reason is the marker used to quantify ATP in a sample[415]. The resonances of PME and PDE are also of interest with respect to rapidly-growing

tumours[416]. The usually long relaxation times (T_1 = 1-5 s) of phosphorus compounds in tissue may necessitate long recycle times and limit temporal resolution.

- ^{23}Na MRS

Of high natural abundance and good MR detection sensitivity ($[Na^+]_o$ = 135-140 mM and $[Na^+]_i$ = 5 mM), ^{23}Na can be considered relatively easy to observe using MRS. The interest of biologists however, is to estimate intracellular levels of Na^+ and observe changes in the transmembrane flux of Na^+, which is sensitive to metabolic stress and the effects of various drugs. To separate these resonances, scientists use paramagnetic molecules that bind Na^+ and shift its resonance in the spectrum upfield approximately 5 ppm. These molecules include lanthanides such as dysprosium triethylenetetraaminehexaacetic acid ($DyTTHA^{3-}$)[417] and thulium Tm-1,4,7,10-tetraazadodecane-N-tetramethylphosphate ($TmDOPT^{5-}$)[418]. These molecules, under normal conditions do not cross the cell membrane and bind reversibly to monovalent cations such as Na^+, K^+ and Li^+ which results in a shift of the resonances displayed in the spectrum. This shift occurs because the cation is in rapid exchange between bound and free states, and experiences two distinct chemical environments. Thus, the acquired signal represents an average of both chemical environments surrounding the ion. Because of toxicity considerations, the concentrations in the perfusate of these substances should not be above 10 mM.

Not all Na^+ is visible to MRS, which makes quantification more difficult than other methods. The ratio of the quantity measured by MRS relative to other methods detecting the total amount is called the *visibility factor*, which may vary between 0.4 and

1.0. The reasons these differences exist are due to the type of molecular bonds and peculiarities in the relaxation times of these nuclei. Na^+ in solution is a free ion and therefore is not involved in a molecular bond. In living organisms, however, Na^+ binds to charged molecules through ionic interactions which restrict its motion and causes linebroadening as a result of its quadrupolar mechanism of relaxation.

- ^{39}K MRS

With much lower intrinsic sensitivity and a higher quadrupolar moment, ^{39}K is much more difficult to observe than ^{23}Na, which makes ^{39}K MRS much less attractive as an investigational tool. Shift reagents can also be used to observe ^{39}K. Its short relaxation times (< 50 ms) allow for rapid pulse repetition times; however 4-5 minutes may be required to achieve a good quality spectrum with an acceptable signal-to-noise ratio from a 1g perfused rat heart.

- ^{7}Li MRS

Lithium is a partial congener of Na^+. It replaces Na^+ in several inward and outward transporters but not Na^+ in the Na^+/K^+ ATPase and Na^+/Ca^{++} exchanger[419,420,421]. Thus, Li^+ is an accepted probe ion for evaluating activity of the Na^+ channels, the Na^+/H^+ exchanger and the $Na^+/K^+/2Cl^-$ co-transporter[422]. Lithium contains two isotopes, ^{7}Li and ^{6}Li; the first has a high relative NMR sensitivity and a high natural abundance. Shift reagent aided ^{7}Li NMR has been used to measure ^{7}Li relaxation times in frog and rat hearts[423,424]. However, the Li^+ concentration (78 mM) used in these experiments was beyond any physiological range. The use of lower concentrations of Li^+ was precluded by

a significant decrease in chemical shift difference between the extracellular (shifted with shift reagent) and intracellular (unshifted) $^{7}Li^{+}$ signals arising from the competition between Li^{+} and Na^{+} for binding to the shift reagent. In the experiments described below, a moderate concentration (15 mM) of Li^{+} was used without shift reagents. This is now an accepted and routine method to assess the effects of drugs on the kinetics of Na^{+} channels[391]. In general, the rate of Li^{+} efflux and its kinetics depend on the following factors: (a) the $[Li^{+}]_i/[Na^{+}]_i$ ratio; (b) the membrane potential (driving force); (c) the heart rate; and (d) the number of channels available and their functional state (activated, resting and inactivated[425]). The largest fraction of Li^{+} efflux from cardiac cells is mediated by voltage-dependent channels and not via the $Na^{+}/K^{+}/2Cl^{-}$ co-transporter or the Na^{+}/H^{+} exchanger[391].

- ^{87}Rb MRS

Rubidium is a well established congener of potassium[426,427,428,429]. The rates of influx and efflux of Rb^{+} have been measured in living tissues and isolated cells by the radioisotope technique, atomic absorption spectrometry, and nuclear magnetic resonance spectroscopy[430,431,432]. Magnetic resonance spectroscopy is the analytical tool of choice for these experiments because of its non-invasive nature. The relatively high natural abundance, low biological abundance, and high NMR sensitivity of ^{87}Rb make it a good tracer for NMR studies of K^{+} kinetics [433, 434]. Rubidium influx data can be approximated to K^{+} if there is no ion selectivity in the different K^{+}-transporting systems. Rubidium replaces K^{+} in the Na^{+}/K^{+} ATPase and in the $Na^{+}/K^{+}/2Cl^{-}$ co-transporter. This has been characterized in isolated chicken, rabbit, and neonatal rat cardiomyocytes, however its

relative contribution to K^+/Rb^+ uptake in the adult rat heart remains unclear[435,436,437]. Potassium channels also account for the influx of Rb^+ because of the inwardly directed electrochemical gradient at the beginning of Rb^+ uptake experiments in cardiomyocytes. With regard to the Na^+/K^+ ATPase, the kinetic properties of K^+ and Rb^+ are similar in cardiac and skeletal muscle, nerves, red cells and other tissues. A direct comparison of ^{86}Rb and ^{42}K fluxes in human erythrocytes revealed identical uptake rates[395]. Further, Rb^+ quantitatively replaces K^+ in electrophysiological determinations of Na^+/K^+ ATPase activity in cardiac tissue and its equilibrium transmembrane potential is similar to that of K^+. This suggests similar ion selectivity of these inward transport systems (Na^+/K^+ ATPase, $Na^+/K^+/2Cl^-$ co-transporter and K^+ channels) but also outward transporters ($Na^+/K^+/2Cl^-$ co-transporter and K^+ channels). Data available from other mammalian cell types show that Rb^+ is quantitatively similar to K^+ in its interactions with the $Na^+/K^+/2Cl^-$ contransporter[438,439,440]. This also seems true for K^+ channels[399].

Table 2.1 - MR properties and applications of biologically important MR-sensitive nuclei

Nucleus	MR frequency at 8.4 T (in MHz)	Natural abundance (%)	Detection sensitivity at constant field	Spin	Biochemical parameters measured
^{1}H	357.64.68	99.9844	1.00	1/2	Lactate, lipid, N-acetyl aspartate
^{2}H	54.9024	0.0156	0.00964	1	Water flow, metabolic products of ^{2}H-labeled compounds
^{3}H	381.4776	?0	1.21	1/2	metabolic products of ^{3}H compounds
^{7}Li	138.9948	92.57	0.294	3/2	Li^{+} influx and efflux (congener for Na^{+})
^{13}C	89.922	1.108	0.0159	1/2	Metabolic products of ^{13}C-labelled compounds
^{14}N	25.8384	99.635	0.00101	1	Ammonium ion, amino acids
^{15}N	36.25104	0.365	0.00104	1/2	Ammonium ion, amino acids
^{17}O	48.5016	0.037	0.000108	5/2	Water flow
^{19}F	336.462	100.0	0.834	1/2	Metabolic products of ^{19}F-labeled drugs, intracellular free Ca^{2+}

					levels
^{23}Na	94.6008	100.0	0.0927	3/2	Intra- and extracellular Na^+ levels
^{31}P	149.9445	100.0	0.0664	1/2	ATP, inorganic phosphate, phosphocreatine, phosphomonoesters, intra- and extracellular pH
^{35}Cl	35.0448	78.54	0.00471	3/2	Extracellular Cl^- levels, extracellular volumes
^{39}K	16.6908	93.08	0.000508	3/2	Intra- and extracellular K^+ levels, K^+ equilibrium potential
^{87}Rb	117.0288	27.20	0.177	3/2	Rb^+ efflux and influx (congener for K^+).

2.5 Infrared Spectroscopy

2.5.1 Basic principles

Infrared radiation[441] is a form of electromagnetic radiation that occurs at frequencies (or wavelength [λ]) between 14,300 to 20 cm^{-1} (or 0.7 to 500 μm) in the electromagnetic spectrum. Infrared spectroscopy (IRS) is the study of the interaction of this type of electromagnetic radiation with matter. In the case of biomedical applications of IRS, the 'matter' in question may be tissue, cells, proteins, nucleic acids, drugs or metabolites.

The fundamental principle of IR spectroscopy is that its interaction with matter results in intra-molecular motion (IRS has also been described as absorption or vibrational spectroscopy). Infrared absorption frequencies and intensities of a molecule in the IR spectrum are directly related to the chemical functional groups present in the molecule. Specific (or "fingerprint") vibrational frequencies have been identified for different motions of specific chemical bonds, which will vary depending on the chemical and physical environment surrounding the bonds (such as temperature, pH, etc.).

From a physical point-of-view, the interaction between electromagnetic radiation and matter can be described as the transfer of energy from the radiation field to energy states of the matter or vice-versa, in a quantized manner. Theoretically, light radiation is considered as discrete packets (or "quanta") of energy called photons. Photons can be absorbed or emitted when an atom or molecule changes energy levels. The total energy of molecules can be considered as the sum of contributions from electronic, vibrational and rotational energies, and is expressed as:

$$E_{total} = E_{el} + E_{rot} + E_{vib}$$

The electronic energy is larger than the rotational and vibrational energies and normally involves energies corresponding to ultraviolet or visible radiation. The rotational and vibrational transitions involve energies corresponding to infrared radiation. Pure vibrational transitions are caused by the less energetic infrared radiation (1 to 15 μm), whereas rotational transitions require even less energy. Changes in the energy levels of a molecule will invariably translate into changes in electronic, vibrational and/or rotational levels of energy. A molecule may then jump from any of the vibrational and rotational levels when absorbing energy to a higher level or excited state. These energy levels are characteristic of the molecule and dependent on properties such as molecular identity, structure, and any chemical process undergone by the molecule.

Molecules in nature consist of many atoms connected by chemical bonds. In any given environment, atoms and their groups undergo complex vibrations, which can be observed at different frequencies. The normal vibration of a molecule involves simultaneous motion of atoms or functional groups within the molecule. The vibration of atoms of a molecule are closely related to the type of vibrating atoms, the forces of their interaction, and the structure of the molecule. A given structure will reflect the spatial arrangement of the molecule defined by symmetry properties.

The fundamental molecular modes of vibration include stretching, bending, wagging, rocking and twisting. The stretching vibration is associated with motion of atoms that cause stretching and shortening of the chemical bond. For a three-atoms system, the stretching motion can be classified as symmetric and asymmetric in nature. A

bending vibrational mode describes an in-plane motion of atoms during which the angle between bonds change; the wagging vibration is an in-phase, out-of-phase motion of atoms, while other atoms of the molecule remain in plane. Rocking vibration describes atoms swinging back and forth in phase in the symmetry plane of the molecule: and if the plane is twisted, then the vibration is called a twisting vibration.

It is possible to isolate a functional group containing two or more atoms for which the amplitude of a given normal vibration predominates over the amplitude of deflection of other atoms in the molecule. In this case, only this functional group participates in the vibration and the mode is assigned to it. This concept of characteristic vibrations provide an enormous practical significance for identification of functional groups in unknown molecules. Therefore it is possible to trace, identify and follow the formation of a given compound or molecule in a chemical reaction, if the vibrational characteristics (derived from the analysis of the IR spectrum) are known. The identification and quantification of specific compounds through the characteristic vibrations of functional groups and tracer molecules in bodily fluids is one of the major applications of IR spectroscopy to biomedical problems.

2.5.2 Instrumentation and Spectral Analysis

Fourier transform infrared (FT-IR) spectrometers are in common use today. The basic constituents of an IR spectrometer include an IR radiation source, a detector, the optical components and computing systems.

The optical arrangement of the FT-IR spectrometer is the so-called Michelson interferometer. It is composed of two adjacent mirrors that are used to produce the

optical signal which contains spectral information from the sample, called the interferogram. The interferogram is recorded in a finite path of optical intervals, and at small, uniform distance intervals. As with magnetic resonance spectroscopy, in order to obtain a spectrum, the acquired signal must be subjected to Fourier transformation. The result, are spectra in which signal intensity is plotted as a function of frequency.

The IR spectrum (or absorption spectrum) shows absorption (A) or transmittance (T) of radiation as a function of frequency. Infrared bands form different tones (the equivalent of the MRS resonances), and combination of tones and overtones in various frequency regions. Traditionally, an infrared band is characterized by the maximum band position expressed in wavenumbers, the position intensity (peak height) and the band half-width. Integration of the band's area is also often used as an analytical parameter.

Peak position is one of the most significant parameters in spectroscopic analysis. It provides frequency information for a particular type of vibration. A shift in the frequency indicates that the molecular structure has changed. The shift may also reflect changes in the chemical environment such as pH, temperature, etc. These characteristics of the IR measurement have been extensively used to study the structure of proteins and their changes in response to a variety of physical and chemical factors.

The maximal peak height (or peak intensity) can be used to determine the concentration of a particular compound in a mixture. Likewise, integration of the band area is often used in analytical chemistry. Alternatively, ratios of peak areas are used as measurable parameters.

The band half-width reflects intermolecular interactions. Increases in temperature affect interactions with adjacent molecules and are often used in the investigation of

biological molecules. Spectra of molecules are characterized by many difficult to resolve, broad and overlapping bands. Techniques such as Fourier self-deconvolution and peak fitting have been developed. Despite their wide application, their accuracy remains a matter of controversy. An alternative way to resolve overlapping peaks in a band is to use the second-derivative method, which mathematically performs the second derivative of the original spectrum, so that unobservable peaks become observable. This technique is powerful and has become popular. In biochemical analysis, where changes in chemical compositions are small and not readily observable, multivariate spectral analysis techniques along with least partial squares and other statistical methods have been used to assess discrete changes of biological fluids.

2.5.3 Biomedical Applications

Recent applications of IR spectroscopic techniques to biomedical problems[442] have suggested a strong potential for them to become accurate diagnostic tools in analytical chemistry. An advantage of IR spectroscopic analysis is that the measurements are not affected by the physical states of the sample: gaseous, liquid, homogenous and inhomogeneous solid samples all can be conveniently studied. Other advantages of using IR techniques in biochemical analyses include: (i) it is reagentless; (ii) little or no sample preparation is needed and minimal technical skills are required from the operator; (iii) the measurement is non-destructive; (iv) it is possible to obtain on-line or high-volume measurements and (v) the method has potential for a rapid multicomponent analysis to be carried out from a single measurement, once a calibration curve has been built. Thus, infrared technology has the potential to be applied to several aspects of biodiagnostics.

Qualitative and quantitative analysis of biochemical components, spectroscopic changes in molecular structures as diagnostic markers of morbid processes and the use of tracer molecules to assess kinetics and follow biochemical reactions or the effect of drugs are among the three most envisaged aspects of infrared technology [443].

2.5.3.1 Qualitative Analysis of Biochemical Components in Biofluids

Infrared spectroscopy offers a number of advantages for the analysis of bodily fluids. Unlike most calorimetric or electrochemical or enzymatic assays, IRS is applicable to a variety of biofluids including whole blood, plasma, synovial fluid, saliva, urine, etc. Quantitative analysis may also provide assessment of clinically relevant parameters in whole blood such as cholesterol and triglycerides levels as well as estimates of total protein content, creatinine, and urea in urine. Current investigations focus on defining the best spectral range for quantitative analyses, whether it be near-IR or mid-IR. Infrared bands in the near-IR region are combination and overtone vibrations arising from functional groups such as C-H, O-H, N-H moieties of molecules. The bands that dominate the mid-infrared region are fundamental groups in molecular backbones. The two regions carry different information content and a combination of these two modalities may increase the accuracy of measurements.

2.5.3.2 Structural Molecular Changes as Indicators of Disease

A dogma for many spectroscopists (MR included) is that all disease processes must be accompanied by changes in the biochemistry of the cells, tissues or organs affected. Any technique that provides information on the biochemical status of cells and tissues is

therefore a potential diagnostic tool. These changes must precede any morphological or symptomatic alterations upon which most diagnostics methods are currently based. Spectroscopic diagnosis should be, at least in theory, possible at a much earlier disease stage and consequently allow a much favorable outcome of treatment than is currently possible.

Because of the complexity of the IR spectra of biomolecules, identification of changes in spectral signature changes relies on sophisticated methods of statistical analyses. Cluster and multivariate analyses along with the development of pattern recognition software[444] have been the most successful approaches. Differential diagnosis of certain forms of leukemia and arthritis are the first examples of the potential use of this technique[445,446].

2.5.3.3 The Use of IR Tracers

In this IR modality, the selected tracer molecule has a unique or readily distinguishable infrared spectroscopic signature, such that it can be characterized among other components in the biological sample. This technique may provide both qualitative and quantitative information. The marker molecule may be internal or natural occurring in the biofluid matrix, or simply be added to the sample. An obvious requirement is that this molecule will not introduce artifacts or collateral effects in the diagnostic process. An example of a near-infrared active tracer is indocyanin green, which has recently been introduced as a cerebral blood flow indicator[447].

2.6 Pertinent Characteristics of Esmolol

Comprehensive reviews describing the pharmacokinetics and pharmacological properties of esmolol under different clinical and experimental conditions have been published[448,449,450,451]. This section will briefly discuss aspects of esmolol pharmacology, chemistry, and metabolism that are pertinent to the scope of this manuscript.

2.6.1 Pharmacological & Pharmacokinetics Peculiarities of Esmolol

Esmolol is a cardioselective β-receptor blocker (β_1 antagonist, $\beta_1/\beta_2 = 35$) with a very short duration of action (9-minute half-life), and is normally used in the critical care setting for treatment of angina pectoris, hypertension and cardiac arrhythmias, as well as to reduce reflex tachycardia during induction of anesthesia and endotracheal intubation[452,453]. Contrary to other preparations available in the market, the use of which was precluded due to long half-lives, esmolol is the first compound available for the critically ill population. Esmolol is easily titratable, cardioselective, with a rapid onset and termination of effect that provides an element of tolerability that was not previously available. More recently, it has proven effective in preventing sudden death after myocardial infarction[454]. The pharmacological concentrations used in patients are approximately 50-200 μg/kg/minute for maintenance infusions. Neither renal nor hepatic impairment significantly alters the pharmacokinetics of esmolol. Its electrophysiological and hemodynamic effects are characteristic of those of the other β–blockers. Its distinguishing feature is its ability to rapidly achieve steady-state β–blockade and the potential to tailor its dosage to the desired effect. The use of esmolol is particular well

suited to the critically ill population, anesthesia, and for surgical procedures requiring brief duration β–blockade.

Electrophysiologically, β–blockers are known to produce, alterations of sinus and AV node function, affect atrial refractoriness and QT interval and have no effect on ventricular conduction and refractoriness. Esmolol, given intravenously to patients[455] 500 μg/kg/min as a bolus for 5 minutes and at maintenance doses of 300 μg/kg/min for 8-40 minutes, prolonged the sinus cycle length, the AV nodal conduction time and AV nodal refractoriness as shown by an increase in the cycle length to Wenckebach. These are not different from the effects of other beta-blockers. The 12% prolongation of the sinus cycle length caused by esmolol is comparable to that of metoprolol (10%)[456], acebutolol (11%)[457], and sotalol (13%)[458], although it is less than that of timolol (24%)[459], and propranolol (28%)[460]. Similarly, the effect of esmolol on AH interval is equivalent to other beta-blockers. The effects on AV nodal refractoriness were generally less pronounced than those of other beta-blockers including timolol, but equally efficient in prolonging the effective or functional AV nodal refractory periods. Esmolol had no direct effect on atrial refractoriness, but this is not atypical of β–blockers.

Severe bradycardia and hypotension have been reported as the major adverse effects of esmolol overdose. These effects are ideal for inducing minimal myocardial contraction or heart arrest during cardiac surgery.

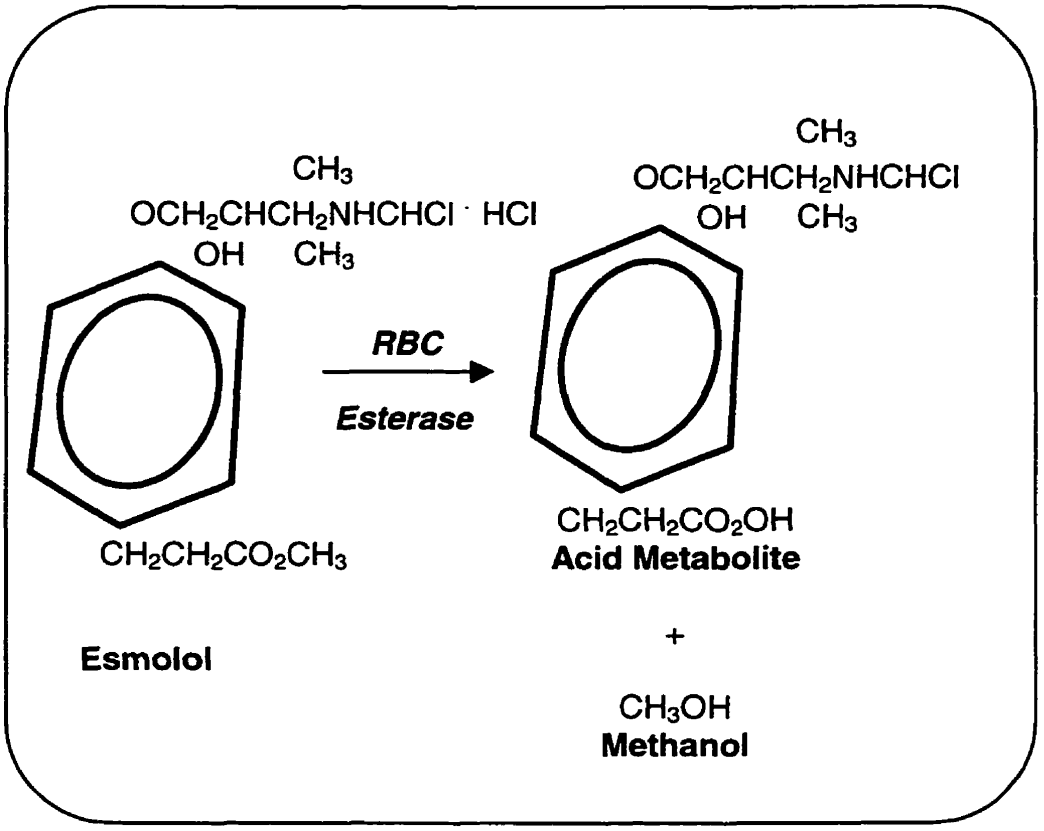

Figure 2.4 - The one-step reaction of the metabolism of esmolol in human blood catalyzed by esterases present mainly in the cytolsol of red blood cells. Esmolol is quickly metabolized into Methanol and its major metabolite, a propionic acid derivative at a 1:1 ratio. The acid metabolite is ~1500 times less powerful than esmolol and is excreted unmodified in the urine. Methanol is further metabolized into formaldehyde, formic acid and is excreted in the urine as NH_4^+.

2.6.2 Chemistry

Esmolol (Brevibloc®, Zeneca Pharma Canada, Inc.), methyl 3-[4-(2-hydroxy-3-[isopropylamino]propoxy)phenyl]-propionate - $C_{16}H_{26}NO_6Cl$, MW = 331.8 kD), is soluble in aqueous solutions and is structurally similar to metoprolol. The molecule of esmolol has an asymmetric carbon, and similarly to other β–blockers containing an oxypropanolamine nucleus, only (-) esmolol is active, whereas (+) esmolol is inactive as a β–blocker. Esmolol has an ethylene-extended methyl ester group in the para-position of the aryloxypropanolamine structure. The addition of the ester group renders the molecule susceptible to rapid hydrolysis by esterases present in the cytosol of erythrocytes to its acid metabolite (3-[4-[2-hydroxy-3- (isopropylamino) propoxy] phenyl] propionic acid) and methanol. There is evidence that esmolol may also be metabolized by tissue esterases[461,462].

2.6.3 Details of the Metabolism of Esmolol

Esmolol is rapidly metabolized by red blood cells cytosol esterases to an acid metabolite (Figure 3) and methanol. The specific enzyme involved in esmolol metabolism has not yet been defined. Very little is known about esterase activity of red blood cells cytosol enzymes. Studies have shown that human hemoglobin[463] and carbonic anhydrases A, B and C can behave as esterases[464], but the structural requirements of these 'pseudo' esterases are fairly strict, with activity limited to phenylactated or phenylactate derivatives. Because of dramatic species differences in the metabolism of esmolol in dog and human blood compared to rat and guinea pig blood, it has been suggested that the esterase responsible for esmolol cleavage in rat blood is an aliphatic esterase, since

aliphatic esterases are absent in man and dog. Other inhibition studies have suggested the esterase responsible for esmolol metabolism in dog and human blood to be an arylesterase, as yet unidentified but apparently different than the commonly known esterases present in blood and responsible for the metabolism of procaine, acetylcholine and succinylcholine[416].

The acid metabolite of esmolol is an extremely weak β-blocker with low affinity for β-adrenergic receptors and is about 1,500-fold less potent than esmolol. Metabolism and elimination of esmolol seems independent of renal or hepatic function[465,466]. Less than 1 to 2% of esmolol is eliminated unchanged in the urine[467]. The acid metabolite is renally eliminated and may accumulate in patients with renal failure[468]. Methanol formed from the metabolism of esmolol is within the range normally found in the untreated population, and at least two orders of magnitude below levels associated with methanol toxicity [413]. In a study carried out with the purpose to measure methanol accumulation, subjects received continuous infusions of esmolol at concentrations of 150 mg/kg/min and 300 mg/kg/min for 24 and 6 hs, respectively. Methanol concentrations remained within the range of normal endogenous levels[469]. Approximately 55% of esmolol and 10% of the acid metabolite is bound to human plasma protein[470].

CHAPTER III - METHODS AND RESULTS

3.1- Effects of Esmolol When Used as a Cardioplegic Agent. Initial Functional Studies

Can esmolol produce reversible cardiac arrest?

3.2 - The Metabolism of Esmolol when used as a Cardioplegic Agent

Does methanol accumulate up to toxic levels?

3.3 - Subcellular Mechanisms of Action of Esmolol as a Cardioplegic Agent. A Multinuclear MRS and Ca^{++} Fluoroscopy Study.

Are there effects other than classical β–blockade?

All animals received humane care in compliance with the Canadian Council on Animal Care regulations[471], under the supervision of the Institute for Biodiagnostics Animal Care Committee. The animals were acclimatized before experimental use (a minimum of 7 days for rats and 14 days for pigs), maintained on a normal laboratory diet and given access to water *ad libitum*.

3.1- Effects of Esmolol when used as a Cardioplegic Agent. Initial Functional Studies

The work was carried out using isolated (Langendorff Preparation) rat and rabbit hearts and a large animal model (pig) under extracorporeal circulation with continuous, undiluted, normothermic blood cardioplegia (37° C). In all 4 protocols functional data (positive and negative deflections of the first derivative of pressure over time [± dP/dt]; heart rate [HR]; left ventricular developed pressure [LVDP]; left ventricular systolic pressure [LVSP]; left ventricular end-diastolic pressure [LVEDP]; electrocardiogram [ECG] signal amplitude [ECGamp]; and developed pressure--heart rate product [RPP]) were monitored. The results obtained were compared to baseline data acquired prior to induction of arrest.

3.1.1 - Materials & Methods

3.1.1.1 - Protocols

3.1.1.1.1 - Evaluation of Esmolol as a Cardioplegic Agent:

Can esmolol produce reversible cardiac arrest?

The initial series of experiments was conducted using an isolated rat heart model (Langendorff preparation). Eight Sprague-Dawley male rats weighing between 500 and

600g were used. The isolated rat hearts were subjected to periods of arrest varying from 20 to 120 minutes (20, 60, 90 and 120 minutes) after which functional indices where measured (± dP/dt; HR, LVDP, LVSP, LVEDP, ECGamp, RPP). The results obtained were compared to baseline data acquired prior to induction of arrest.

3.1.1.1.2 - Dose Response Curves

Dose response curves were performed using isolated Langendorff rat and rabbit hearts (n = 6). The final concentrations of esmolol varied from 8.5×10^{-5} to 6.8×10^{-3} mol/L and from 1.2×10^{-4} to 1.45×10^{-3} mol/L in the rat and rabbit experiments, respectively.

3.1.1.1.3 - Effects on the Acutely Damaged Rat Heart - Esmolol Arrest *vs.* Potassium Arrest

The effects of an acute ischemic insult (no-flow ischemia, 20 min at 37 ° C) were assessed on isolated rat hearts perfused with normothermic (37 ° C) esmolol -containing Krebs-Henseleit solution and compared with the results obtained on hearts perfused with high-potassium KH solution (KCl = 25 mmol/L). Nineteen rats were divided into two groups and two subgroups. The hearts in Group A (n = 9) hearts were perfused (and arrested) with either esmolol or potassium (groups AE and AP) for 20 minutes followed by 20 min of no-flow ischemia at 37° C. Hearts in Group B hearts (n = 10) received the same ischemic insult before being perfused with either esmolol or potassium (groups BE and BP).

3.1.1.1.4 - Esmolol Cardioplegia in a Large Animal Model Under Normothermic Bypass

This protocol evaluated the effects of esmolol in a more clinically relevant experimental model. Eleven pigs were divided into esmolol (n = 6) and potassium (n = 5) groups and subjected to normothermic cardiopulmonary bypass and a one-hour period of cardiac arrest.

3.1.1.2 - Instrumentation & Experimental Design

3.1.1.2.1 - Isolated Rat and Rabbit Hearts (Langendorff Preparation)

The animals were anesthetized with isoflurane at a concentration of 3 - 5 % in oxygen (100%) at a rate of 2 L/ min and were maintained with 1.5 - 2.0 % at an oxygen flow rate of 1 L/ min. After achieving a surgical plane of anesthesia, a median thoracotomy was performed and the heart was removed. The isolated rat and rabbit heart experiments were performed in a Langendorff perfusion apparatus using oxygenated KH solution containing (in mmol/L) NaCl 118, $NaHCO_3$ 25, KCl 4.7, $CaCl_2$ 1.75 (~ 1.1 mmol/L free Ca^{++}), $MgSO_4$ 1.2, EDTA 0.5 and glucose 11. The perfusate was equilibrated with 95% O_2/ 5% CO_2, with the pH maintained at 7.4. The hearts were initially perfused at a constant pressure of 90 mmHg under normothermic (37° C) conditions. The perfusion mode was then switched to a constant flow mode after a 10-minute stabilization period. Mechanical function was measured using a water-filled compliant latex balloon inserted into the left ventricle, secured with a 4-0 silk suture and attached to a pressure transducer.

Perfusion with high-potassium KH solution (25 mmol/L) was provided by a separate reservoir. Esmolol (Brevibloc®; Zeneca Pharma Inc., Mississauga, Ontario, Canada) was provided in vials containing 10 mL of a 250 mg/mL solution. One vial was

diluted in 990 mL of oxygenated KH solution, yielding a concentration of 2.5 mg/mL. The solution was infused using an electronic syringe pump attached to a three-way stopcock inserted immediately above the heart, and was mixed with the bulk of the perfusate. The final concentration of esmolol reaching the heart was determined by the ratio of the rate of drug infusion and the perfusion rate.

For the initial and ischemic protocols (items 3.1.1.1 and 3.1.1.3), the syringe pump infusion rate was set at 5 mL/min (2.5 mg/mL x 5 = 12.5 mg/min) until complete arrest was achieved. At this time, the infusion rate was titrated to the minimum dose necessary to maintain arrest, usually about 1.0 to 1.5 mL/min (2.75 to 3.75 mg/min). The measured coronary flow for a ~ 1g rat heart was 20 mL/min while beating and 18 mL/min during arrest. For calculation of the concentrations of esmolol in the rat heart, we used an average perfusion rate of 22 mL/min at constant flow and the expression:

$$IR_{E\text{or}K} = \frac{[C] \cdot MW \cdot Cf}{S_{[E\text{or}K]}} \cdot 60$$

Where:

- [C] is the desired concentration in the perfusate (in mmol/L);
- MW is the molecular weight of esmolol or KCl;
- Cf is the coronary flow in mL/min;
- S is the concentration of esmolol or KCl in the syringe in g/mL;
- 60 is the correction factor that will yield the data in mL/h.

In protocols 1 and 3 the esmolol concentration used for inducing arrest was calculated as 1.7×10^{-3} mol/L, and for maintenance the value was 5.0×10^{-4} mol/L.

3.1.1.2.2 - Large Animal Model (pig) under Extracorporeal Circulation

Eleven Yorkshire pigs of either sex, weighing 35 to 50 kg were subjected to extracorporeal circulation under normothermic conditions (37° C), during which positive and negative first derivative of pressure (± dP/dt), heart rate, LVSP, LVEDP, LVDP, and electrocardiograph signal amplitude were monitored (ECGamp).

After overnight fasting, the pigs were preanesthetized with intramuscular ketamine (20 mg/kg), midazolam (0.3 mg/kg), and atropine (0.015 mg/kg). The animals were intubated and ventilated with a mixture of oxygen (40%), medical air (58%) and isoflurane (2%) at a flow of 2 to 4 L/min. To maintain muscle paralysis, pancuronium (0.15 mg/kg) was given every hour during the procedure. During extracorporeal circulation, isoflurane was administered (1.0 to 2.0 %) directly into the pump oxygenator. An arterial pressure catheter was placed in the carotid artery; a central venous pressure line was inserted through the jugular vein. A thermocouple was inserted into the esophagus for monitoring temperature, which was kept at 37° C by active rewarming with a heat exchanger. The arterial and central venous pressures were monitored continuously, as were the blood gases and electrolytes, which were kept within the physiologic range.

The perfusion system consisted of a membrane oxygenator (COBE Inc., Scaraborough, Ontario, Canada), a 40 μm arterial blood filter (Dideco, Mirandola, Italy), and a centrifugal pump (St. Jude Medical Inc., Chelmsford, MA, USA) placed in the arterial line (in the first two experiments, a roller-pump [COBE] was used for one experiment in each group). Cardioplegia was delivered in an antegrade fashion using a roller-pump connected to a cannula (DLP, Grand Rapids, MI, USA) inserted in the ascending aorta and secured by a 3-0 Ethibond® double purse string suture. Esmolol and

potassium were injected in this cardioplegia line by means of an electronic syringe-pump through a side connector and a three-way stopcock.

After reaching a surgical plane of anesthesia, a median sternotomy was performed and heparin (500 UI/kg) was injected systemically. The activated clotting time was monitored periodically and maintained above 600 seconds. After completing purse-string sutures on the ascending aorta and on the right atrial appendage, two cannulae were inserted in the ascending aorta: one for the arterial input from the pump and a second for cardioplegia delivery. Venous return was ensured using a two-stage atriocaval cannula (DLP) inserted through the right atrial appendage. Before initiating bypass, a 10-minute period was allowed for acquisition of initial baseline functional data. Normothermic cardiopulmonary bypass was initiated at a flow rate of 60-100 mL/kg/min, and another 10-minute period was allowed for data acquisition. Antegrade cardioplegia was delivered continuously immediately after aortic cross-clamping at a flow rate of 150 to 250 mL/min.

The animals were divided into esmolol and potassium groups. The potassium group (n = 5) received KCl and magnesium sulfate ($MgSO_4$ at 10%) infused according to the nomograms developed by LeHouerou and colleagues[309] and previously described in section 2.3.4.2. The esmolol group (n = 6) received esmolol as the only cardioplegic agent at a concentration in the syringe pump of 10 mg/mL.

3.1.1.2.3 Esmolol and Potassium Cardioplegia Concentrations

The potassium concentration in the cardioplegia line was 25 mEq/L for induction and 12 mEq/L for maintenance of arrest. Undiluted continuous normothermic cardioplegia was administered as described previously (309).

The esmolol concentrations in the cardioplegic line were as follows:

- *induction*: syringe-pump rate 15 mL/min (150 mg/min) , cardioplegia roller-pump flow 150 mL/min = 0.91 mg. mL^{-1}. min^{-1}; approximately 2.7 x 10^{-3} mol/L; and
- *maintenance*: syringe-pump rate 5 mL/min (50 mg/min), cardioplegia roller-pump flow rate 150 mL/min = 0.31 mg. mL^{-1}. min^{-1}; approximately 9.0 x 10^{-4} mol/L.

After 1 hour of normothermic cardioplegic arrest, the aortic cross-clamp was released, cardioplegia infusion was stopped, and the heart was allowed to beat spontaneously while maintaining total cardiopulmonary bypass. Functional data (± dP/dt, LVSP, LVEDP, LVDP, and heart rate) were acquired during the recovery period. This period was composed of two phases: an initial phase of recovery when the heart was beating empty and the arterial pump maintained the systemic flow, and a second in which the animal was weaned off bypass and the heart resumed the hemodynamic load and maintenance of arterial pressure. Each phase lasted 20 minutes, and no inotropic support was provided. After acquisition of the last data set, the animal was euthanized by circulatory arrest and exsanguination under anesthesia.

3.1.1.2.4 Statistical Analyses

Student's *t* test was used in all analyses with dependent or independent variables when applicable, supported by the Mann-Whitney U test for the independent variables and the

Wilcoxon matched-pairs test for the dependent variables. In addition, because of the limited number of animals, the Exact Permutation test was used in both types of analyses[472]. Differences are expressed in P values.

3.1.2 - Results

3.1.2.1 - Isolated Rat Hearts

In all experiments, cardiac arrest was achieved 45 to 60 seconds after beginning the infusion at a syringe-pump infusion rate of 5 mL/min, approximately 1.7×10^{-3} mol/L. At this time, infusion was switched to the maintenance mode by decreasing the syringe-pump infusion rate to 1.5 mL/min, about 5.0×10^{-4} mol/L. The minimal dose was always titrated and varied within the range of 1.0 to 1.5 mL/min, approximately 3.4×10^{-4} mol/L at an average coronary flow of rate of 22.2 mL/min. The longer the induction period, the greater the stability of arrest during the maintenance period (i.e., shifting to lower doses without resumption of heart activity). After titration of the minimal dose required, cardiac arrest was maintained for periods of up to 120 minutes. Under these conditions (minimal dose, regardless of the length of the arrest period), the first beat was usually observed within 30 seconds of interrupting the infusion of esmolol. Occasional arrhythmias (early after-depolarizations, or extrasystoles) were observed in some cases during the first 5 to 10 minutes of "reperfusion". In all experiments, sinus rhythm and preinjection contractile values were reestablished within 20 minutes of recovery (Figure 3.1).

The LVEDP increased during arrest. The increase in LVEDP was reversible, declining to prearrest values after stopping drug infusion. The data indicate that esmolol induces and maintains reversible heart arrest within clinically relevant time frames.

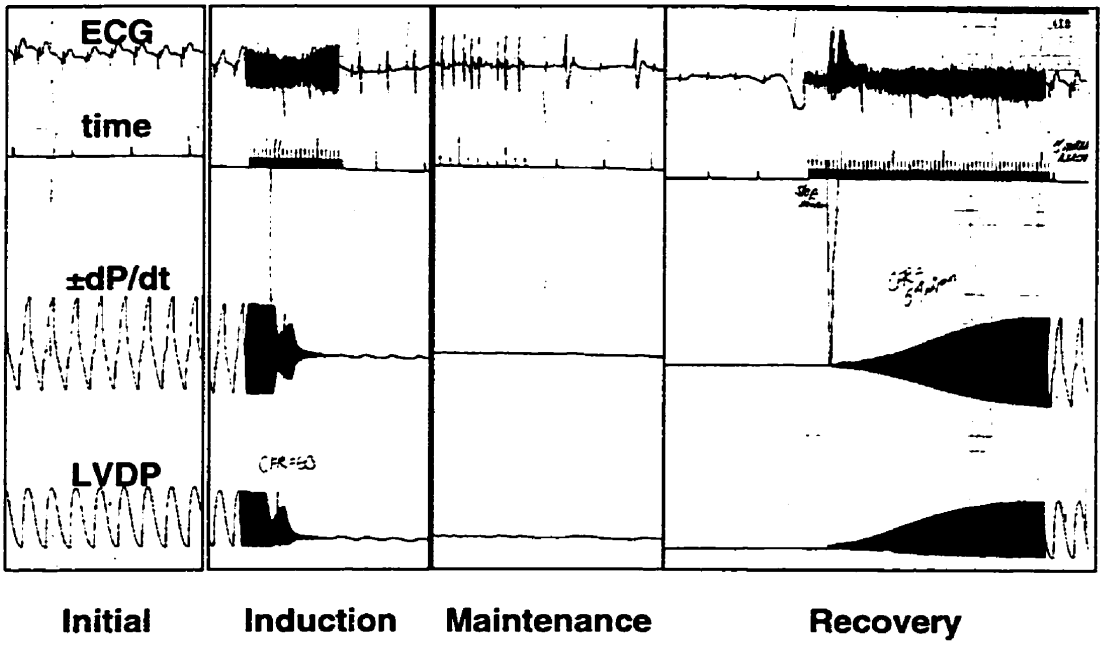

Figure 3.1 - Polygraph traces of esmolol-perfused rabbit heart during induction, maintenance and recovery of cardiac arrest. Note the electromechanical dissociation. (± dP/dt = first derivative of pressure over time, ECG = electrocardiogram; LVDP = left ventricular developed pressure.

Table 3.1 - Concentrations required to induce cardiac mechanical and electrical arrest.

	Rat	Pig	Rabbit
Mechanical Arrest	1.36×10^{-3} M	9.0×10^{-4} M	4.2×10^{-4} M
Cessation of Electrical Activity	1.7×10^{-3} M	Not achieved	6.0×10^{-4} M

3.1.2.2 - Dose-Response Curves using Isolated Rat and Rabbit Hearts

Mechanical indices such as ± dP/dt and LVDP reached 0 at a 4 mL/min dose (0.45 mg . mL^{-1} . min^{-1}; approximately 1.36 x 10^{-3} mol/L). At 5 mL/min (0.56 mg . mL^{-1} . min^{-1}; about 1.7 x 10^{-3} mol/L), all indices reached zero except LVEDP (Figure 3.2 (a) and (b)). At a dose of 4.0 mL/min, the end of the infusion period (fifth minute) was marked by mechanical arrest in the presence of electrical activity (ECG signal, P waves and QRS complexes). In the experiments using isolated rabbit hearts, mechanical arrest was achieved at 0.04 mg. mL^{-1}. min^{-1} (approximately 4.2 x 10^{-4} mol/L), whereas cessation of electrical activity was obtained at 0.2 mg . mL^{-1}. min^{-1} (approximately 6.0 x 10^{-4} mol/L).

Unlike the other indices, LVEDP increased during the infusion period. During arrest (concentrations > 4.2 x 10^{-4}), LVSP was equal to LVEDP measured by the intraventricular balloon. The LVEDP returned to prearrest values after 20 minutes of "reperfusion" in the recovery period, in the absence of the drug. In both curves, each heart was used to assess the effects of increasing drug concentrations. A cumulative effect on the LVDEP was observed such that the "resting" pressure gradually increased throughout the experiment.

All other indices showed nearly 100% recovery 20 minutes after stopping the infusion of esmolol. Even at higher doses, the recovery levels were greater than 80% at 20 minutes after "reperfusion", with the exception that 35 minutes of "reperfusion" was required for recovery after the 20-mL/min dose (Figure 3.3, (a) and (b)). The duration of the recovery period was directly proportional to the amount of drug infused.

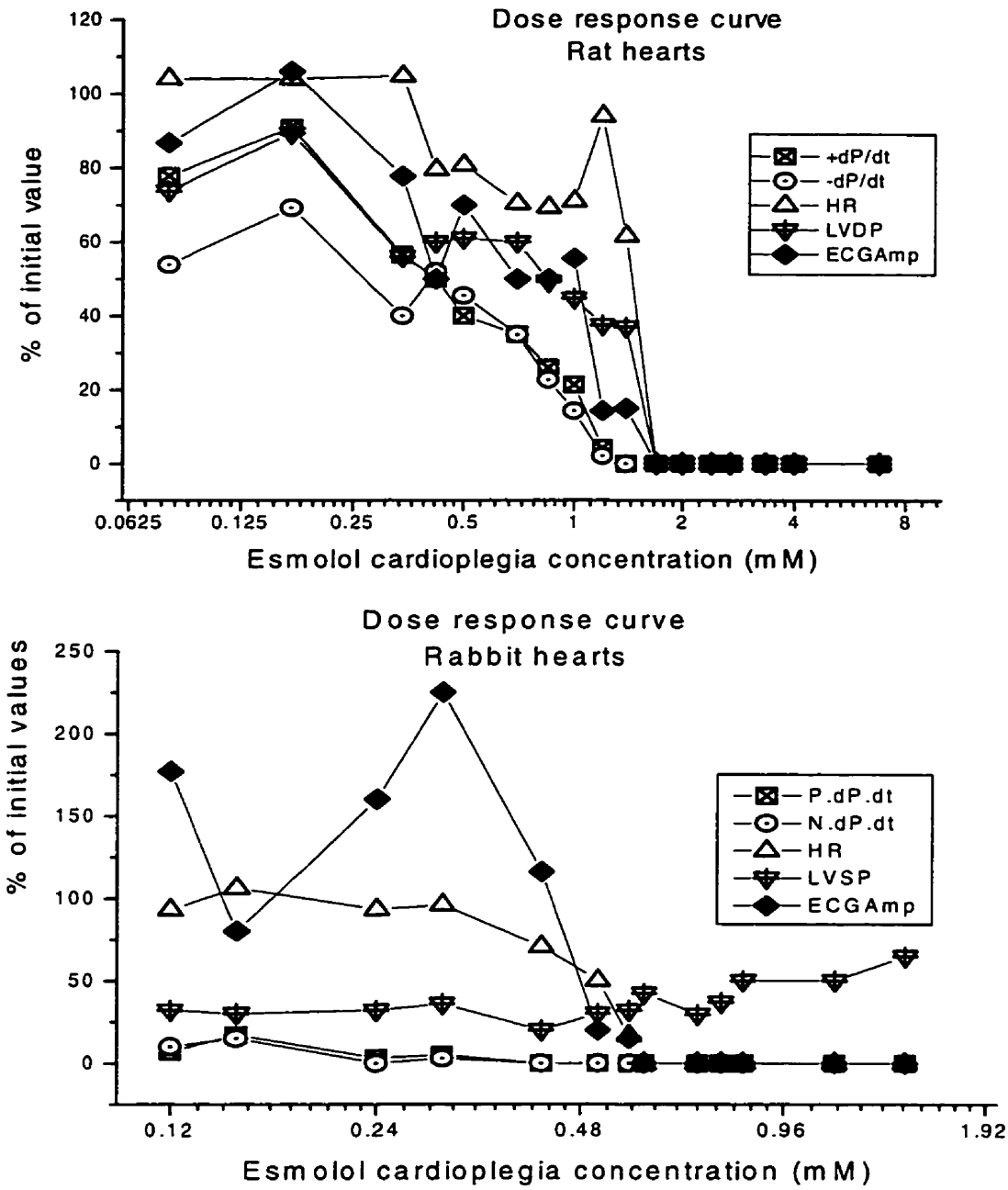

Figure 3.2 - Dose-response curves of esmolol-perfused isolated rat and rabbit hearts (n = 6, Langendorff preparation). In (a), concentrations varied from 0.084 to 6.788 mmol/L (rat hearts); in (b), concentrations varied from 0.12 to 1.45 mmol/L (rabbit hearts). During arrest (concentrations > 0.42 mmol/L), the left ventricular systolic pressure (LVSP) was equal to the left ventricular end-diastolic pressure (dP/dt = first derivative of pressure; ECG = electrocardiogram; HR = heart rate; LVDP = left ventricular developed pressure; P = positive; N = negative).

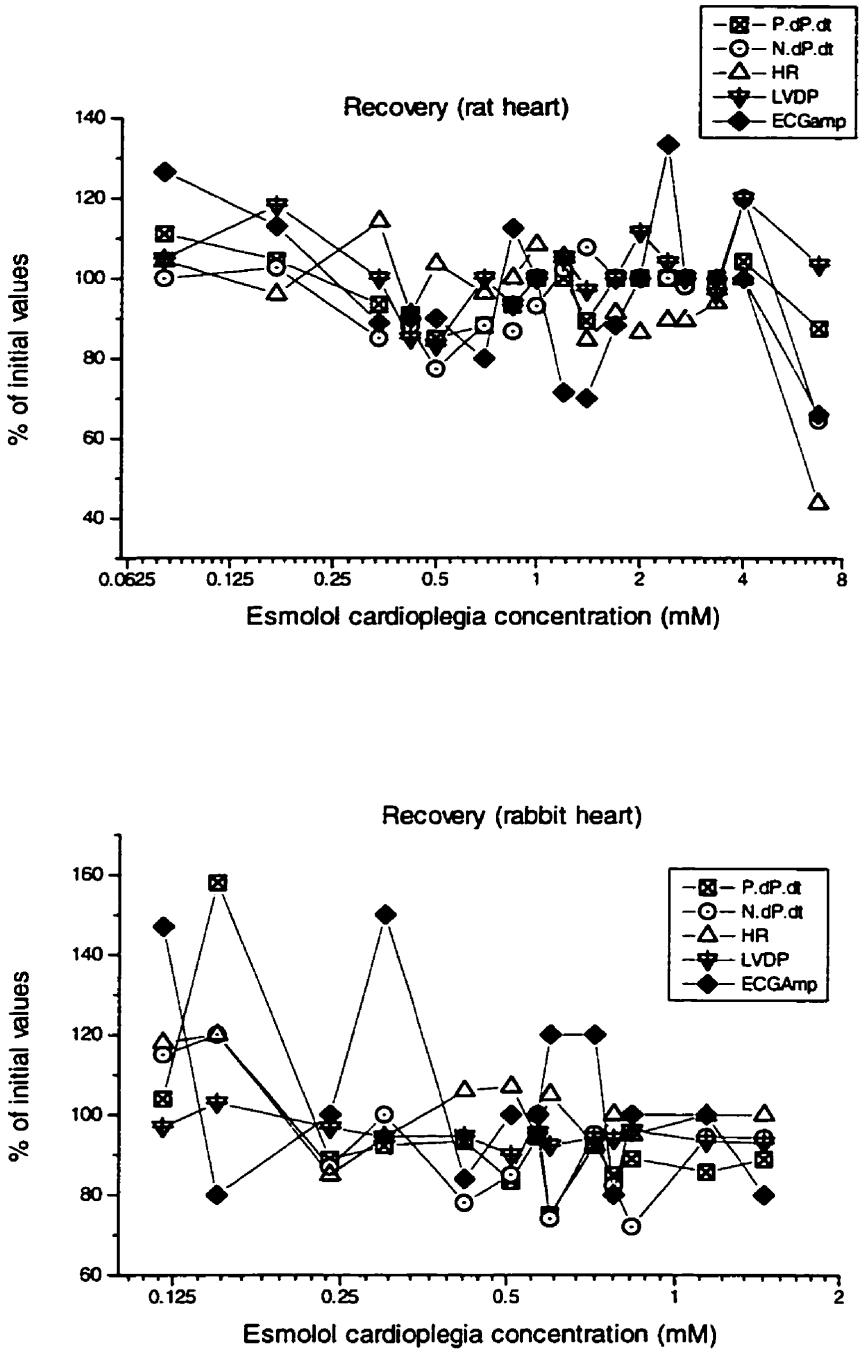

Figure 3.3 - Recovery of contractile parameters in the isolated rat and rabbit hearts as a function of esmolol concentration. All contractile parameters returned to pre-arrest values upon 20 minutes of recovery of infusion with the exception of the 6.788 mmol/L dose in the rat heart experiments. (Abbreviations are as Fig. 3.2)

3.1.2.3 - Effects of Ischemia in Esmolol and High-Potassium Arrested Hearts

Overall, the recovery of contractile indices was higher in the esmolol-treated hearts than in the potassium-treated hearts. The data are presented as percentage of initial values ± standard deviation. In Group A, where the ischemic insult was inflicted after induction of arrest, esmolol-arrested hearts showed better recovery of the following parameters: positive dP/dt ($P < 0.01$), LVSP ($P < 0.009$), and LVDP ($P < 0.009$). In group B, which tested the effects of esmolol in the acutely damaged myocardium, esmolol-treated hearts also showed better outcome. Statistically significant differences were found in positive and negative dP/dt ($P < 0.01$), LVSP ($P < 0.01$), LVDP ($P < 0.009$), and heart rate ($P < 0.009$) (Table 3.2 and Figures 3.4 and 3.5 A through D).

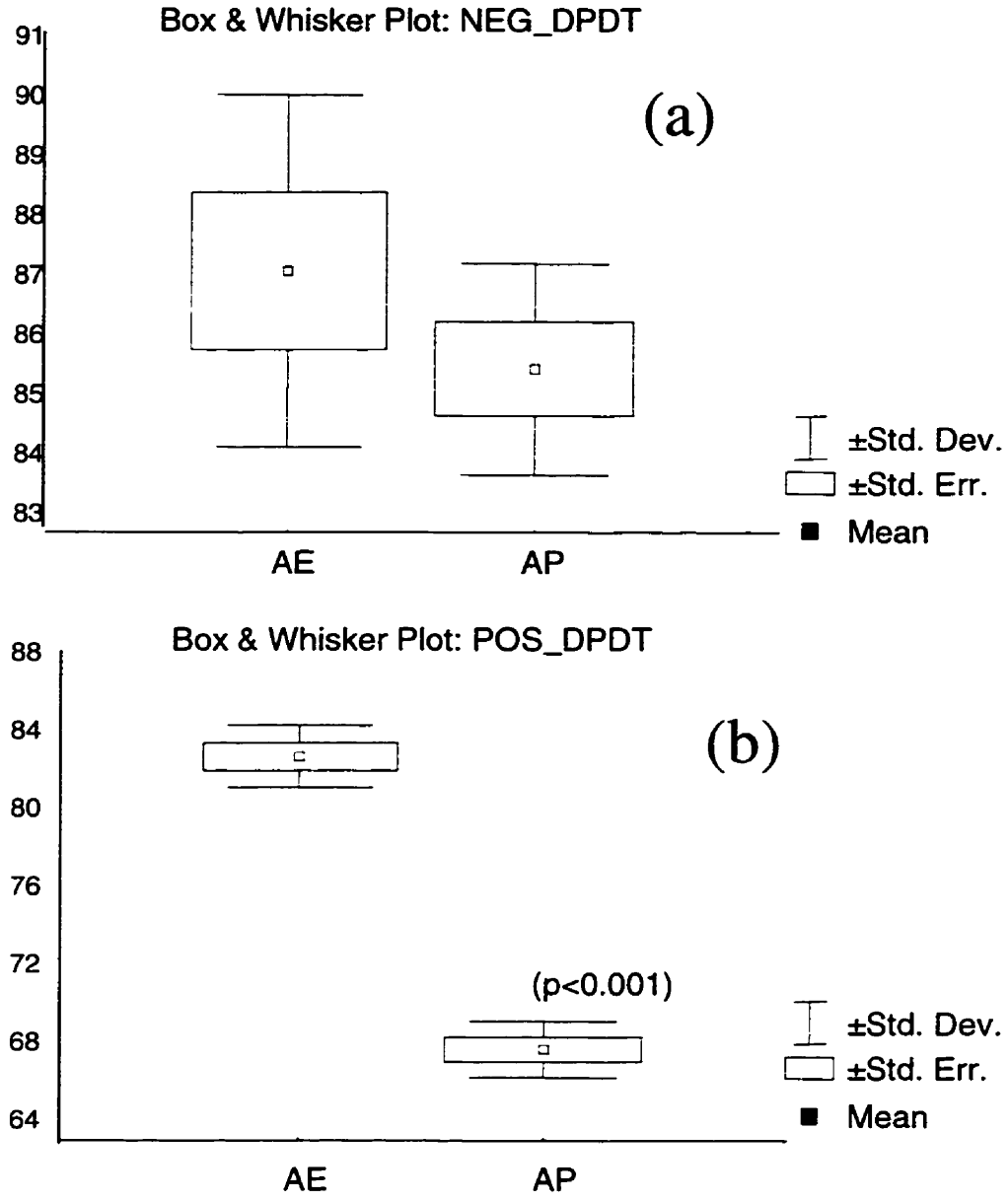

Figure 3.4 - A - Effects of Ischemia on group A, ischemia after induction of arrest (AE vs. AP). In (a), effects on the negative deflection of the first derivative of pressure over time (Neg dP/dt, P = NS). In (b), statistically significant difference was found in recovery values of the positive deflection of the first derivative of pressure over time (Pos dP/dt) between esmolol- and potassium-arrested hearts Data are expressed as percentage of pre-arrest values.

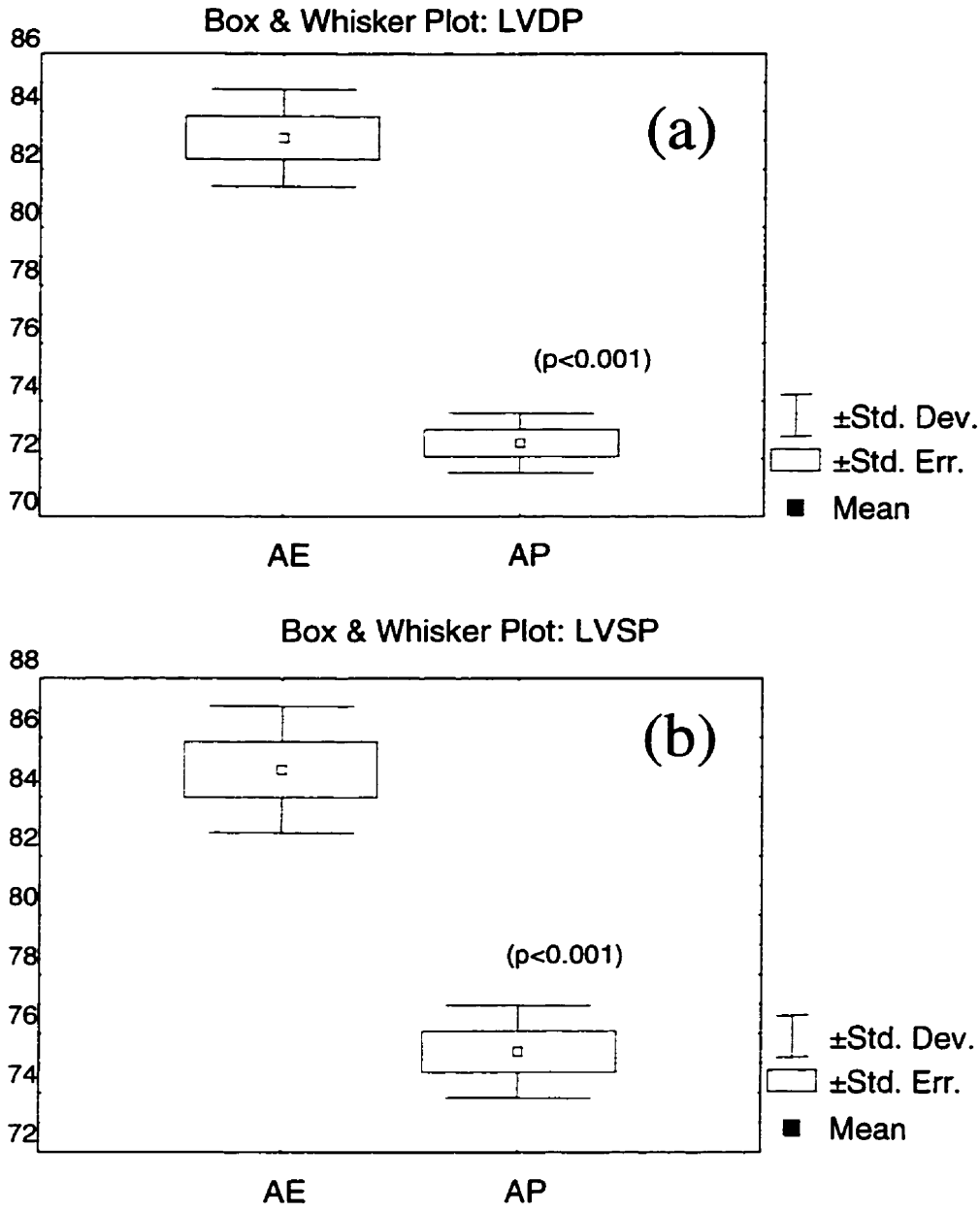

Figure 3.4 - B - Effects of Ischemia on group A, ischemia after induction of arrest (AE vs. AP). Recovery values of left-ventricular developed (a) and systolic (b) pressures (LVDP and LVSP) were higher in esmolol arrested hearts relatively to potassium-treated hearts. Statistically significant differences were found in both measured parameters. Data are expressed as percentage of pre-arrest values.

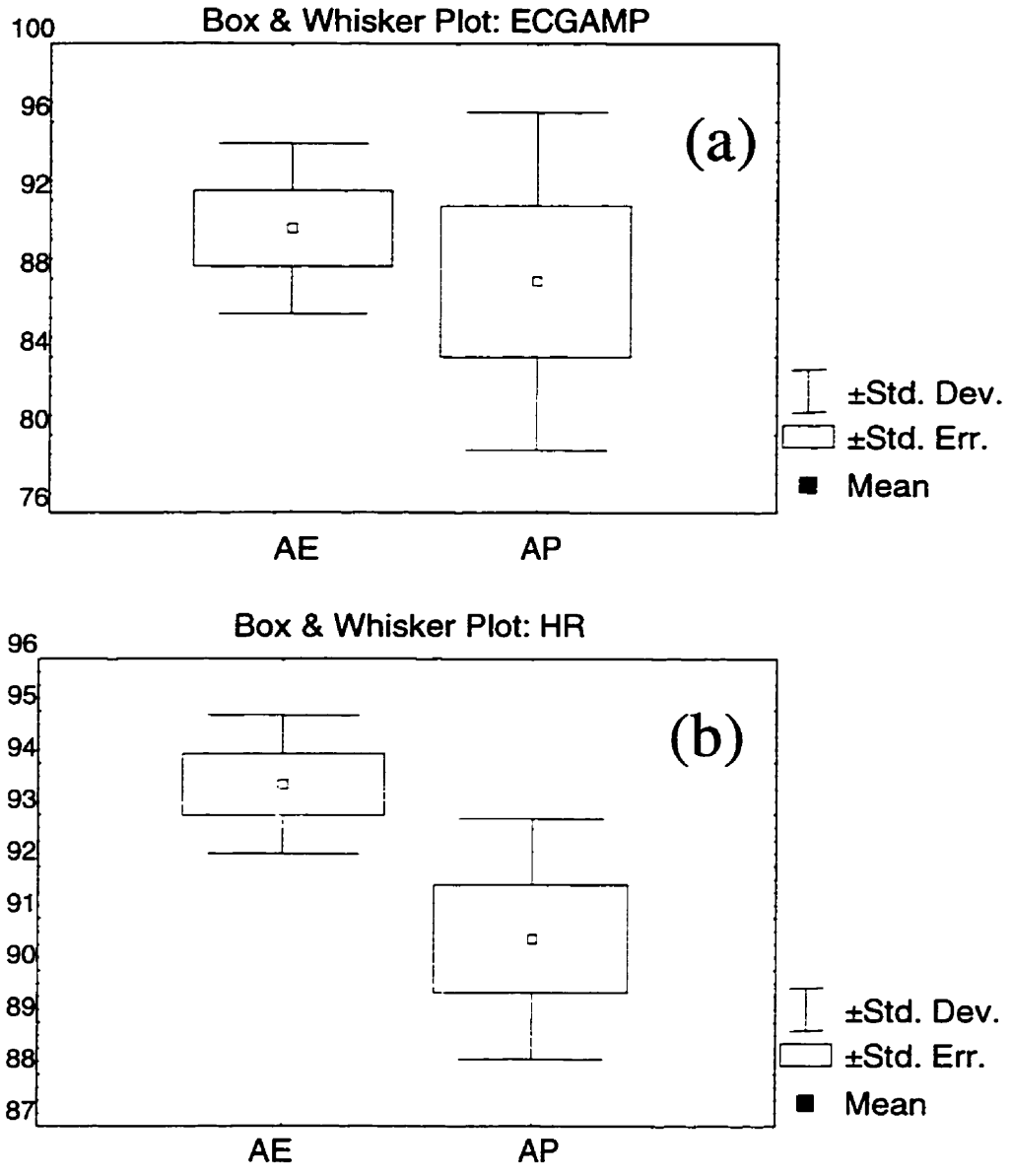

Figure 3.4 - C - Effects of Ischemia on group A, ischemia after induction of arrest (AE vs. AP). Recovery values of electrocardiogram signal amplitude (ECG amp, (a)) and systolic heart rate (HR, (b)). No statistically significant differences were found in both parameters measured. Data are expressed as percentage of pre-arrest values.

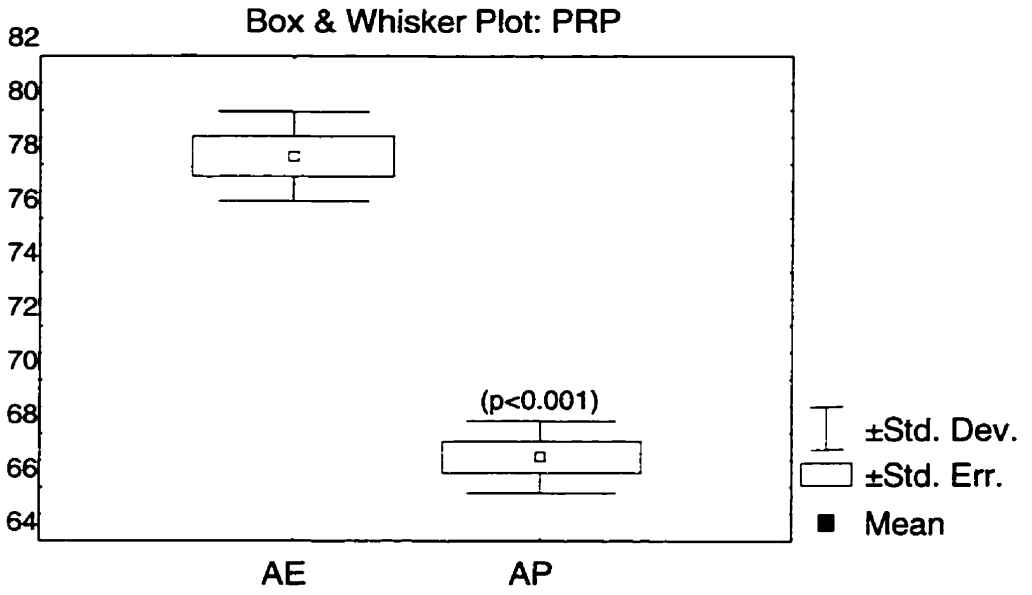

Figure 3.4 - D - Effects of Ischemia on group A, ischemia after induction of arrest (AE vs. AP). Recovery values pressure-rate product (PRP, = LVDP x HR). A significant difference was found between potassium and esmolol-treated hearts. Data are expressed as percentage of pre-arrest values.

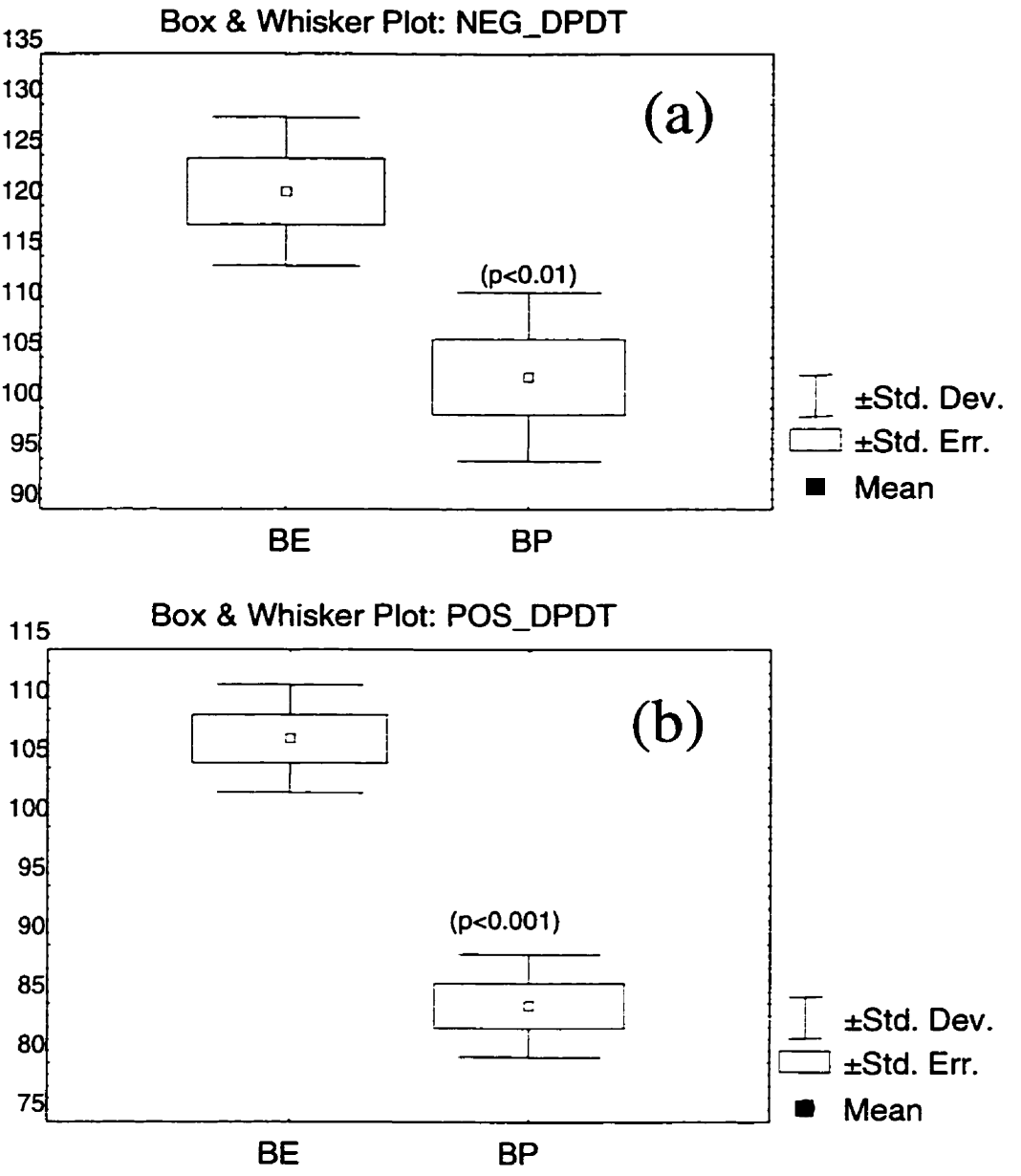

Figure 3.5 - A - Effects of Ischemia on group B, ischemia before induction of arrest (BE vs. BP). In (a), effects on the negative deflection of the first derivative of pressure over time (Neg dP/dt). In (b), recovery values of the positive deflection of the first derivative of pressure over time (Pos dP/dt) between esmolol- and potassium-arrested hearts Statistically significant differences were found in measurements of both parameters. Data are expressed as percentage of pre-arrest values.

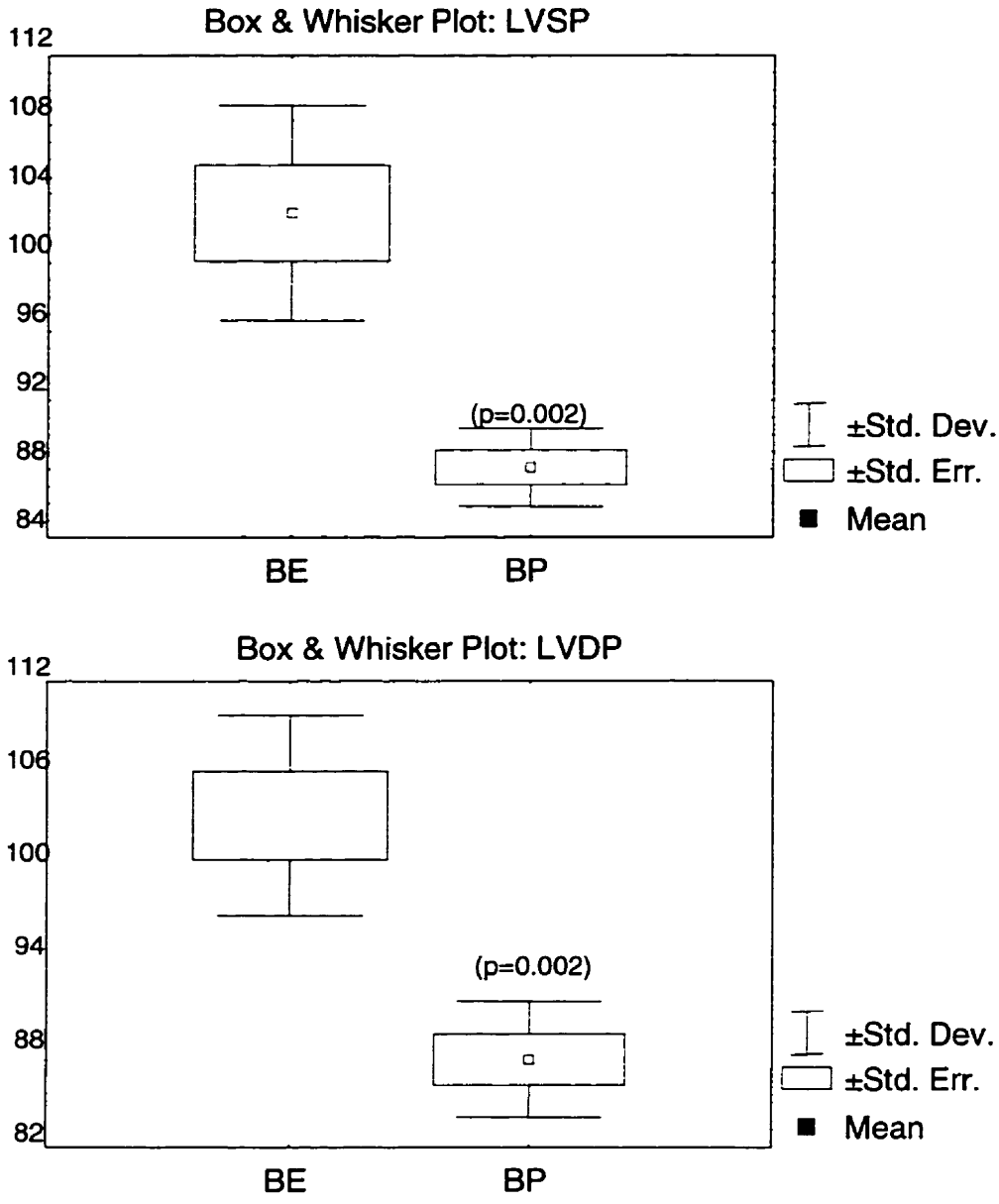

Figure 3.5 - B - Effects of Ischemia on group B, ischemia before induction of arrest (BE vs. BP). Recovery values of left-ventricular developed (a) and systolic (b) pressures (LVDP and LVSP) were higher in esmolol arrested hearts relatively to potassium-treated hearts. Statistically significant differences were found in both measured parameters. Data are expressed as percentage of pre-arrest values.

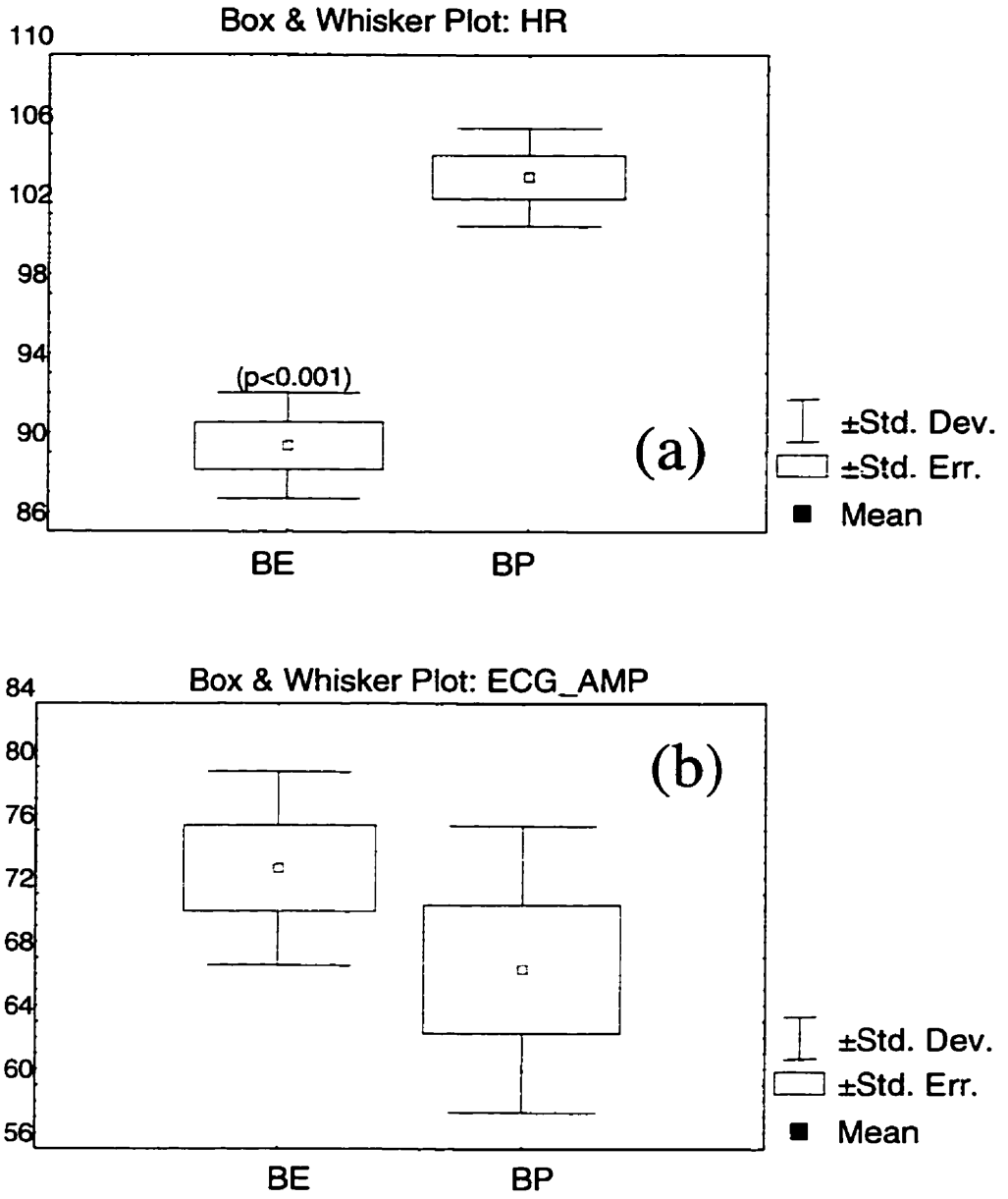

Figure 3.5 - C - Effects of Ischemia on group B, ischemia before induction of arrest (BE vs. BP). Heart rate recovery values of potassium arrested-hearts were significantly ($p<0.001$) higher relative to esmolol-treated hearts (a). No statistically significant differences were found in electrocardiogram signal amplitude (ECG amp, (b)) in either groups. Data are expressed as percentage of pre-arrest values.

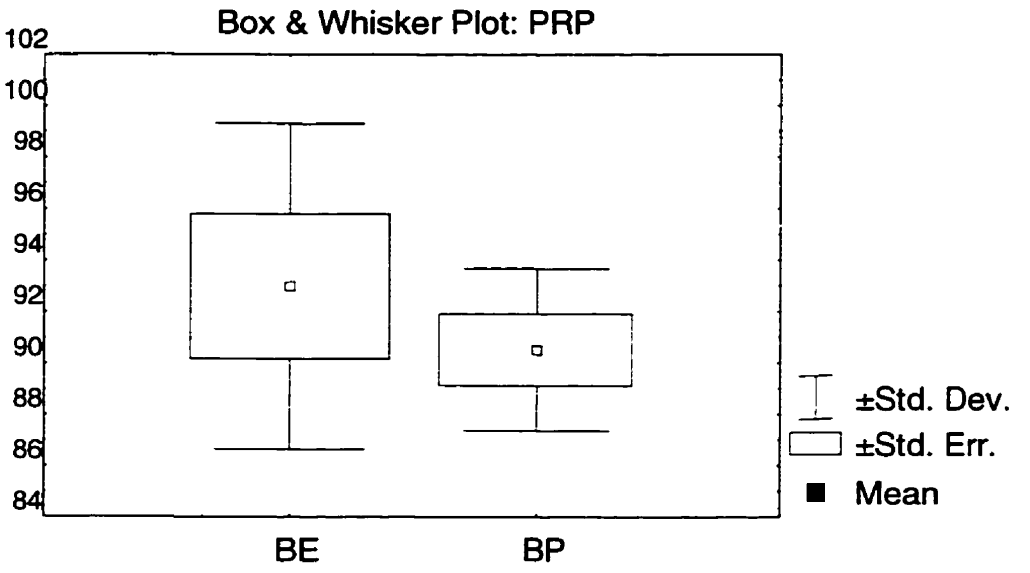

Figure 3.5 - D - Effects of Ischemia on group B, ischemia before induction of arrest (AE vs. AP). Recovery values pressure-rate product (PRP = LVDP x HR). No significant difference was found between potassium and esmolol- treated hearts. Data are expressed as percentage of pre-arrest values.

Table 3.2 - Statistical analyses of physiological parameters obtained from isolated rat hearts subjected to ischemia (20 min, 37° C) prior to, or after, treatment with Esmolol or potassium.

	Groups				**Statistical tests**					
					Student's t		**‡Exact Perm.**		***Mann- Whit. U test**	
	+AE	**+AP**	**#BE**	**#BP**	GroupA	Group B	Group A	Group B	Group A	Group B
	(% of initial values, means ± sd)				*p values*					
+dP/dt	84±2	69±1	107±5	85±4	0.00001	0.00004	0.0079	0.0079	0.0090	0.0090
-dP/dt	87±3	86±2	121±7	103±8	0.33163	0.0061	0.3175	0.0079	0.4647	0.0088
HR	94±1	91±2	90±3	104±2	0.0375	0.00003	0.0476	0.0079	0.0749	0.0088
LVSP	85±2	75±2	103±6	88±2	0.00004	0.001	0.0079	0.0079	0.0090	0.0090
LVDP	83±2	73±3	103±6	88±4	0.000002	0.0015	0.0079	0.0079	0.0088	0.0088
ECGamp	90±4	88±9	74±6	67±9	0.5492	0.2273	0.5633	0.2222	0.7510	0.1732
RPP	78±2	67±1	93±6	90±3	0.00003	0.45	0.0079	0.4762	0.0090	0.6015

+ Ischemic insult inflicted after (A) induction of arrest with Esmolol (E) or Potassium (P).
# Ischemic insult inflicted before (B) arrest with Esmolol (E) or Potassium (P).
* Mann-Whitney U test.
‡Exact Permutation test.

3.1.2.4 - Cardiac Arrest in the Pig *In Vivo* Under Cardiopulmonary Bypass

Pigs were subjected to esmolol arrest for 1 hour, and hemodynamic functions were evaluated after interrupting cardiopulmonary bypass. The flow rate of antegrade cardioplegia was maintained at 150 to 200 mL/min at an aortic pressure of 75-80 mmHg. In potassium-treated pigs, it was not possible to maintain cardiac arrest with an infusion of 12-mEq/L KCl. To obtain arrest the infusion of 25 mEq/L was maintained. Despite a systemic kalemia of 9.5 mmol/L after the hour of arrest, the pigs could be weaned from bypass without the need for inotropic support. In 2 animals treated with potassium to maintain arrest, systemic kalemia reached 17 mmol/L; these animals could not be weaned off bypass 20 minutes after removal of the aortic cross-clamp and interruption of cardioplegic infusion and these data were not included in the analysis. The length of time required to induce arrest and to recover cardiac mechanical function were comparable in the esmolol and potassium groups. Cardiac arrest was easily achieved in both groups within 1-3 minutes (at induction doses of [esmolol] = 0.91 mg. mL^{-1}. min^{-1}; ca. 2.7 x 10^{-3} mol/L and [KCl] = 25 mEq/L). The maintenance doses in the esmolol group were ~0.31 mg. mL^{-1}. min^{-1}, approximately 9.0 x 10^{-4} mol/L (Table 3.1) whereas the maintenance dose in the KCl group was kept at 25 mEq/L. Except for the two initial pigs treated with potassium, all the pigs were weaned from bypass without the use of inotropic support at the 20th minute of "reperfusion". The recovery values of contractile parameters after 1h of esmolol or potassium cardioplegic arrest were similar in both groups. However, differences were observed in heart rate (Student's *t* test, P = 0.043, not supported by the other tests), and in LVDP (Mann-Whitney U test, P = 0.044, not supported by the other tests; Table 3.3).

Table 3.3 - Statistical analyses of contractile parameters obtained from pigs under extracorporeal circulation subjected to continuous, undiluted, normothermic blood cardioplegia. Arrest crossclamp time: 60 min.

	Esmolol	Potassium	Student's t	‡Exact Perm.	*M-W U t
Recovery (% of initial values, means ± sd)				*p values*	
+dP/dt	96±13	111±35	0.352	0.348	0.273
-dP/dt	91±20	93±37	0.862	0.880	0.855
HR	85±15	116±27	0.043	0.045	0.068
LVDP	93±14	110±22	0.146	0.277	0.045

*Mann-Whitney U test
‡Exact Permutation test.

3.2 - The Metabolism of Esmolol When Used as a Cardioplegic Agent

Does methanol accumulate up to toxic levels?

The initial concern for studying the metabolism of esmolol came about from the results of the previous protocols in which the doses used for inducing arrest were judged high and would possibly preclude the clinical use of esmolol. Relative to potassium which has already proven its safety in a large number of patients over its decades of use, the introduction of esmolol as a cardioplegic agent could be seen as adding another problem rather than providing a practical alternative. It became important to monitor methanol, a product of esmolol metabolism. Methods for assessing concentrations of methanol and esmolol have been published and are based mainly on chromatographic analyses, which were used in clinical trials when esmolol was introduced on the market[473, 474].

Our concern however, was to follow the metabolism of esmolol in a continuous fashion, during surgery. A pilot series of *in vitro* experiments was designed to examine this possibility using infrared spectroscopy for measurements of methanol levels in blood and plasma. These results lead to the development of custom-built sample holders adapted to the bypass circuit for continuous, on-line measurements. Another series of experiments was performed using the pig model of cardiopulmonary bypass subjected to a 1h period of normothermic cardiac arrest with esmolol. During these experiments mid- and near-infrared spectroscopy were used to measure in a continuous fashion the levels of methanol in the venous blood returning from the pig (venous return line) and in the

exhaust gas from the pump oxygenator. Additional blood samples were collected for off-line measurements using gas chromatography.

3.2.1 - Metabolic Considerations

The metabolism of esmolol has been previously described (Figure 2.4). We have compared the doses recommended for its use and the strategy used in our experimental setting:

Based on the literature and on product information[475, 476], the recommended procedure for administration of esmolol is as follows:

- loading dose (bolus given over 1 minute): 500 mg/kg
- maintenance dose (given over an arbitrary period of 59 minutes): 50 - 300 mg/kg/min

In this situation, after a 60-minute period of treatment, the total amount of esmolol administered will be:

258.75 - 1365.0 mg (0.78 - 4.11 mmoles)

One of the metabolic products of esmolol is methanol. Methanol is produced in a 1:1 ratio:

Esmolol → propionic acid derivative + methanol (CH_3OH)[477]

Assuming no other losses of methanol, 0.78 to 4.11 mmol of methanol will be formed at the end of 1 h of administration.

The toxic level of methanol in human blood is considered to be 6.24 mM[478]. Assuming that methanol is highly diffusible, and fast and homogeneous distribution in total body water, administration of these concentrations of esmolol in a 75 kg human patient will result in a methanol concentration 480 to 91 times lower than its toxic levels, in agreement with published data ("two orders of magnitude below toxic levels") [448].

In our experimental setting, using the porcine model under normothermic bypass and continuous, undiluted high-concentration esmolol cardioplegia for 1h of cardiac arrest, the dosages were as follows[12]:

- loading dose (as a bolus, for the 1st minute): 1.36 mmol
- maintenance dose (for the following 59 minutes of arrest): 300 - 500 µmol/minute

After a 1h period of arrest, the total amount administered was:

19.06 - 30.86 mmol (6324 - 10239 mg), an 8 to 28.5 fold higher concentration than described above for current use in humans.

Assuming the same metabolic and pharmacokinetic patterns described above, 19.1 to 30.9 mmoles of methanol should be formed following metabolic degradation of esmolol under these conditions.

Assuming the same toxic levels for methanol as above, for a 40 kg pig, the methanol concentration would be 6.4 to 10.6 fold lower than the toxic methanol

concentration. If the same protocol were used in a 75 kg human patient, these levels would still be 19.5 to 12 fold lower than the toxic methanol concentration.

Based on the above, one could assume that the accumulation of methanol poses no problem even at the relatively high doses proposed. In spite of these theoretical considerations, subsequent pilot experiments in pigs (n = 6) were conducted to verify the theoretical assumptions; the results of which will be described in the following section.

3.2.2 - Detection Using Infrared Spectroscopy

Six pilot experiments using the *in vivo* porcine model of cardiopulmonary bypass and continuous normothermic blood cardioplegia were carried out. The objective was to test the possibility of continuously monitoring the levels of methanol and esmolol at pre-arrest, during arrest and recovery. Infrared spectroscopy was used for on-line measurements in blood and in the gas exhaust of the pump-oxygenator. Throughout the experiments, blood samples were also acquired for gas chromatography *post-hoc* analyses.

Initial *in vitro* experiments were performed to identify esmolol and methanol in IR spectra and to follow the metabolic reaction in plasma.

3.2.2.1 - Materials and Methods

Animal preparation and setup for cardiopulmonary bypass followed the procedures previously described in section 3.1.1. The pig was placed under normothermic cardiopulmonary bypass and subjected to 1-hour cardioplegic arrest either with high K^+ (25 mM) or esmolol (n = 3, each).

3.2.2.1.1 - Measurements in Blood

Two infrared cells (for NIR and MIR) were placed in the venous return line directly before the venous reservoir. The MIR cell (CIRCLE® Cell, Spectra-Tech, Shelton, CT) containing a crystal rod made of ZnSe, was placed in the sample compartment of one of the two FTIR spectrometers (FTS-7, BioRad, Cambridge, MA) and used for ATR (Attenuated Total Reflection) measurements[479] of venous blood during bypass. The

reflections of the infrared beam within the crystal rod provide sufficient intensities for spectral analysis and the experimental design made the system path length independent. The NIR cell was made of Plexiglass® and designed for fiber optics measurements in continuous blood flow experiments. The cell was placed in the venous return line immediately above the venous reservoir, holding two NIR fiber bundles in place, which were connected to the second FTIR instrument (FTS-40, BioRad, Cambridge, MA). This particular arrangement of fibers allows blood flow to be monitored in transmission mode with a variable path length of 0.5 to 5 mm. Figures 3.7 and 3.8 show the experimental setup and the custom-built NIR sample holder.

3.2.2.1.2 - Measurement in the Gas Line from the Pump-oxygenator

A third infrared cell (Multi Pass, Variable Path Length Gas Cell, Harrick, Ossining, NY) was inserted in the exhaust line of the oxygenator to measure the possible escape of methanol through the membrane oxygenator. This MIR gas cell was placed in the sample compartment of an FTIR spectrometer (FTS-7, BioRad, Cambridge, MA). The multi pass feature of this cell allowed measurements of a relatively small volume of gas by reflecting the infrared beam several times through the gas cell. This generated a total path length of up to 30 m and significantly improved the detection limit of trace gas molecules. The experimental design and the instrumental setup are shown in Figure 3.9. Infrared spectra were acquired at 20 seconds intervals prior to arrest, during arrest and recovery. Intensity and changes in isoflurane (the anesthetic drug) bands were used for calibration.

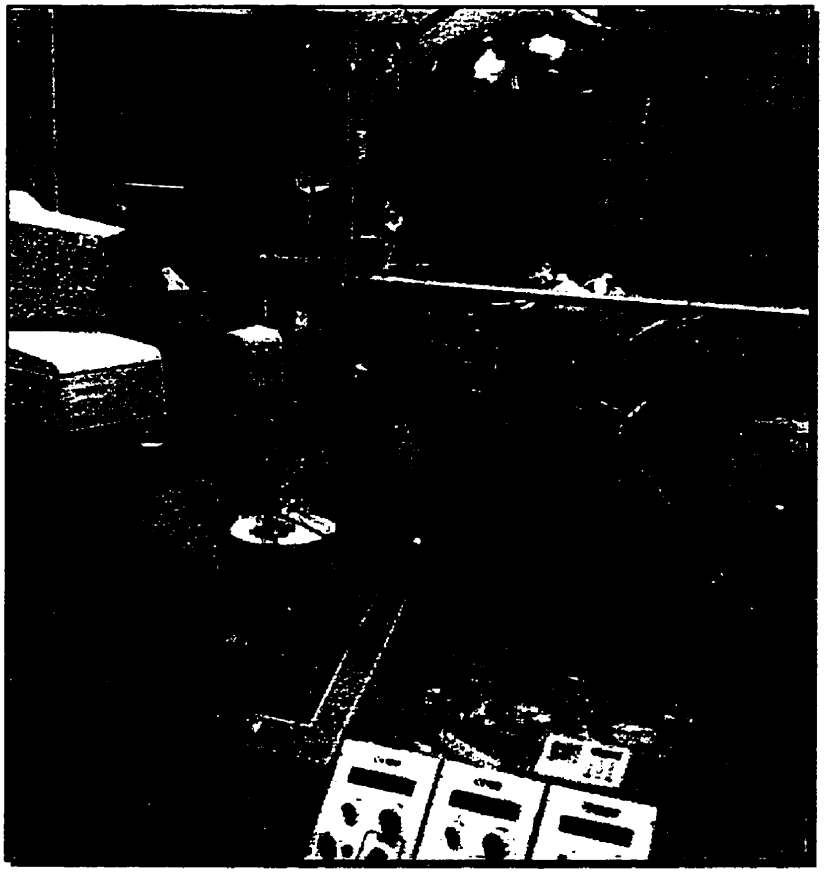

Figure 3.6 – The perfusionist's view of the operating room during cardiopulmonary bypass and cardioplegic arrest with esmolol. In the upper left, the two infrared spectrometers monitoring levels of methanol in blood returning to the venous reservoir. In the foreground lower right, the bypass pump consisting of roller-pumps for the suction and cardioplegia lines, the arterial (systemic) line was attached to a centrifugal (St. Jude Medical Inc.) pump.

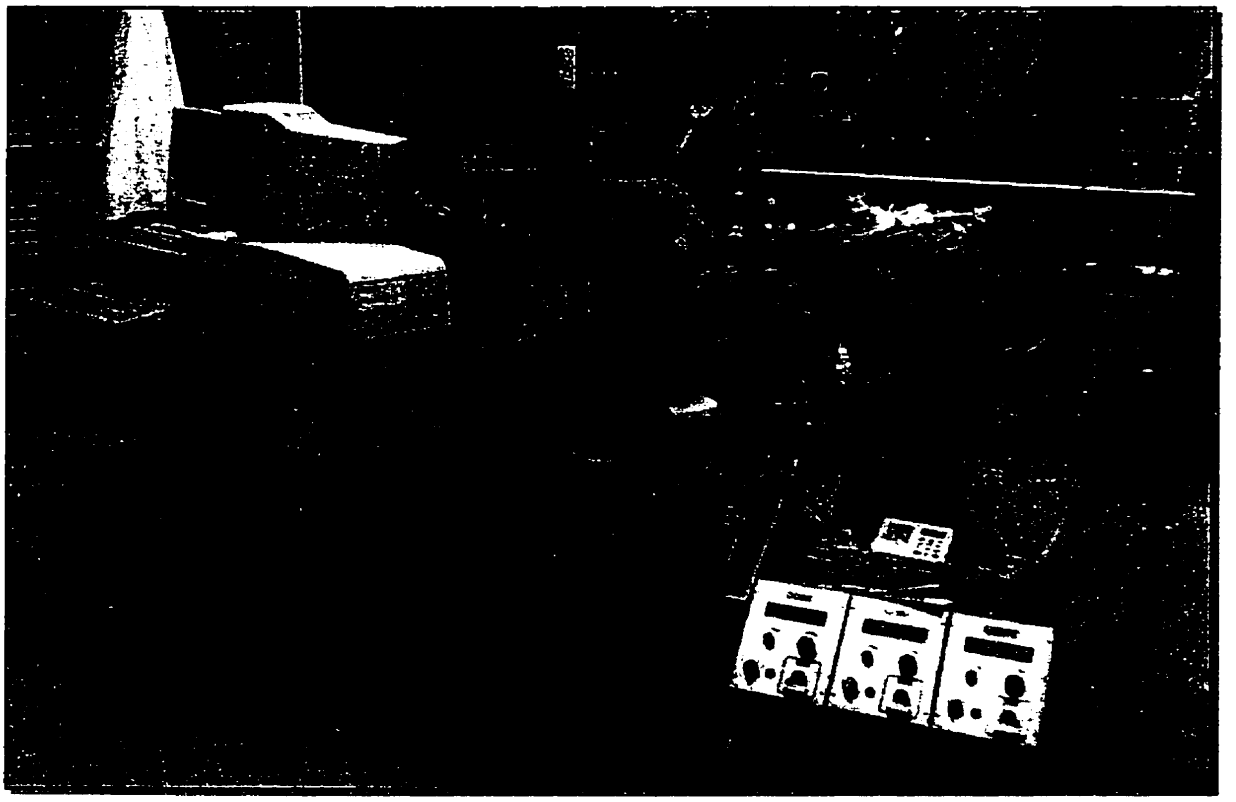

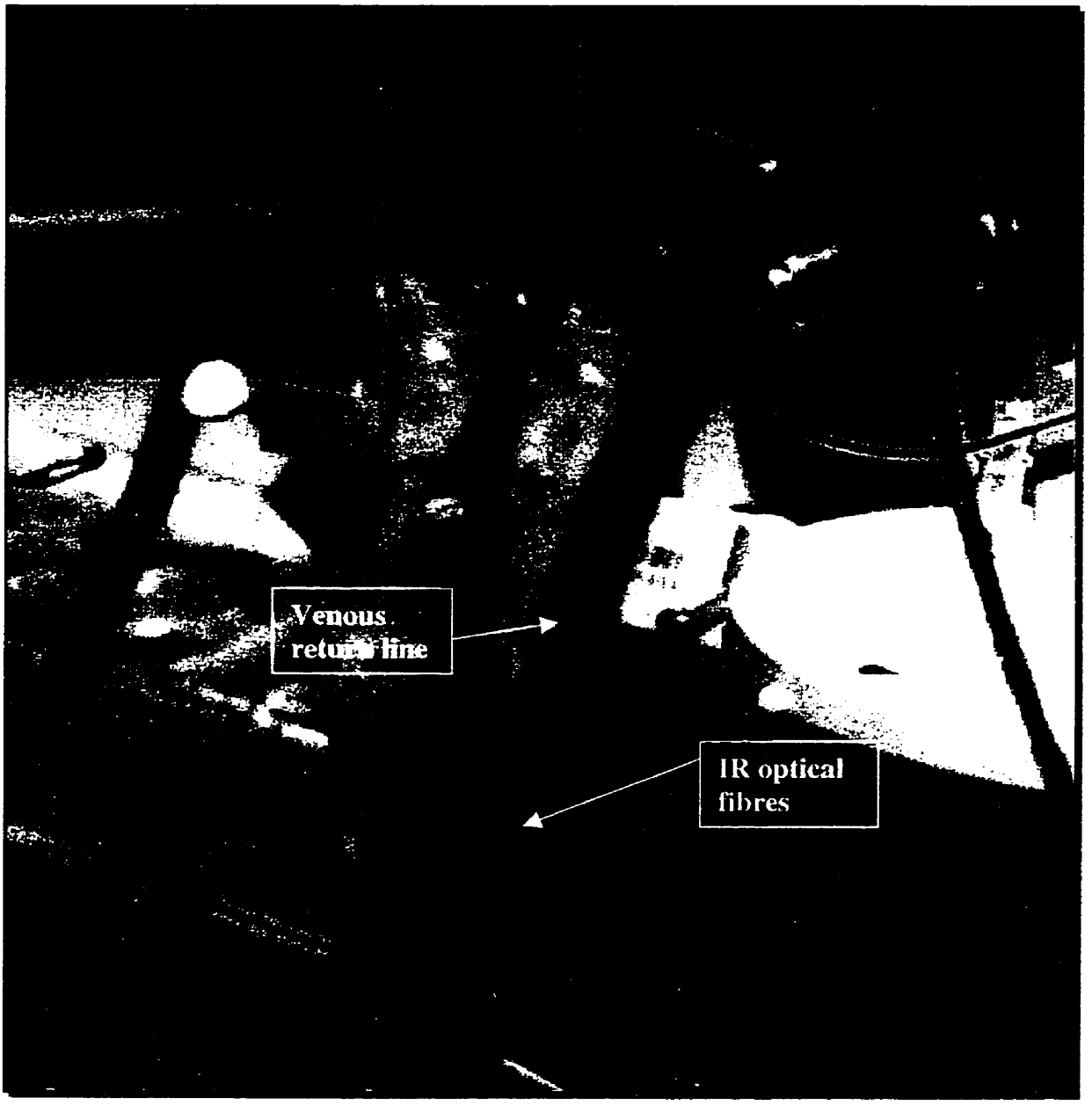

Figure 3.7 – The near-infrared (NIR) custom-built sample holder used for continuous monitoring of esmolol and methanol levels during normothermic cardiopulmonary bypass in the pig. The sample holder was interposed in the ½" venous return line of the bypass circuit. Its interior is designed to expose a 4.0 mm length path of continuous laminar flow of blood (delimited by two CaF_2 windows and diverted from the main venous return line) to the near-infrared radiation via an optical fiber connection.

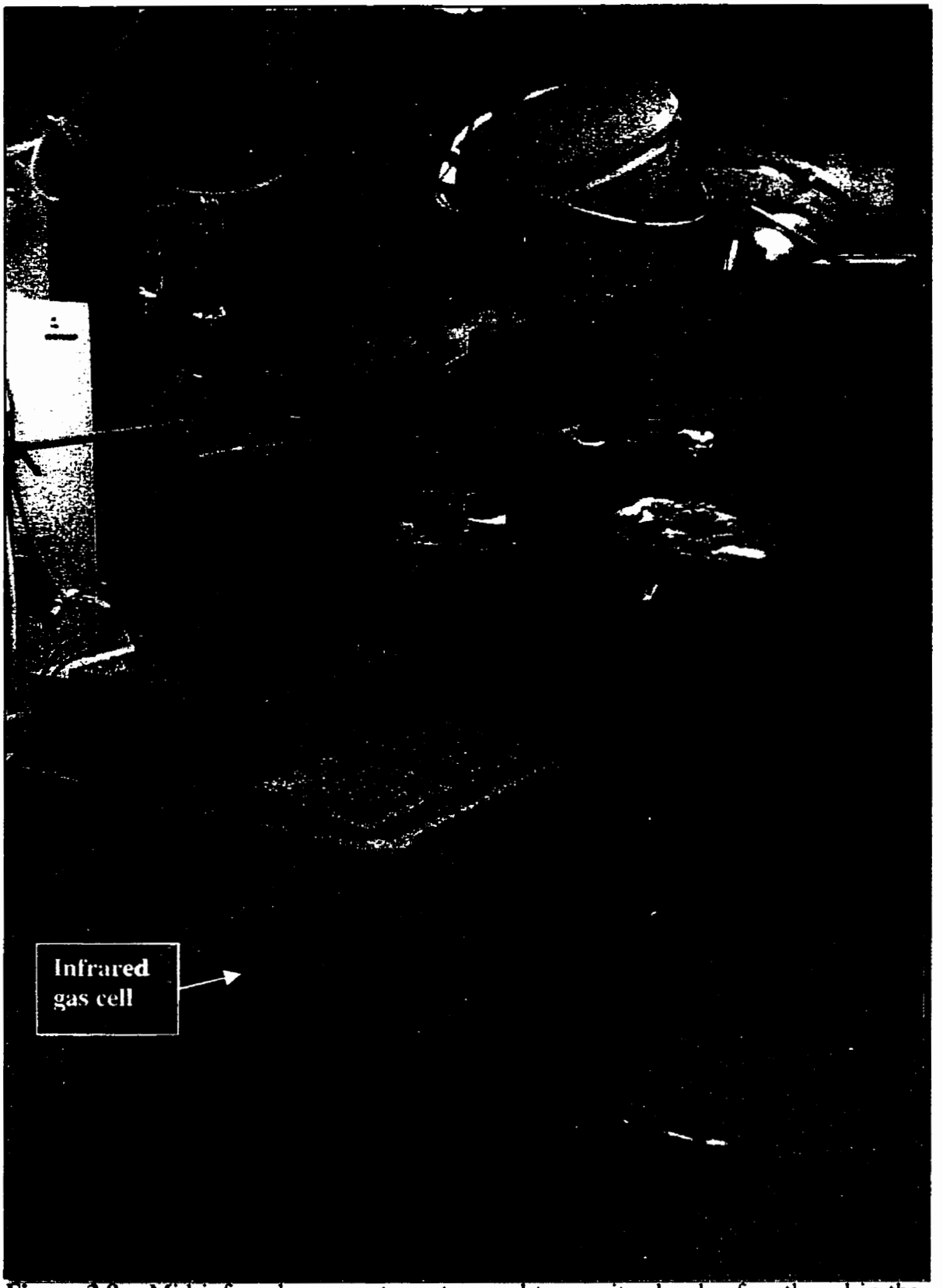

Figure 3.8 – Mid-infrared gas spectrometer used to monitor levels of methanol in the gas exhaust leaving the oxygenator in the bypass circuit.

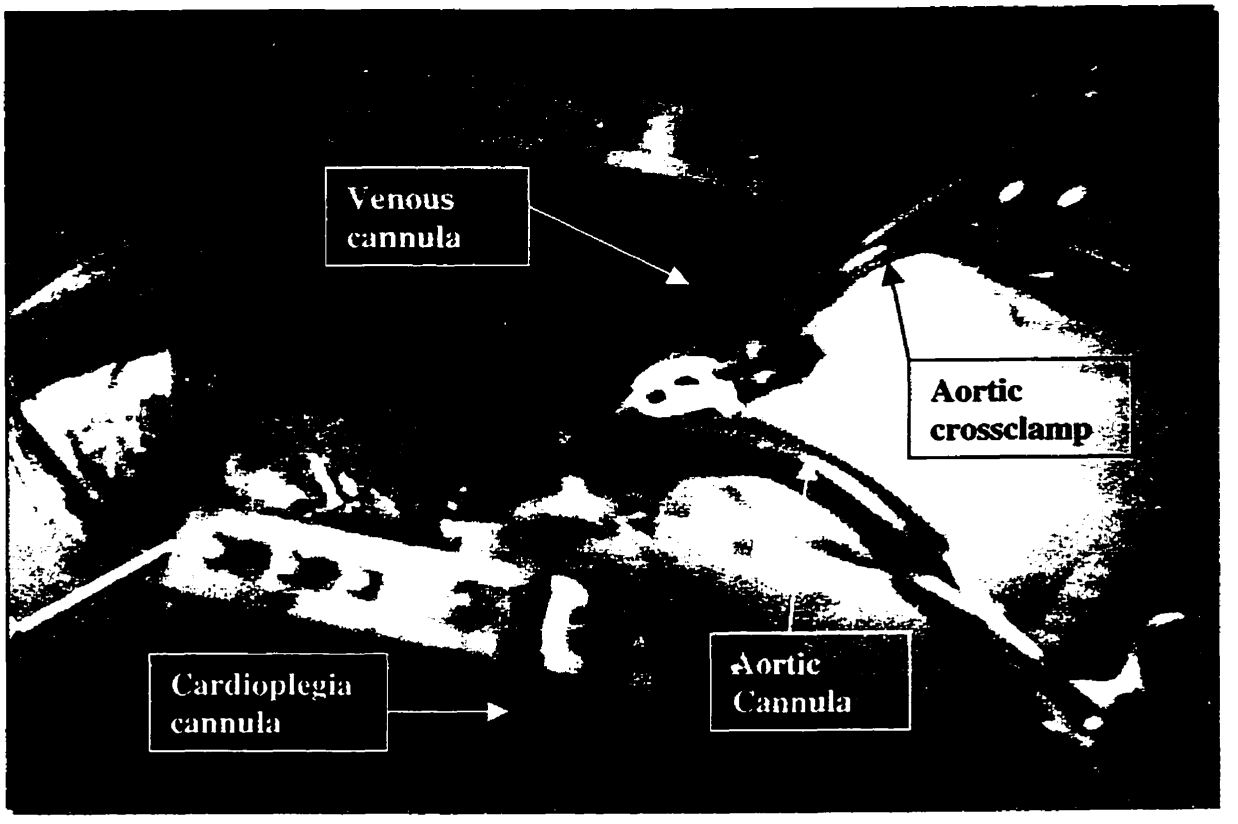

Figure 3.9 – The pig heart arrested with continuous infusion of esmolol (at titrated concentrations to maintain minimal myocardial contraction) injected via the cardioplegia line (first, left to right counterclockwise) inserted in the ascending aorta. Blood returns to the pig from the pump-oxygenator via the aortic cannula (second, left to right, counterclockwise). The two-staged atriocaval cannula (last, left to right, counterclockwise) drains the venous blood from the right atrium to the venous reservoir. In between the venous and the aortic cannula lies the aortic clamp, placed in the ascending aorta in between the cardioplegia and the aortic cannulae.

3.2.2.2.- Results

3.2.2.2.1 - Initial *in vitro* Experiments

The basic metabolic degradation pathway of esmolol in human blood is via an esterase enzyme reaction that splits the methyl ester bond in esmolol into the carboxylate metabolite and methanol, which was presented in Chapter 2.6. The general reaction of esmolol inactivation is presented in Figure 3.11A. Infrared spectra of these three components display specific bands of the different chemical groups present in these molecules e.g. carboxylate, ester and alcohol, which is shown in Figure 3.11B. Starting from the baseline, infrared difference spectra generated during the enzyme reaction, show bands indicating an increase in metabolites (carboxylate and alcohol), as well as a decrease in the amount of esmolol (ester) and water. *In vitro* experiments with esmolol were conducted by incubating blood and saline with pig liver esterase (Sigma-Aldrich Canada, Oakville, ON) at room temperature and were monitored for 100 minutes by infrared spectroscopy (see Figure 3.11C). In the experimental setup, the MIR circle cell was used under continuous flow conditions, pumping 20 ml of solution in a closed loop at the rate of 30 ml/min. All the expected infrared bands were observed during the experiment and are indicated in Figure 3.11C by arrows (directed upwards for the metabolites and directed downwards for esmolol). The enzyme reaction performed in saline showed kinetic constants of 23.1 µmol/min for esmolol incubated with pig liver esterase, within the expected range of the enzyme activity (200 µmol/min for butyric acid, ethyl ester). The same reaction performed in 10% albumin solution was not significantly reduced (compared to in water), whereas the experiment performed in isolated pig blood using red blood cell esterase showed a reduced enzyme activity (< 50 %), indicating a

lower metabolic rate of esmolol in whole blood. A possible explanation for the reduced enzyme activity could be the slower process of esmolol diffusion into the red blood cells, relative to a cell-free system. The promising results of esmolol degradation monitored by infrared spectroscopy demonstrate the suitability of this method for monitoring this enzyme *in vivo*.

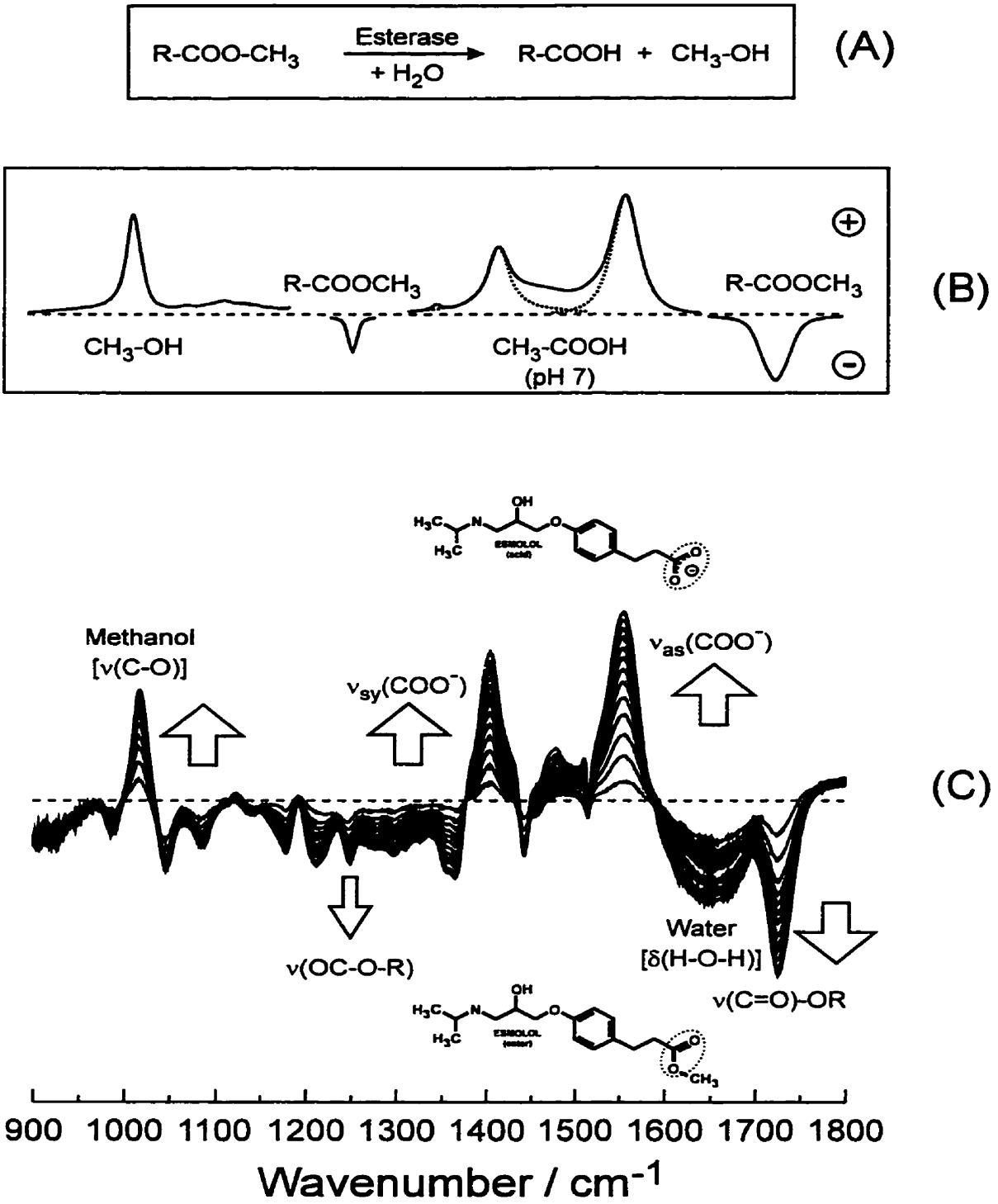

Figure 3.10 - Metabolic degradation pathway of esmolol in human blood. (A) represents the enzyme reaction transforming esmolol into the carboxylic acid metabolite and methanol. (B) reflects the location of marker bands in the infrared difference spectrum of esmolol and (C) shows the result of an esmolol solution (pH 8) incubated with pig liver esterase extract (at 25 °C). The arrows directed upwards reflect an increase in metabolites and the downward arrows the disappearance of esmolol (ester).

3.2.2.2.2 - Detection in Blood

The *in vivo* measurements assessed the capability of the infrared spectroscopy to measure the concentration of esmolol and its metabolites on-line in flowing blood. Experiments to determine the spectral signature of esmolol and methanol in water, plasma and whole blood, are shown in Figure 3.12 A-F. The IR spectrum of a dried film of esmolol in (A) demonstrates the relative dominance of the ester vibration band (at 1736 cm^{-1}), whereas esmolol in solution clearly shows a strong band 1045 cm^{-1} representing a structural vibration specific for the molecule. The latter can be detected in concentrated solutions of esmolol and allows a minimal detectable concentration of 0.1 mM for for esmolol, *in vitro*. The detection limit of methanol in the circle cell system under flow conditions was determined to be at 1 mM, *in vitro* (see Figure 3.12D-F). This value was determined by dilution experiments of methanol in water, saline, plasma, and whole blood using a strong band at 1018 cm^{-1} typical for methanol in solution. The C-O band in pure methanol is located at 1033 cm^{-1}, but shifts when methanol is diluted in water-based solutions.

In the *in vivo* experiments, infrared spectra of the venous blood were continuously recorded (one averaged spectrum (128 scans) per min) and analyzed. Figure 3.13 shows a series of representative spectra acquired on-line from an esmolol group bypass experiment. Several changes could be observed in the different peaks over time. Three typical sugar bands at 1020, 1040 and 1080 cm^{-1} quickly decreased in intensity early in the experiment upon initiation of bypass as a result of the diluting effect of the Ringers/mannitol solution initially present in the priming solution of the bypass system. This loss of intensity could be monitored over the first 10 measurements (5 min) before additional mannitol was added to the circuit. The bands for esmolol (at 1045 cm^{-1}) and

methanol (at 1018 cm^{-1}) overlap with bands coming from mannitol (located at 1020 and 1040 cm^{-1}). The detection of small amounts of methanol is therefore only possible after calibrating the band at 1020 cm^{-1} with a constant mannitol band at 1080 cm^{-1}. Changes in both bands can then reflect alterations in the methanol content, which were not different in either group. Because the sensitivity of the on-line methanol detection by IR spectroscopy is limited to 1mM, it was assumed that the concentration of methanol was below this level. Many other bands in the IR spectrum showed changes during the bypass experiment e.g. a band with increased intensity at 1142 cm^{-1}, but were not analyzed in this study.

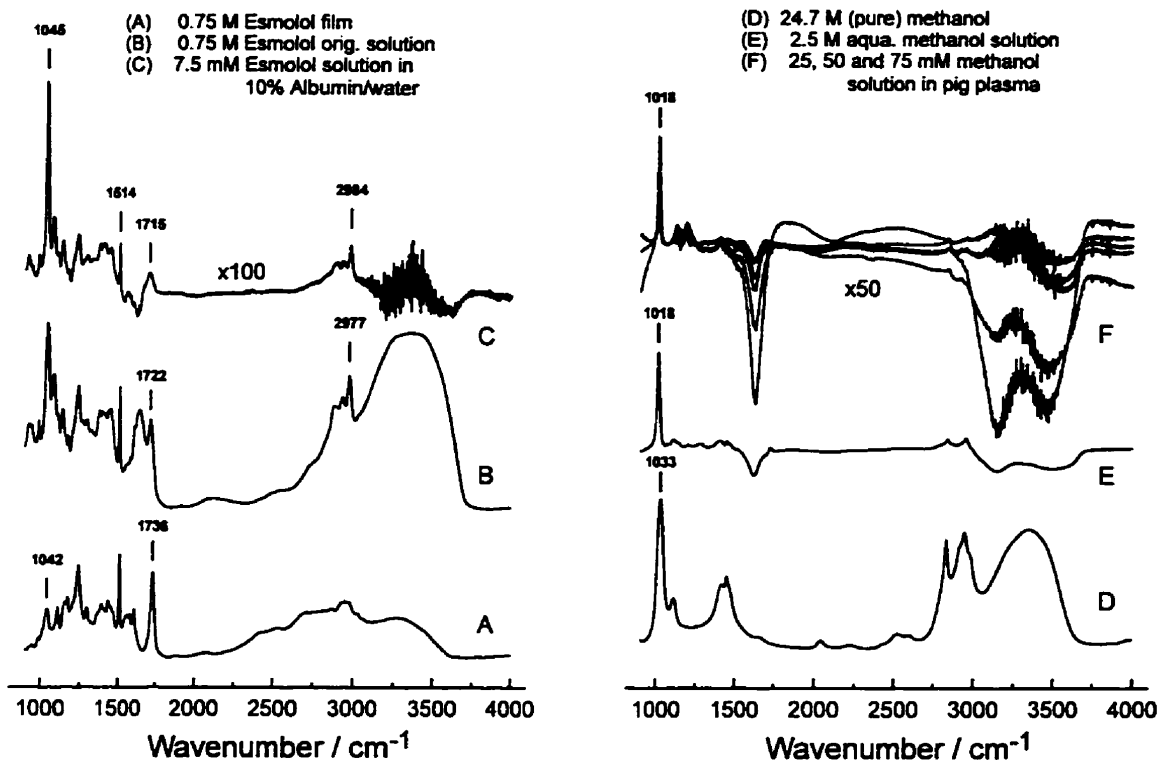

Figure 3.11 - **(A)** Infrared spectra of esmolol as a dried film on BaF_2. **(B)** Esmolol solution between two CaF_2 windows with 4 μm path length and **(C)** a 7.5 mM esmolol solution in pig plasma measured in a flow cell. **(D)** Methanol solution between two CaF_2 windows with 4 μm path length and **(E)** shows the same alcohol diluted in and subtracted from water indicating a significant wavenumber shift of the strong ν(C-O) band in water from 1033 cm^{-1} to 1018 cm^{-1}, **(F)** shows smaller concentrations of methanol diluted in pig plasma.

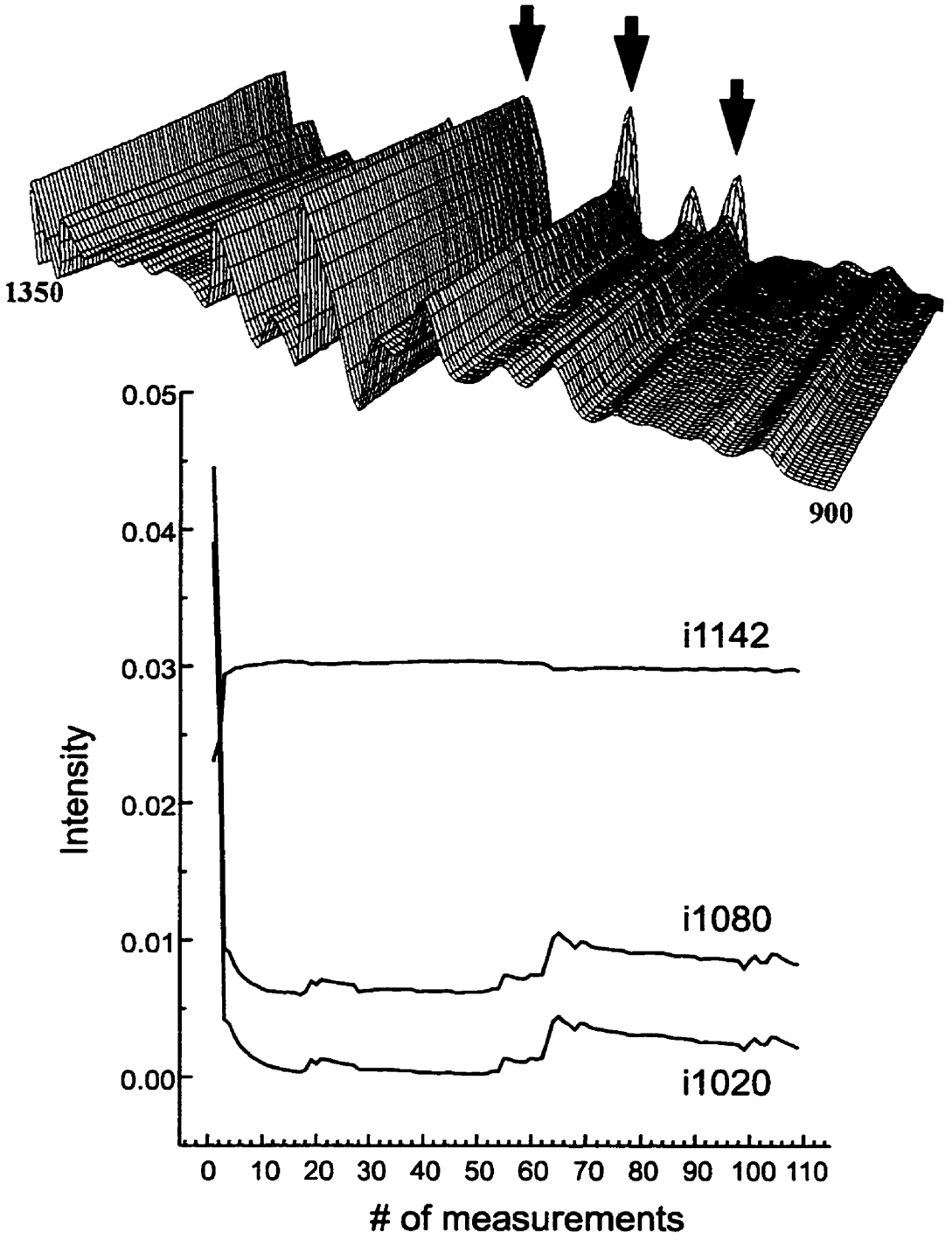

Figure 3.12 - Mid-infrared spectra obtained on-line from circulating blood in an esmolol bypass experiment. Typical sugar bonds presumably indicating mannitol and its change in concentration throughout the experiment could be identified. Methanol overlaps with the band at 1020 cm^{-1} and could not be detected on-line.

3.2.2.2.3 - Detection in the Gas Exhaust Line of the Pump-oxygenator

The pump-oxygenator in the by-pass circuit provided a possible site for methanol to escape the system. To measure the amount of methanol that could be released, an infrared gas cell (30-cm length) with an effective IR path length of 30 m was inserted in the gas exhaust line. Figure 3.14 displays typical IR gas spectra of small concentrations of methanol and isoflurane. Both gases can easily be distinguished due to specific marker bands. Methanol displays two very sharp bands at 1033 and 2843 cm^{-1} that are accessible by on-line monitoring of the gas stream. These bands also do not overlap with any other absorptions of molecules present in the exhaust line. In contrast, isoflurane shows different IR bands, the two strongest being at 1164 and 1214 cm^{-1} are (Figure 3.14). There are also two additional minor IR bands visible at 3003 and 3046 cm^{-1} that became very intense during the experiment when the anesthetic flow is increased to 3% isoflurane (Figure 3.14). These bands can easily be followed and monitored indicating the amount of the anesthetic used at any time of the experiment.

The marker band for methanol at 2843 cm^{-1} appears in this spectral region and can be monitored and quantified. No methanol was detected at any time in the gas exhaust line of the oxygenator in any of the gas cell-monitored experiments (n = 6). As a test, 10 µl methanol was injected into the gas exhaust line and monitored over a short period of time (Figure 3.15). Thirty spectra were recorded at 3 min intervals and the methanol marker band was monitored during the experiment to simulate the effect of methanol escape from the oxygenator.

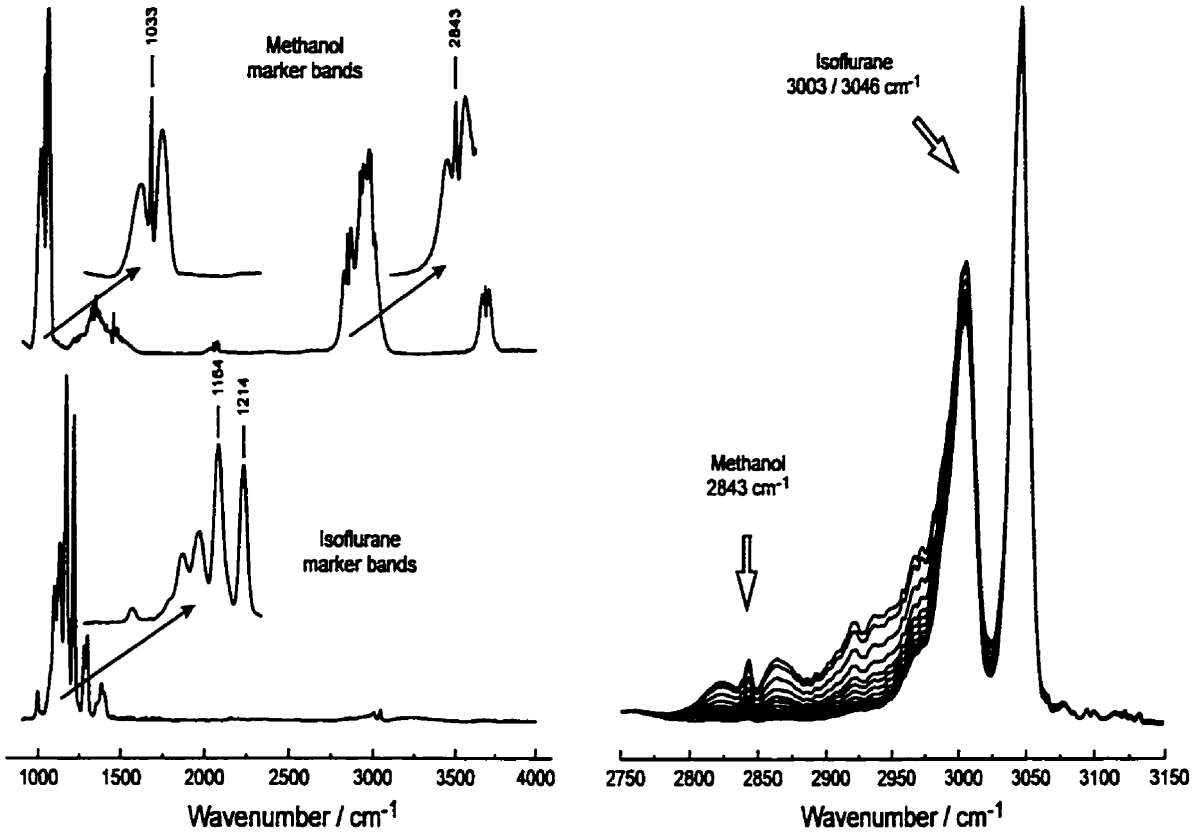

Figure 3.13 - Infrared gas spectra of isoflurane (bottom/left) and methanol (top/left) under normal atmospheric pressure conditions (showing marker bands). On the right: series of gas infrared spectra measured on-line during bypass (pig heart surgery) - pulse of methanol (10 µl) in a 3% isoflurane stream.

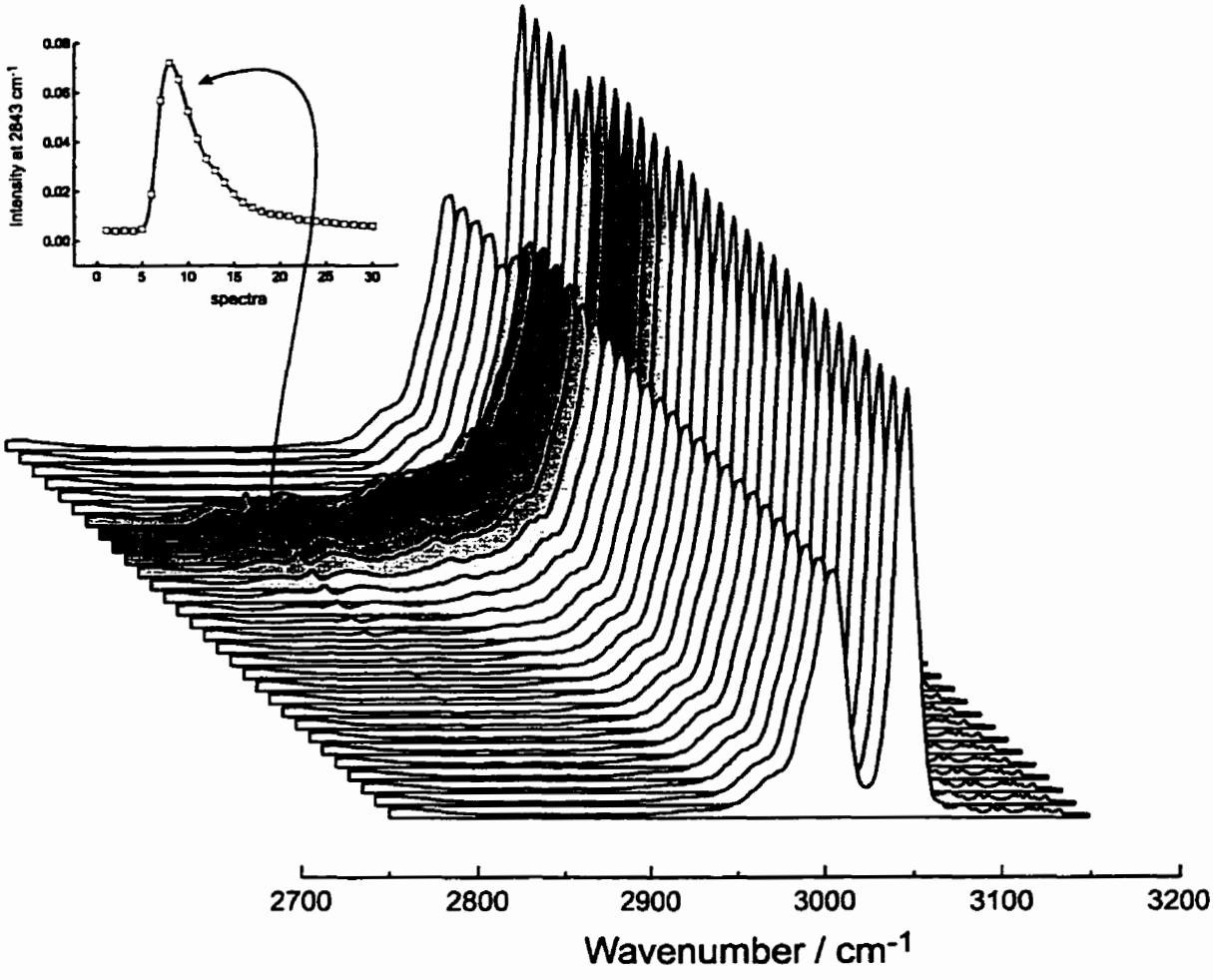

Figure 3.14 - Infrared spectra obtained over time from a gas cell placed in the oxygenator exhaust line during an esmolol pig bypass experiment. The methanol peak at 2843 cm^{-1} could be identified only after a pulse of 10μL methanol into the line leaving the oxygenator. The other large peaks in the spectra are believed to represent isoflurane.

3.2.3 - Detection Using Gas Chromatography

The "gold standard" for measurement of alcohols in blood is gas chromatography (GC)[480]. As an initial approach to detecting methanol in blood, 6 experiments using the porcine model under extracorporeal circulation and one hour of normothermic cardioplegic arrest with either esmolol or potassium (n = 3, each) were carried out. Animal preparation, anesthesia and surgical techniques were as described previously. Throughout each experiment, a total of five blood samples was acquired. A first baseline sample was acquired during initiation of bypass, followed by 2 samples collected at 30 and 60 minutes of cardioplegic arrest. Two final samples were collected during partial bypass and upon recovery, immediately before weaning the animal off bypass. All samples were obtained from the same site in the circuit (from the stop-cock attached to the vent of the arterial filter) and collected in gray-cap Vacutainers, immediately sealed and stored at 4° C to avoid volatilization of methanol for analysis. The biochemist responsible for the measurements was blinded to the cardioplegic agent.

3.2.3.1 - Materials & Methods

Methanol concentration in plasma was determined using a 5890 Hewlett Packard Gas Chromatographic System. Separation was achieved on a Supelcowax 10™ fused silica capillary column (30 m *x* 0.25 mm, 0.25 μm) using hydrogen as carrier gas and nitrogen as make-up gas. Sample injection was done using a split capillary injection with sample size of 0.20 mL. Based on initial experience, optimal temperatures for methanol separation were determined to be 40° C for the column (isocratic), 200° C for the

injection port and 250° C for the Flame Ionization Detector (FID). Millennium Chromatographic Manager Software was used to acquire and process the data.

Before final storage, the samples were centrifuged for 15 min. at 4° C , the plasma was separated from the red blood cells, sealed under a blanket of nitrogen and stored at -75° C.

Before injection, the plasma samples were centrifuged for 3 min. at 4° C and deproteinized by addition of 50 mL 0.8 M sodium tungstate and 50 mL 0.8 M cupric sulfate to 500 mL of plasma. Following centrifugation, the supernatant was injected onto the gas chromatography apparatus for the analyses of methanol.

3.2.3.2 - Results

Based on previous experiments and calibration curves carried out using known standards, the method revealed an 88% recovery of methanol with a correlation index of 0.988 for manual injection precision. Standard retention times determined for methanol and ethanol were 4.4 and 5.2 minutes, respectively. Retention time for formaldehyde was 4.35 minutes. The detection limit for methanol under these conditions was determined to belong to the $1:1x10^7$ dilution or 0.3125 μM.

Based on the total esmolol dose administered during the experiments (1 vial, 2.5 g) and the total volume of the system (4.5 L) the calculated methanol yield would be 1.67 mmol/L. Figures 3.16 and 3.17 ((a) through (e)) show representative chromatograms obtained from samples collected during the different phases of esmolol and potassium bypass experiments. The methanol peak which was undetectable prior to induction of esmolol arrest, became increasingly higher, reaching its maximal level at the end of the

arrest period. At this point, the methanol concentration was determined to be 312.5 μM, approximately 20 % of the theoretical yield. A smaller peak close to the methanol peak with a retention time of ~ 4.38 minutes appeared in samples obtained during the arrest period, which may possibly reflect rapid metabolism of methanol into formaldehyde. Samples obtained after interrupting infusion of esmolol and during the recovery period showed a return to prearrest levels. Blood levels of methanol detected under these conditions were less than 5% of the methanol toxicity level (6.24 mmol/L). In samples obtained from pigs belonging to the potassium group, methanol and formaldehyde levels were undetectable. Other peaks could be observed in the chromatograms and they presumably represent the gaseous anesthetic isoflurane used during surgery and/or products of its metabolism. These peaks were consistent in samples obtained from both groups.

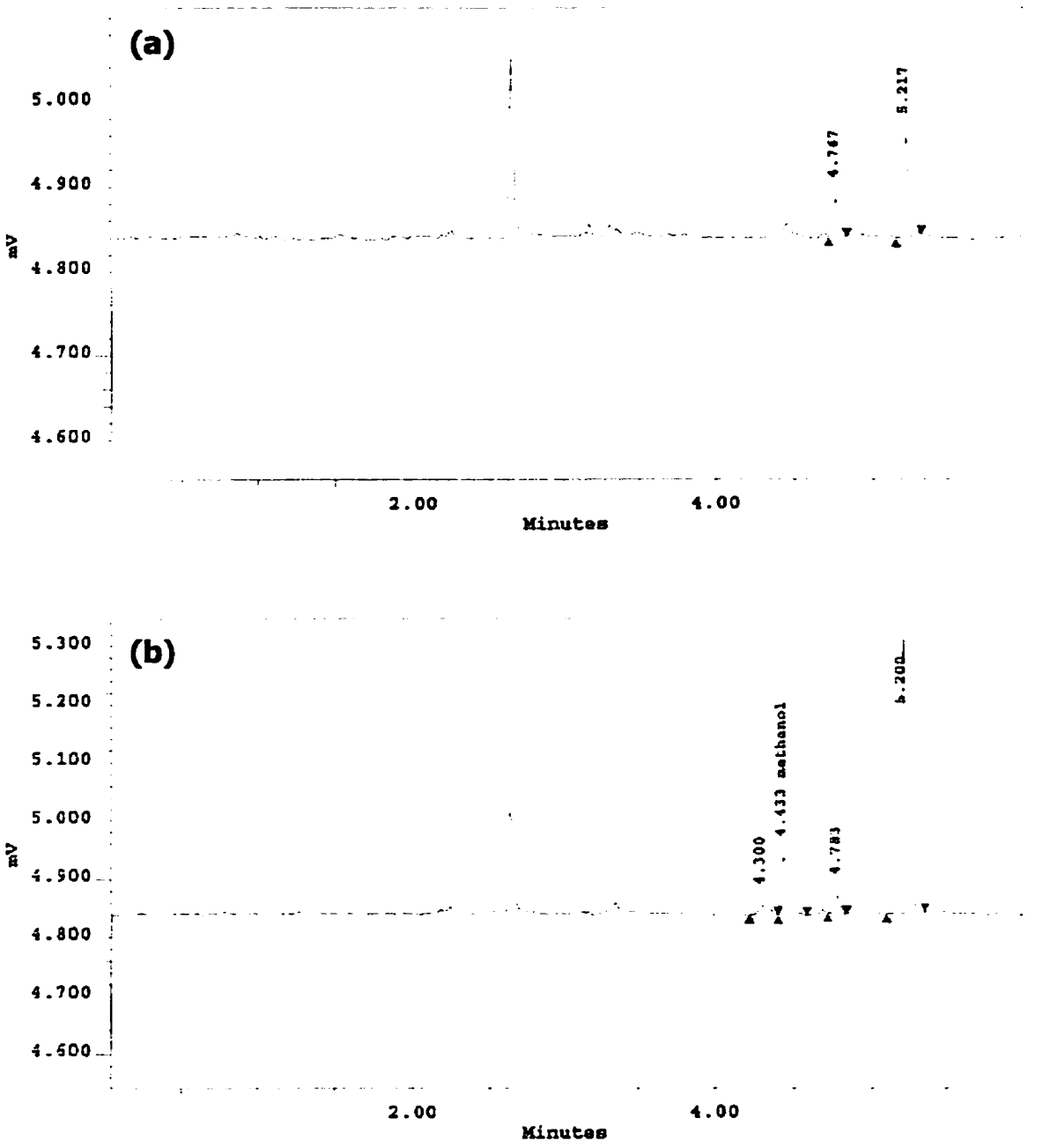

Figure 3.15. (a) and (b) – Gas chromatograms obtained from blood samples of pigs subjected to cardiopulmonary bypass and 1 hour of esmolol-induced cardioplegic arrest. (a) prearrest sample; (b) sample obtained 30 minutes after induction of cardioplegic arrest with esmolol. Note the methanol peak at 4.4 minutes retention time.

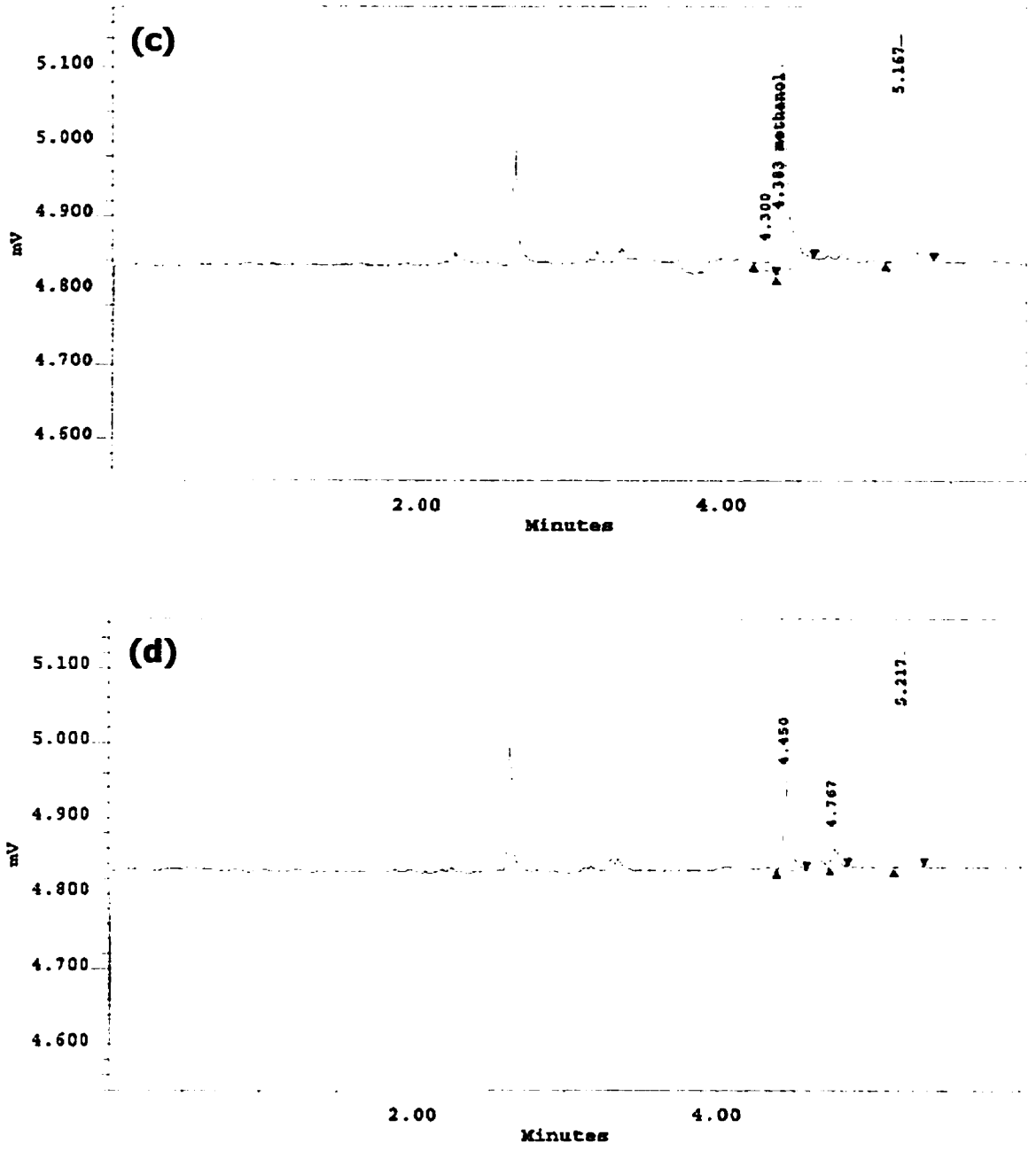

Figures 3.15. (c) and (d) – Gas chromatograms of esmolol group pigs at (c) the end of the cardioplegia period (1h) and (d) during partial bypass.

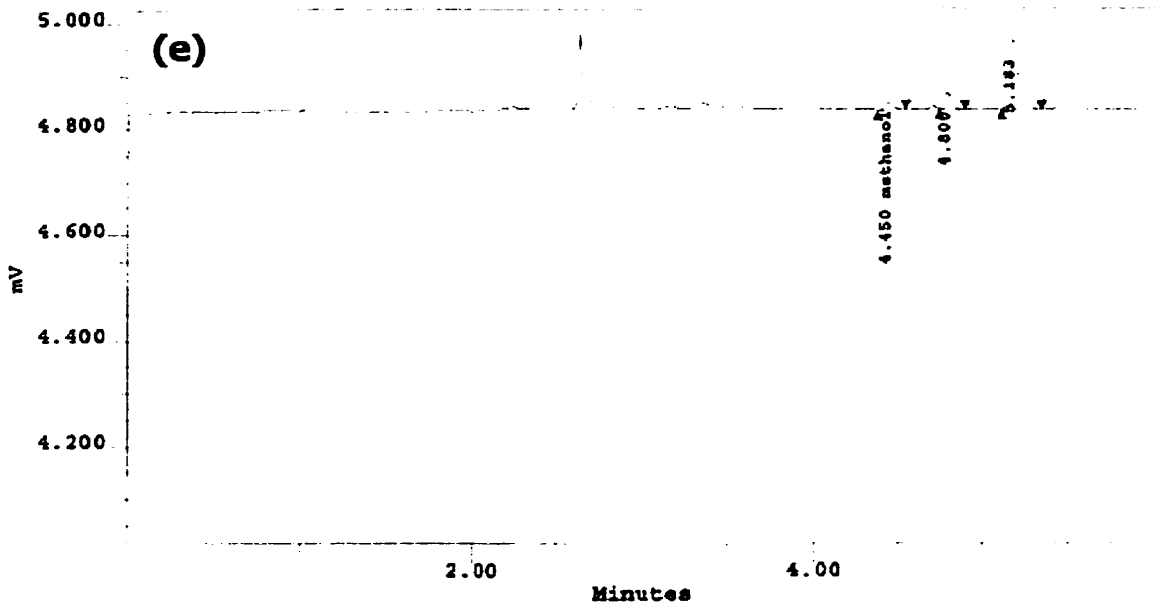

Figure 3.15.(e) – Gas chromatogram obtained immediately before weaning the pig off bypass, approximately 30 minutes after interrupting the one hour period of esmolol-induced cardioplegic arrest, showing an almost complete return to prearrest levels of the methanol peak. The peak at ~ 5.2 minutes represents alcohol injected during the process of methanol analysis. Additional peaks are believed to represent the anesthetic isoflurane and/or products of its metabolism.

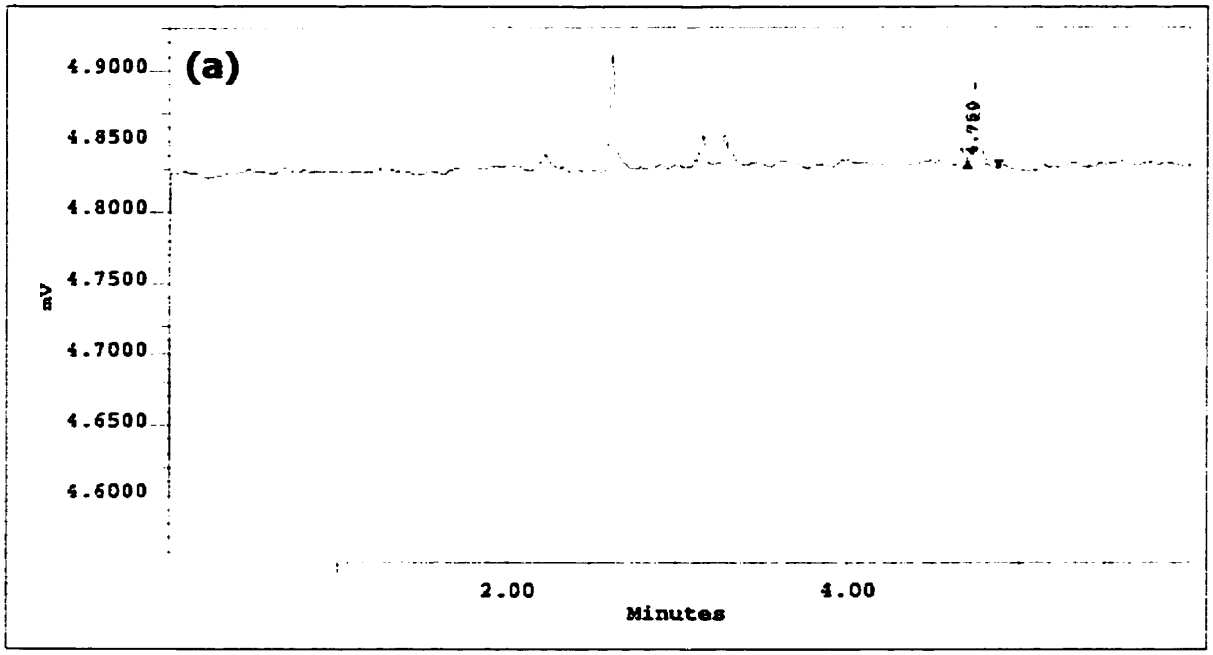

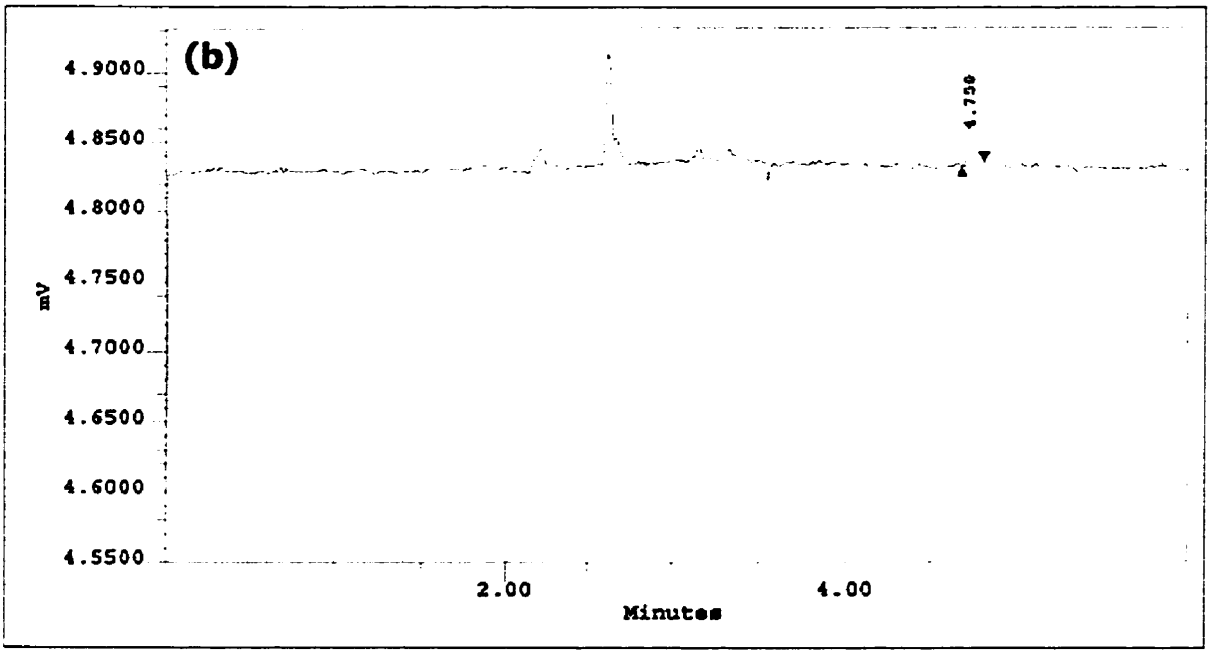

Figure 3.16. (a) and (b) – Gas chromatograms obtained from blood samples of pigs subjected to cardiopulmonary bypass and 1 hour of cardioplegic arrest induced with high K^+ (25 mM). (a) prearrest sample; (b) sample obtained 30 minutes after induction of cardioplegic arrest.

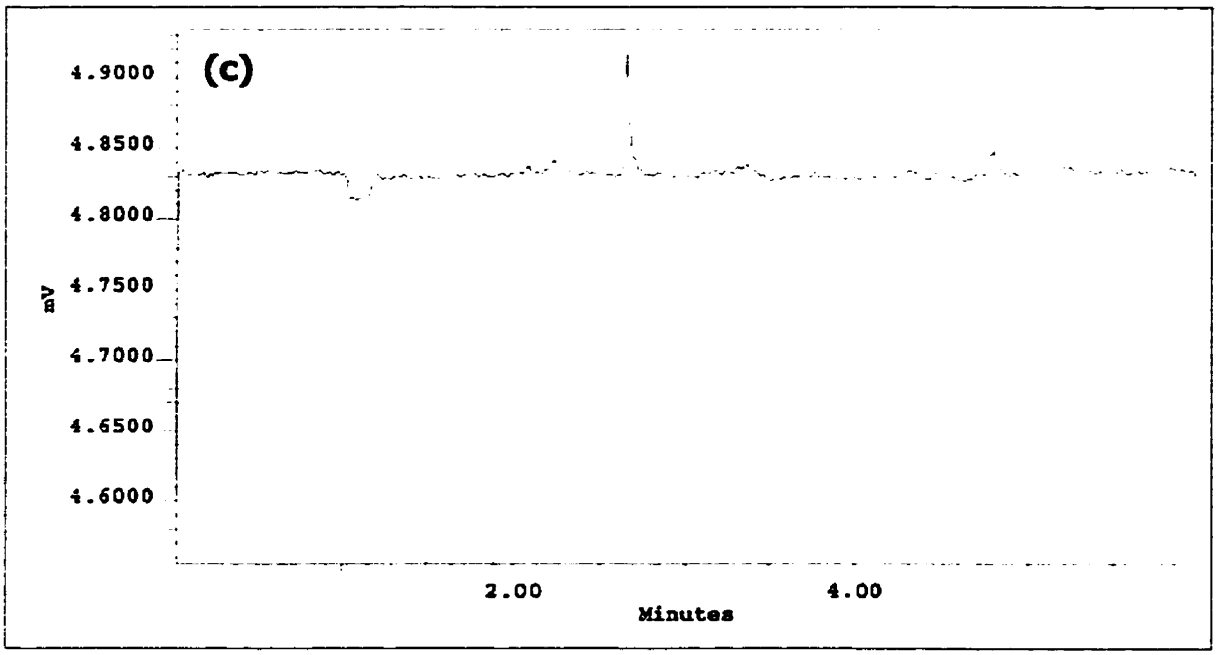

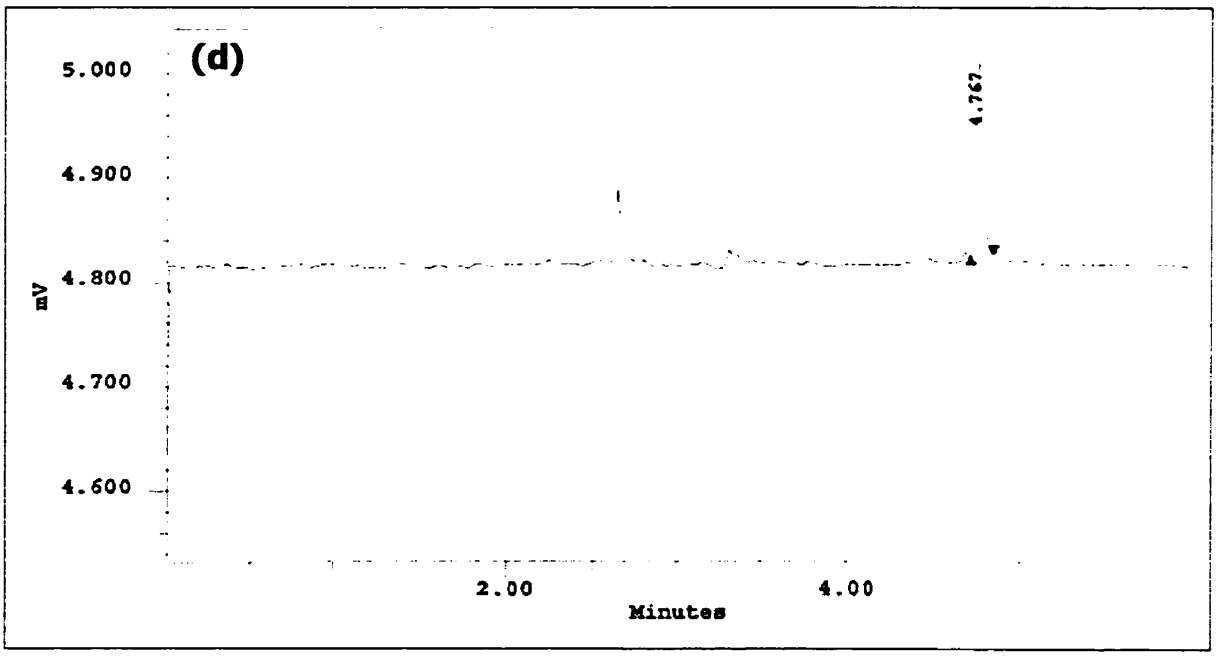

Figures 3.16. (c) and (d) – Gas chromatograms of potassium group pigs at (c) the end of the cardioplegia period (1h) and (d) during partial bypass.

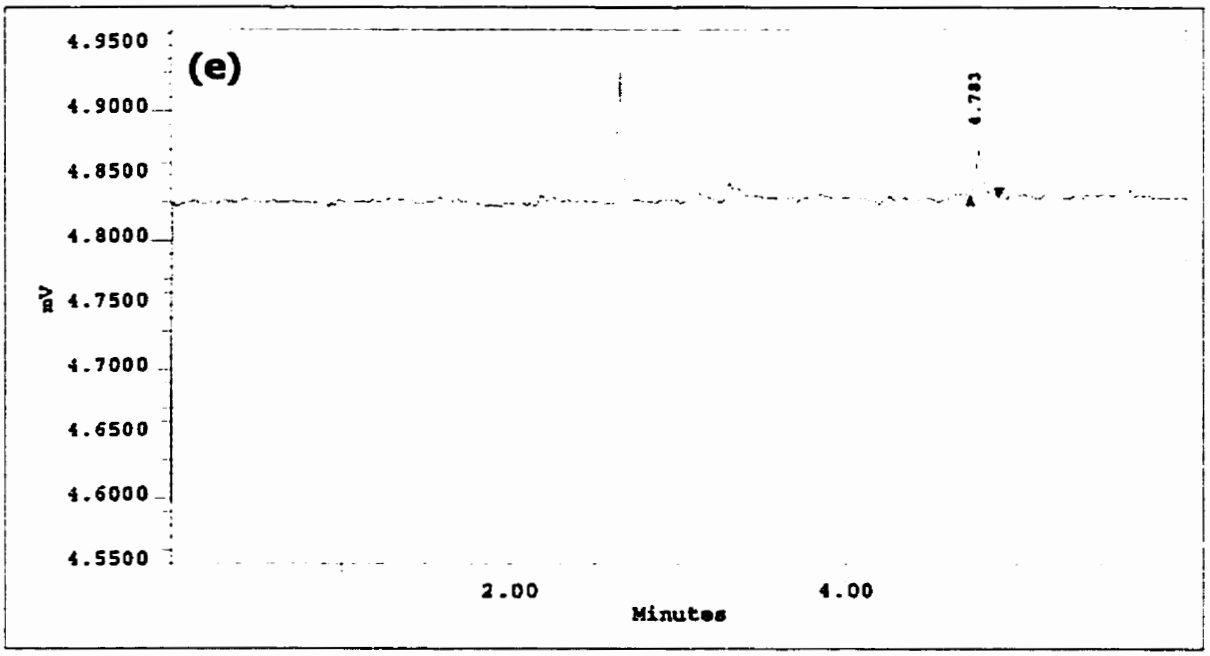

Figure 3.16. (e) – Gas chromatogram obtained immediately before weaning the pig off bypass, approximately 30 minutes after interrupting cardioplegic arrest. No methanol peaks could be detected in any of the chromatograms obtained from pigs subjected to KCl-arrest. The peaks observed are believed to correspond to the anesthetic isoflurane and/or products of its metabolism.

3.3 - Subcellular Mechanisms of Action of Esmolol as a Cardioplegic Agent. A Multi-nuclear MRS and Ca^{++} Fluoroscopic Study.

Are there effects other than classical β–blockade?

The main objective of the work was to identify mechanisms other than beta-blockade by which esmolol induced and maintained arrest in the rat heart. ^{87}Rb and ^{7}Li MRS were used to assess changes in membrane permeability to K^+ and Na^+, respectively, reflecting effects of esmolol on K^+ and Na^+ channels in 39 rat hearts. To follow changes in high-energy phosphates in the heart during arrest and recovery, ^{31}P MRS was performed on 24 isolated rat heart preparations. Two series of 12 experiments were carried out: the first series included esmolol (n = 8) and potassium (n = 4) arrested hearts in which ^{31}P spectra were acquired for 15 min prearrest, during 60 min of arrest (with either esmolol or high K^+) and 30 minutes of recovery. The second series followed the same protocol but included a 90 minute recovery period and a control group (n = 4, each). The latter group was added to take into account the effects of continuous perfusion without drug. A final set of experiments was carried out using fluorescent microscopy to assess changes in intracellular Ca^{++} transients in the presence of esmolol relatively to 25 mM potassium in isolated cells preparations (n = 12).

3.3.1 - Materials & Methods

3.3.1.1 - NMR Experiments

For the ^{87}Rb experiments, the hearts were perfused with phosphate-free Krebs-Henseleit (KH) buffer containing (in mmol/L) NaCl 118, $NaHCO_3$ 25, KCl 4.7, $CaCl_2$ 1.75 (~ 1.1 mmol/L free Ca^{++}), $MgSO_4$ 1.2, EDTA 0.5 and glucose 11. The perfusate was equilibrated with 95% O_2/ 5% CO_2, with the pH maintained at 7.4. The KH buffer used for Rb^+ loading contained [Rb^+] 0.94 mmol/L and [K^+] 3.76 mmol/L instead of 4.7 mmol/L K^+. For the ^7Li MRS experiments the Li^+-containing solution was prepared by adding 15 mmol/L LiCl to the KH buffer described above. For the ^{31}P on the esmolol group experiments, the hearts were perfused with KH buffer. In the potassium group, 20.3 mmol/L KCl was added to the perfusate to reach a 25 mM [K^+].

Esmolol was a gift from Zeneca Canada Inc. consisting of 10 mL vials containing 250 mg/mL. Prior to utilization, 10 mL of esmolol were diluted into 90 mL of oxygenated KH solution and placed in a syringe-pump for infusion. A high concentration (200 mg/mL, 2684 mmol/L) stock solution of KCl was prepared and injected using a syringe-pump to achieve a concentration of 25 mM in the perfusate. The syringe-pump infusion rate for esmolol and potassium injections were calculated using the expression:

$$IR_{EorK} = \frac{[C] \cdot MW \cdot Cf}{S_{[EorK]}} \cdot 60$$

Where:

- IR_{EorK} represents the infusion rates for esmolol or potassium;
- $[C]$ is the desired concentration in the perfusate (in mmol/L);
- MW is esmolol or KCl molecular weight;

- C_f is the coronary flow in mL/min;
- S is the concentration of esmolol or KCl in the syringe in g/mL;
- *60* is the transformation factor to yield values in mL/h

3.3.1.2 - Animal Preparation

Thirty-nine Sprague-Dawley rats (male, 350-500g) were injected intraperitoneally with pentobarbitol (Tiopental®, 120 mg/kg). After reaching a surgical plane of anesthesia (absence of central and peripheral reflexes), a median thoracotomy was performed, the heart rapidly excised and dropped in cold (~ 4°C) oxygenated KH solution. The heart was then placed in the perfusion apparatus secured by a cannula inserted in the aorta (modified Langendorff apparatus) and perfused retrogradely with KH solution initially at constant pressure (85 cmH_2O) and subsequently at a constant flow (14-15 mL/min) from a roller-pump. After opening the left atrium, a latex balloon attached to a pressure line and a transducer was placed inside the left ventricle and secured with a 4-0 silk suture. End-diastolic pressure was set to approximately 8 mmHg. An NMR compatible electrocardiogram (ECG) electrode was placed on each ventricular wall. Functional data and ECG waveforms were acquired using a computer (software: System Integrator DMSI-200 Version 1.07c, Micro Med Inc., Louisville, KY). The temperature of the perfusate was maintained at 37° C by means of a water-bath. The pressure-rate product (PRP), the product of developed pressure (systolic minus diastolic pressures) and heart rate, was used as an index of ventricular function. The coronary flow rate was monitored with an ultrasonic blood-flow meter (Transonic Systems Inc.) and perfusion pressure was measured continuously through the catheter connecting the aortic

line and the pressure transducer and transferred to the computer. Functional data and coronary flow were measured simultaneously with acquisition of the NMR spectra. After a 10-15 minute stabilization period, the heart was placed inside the bore of an AM-360 MHz magnet (8.7T, Magnex Inc., England) attached to the Bruker console (Aspect 3000, Bruker, Germany) (Figure 3.18 (a), (b), and (c)).

3.3.1.3 - Experimental Protocols

All hearts were perfused for 10-15 minutes with KH buffer before beginning spectral acquisition according to Diagram 1. In the Rb^+ experiments, the hearts were randomly divided into esmolol (n = 15) and control (n = 5) groups. NMR spectral acquisition was performed during loading and washout of Rb^+. In the Li^+ experiments, the hearts were randomly distributed into esmolol (n = 15) and K^+ (n = 4) groups. In all Li^+ experiments (n = 19) a complete set of control data was acquired prior to treatment with esmolol or potassium (Diagram 1). Two series of ^{31}P MRS experiments were performed. The first series included a 60-minute period of arrest (induced by esmolol [n = 8] or potassium [n = 4]) followed by 30 minutes of recovery whereas in the second series (n = 12) the recovery period was extended to 90 minutes and a control group was added (in which no drug was infused). ^{31}P MRS spectra were acquired throughout the periods of arrest and recovery in both series.

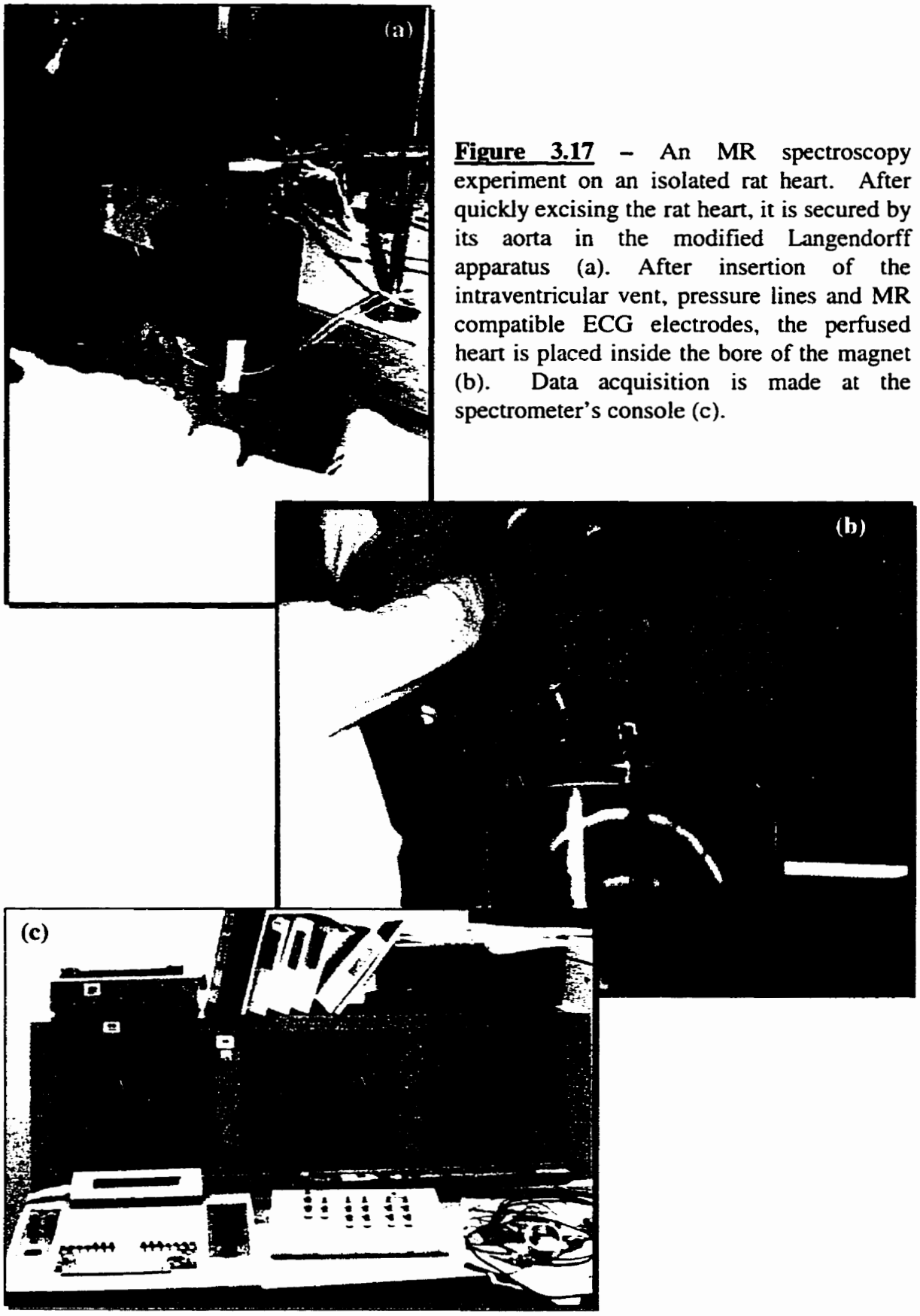

Figure 3.17 – An MR spectroscopy experiment on an isolated rat heart. After quickly excising the rat heart, it is secured by its aorta in the modified Langendorff apparatus (a). After insertion of the intraventricular vent, pressure lines and MR compatible ECG electrodes, the perfused heart is placed inside the bore of the magnet (b). Data acquisition is made at the spectrometer's console (c).

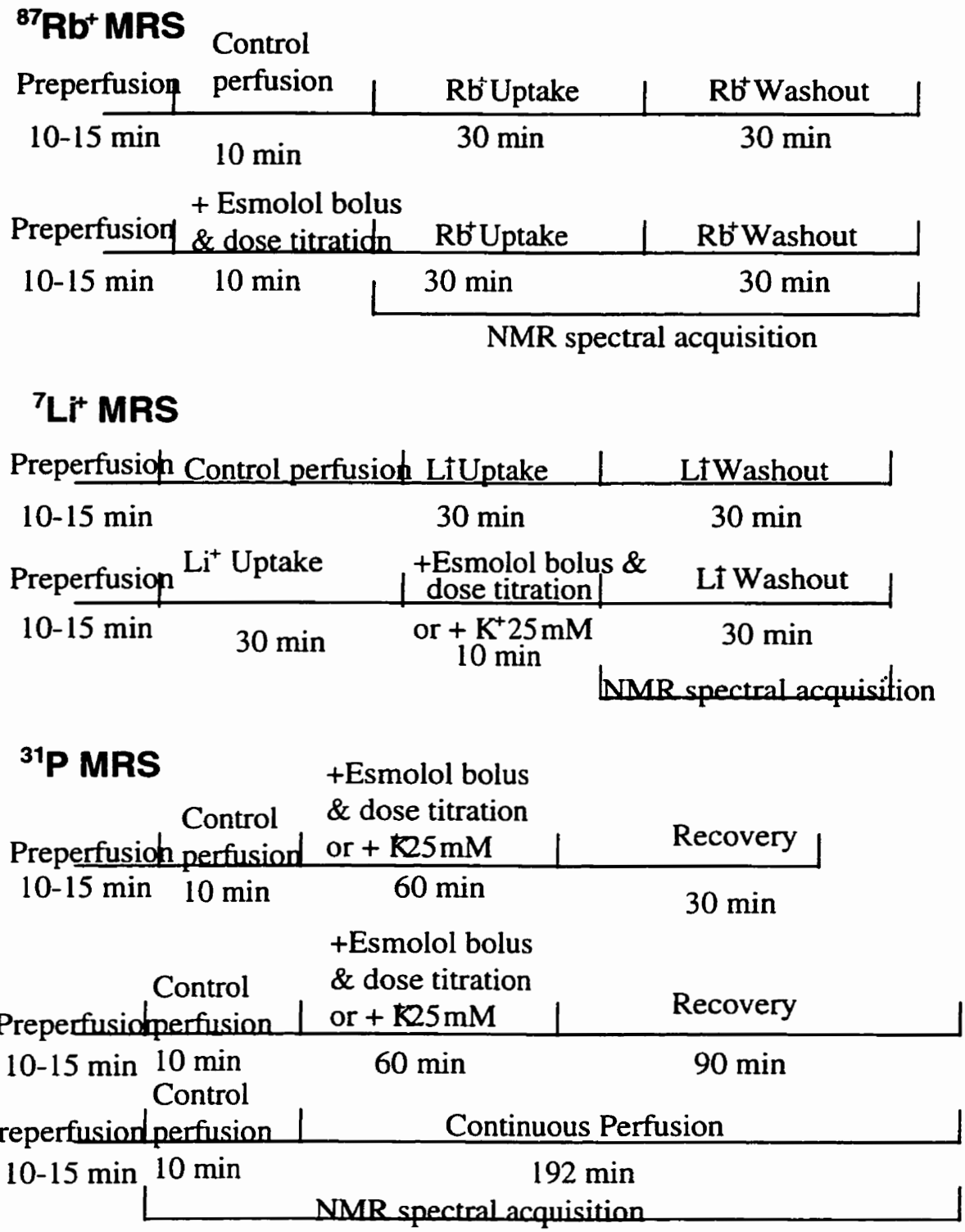

Diagram 3.1 – Schematic representation of experimental protocols carried out in ^{87}Rb, ^{7}Li and ^{31}P NMR spectroscopy experiments in isolated, buffer-perfused rat hearts (modified Langendorff preparation). See text for details.

3.3.1.3.1 - Measurements of Rb^+ Uptake/Washout

To measure Rb^+ uptake/washout, the perfusate was switched to a Rb^+-containing KH solution for 30 minutes and was then switched back to a normal KH solution for observation of Rb^+ washout (also 30 minutes). In the esmolol-treated group, the heart was arrested with esmolol as a bolus injection at 1.36 mmol/L (infusion pump rate was calculated using the formula described above) and the minimal dose needed to maintain arrest was titrated for approximately 10 minutes. Once the arresting dose of esmolol was established and there were no signs of ventricular contraction (completely flat pressure trace), the perfusate was switched to a Rb^+-containing solution and Rb^+ loading was followed for 30 minutes. At the end of the loading phase, while still in the presence of esmolol, Rb^+ washout was started by switching to normal KH solution for 30 minutes. The acquisition of $^{87}Rb^+$ MRS spectra took place throughout loading and washout. To reduce the contribution of the Rb^+ signal in the bath surrounding the heart, the hearts were perfused in a "dry" mode[481]. Previous work has showed no marked change in Rb^+ kinetics or function using this "dry perfusion" technique[486,482]. The temperature was controlled and maintained at 37°C by N_2 gas flow at 10-15 L/min through a heating element placed inside the bore of the magnet. A total of 13 different doses varying from 209 to 544 μmol/L were used. In two other experiments, esmolol at 1.36 and 1.7 mmol/L was used to maintain arrest and eliminate electrical activity. An additional 5 experiments, in which no esmolol was used served as controls.

3.3.1.3.2 - Measurements of Li^+ Washout

For these experiments, NMR spectral acquisition was performed only during washout, because it is not possible to detect intracellular loading of Li^+ in the presence of the high background signal originating from Li^+ in the extracellular space and in the bath. Loading was achieved by switching the perfusate to a Li^+-containing KH solution (LiCl, 15 mM) and perfusing the heart for 30 minutes. A decrease in contractile function was observed at the beginning of Li^+ loading, which was attributed to the higher than normal osmolarity of the Li^+-containing perfusate[422]. This decrease in function was transient and dissipated within 5-10 minutes. In all experiments a control washout curve was obtained by switching the perfusate to a Li^+-free solution and acquiring one set of NMR data prior to treatment with esmolol or K^+. In the esmolol experiments (n = 15), the hearts were arrested at the end of the Li^+ loading period with a bolus injection of esmolol and the maintenance dose was titrated for 10 minutes. After determining the minimal dose required to maintain arrest, the perfusate was switched to Li^+-free KH solution and NMR data were acquired during Li^+ washout, in the presence of esmolol at the titrated minimal maintenance dose. In the K^+ group (n = 4), the same protocol was followed with the exception that arrest was induced with an injection of potassium at a constant dose of 25 mmol/L. To minimize the NMR signal from Li^+ in the bath during Li^+ washout, the hearts were superfused with KH Li^+-free flushing solution using a roller-pump at a constant flow rate 5 times greater than the coronary flow (~ 60 mL/min). A total of 10 experiments were performed in this manner and the arresting concentrations of esmolol varied from 356 to 586 μM. In five other experiments, higher maintenance doses (1.0, 1.5, 1.7 and 2.0 mM) were used to maintain electrical arrest. In all experiments Li^+

washout kinetics were observed with either esmolol or potassium for a total period of 30 minutes.

3.3.1.3.3 - Measurements of High-energy Phosphates Levels (^{31}P MRS)

In the esmolol group, the hearts were subjected to a 60 minute period of arrest with an initial bolus injection at 1.36 mmol/L (16.24 mL/h at $S_{[E]}$ = 0.025 g/mL) followed by titration of the minimal dose required to maintain cardiac arrest (which varied from 0.293 to 0.586 mmol/L). In the potassium group, cardiac arrest was obtained by switching the KH perfusate to a "high-K" KH solution which contained [KCl] = 25 mM provided by a separate reservoir. In both groups, spectral acquisition took place throughout a 60-minute arrest period and a 30-minute recovery period. A minimum of 16 spectra were acquired during each experiment. In the second series of experiments, the same protocol was used for both the esmolol and potassium groups with the exception that the recovery period was extended to 90 minutes. A control group was also added to the protocol (n = 4) in which no drug was added to the perfusate, and the heart was left beating throughout the protocol, to account for changes in the high-energy phosphates content due to experimental conditions. In this series a total of 40 spectra were acquired for each experiment.

3.3.1.4 - NMR Spectroscopy

NMR data were acquired using a Bruker AM-360 NMR spectrometer and 20-mm broadband probes (Morris Instruments, Ottawa, ON, Canada or Bruker, Bremen,

Germany). Shimming was optimized using the ^{23}Na signal from the heart and the surrounding bath. A maximal line width < 15 Hz was considered acceptable.

3.3.1.4.1 - $^{87}Rb^{+}$ MRS

Rubidium spectra were acquired at 117.84 MHz, the sweep width was 15 kHz and 512 data points were collected with a 2.5 minute time resolution (90° pulse, 60 μs; recycle time 14 ms), allowing 10240 scans per spectrum. A total of 32 spectra were acquired for each experiment (loading + washout). A capillary containing 1 mol/L RbCl + 5 mol/L KI (10 to 15 μmol Rb) was used as a concentration reference. After the shimming procedure, the perfusate was aspirated from the bottom of the NMR tube maintaining a minimal amount of fluid around the heart ("dry" mode). This practice does not lead to any detectable broadening of the $^{87}Rb^{+}$ resonance (~ 350 Hz), changes in mechanical function or changes in Rb^{+} influx or efflux relative to hearts that were immersed and flushed from outside with a Rb^{+}-free solution [486,487].

3.3.1.4.2 - $^{7}Li^{+}$ MRS

Lithium spectra were acquired using a broadband probe operating at 139.93 MHz, a spectral width of 5 kHz, collecting 512 data points. The repetition time was 2.2 s (60° pulse) providing 52 scans and a time resolution of ~ 2 minutes per spectrum. A capillary containing 0.5 M LiCl + 50 mM $(Tris)_3$DyTTHA-3Tris.HCl (7 mmol of Li; TTHA = triethylenetetraminehexaacetate) was used as concentration and chemical shift reference. The repetition time (2.2 s) and pulse length (60°) were chosen to increase the contribution

from the intracellular Li^+ signal (~ 0.7 < T_1 < 7.0 s) and accordingly, decrease the contribution from the extracellular and bath Li^+ signals (T_1 > 15 s).

3.3.1.4.3 - ^{31}P MRS

Phosphorus spectroscopy was carried out using a Bruker broadband probe tuned to 145.78 MHz. ^{31}P MRS spectra were acquired with a 4-min time resolution (60° pulse = 24 μs, recycle time = 2.2 s). A total of 144 scans was acquired for each spectrum, yielding a time resolution of ~ 5 minutes per spectrum. The sweep width was 10 kHz and 4k data points were collected. A sealed capillary containing 1M solution of phenylphosphonic acid (10 μmol of P) was used as a reference.

3.3.1.5 - NMR Data Processing, Kinetics and Statistical Analyses

All spectra were processed with the help of a software package (1D WinNMR® , Bruker, Bremen, Germany) in a personal computer. Curve plots, calculations of slopes and statistical analyses were done using Microcal Origin® and Statistica® software. Prior to Fourier transformation, automatic phase and baseline correction routines were performed along with a linebroadening factor of 20 Hz for Li^+ spectra, 150 Hz for Rb^+ spectra and 30 Hz for phosphorus spectra. Both areas and peak heights were used for spectral quantification using peak picking and integration subroutines provided by the Bruker software. Lithium and Rb^+ experiments were modeled as first-order kinetics and the slopes (k) of the curves obtained from linear regression of the logarithmically-transformed curves of the ratios peak/reference x time were compared. In the Rb^+ experiments the rate of accumulation (uptake) was calculated using two different models:

(a) from the slope of the initial (considered linear) portion of the uptake curve (initial six data points less the first point, ~ 12 minutes); and (b) using the exponential growth equation (see Results) to obtain *k* values. The first point in Rb^+ and Li^+ experiments (in uptake and washout curves) were excluded from the analysis to reduce interference from the kinetics of equilibration of the extracellular spaces. The Student's *t* test was used for intragroup comparisons; repeated measurements ANOVA and the Tukey test were used for multi-variable analyses. The statistical significance level was considered to be 0.05. All data are expressed as means ± standard deviation unless otherwise stated.

3.3.1.6 - Calcium Fluorescence Measurements

3.3.1.6.1 - Myocyte Preparation

The isolation and preparation of myocytes have been described in detail elsewhere[483,484]. Briefly, adult Sprague-Dawley rats weighing between 450 and 550 g were obtained from the IBD Animal Facility and anesthetized following the procedure described above for the other isolated rat heart preparations. All solutions are detailed in Table 3.4. Following placement of the heart on a modified Langendorff apparatus, the heart was perfused with 50 mL of oxygenated Ca^{++}-free KH solution at room temperature (~ 22° C) to wash blood from the vasculature. Infusion of enzyme solution immediately followed the perfusion with Ca^{++}-free KH solution for 25-35 minutes. Ca^{++} tolerance was induced initially with perfusion of solution B (0.1 mM Ca^{++}) infused for 1-2 minutes to washout enzyme solution. The heart was then removed from the apparatus and placed in a beaker with ~ 30 mL of solution B. The ventricles were dissected free, minced with scissors and the beaker containing the cells was placed in a water bath at 37° C under

100% oxygen for 10-15 minutes to allow the cells to settle. After the cells settled, the supernatant was removed (~ 25 mL) and 30 mL of solution C (0.5 mM Ca^{++}) were added. The beaker was then returned to the water bath for another period of 10-15 minutes to allow the cells to settle. The supernatant was again removed (~ 25 mL) and replaced with ~ 30 mL of solution D (1.0 mM Ca^{++}) and repeated once with Hepes buffer. Calcium tolerance was induced slowly, over 30 minutes during which time the cells were maintained in suspension by gentle agitation and continuously gassed with oxygen 100%. Final [Ca^{++}] was 1.0 mM. The minimal acceptable yield rate (field estimation) was set at 70%. All experiments were completed within 5 h of the final addition of $CaCl_2$[459, 485].

Cells were chosen for inclusion in the study based on the following criteria: rod shape; quiescent until stimulated to contract by field stimulation (contraction verified by visual observation); and when not being stimulated to contract, the ratio of the 340- to the 380-nm fluorescence intensity was required to be < 1.0 ($[Ca^{++}]_i$ ~ 100 nM.

Table 3.4 – Composition and concentrations of the different solutions used in the protocol for myocyte isolation and preparation for Ca^{++} fluorescence microscopy

	Ca^{++}-free KH (in mM)	***Solution B***	***Solution C***	***Solution D***	***Enzyme Solution***	***Tyrode Hepes Buffer***
NaCl	123	123	123	123	123	137.5
$MgSO_4$	0.58	0.58	0.58	0.58	0.58	1.2
KCl	5.3	5.3	5.3	5.3	5.3	5.4
KH_2PO_4	1.2	1.2	1.2	1.2	1.2	1.2
$NaHCO_3$	20	20	20	20	20	--
Glucose	6	6	6	6	6	10
Hepes	--	--	--	--	--	20
$CaCl_2$	--	100µM Ca^{++}	500 µM Ca^{++}	1.0 mM Ca^{++}	1.25 mM Ca^{++}	--
Collagenase II	--	--	--	--	50 mg	--
Taurine	--	--	--	--	375 mg	--
DL-glutamic acid	--	--	--	--	59 mg	--

3.3.1.6.2 - Cell Loading

Isolated cells were loaded with Fura-2/acetomethyl ester (AM) (Molecular Probes, Eugene, OR) in a dark room to a final concentration of 2.0 μM by adding 10 μL of 1.0 mM Fura-2 AM stock solution in dimethyl sulfoxide to a 5-mL aliquot of cell-containing solution in a flat bottom vial wrapped in foil paper and placed into a 37° C water bath. The vial was removed from the water bath and gently shaken every 10 minutes; the total loading time was 45 minutes. The cells were then rinsed for 30 minutes with 1.0 mM Ca^{++} Tyrode solution at 37° C to remove any remaining Fura-2 from the extracellular medium[459].

3.3.1.6.3 - Microfluometry

Calcium transients were measured in a manner similar as previously described[459]. Briefly, the cell superfusion chamber consisted of a Plexiglass® block machined to accommodate a thin glass cover slip as a bottom. A droplet of cell suspension was placed in the chamber, and a thin sheet of buffer continuously flowed across the cells. The superfusion chamber was mounted on a Olympus inverted microscope attached to a PTI spectrofluorometer (PTI Industries, New Jersey, USA) in which the cells were localized by visualization. The rotational period of the interference wheel (chopper) was set at 100 ms such that a ratio was obtained every 10 ms. Cardiomyocytes were sequentially excited with 340 and 380 nm wavelength light derived from the dual wavelength spectrofluorometer. The emitted fluorescent images of the myocyte at 510 nm were recorded and quantified with photomultiplier tubes coupled to a computer. Two separate signals corresponding to 340- and 380-nm signals were fed to the computer equipped

with data acquisition software system (FeliX®, PTI Inc.). Fluorescence signal ratios were converted to concentrations based on a previously established calibration curve[459] and stored by FeliX® and were later transferred into a spreadsheet format (Microsoft Excel®) for averaging and statistical calculations. Because the cells exhibit beat-to-beat variability in amplitude of response, the data are presented as averages of 5-6 consecutive responses ± standard deviation of the mean. Average peak height was calculated for each cell. The Tukey test for significant differences along with repeated measurements ANOVA were used for statistical evaluation of differences.

3.3.2 - Results

3.3.2.1 - Effect of Esmolol Arrest on K^+ Kinetics (^{87}Rb MRS)

3.3.2.1.1 - Effects on Rb^+ Uptake

The uptake curves were modeled as a first order reaction. The ascending portions of the curves (first six data points after discarding the first point) were considered to be linear.

Linear regression analyses as described by the expression

$$y = A + B * X$$

were carried out to calculate rate constants (B term). Based on this model, esmolol did not affect the uptake of Rb^+ (mean $k = 0.032 \pm 0.014$ for esmolol experiments *vs.* control mean $k = 0.036 \pm 0.008$, P = 0.184) (Figures 3.18 and 3.19).

An alternative approach to modeling the uptake curves was carried out using the exponential association function

$$y = y_0 + A1 * [1-e^{(-x/t1)}] + A2 * [1-e^{(-x/t2)}]$$

where A2 = 0 and k = 1/t1. This approach showed no difference between the rate constants for the esmolol and control groups ($k_{control} = 0.045 \pm 0.018$ *vs.* $k_{esmolol} = 0.036 \pm 0.017$, P = 0.415) (Figure 3.20).

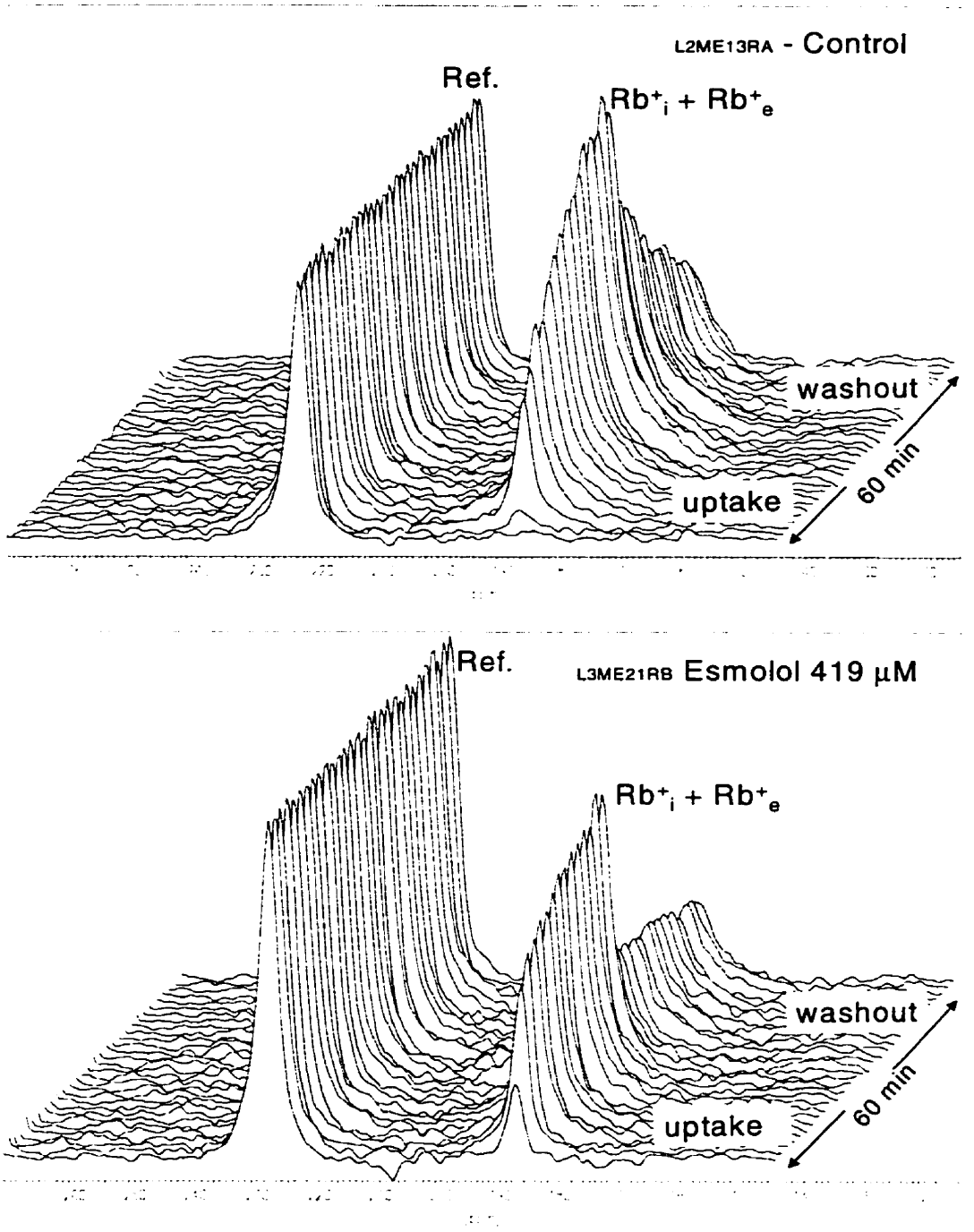

Figure 3.18 - Representative $^{87}Rb^+$ NMR spectra obtained during one hour of control perfusion (upper panel) and esmolol arrest (lower panel). **Ref.** = reference peaks (~230 ppm) containing 1.0 M RbCl in a sealed capillary tube placed beside the heart. $\mathbf{Rb^+_i}$ + $\mathbf{Rb^+_e}$ peaks (~190 ppm) represent myocyte uptake (initial 30 minutes) and washout (following 30 minutes) over time of Rb^+ from the intracellular space. Contributions from the extracellular compartment are considered insignificant 3-5 minutes after switching to non Rb^+-containing perfusate. The rates by which the right-hand peak changes over time are indicative of K^+ kinetics across the cellular membrane.

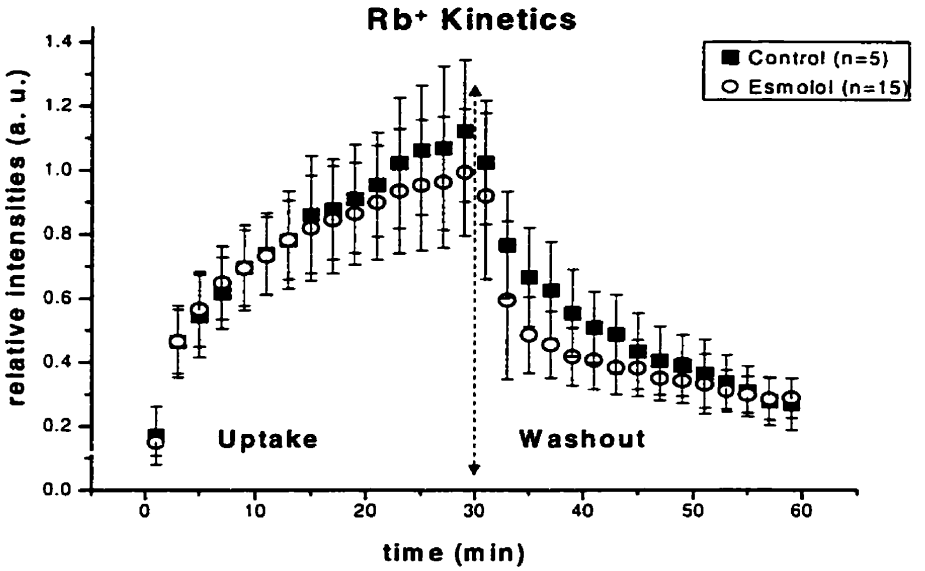

Figure 3.19 – Relative (to reference peak) peak intensities of Rb^+ uptake and washout of all control (n = 5, squares) and esmolol (n = 15, circles) experiments. Statistically significant differences between the slopes of the two curves were observed during the washout period. There was no significant differences between the slopes of the curves during uptake using a linear regression model.

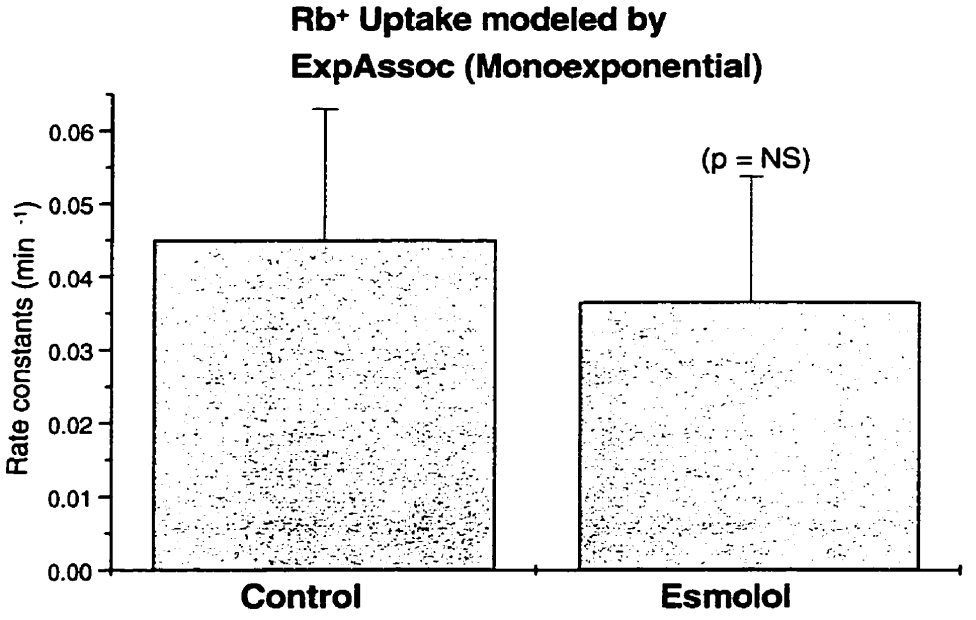

Figure 3.20 – Average rate constants of rubidium uptake (initial 30 minutes) obtained from control and esmolol experiments using the exponential association function for modeling uptake curves. No significant differences were found between the uptake rates of control and esmolol-arrested hearts, suggesting the absence of any effect of esmolol at the concentrations used to maintain arrest, on inward kinetics of Rb^+ (and K^+).

3.3.2.1.2 - Effects on Rb^+ Washout

The washout curves were modeled as monoexponential decay curves as described by the function:

$$y = y_0 + A1 * e^{(-(x-x0)/t1)}$$

Where $k = 1/t1$

The average calculated rate constants of esmolol-arrested hearts indicate that rubidium washout was 30 - 40% inhibited relative to control as monitored by reduced Rb^+ efflux during the washout period ($k_{esmolol} = 0.025 \pm 0.007$ *vs.* $k_{control} = 0.036 \pm 0.009$, P= 0.0101) (Figure 3.21). These data suggest that esmolol may alter the rate at which rubidium (and potassium) exits the myocyte when compared to controls.

3.3.2.1.3 - Effects of Esmolol Concentration on Rb^+ Uptake and Washout

In the different experiments, the dose of esmolol required to maintain arrest was titrated over a period of approximately 10 minutes. The doses varied among the different hearts from: 209-544 μM. To observe whether different concentrations affected the uptake and/or washout rates of rubidium, the rate constants were plotted against the concentrations of esmolol used to maintain arrest during each experiment. Linear regression analyses were performed to correlate the data (Figure 3.22). Neither the uptake nor the washout rate constants correlated with the different concentrations of esmolol. The correlation coefficients were: $r_{uptake} = 0.03$ and $P_{uptake} = 0.92$; and $r_{washout} = 0.15$ and $P_{washout} = 0.62$.

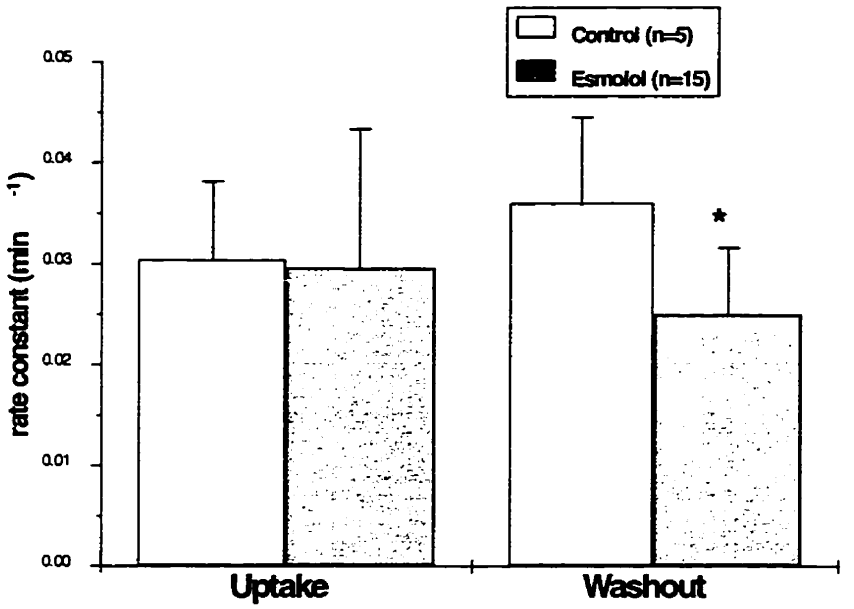

Figure 3.21 – Averages of calculated rate constants obtained from uptake and washout curves (modeled as first-order kinetics) of control and esmolol groups. Rate constants were significantly reduced (P = 0.01) relative to control during the Rb^+ washout period in esmolol-arrested hearts.

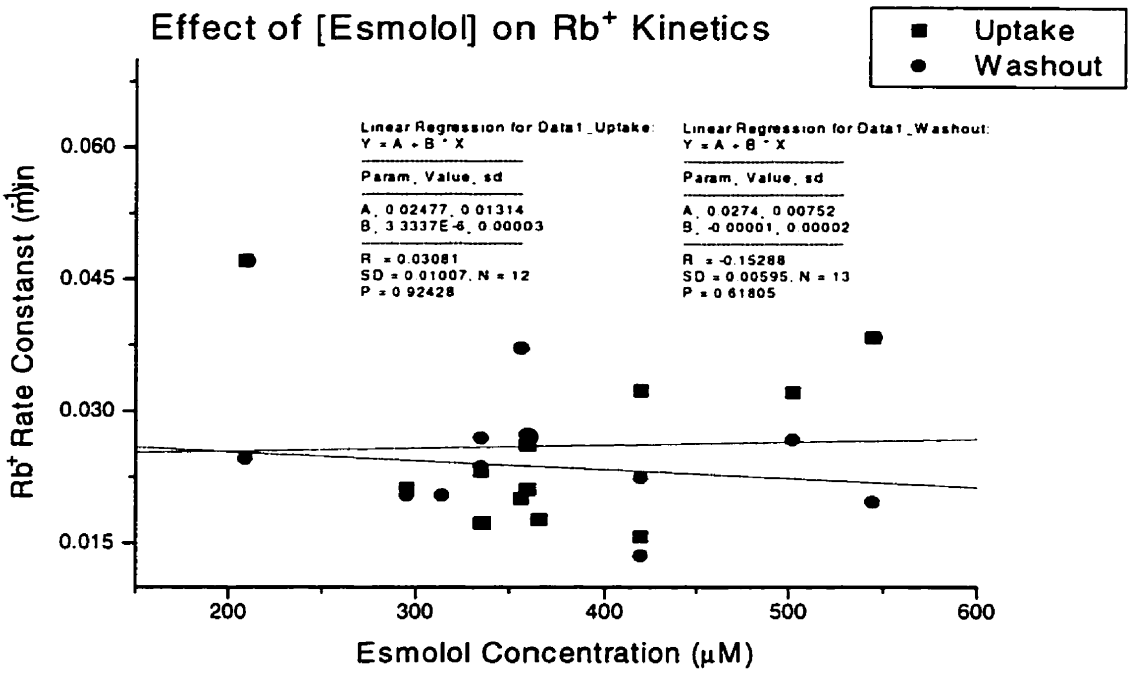

Figure 3.22 – Calculated rate constants of Rb^+ uptake and washout plotted against their individual concentrations. In both curves, no correlation (neither up or downwards) could be established between the calculated rate constants and the different concentrations used to maintain arrest. Uptake: r = 0.03, P = 0.92; Washout: r = 0.15, P = 0.61.

3.3.2.2 - Effects of Esmolol Arrest on Na^+ Kinetics ($^7Li^+$ MRS)

3.3.2.2.1 - Li^+ Washout

The analyses of Li^+ efflux curves followed the same model as the Rb^+ experiments, i.e., using the monoexponential decay function and $k = 1/t1$. Lithium efflux was significantly inhibited, ~ 62% and 57% in esmolol- and potassium-arrested hearts, respectively: $k_{control} = 0.0835 \pm 0.007$, *vs.* $k_{esmolol} = 0.0319 \pm 0.009$, and $k_{potassium} = 0.0366 \pm 0.007$, $P < 0.001$ for both groups. The slopes for esmolol and potassium differ significantly from the controls, but not from each other, ($P_{E \times P} = 0.32$), suggesting that the strong inhibition of Li^+ efflux observed during the washout period in the presence of esmolol or potassium may be due to the same mechanism (Figures 3.23 through 3.25, Table 3.5).

3.3.2.2.2 - Effects of Esmolol Concentration on Li^+ Washout

In the Li^+ experiments, the titrated doses of esmolol required to maintain arrest were in the same range as those seen during the Rb^+ experiments: 356 to 586 μM. The effect of esmolol concentration on Li^+ washout was evaluated by the same method as for Rb^+, using linear regression analysis. As shown in Figure 3.26, there was no correlation between the Li^+ washout rate constants and the esmolol concentrations used ($r = 0.27$, $P = 0.44$).

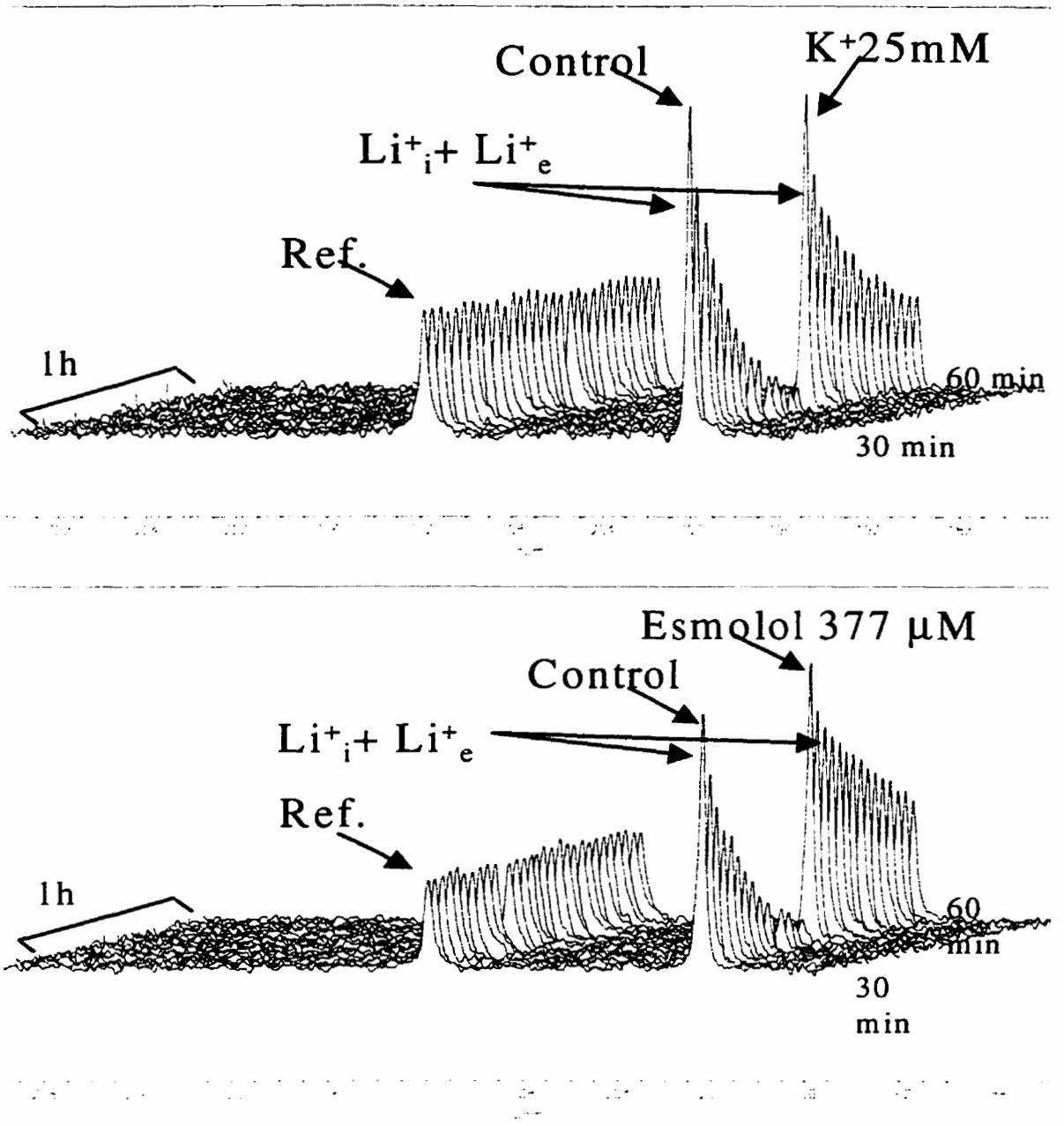

Figure 3.23 - ^{7}Li MR spectra obtained over 1h of perfusion under control and experimental conditions (30 min each). Ref. = 0.1M LiCl reference peak at ~212 ppm. The peak at ~200 ppm represents mainly Li^+ efflux from the myoplasm. Contributions from the extracellular space are minimal after 3-5 minutes because Li^+ in the extracellular space is quickly washed out upon switching to non-LiCl containing perfusate. In **a)**, Lithium washout spectra during the control period and in the presence of 25 mM of KCl; In **b),** spectra obtained during the control period and in the presence of 377µM of esmolol. Note the important inhibition of Li^+ efflux in the presence of both potassium and esmolol as seen by the different decay rates of the ~200 ppm peak.

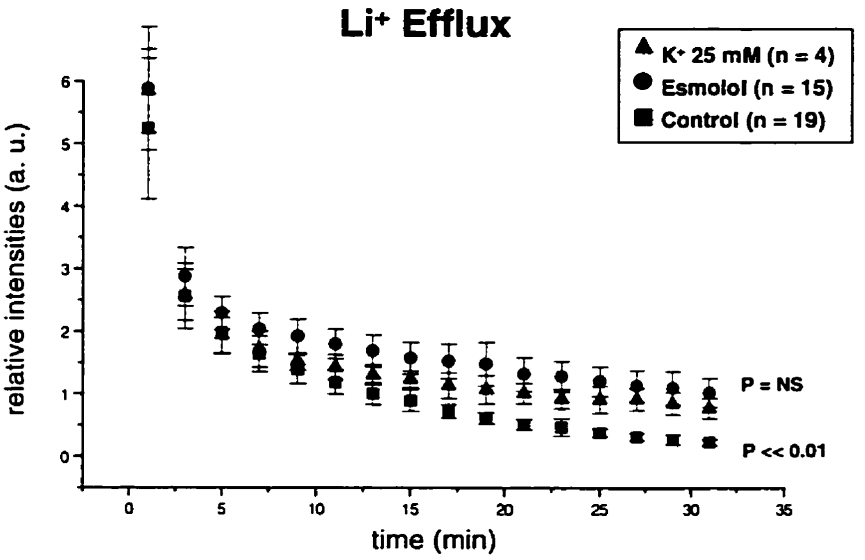

Figure 3.24 – Relative peak intensities (to reference peak) of Li^+ washout of all control (n = 19, squares), esmolol (n = 15, circles) and potassium (n = 4, triangles) experiments. Statistically significant differences (P << 0.01) occur between the slopes of the esmolol and potassium-treated animals relative to controls during the washout period. There were no significant differences between the slopes of the esmolol and potassium groups relative to each other.

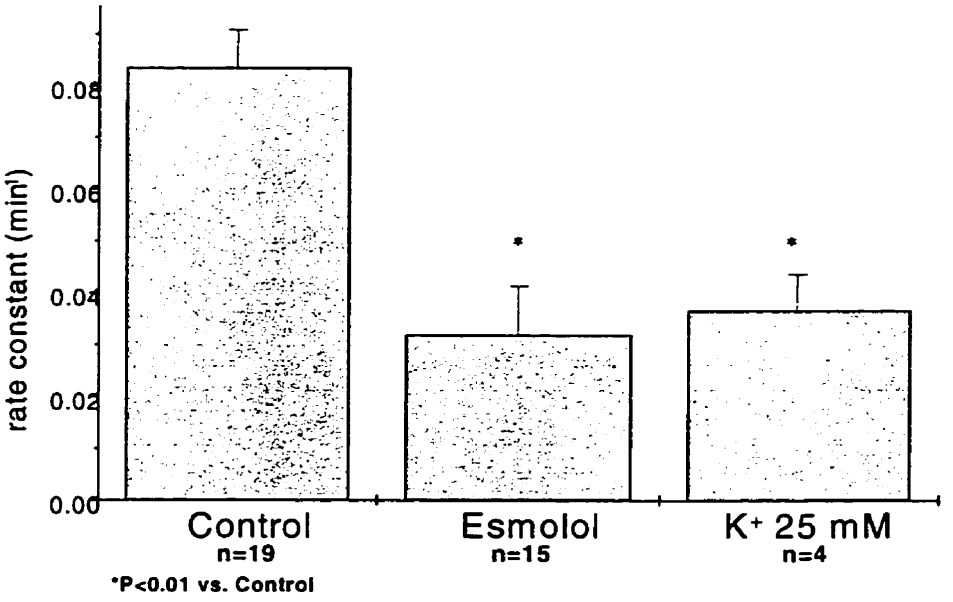

Figure 3.25 – Averages of calculated rate constants (± standard deviation) of control, K^+ and esmolol-arrested hearts. The Li^+ washout slopes of both potassium and esmolol groups were significantly different from control indicating strong inhibition of Li^+ efflux from the intracellular space during washout periods. The esmolol and potassium curves did not differ from each other suggesting a common inhibitory mechanism of Li^+ (and therefore, Na^+) kinetics.

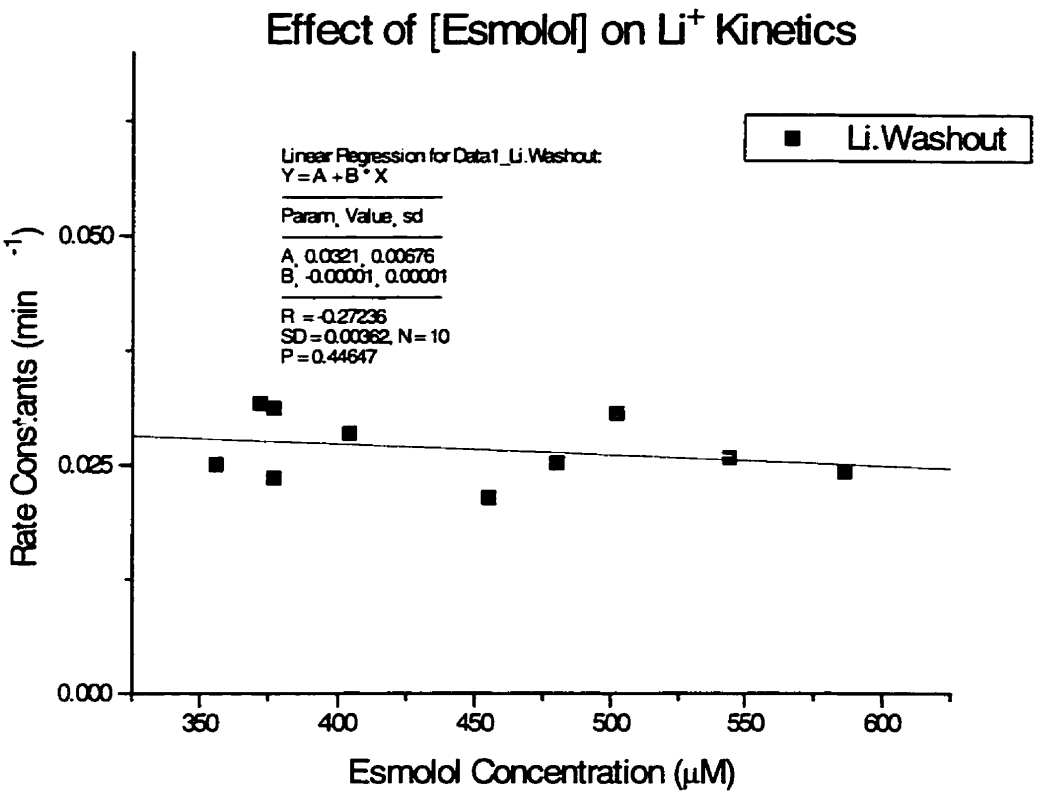

Figure 3.26 – Li^+ washout rate constants obtained from esmolol-arrested hearts plotted against the concentrations of esmolol used to maintain arrest. A correlation between the different concentrations of esmolol (within the range of 356 – 586 µmol/L) and the effect on the rate constants could not be established using a regression analysis (r = 0.27, P = 0.44).

Table 3.5 – Statistical comparisons of the average rate constants from $^7Li^+$ and $^{87}Rb^+$ MRS experiments during the uptake and washout phases of control, esmolol- and potassium-arrested hearts.

	Li^+ Kinetics					Rb^+ Kinetics					
						Uptake			*Washout*		
	means	*± sd*	*P*		*n*	*means*	*± sd*		*means*	*± sd*	*P*	*n*
Control	0.083	0.007	*vs C*	*E vs K*	19	0.036	0.008	-	0.036	0.009	-	5
Esmolol	0.032	0.009	6.53E-16	-	15	0.032	0.014	0.184	0.025	0.007	0.0101	15
K+	0.037	0.007	1.45E-04	0.32	4							

3.3.2.3 - Effects of Esmolol Arrest on High-energy Phosphates Content

^{31}P MR spectroscopy was performed on esmolol (n = 8) and potassium (n = 4) arrested hearts prior to arrest, during a 60-minute arrest period and a 30-minute recovery period. Figure 3.27 (a) shows typical spectra of esmolol and potassium treated hearts during arrest and recovery. In these spectra, phosphocreatine (PCr), β–ATP and Pi were the variables studied. As mentioned previously, the β–ATP peak most accurately reflects any changes in the ATP content in the heart.

Figure 3.27 (b), (c) and (d) show the changes in PCr, β–ATP and Pi throughout the experiments and in the different groups. The PCr content was significantly less after recovery of function (ER and KR) than prior to arrest (EC and KC) and arrest periods (EA and KA) in both groups (Figure 3.29). In addition, in the esmolol group, the levels of PCr during the recovery period were significantly lower than in the potassium group (PCr peak /reference integral = 0.256 ± 0.02, n = 15, for the esmolol group vs. 0.433 ± 0.02, n = 14 for the potassium group, $P<0.01$).

The β–ATP levels declined similarly in both the esmolol and potassium groups relative to controls during arrest. During the recovery period (ER), in the esmolol group, the β–ATP levels were significantly different from the arrest (EA) and control (EC) levels (β–ATP peak /reference integral = 0.30 ± 0.02 (ER), n = 16; vs. 0.425 ± 0.016 (EA), n = 32, $P < 0.01$ and vs. 0.592 ± 0.032 (EC), n = 10, $P < 0.01$). In the potassium group, recovery levels of ATP were not different from the arrest levels but did differ from the control (prearrest) levels: 0.398 ± 0.024 (KR), n = 14 vs. 0.467 ± 0.023 (KA), n = 16, P = NS; but KR vs. 0.547 ± 0.032 (KC), n = 8, $P < 0.01$. The recovery levels of β–ATP

in both esmolol and potassium groups were not different from each other: 0.30 ± 0.022 (ER), n = 16; vs. 0.398 ± 0.024 (KR), n = 14, P = 0.09.

Inorganic phosphate levels were reduced in both groups during arrest relative to the prearrest and recovery values, but did not differ from each other: 0.09 ± 0.012 (EA), n = 17 vs. 0.129 ± 0.012 (KA), n = 16, P>0.05; but vs. 0.202 ± 0.017 (KC), n = 8 and 0.248 ± 0.016 (EC), n = 10, P<0.01 in both cases and vs. 0.207 ± 0.013 (KR), n = 14 and 0.242 ± 0.013 (ER), P<0.01 also in both cases. In the esmolol and potassium groups, Pi levels returned to values similar to those observed prior to arrest (Figure 3.28).

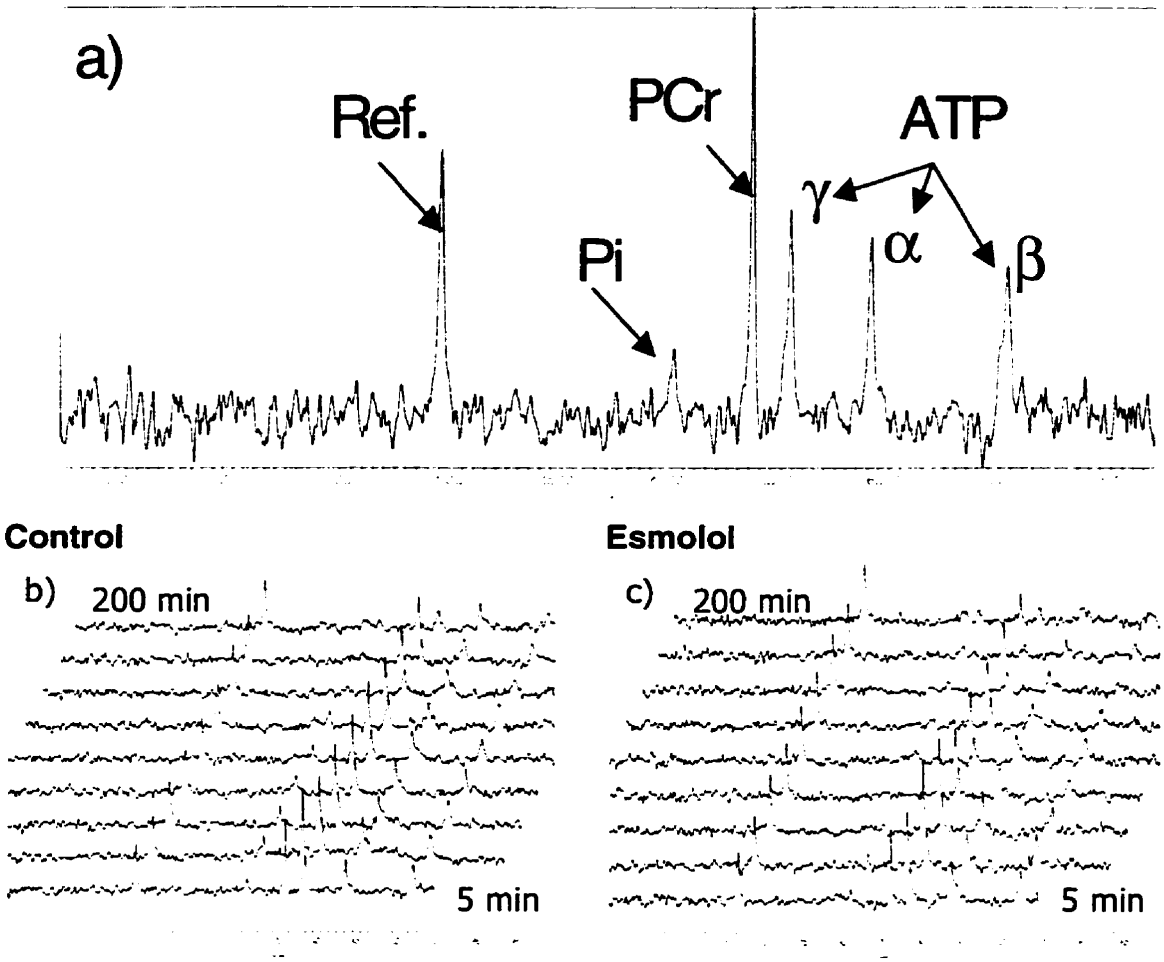

Figure 3.27 – In (a), typical ^{31}P NMR spectrum obtained from an isolated, buffer-perfused rat heart. Ref. = reference peak corresponding to the signal from a capillary tube placed beside the heart and inside the magnet bore, containing a 1.0 M solution (10 μM of P) of phenyl-phosphoric acid (PPA). Pi = Inorganic phosphate peak; PCr = phosphocreatine; α–, β– and γ– ATP peaks represent the MR signal arising from the three phosphorus groups of the adenosine tri-phosphate molecule. Because each of these groups experiences a different chemical environment, their NMR signals translate into different positions in the NMR spectrum. In b), c) and d), representative sequential spectra obtained from each group over a 200 min perfusion period.

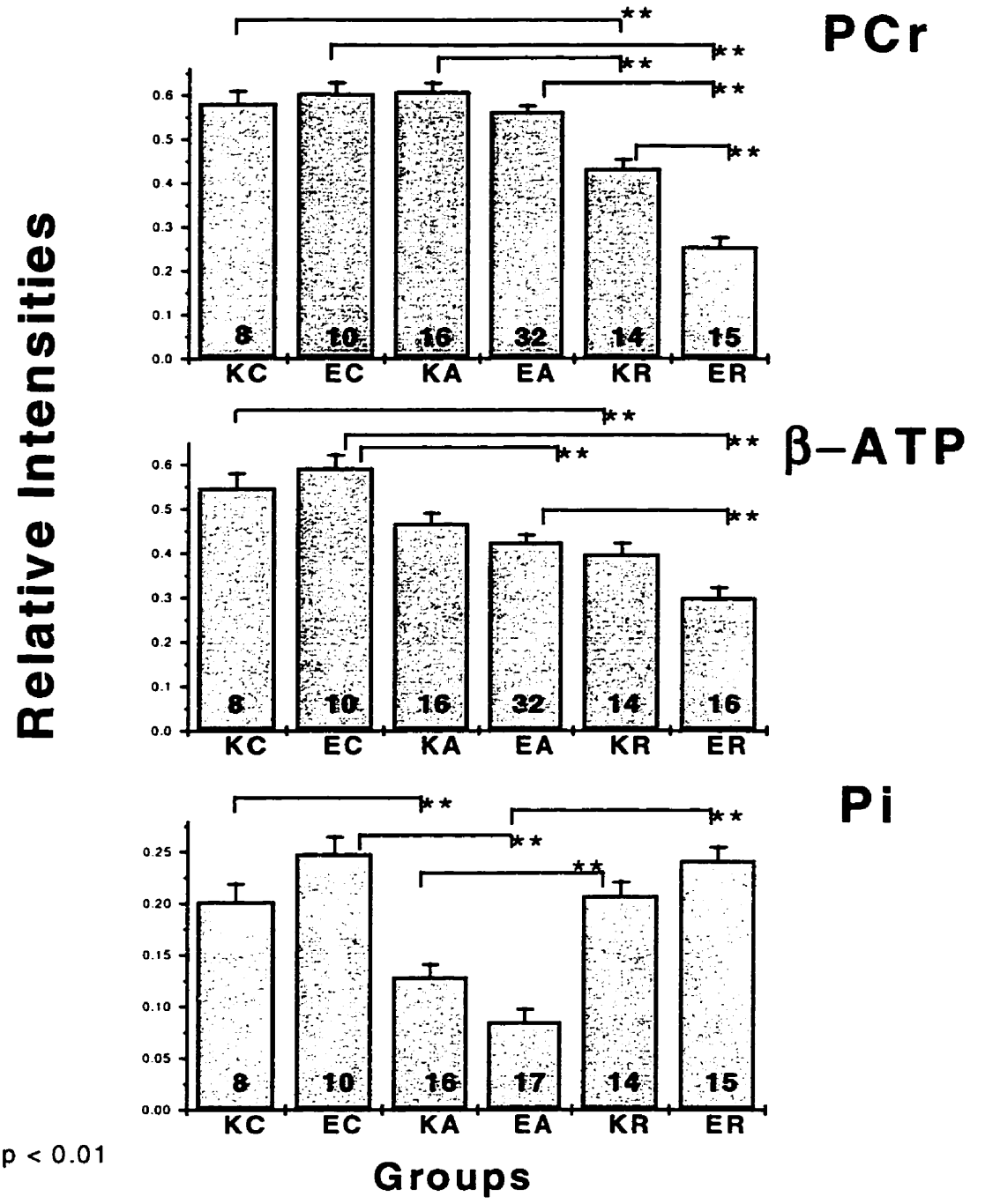

Figure 3.28 – Statistical analyses of high-energy phosphate contents of isolated rat hearts arrested with esmolol (n = 8) and potassium (n = 4). The repeated measurements ANOVA was used for multiple comparisons. K = potassium group, E = esmolol group; C = control (prearrest), A = arrest period, R = recovery period. The numbers inside the columns represent the number of data points in each group used for comparison. Physiologically relevant differences are described in the text. Data are expressed as means of relative peak intensities (peak areas/area of the reference peak) ± standard deviation of the mean.

Because changes were observed in the PCr content of the hearts, a second series of 12 experiments was designed with a longer recovery period and the incorporation of a control group to account for changes in high-energy phosphate content that were independent of esmolol or potassium effects, (e.g., due to the experimental conditions and lengthy perfusion recovery times). The hearts were divided into esmolol, potassium and control groups (n = 4, each). In the esmolol and potassium groups, the hearts were subjected to 60 minutes of arrest and 100 minutes of recovery, while in the control group the hearts were allowed to beat for ~ 200 minutes. ^{31}P MR spectra were acquired throughout the experiments. A total of 40 spectra per experiment were accumulated at ~ 5 minutes intervals.

To analyze the data, the experiments were subdivided into pre-arrest, arrest and recovery periods and a 3-way comparison was established using the Tukey test and repeated measures ANOVA. The significance level was set at 0.05. Table 3.6 shows P values from all possible 3-way comparisons. During recovery, no statistically significant difference was found between the potassium, esmolol and control groups. The PCr levels in the potassium group were slightly higher than control during the arrest period: PCr_K = 1.253; $PCr_{control}$ = 0.976, P = 0.044; but did not differ from the esmolol group: $PCr_{esmolol}$ = 1.127, P = 0.423; a significant, but borderline statistical difference was seen relative to control levels. No statistical difference was observed in the β–ATP levels in any of the three periods. The levels of Pi were reduced during arrest in both the esmolol and potassium groups relative to controls but did not differ from each other, and did not differ during the other periods (Table 3.6).

Pre-Arrest

	Potassium			Esmolol		
	PCr	β–ATP	Pi	PCr	β–ATP	Pi
	(1.164)	(0.510)	(0.224)	(1.117)	(0.520)	(0.252)
Potassium						
Esmolol	0.893	0.735	0.654			
Control	0.999	0.841	0.384	0.876	0.889	0.875

Arrest

	Potassium			Esmolol		
	PCr	β–ATP	Pi	PCr	β–ATP	Pi
	(1.253)	(0.535)	(0.327)	(1.127)	(0.403)	(0.129)
Potassium						
Esmolol	0.423	0.209	0.343			
Control	0.044*	0.586	0.908	0.310	0.694	0.559

Recovery

	Potassium			Esmolol		
	PCr	β–ATP	Pi	PCr	β–ATP	Pi
	(0.829)	(0.298)	(0.222)	(0.535)	(0.228)	(0.156)
Potassium						
Esmolol	0.069	0.384	0.071			
Control	0.719	0.715	0.664	0.157	0.143	0.231

Table 3.6 - Statistical analyses (P values) of changes in levels of phosphocreatine (PCr), the β– fraction of adenosine triphosphate (β–ATP) and inorganic phosphate (Pi) prior to arrest (30 min), during arrest (60 min) and recovery (110 min). Values in parentheses are mean values of relative peak intensities of each parameter at a given period of the experiment (Pre-arrest, Arrest, or Recovery). Statistical analyses were performed using the Tukey test and repeated measures ANOVA; the significance level is set as $P < 0.05$ and is denoted with an *.

3.3.2.3.1 – Temporal Effects on the Levels of HEP in the Control and Experimental Groups

Figures 3.29 through 3.31 show the changes in PCr, β–ATP and Pi prior to arrest, during arrest and recovery in the esmolol, potassium, and control groups. During each period, linear regression analyses were performed on each data set and the corresponding slopes of the curves were calculated. Table 3.7 shows the statistical comparisons that could be established between the slopes. During the arrest and recovery periods, a 3-way analysis revealed significant differences (Arrest $P < 0.0001$; Recovery $P = 0.0009$) between the slopes obtained for the PCr variable. Two-way comparisons (using Bonferroni's correction for the level of significance of the P value) were performed to locate the differences between the groups. No differences were found in the slopes of β–ATP regression curves during arrest ($P = 0.956$) or recovery ($P = 0.181$). Significant differences in the regression slopes of Pi were found during the recovery period ($P = 0.04$; during arrest $P = 0.974$) using a 3-way comparison model. A two-way comparison analysis (using Bonferroni's correction) revealed no significant ($P < 0.15$) differences. No difference was found for any variable during the prearrest period.

The statistical method used for comparison of regression curves can generally be described as:

$$y = b_0 + b_1 x_1 + b_2 x_2 + b_3 x_1 x_2 + E$$

Where x_1 = a given drug concentration and

x_2 = a given drug product

Substituting $x_2 = 0$ and $x_2 = 1$ respectively for two different drugs, the generic equation for a given drug A will be

$$E(y) = b_0 + b_1 x_1$$

And for drug B will be

$$E(y) = b_0 + b_1 x_1 + b_2 + b_3 x_1 = (b_0 + b_2) + (b_1 + b_3) x_1$$

The parameters in the model can be interpreted in terms of the slopes and intercepts associated with these regression lines:

b_0 : y-intercept for product A regression line

b_1 : slope of product A regression line

b_2 : difference in the y-intercept of the regression line for products B and A

b_3 : difference in the slopes of the regression lines for products B and A.

The objective is the comparison between slopes of the regression lines. A difference in slopes would indicate an effect in the rate of decay (relative to control) of a given metabolite (ATP, PCr, or Pi). A statistical test of the equality of the slopes is required ($\alpha = 0.05$). Using the complete model described above, we can obtain a least squares fit for each variable. The reduction in the sum of squares (SS) for error attributed to x_1x_2 is

$$SS_{drop} = SSE_a - SSE_b$$

using

$$MSE_a = SSE_a/df$$

Where MSE = mean sum of squares error and df = degrees of freedom, the F value can be obtained in order to test H_0 (the null hypothesis, $b_3 = 0$) at a 0.95 confidence level by using:

$$F = MS_{drop}/MSE_a$$

This method for comparing slopes of two regression lines can be extended to the comparison of three regression lines by including additional dummy variables and all possible interaction terms between the quantitative variables x1 and the dummy variables (D1 and D2). The Boniferoni's correction should also be applied by dividing the previous α value (0.05) by the number of comparisons. In the case of the above data, significance was set at 0.0167 because there were three curves (0.05/3). Applying this strategy to our experimental data, we have:

$$y = b_0 + b_1D_1 + b_2D_2 + b_3x_1 + b_4D_1x_1 + b_5D_2x_1 + E$$

Defining D1 and D_2 variables according to the different groups, we have:

	D1	D2
Esmolol	1	0
Potassium	0	1
Control	0	0

Then for esmolol, $D_1 = 1$ and $D_2 = 0$, we get:

$$y = b_0 + b_1 + b_3x_1 + b_4x_1 + E = (b_0 + b_1) + (b_3 + b_4)x_1 + E$$

For potassium, $D_1 = 0$ and $D_2 = 1$:

$$y = b_0 + b_2 + b_3x_1 + b_5x_1 + E = (b_0 + b_2) + (b_3 + b_5)x_1 + E$$

And for control, $D_1 = 0 = D_2$,

$$y = b_0 + b_3x_1 + E$$

The coefficients are interpreted as before.

Two-way comparisons (esmolol group vs. control group, potassium vs. esmolol and potassium vs. control groups) were undertaken using the Bonferroni correction for the statistical level of significance ($\alpha = 0.05/3 = 0.0167$) in the groups (time periods and variables) in which the 3-way comparisons revealed statiscally significant differences. For the PCr variable, differences were observed during the arrest and recovery periods. The rate of decay (k) of PCr was significantly faster during the arrest period in esmolol-treated hearts than in potassium-treated hearts ($k_{esmolol}$ = (-) 0.00875 ± 0.00097 vs. $k_{potassium}$ = (+) 0.00172 ± 0.00164; P = 0.00001), and faster than in control hearts (k = (-) 0.00324 ± 0.00061; P = 0.004). The rate of the decay of PCr in potassium treated hearts was also different from control (P = 0.0056) during the arrest period (Table 3.7). During recovery, the PCr regression slope of the esmolol-treated hearts became much less steep ($k_{esmolol}$ = (-) 0.00134 ± 0.00029) and significantly different from those of the control and potassium groups ($k_{control}$ = (-) 0.00328 ± 0.00026, P = 0.00003; $k_{potassium}$ = (-) 0.00398 ± 0.00071, P = 0.00028). The slopes of the potassium group did not differ from the control group (P = 0.407).

For the Pi variable, the differences found in the initial 3-way analysis (P = 0.04) were not confirmed by the paired comparisons between control vs. potassium-treated hearts (P = 0.206) nor for the potassium vs. esmolol-arrested hearts (P = 0.239). However, comparison of the slopes of the esmolol vs. the control groups revealed a

borderline difference ($k_{control}$ = (-) 0.00093 ± 0.00022 vs. $k_{esmolol}$ = (-) 0.00012 ± 0.00019; P = 0.013), using the Bonferroni corrected level of significance.

Table 3.7 – Regression slopes (*k* values) obtained from ^{31}P MR spectra for phosphocreatine (PCr), β–ATP and inorganic phosphate (Pi) prior to arrest, during arrest and recovery of isolated rat hearts during control, esmolol and potassium arrest (Langendorff preparation). Data are expressed as averages ± standard deviation of the mean (respective peak heights / reference / time (min).

	PCr		
	Control	*Esmolol*	*Potassium*
Prearrest	(-) 0.00486 ±0.0036	(-) 0.00213 ± 0.00212	(-) 0.00172 ± 0.00324
Arrest	(-) 0.0034 ±0.00061	(-) 0.00875 ± 0.00097	(+) 0.00172 ± 0.00164
Recovery	(-) 0.00328 ±0.00026	(-) 0.00134 ± 0.00029	(-) 0.00398 ± 0.00071
	β–ATP		
	Control	*Esmolol*	*Potassium*
Prearrest	(-) 0.00129 ±0.00095	(+) 0.00035 ± 0.00143	(+) 0.00004 ± 0.00224
Arrest	(-) 0.00173 ±0.00051	(-) 0.0025 ± 0.0005	(-) 0.00074 ± 0.00072
Recovery	(-) 0.00141 ±0.00017	(-) 0.00089 ± 0.00029	(-) 0.0016 ± 0.00023
	Pi		
	Control	*Esmolol*	*Potassium*
Prearrest	(-) 0.00042 ±0.00115	(-) 0.00089 ± 0.00188	(+) 0.00073 ± 0.00103
Arrest	(-) 0.00206 ±0.00047	(-) 0.00043 ± 0.0004	(+) 0.00029 ± 0.00073
Recovery	(-) 0.00093 ±0.00022	(-) 0.00012 ± 0.00019	(-) 0.0005 ± 0.0002

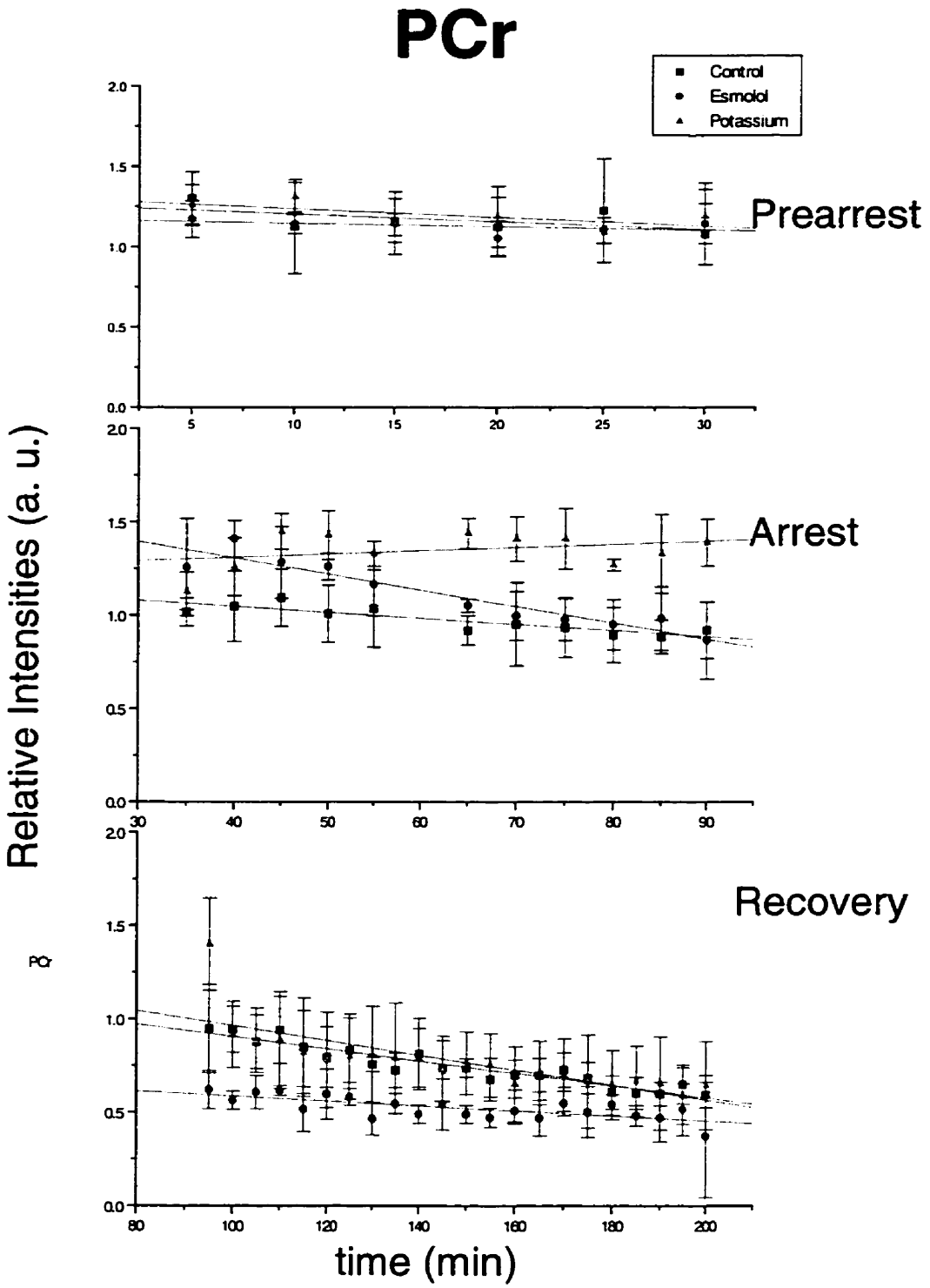

Figure 3.29 – The rates of decay of PCr (phosphocreatine) prior to arrest, during arrest and recovery of isolated rat hearts subjected to 1 h arrest with esmolol or potassium (n = 4, each). The control group (n = 4) consisted of isolated hearts allowed to beat for 200 minutes. ^{31}P MR spectroscopy was carried out throughout the protocol. Data are expressed as the intensity of the PCr peak relative to the reference ± sd.

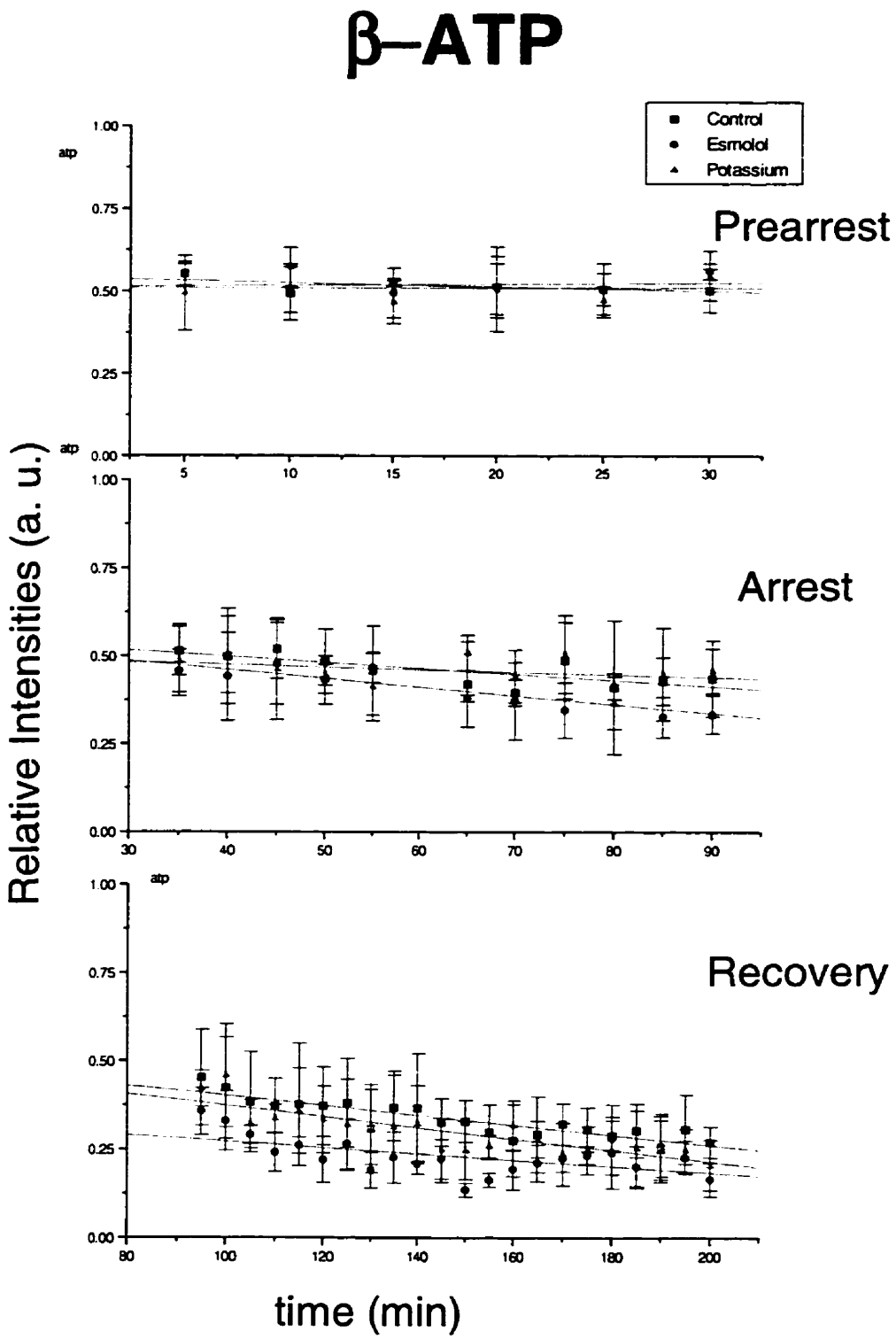

Figure 3.30 – The rates of decay of β–ATP prior to arrest, during arrest and recovery of isolated rat hearts subjected to 1 h of arrest with esmolol or potassium (n = 4, each).

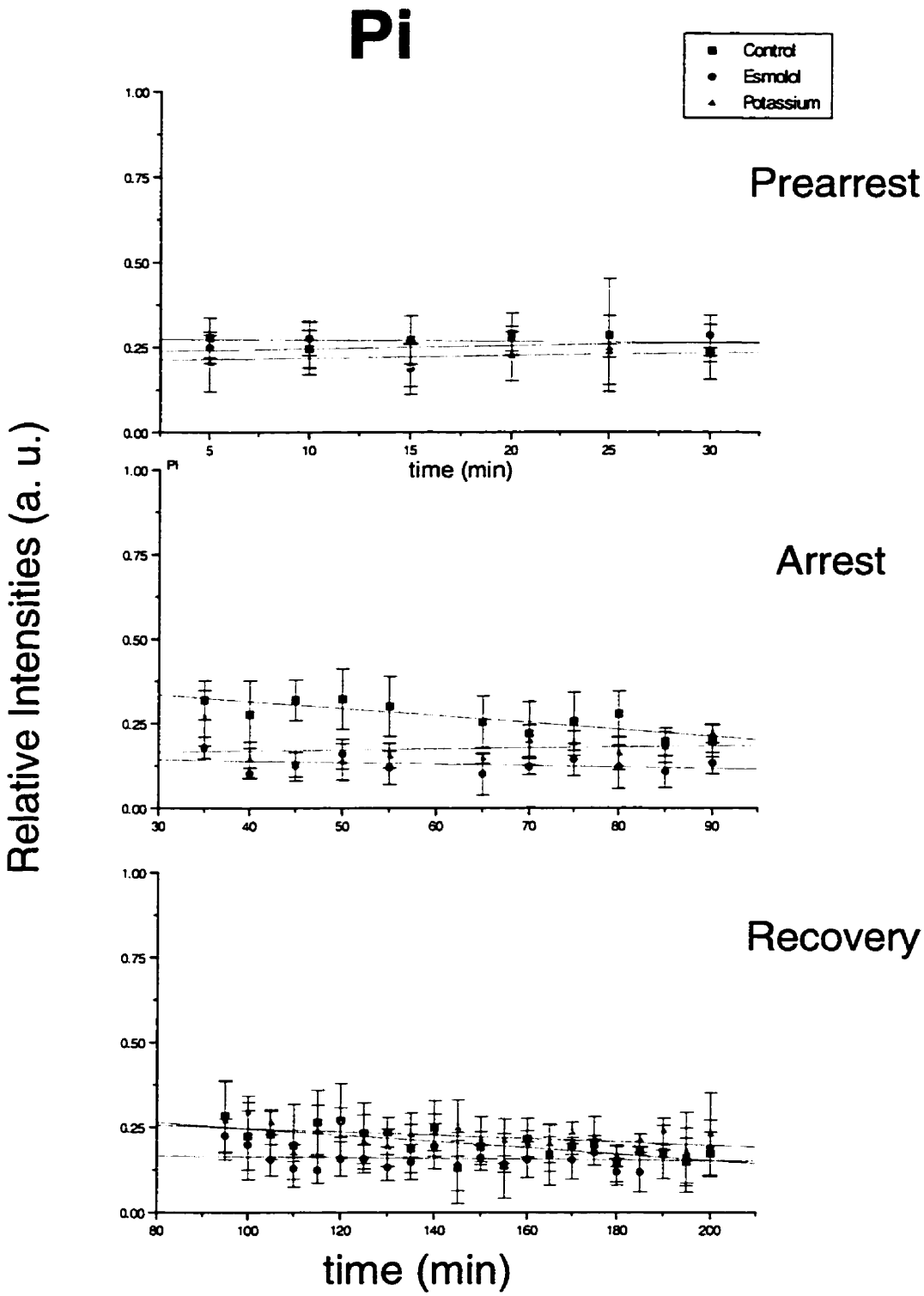

Figure 3.31 – The rates of decay of Pi (inorganic phosphate) prior to arrest, during arrest and recovery of isolated rat hearts subjected to 1 h arrest with esmolol or potassium (n = 4, each).

3.3.2.3.2 – The Effects of Esmolol Concentration on PCr during the Arrest Period

As in the Rb^+ and Li^+ experiments described earlier (Sections 3.3.2.1 and 3.3.2.2), a relatively wide variation in the concentrations of esmolol required to maintain cardiac arrest was observed in the two series of ^{31}P experiments performed. To evaluate whether the effect seen on PCr levels in the esmolol-arrested hearts was concentration-dependent, the data from both series of phosphorus experiments were combined (n = 12). In both series, the arrest period was 1h and phosphorus spectra were acquired under identical experimental conditions. A total of 11 different concentrations (in two experiments 502 μM was used) varying from 293 to 628 μM were plotted against their respective rate constants (Figure 3.32). No correlation was established between the different slopes and the respective concentrations over the range used ($r = 0.16$, $P = 0.63$).

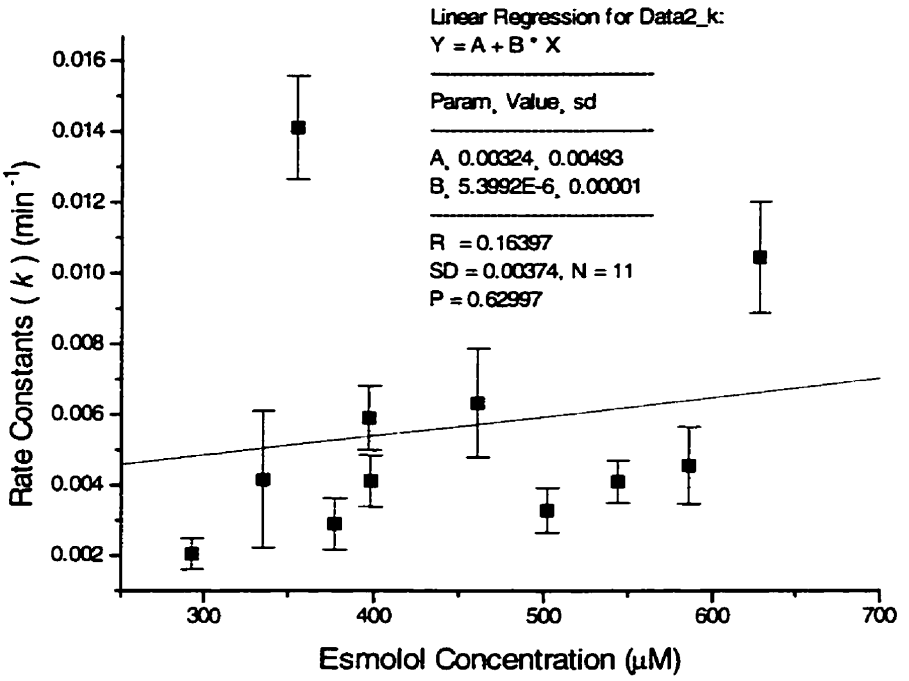

Figure 3.32 – Rate constants (*k* values) from all phosphorus experiments plotted against the different esmolol concentrations required to maintain cardiac arrest. The concentrations (n = 12) varied from 293 to 628 μM (293, 335, 355, 377, 397, 398, 461, 502, 586, and 628 μM). In two experiments, a maintenance dose of 502 μM was used and the rate constants were averaged.

3.3.2.3.3 - Effects on Intracellular pH

Phosphorus (^{31}P MRS) spectroscopy is useful for assessing intracellular pH. The shift of the Pi peak relative to the PCr peak in the phosphorus spectrum is indicative of intracellular pH when compared to a calibration curve. The chemical shift of the Pi peak was analyzed in the spectra obtained from all groups and throughout the different periods. The average pH values for each experimental period (prearrest, arrest, and recovery) were compared. Figure 3.33 shows the intracellular pH values at different times in the esmolol, potassium and control groups. Repeated measures ANOVA along with the Tukey test were used for statistical analyses and no differences were found prior to arrest or during the arrest and recovery periods in any of the groups. During arrest, the average pH_i value for the esmolol group was higher than in the control group ($pH_{i\ esmolol}$ = 7.22 ± 0.2 vs. $pH_{i\ control}$ = 7.09 ± 0.03, P = 0.009) but did not differ from the potassium group ($pH_{i\ potassium}$ = 7.13 ± 0.2, P = 0.053). During recovery, the pHi values returned to prearrest levels and no statistical differences were observed in three-way comparisons between the esmolol, potassium, and control groups (Table 3.8).

Table 3.8 – Statistical analyses (P values) of intracellular pH values measured during the arrest period in esmolol-, potassium-arrested, and control hearts. Repeated measurements ANOVA along with the Tukey test were used in the various 3 – way comparisons. No differences were seen during the pre-arrest and recovery periods.

	Arrest Period		
	Control	*Esmolol*	*Potassium*
Control	_		
Esmolol	0.0037*	_	
Potassium	0.9105	0.053	_

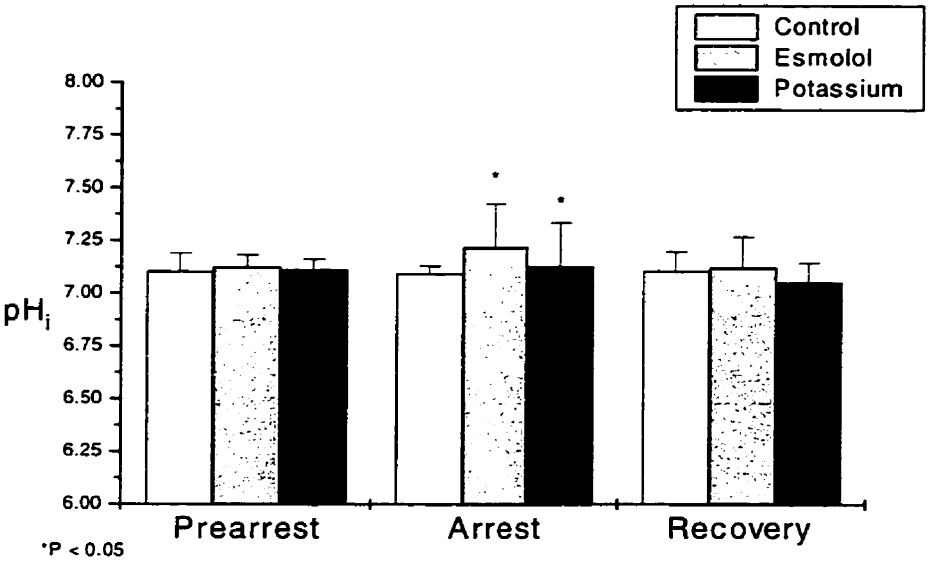

Figure 3.33 – Effects of esmolol and high K^+ perfusion on intracellular pH measured using ^{31}P NMR spectroscopy. Intracellular pH values were obtained from the chemical shift of the Pi peak relative to the PCr peak in ^{31}P NMR spectra of isolated rat hearts and calculated using a calibration curve (P_k = 6.75 for PCr-Pi chemical shift pH determinations). Spectra were acquired prior to arrest, during arrest, and recovery from esmolol or potassium-induced cardiac arrest (n = 4, each). The control group (n = 4) consisted of hearts that were perfused with KH buffer without esmolol or potassium. The maintenance arrest dose of esmolol varied in these experiments from 335 to 628 µmol/L with an average of 444.75 ± 134.1 µmol/L. The data are expressed as averages ± standard deviation of the mean.

3.3.2.4 - Effects of Esmolol and Potassium in Intracellular Calcium Transients

Fluorescence microscopy was used to assess whether esmolol at the concentrations used to induce and maintain cardiac arrest, had any effect in Ca^{++} movement across the membrane. In a preliminary assessment, isolated adult rat myocytes were exposed to esmolol at 1.36 or 1.7 mmol/L and high K^+ at 25 mEq/L and paced for the course of the experiment. A dose-response curve was built with esmolol concentrations varying from 0 (controls) to 2.0 mmol/L (at 0.5 mmol/L intervals). An average of six consecutive measurements per cell was obtained.

Exposure of the isolated myocytes to high K^+ KH solution (n = 3, average of 6 measurements each), resulted in an increase of up to 20% in the fluorescence ratio (F_{340}/F_{380}, ΔF), corresponding to an increase in $[Ca^{++}]_i$ to ~ 200 nM, without pacing. Field pacing was performed on three additional batches of cells and no response to the electrical stimulation was observed (Figure 3.34 (a)). In other three cells, exposure to esmolol at 1.36 and 1.7 mM resulted in minimal (1.36 mM) and no change (1.7 mM) in $[Ca^{++}]_i$ upon field stimulation (Figure 3.34 (b) and (c)).

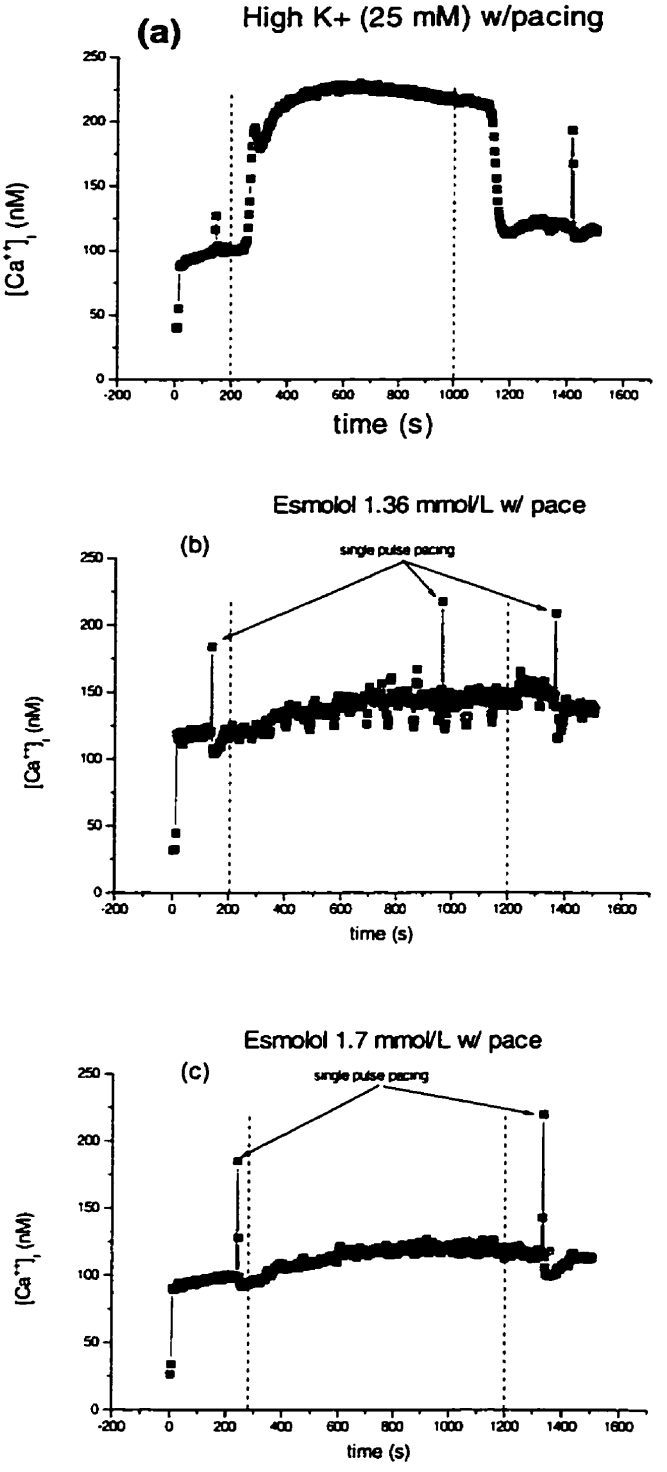

Figure 3.34 – Intracellular calcium fluorescence measured in isolated rat myocytes exposed to (a) potassium and esmolol at (b) 1.36 and (c) 1.7 mmol/L concentrations. Data were acquired over a period of 1500 s and the cells were field stimulated (paced) at least four times during each exposure.

Because the time resolution was poor in the initial experiments (0.3 data point/second, 1500 seconds acquisition time), and quantification of the increase of $[Ca^{++}]_i$ upon stimulation was inaccurate, a second series of experiments that included dose-response curves was undertaken. For these experiments, a time resolution of 10 ms was obtained (100 data points/second) and the cells were exposed to different concentrations of esmolol for 250 seconds each. Doses varied randomly from 0 (controls, n = 12) to 2.0 mM in 0.5 mM increments (0.5, 1.0, 1.5 and 2.0 mM, n = 6 each, average of six stimulations per cell). The maximal changes of the fluorescence ratio (ΔF) following field stimulation between control and esmolol groups were measured and the averages of 6 stimulations per cell at each concentration are plotted in Figure 3.35. The fluorescence ratios were smaller at higher doses of esmolol and inversely proportional to increasing concentrations (r^2 = - 0.95, P = 0.004). The intracellular Ca^{++} transients were progressively smaller up to 1.5 mM and at 2.0 no change was observed in ΔF, indicating no increase in $[Ca^{++}]_i$ despite electrical stimulation.

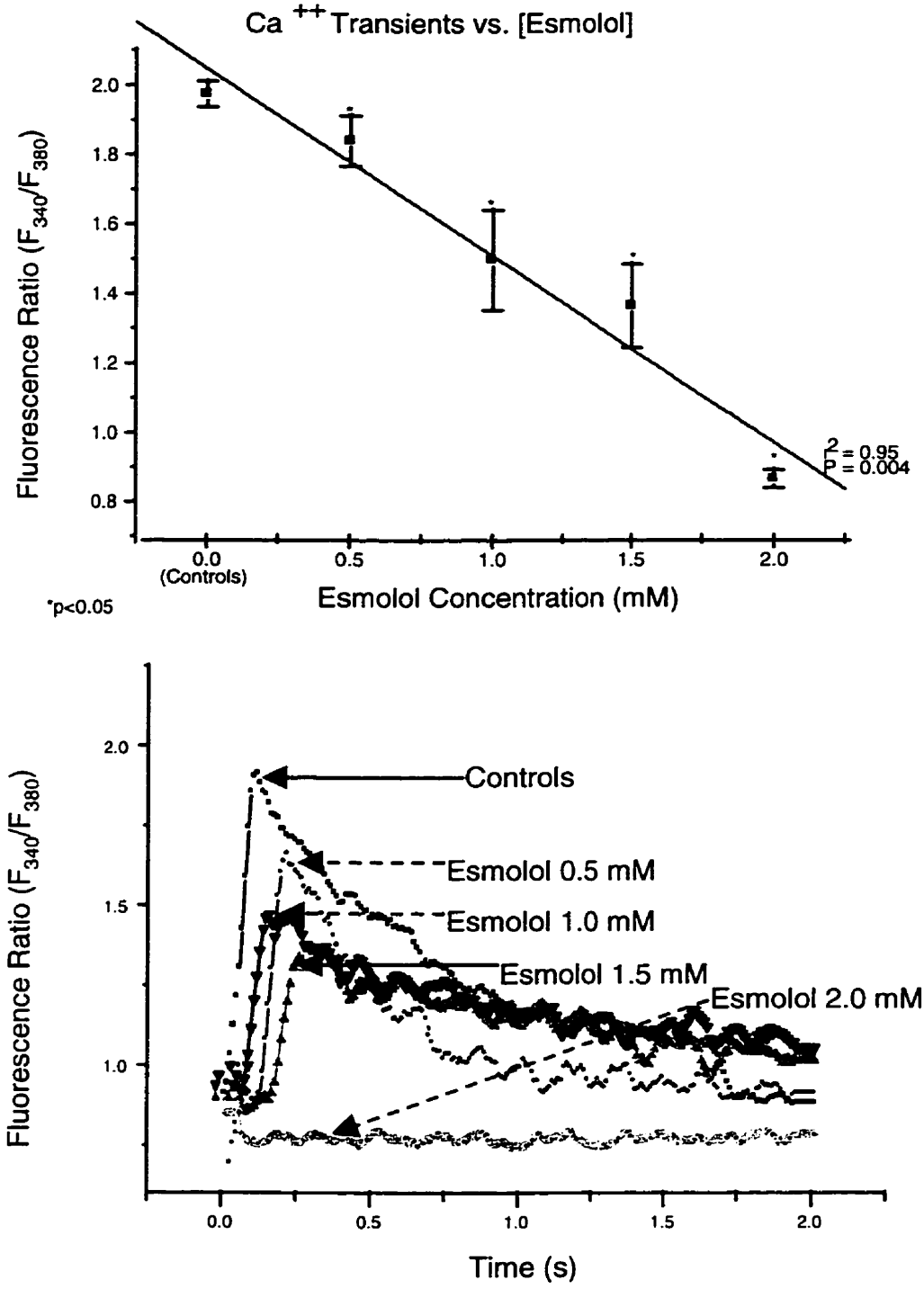

Figure 3.35 – *Upper panel:* Dose-response curve of the peak fluorescence ratio (ΔF) from isolated myocytes subjected to different concentrations of esmolol. Each data point is an average of 6 stimulations of n = 6 cells (controls, n = 12). Time resolution: 10 ms. *Lower panel:* representative fragments of actual Ca^{++} transients captured from a single stimulation of isolated myocytes exposed to different concentrations of esmolol. Note the difference in spike height with increasing concentrations of esmolol.

3.3.2.5 - Functional Analyses

Analysis of the functional outcome of the experiments was performed on two separate series of experiments in which the pressure-rate product (PRP) and the developed (systolic – end-diastolic) pressure were measured. The data were acquired during the rubidium and the phosphorus series of experiments, in which the total exposure time to esmolol was 1h. In the rubidium series, data from the esmolol group are compared to controls (prearrest and recovery in the case of esmolol-arrested hearts) at the same time points as the control group. In the phosphorus experiments, the functional data obtained from the esmolol group are compared with the control and potassium groups at the same time points (prearrest and recovery in the case of esmolol and potassium groups).

3.3.2.5.1 - Results

No significant differences were found in any of the series analyzed.

In the phosphorus series, after 30 minutes of recovery PRP values of esmolol-arrested hearts were not different from prearrest values: $PRP_{E\ prearrest}$ = 25903.574 ± 3935.692 vs. $PRP_{E\ recovery}$ = 22980.505 ± 4618.4565 ; P = 0.94, n = 8. Potassium arrested hearts showed similar recovery: $PRP_{P\ prearrest}$ = 31560.545 ± 3571.4743 vs. $PRP_{P\ recovery}$ = 28360.266 ± 2096.7681 ; P = 0.91, n = 4. Esmolol and potassium recovery values did not differ from each other (P = 0.93). (Figure 3.36, upper panel)

In the rubidium series of experiments, comparisons were made against a control group. No differences were found at the end of the 30-minute recovery period following 1h of esmolol arrest relative to control hearts, which were allowed to beat for the entire

duration of the experiment: $PRPe_{recovery}$ = 26479.82 ± 4994.503 (n = 12) vs. $PRPc_{recovery}$ = 26968.93 ± 4179.794 (n = 5), P = 0.99. Functional parameters in esmolol arrested hearts did not differ from their respective prearrest values: $PRPe_{prearrest}$ = 29442.68 ± 4129.291, P = 0.95, n =12. (Figure 3.36 lower panel).

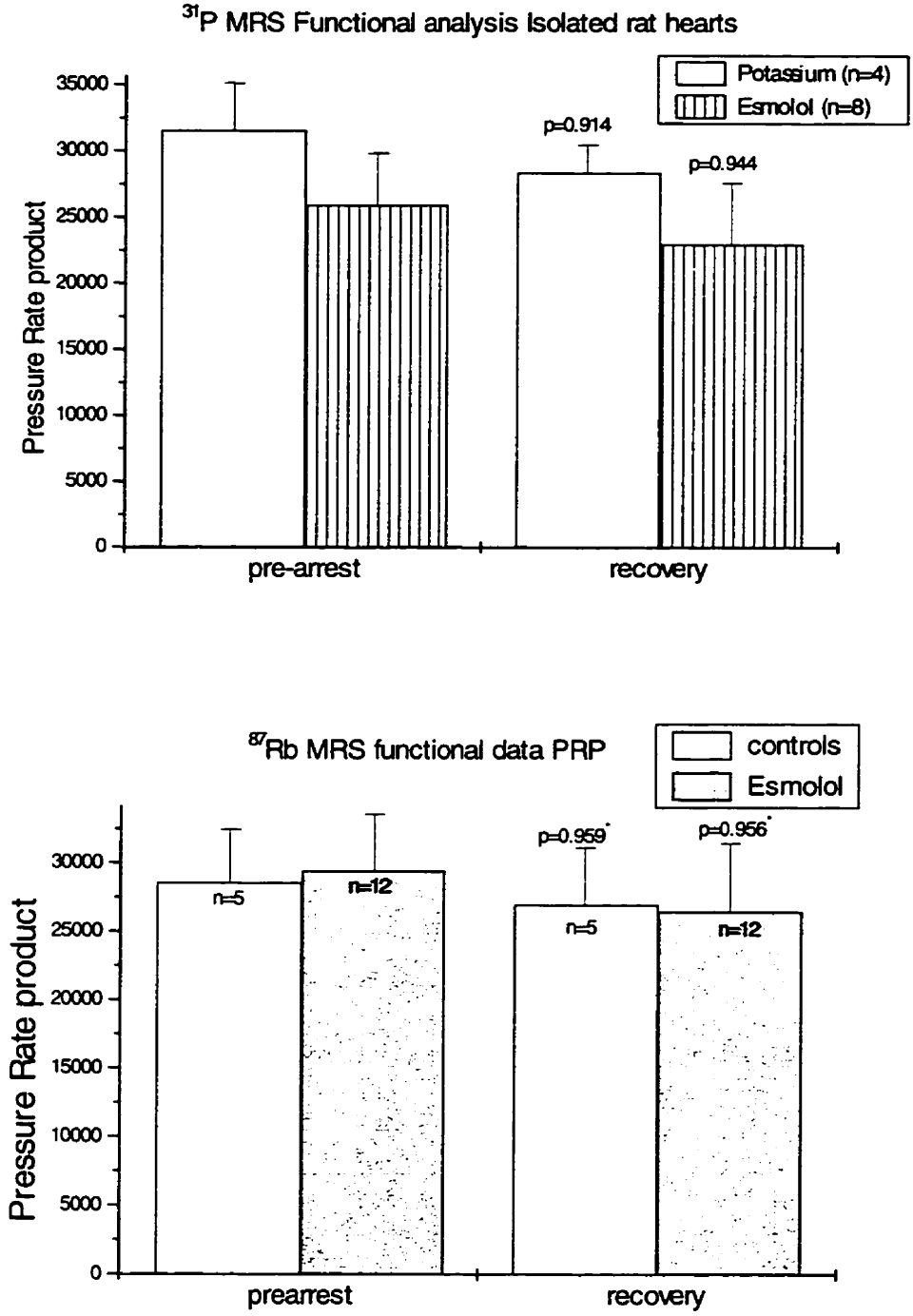

Figure 3.36 – Functional data obtained from ^{31}P (upper panel) and ^{87}Rb (lower panel) MRS experiments on isolated rat hearts prior to arrest (15 min), and recovery (30 min). Data are expressed as pressure rate product (HR x LVDP) and are averages of the last 15 minutes of each period ± standard deviation of the mean.

3.3.2.6 - Histological Analyses

Hearts used in the ^{31}P and ^{87}Rb MRS experiments were also used for histological analyses.

3.3.2.6.1 - Methods and Slide Preparation

At the end of each experiment, the hearts were removed from the Langendorff apparatus and immediately dropped into flasks containing Forman 18% and refrigerated (4° C, for 24h). The flask labels contained only information regarding the name of the investigator, date and order of the experiment in any given day (i.e., date-phosphorus-A; date-rubidium-C, etc.). Sections of the left and right ventricle as well as of the interventricular septum were fixed in formalin for 48 h, areas which were selected before dehydration from 70% alcohol to absolute alcohol. The tissue was cleared in xylene and embedded in paraffin. Five μm thick slices were cut and H & E stained (Mayer's hematoxilyn and eosin), mounted in paramount and examined by a pathologist (Dr. L Yang) under a regular light microscope. The pathologist was blind to the groups (esmolol, potassium or control) to be examined.

3.3.2.6.2 - Results

No significant morphological alterations in the slices submitted for evaluation under light microscopy were observed. Figures 3.37 through 3.39 shows slices obtained from control potassium- and esmolol-arrested hearts. Small hypereosinophylic areas were identified in esmolol-arrested hearts at 400x magnification (Figure 3.39, lower panel).

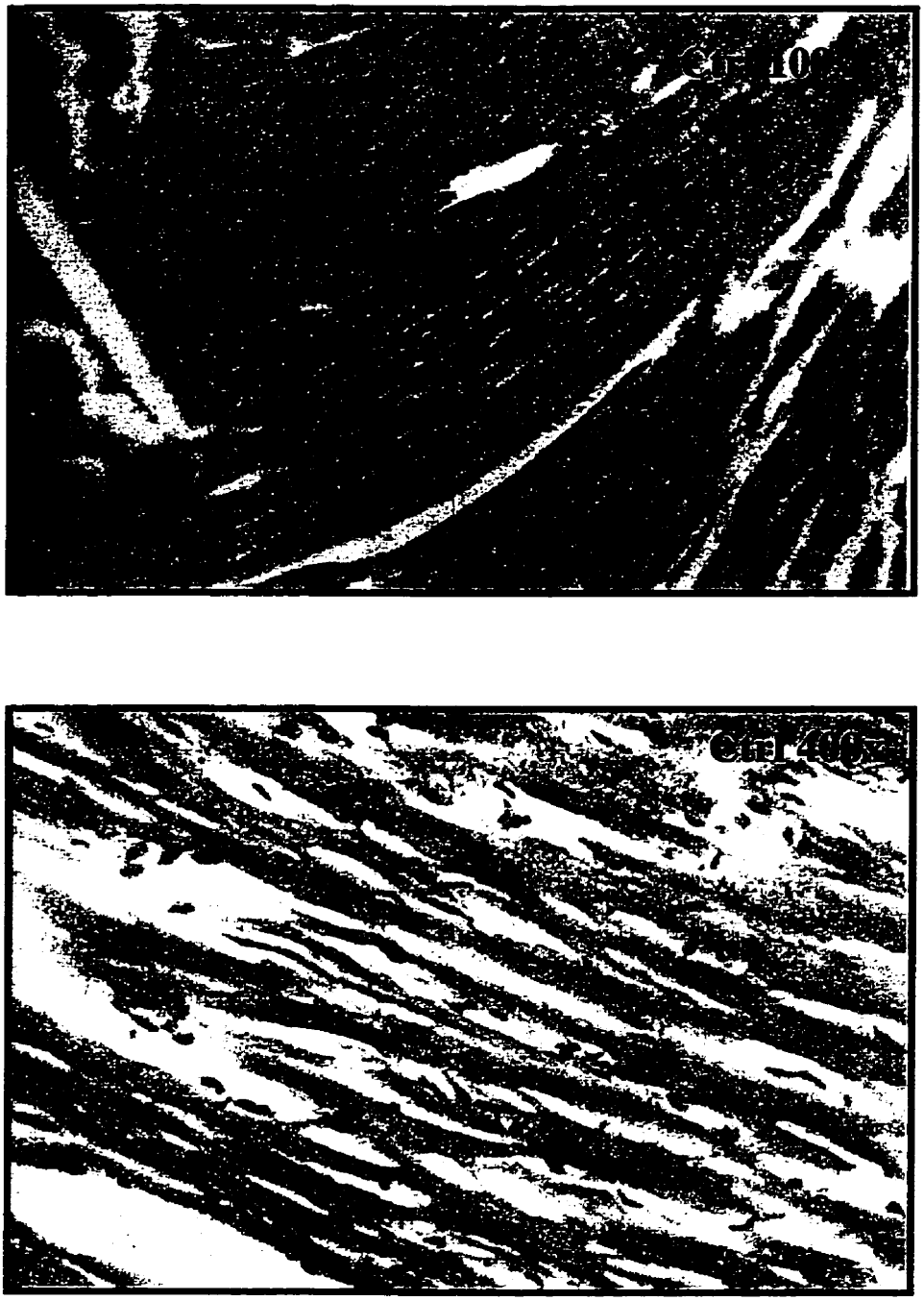

Figure 3.37 - Histological sections of rat myocardial cells obtained from ^{31}P and $^{87}Rb^{+}$ MR studies of control hearts. Stain: H&E.

Figure 3.38- H&E stained slide of rat myocytes obtained from hearts subjected to high (25 mM) KCl cardioplegic arrest. Magnification: 400x.

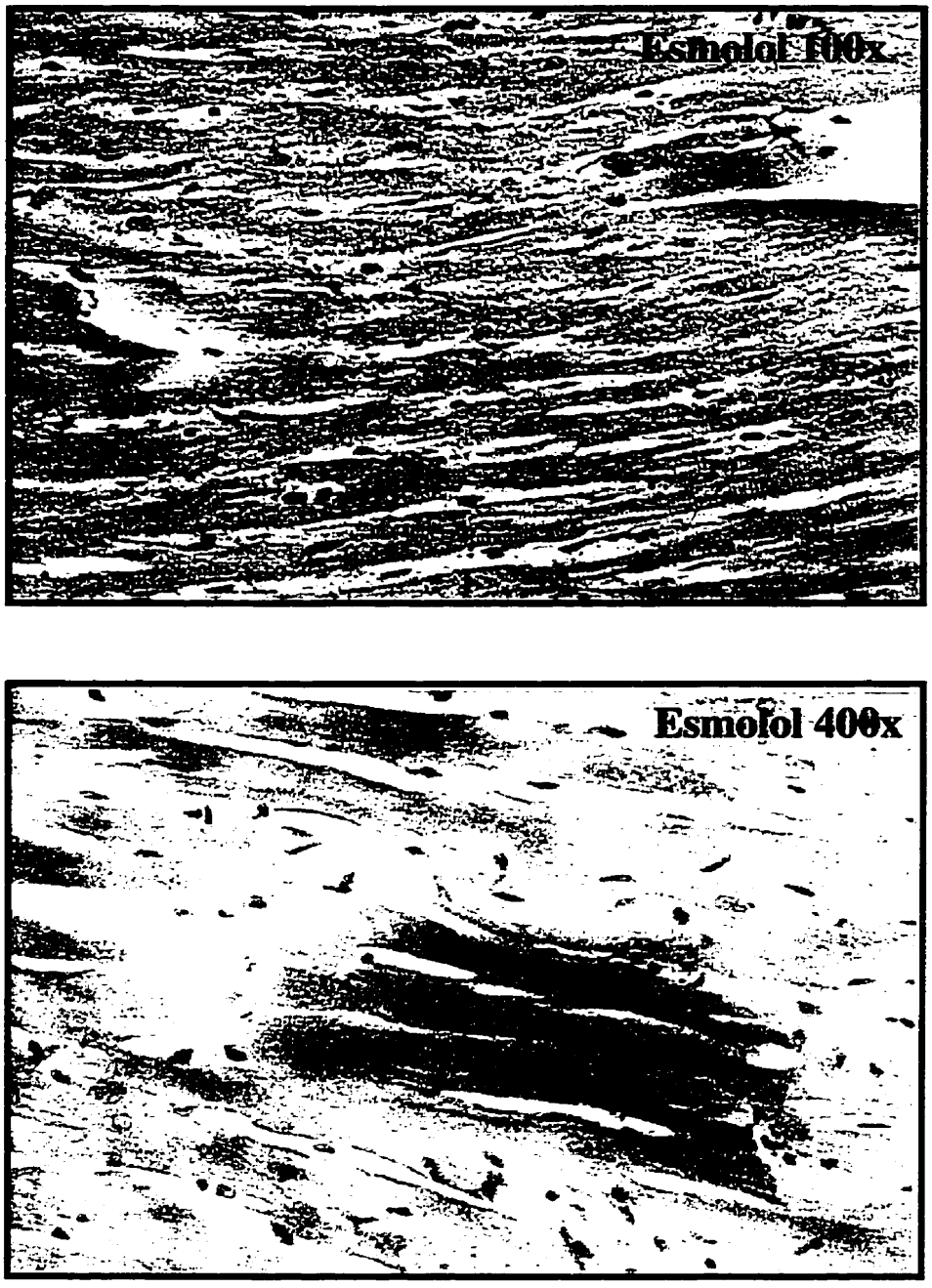

Figure 3.39 - Slides obtained from esmolol-arrested isolated rat hearts. Upper panel: 100x magnification; lower panel: 400x magnification; note the apparent hypereosinophylic area in one of the slides.

CHAPTER 4.0 – DISCUSSION

The work described in the previous chapters was aimed at finding a realistic alternative to existing myocardial protection techniques used in the context of normothermic cardiac operations and normothermic cardioplegia. The benefits and pitfalls of the normothermic approach have been discussed in the section Warm Heart Surgery in Chapter 2 of this thesis. The following paragraphs will focus on the use of potassium as a cardioplegic agent and will discuss aspects of the use of esmolol as a potential alternative approach. A brief justification of methods, techniques, and protocols employed during the different studies will follow, and the actual results and their implications in the use of esmolol as part of a myocardial protection strategy will be discussed.

➢ *Is there a clinical need for an alternative for K^+?*

The mortality rate of classical open-heart surgery may be considered acceptable if it is around 3%, but not higher than 5%, in the most busy centres, worldwide. In these centres, the most common procedure performed is by far myocardial revascularization. Complications, such as perioperative myocardial infarction, stroke, renal failure, neurovascular and aortic injury, respiratory failure and coagulation abnormalities, can still occur in a small number of patients. The so-called "snow-ball" effect of one complication leading to another, is an ever-present threat in the minds of the crew responsible for immediate post-operative care. A variety of responses that include leukocyte-mediated inflammation, coagulopathy due to trauma to blood elements, deleterious effects of hemodilution, and embolisms caused by air and atherosclerotic debris, with the potential

risk of post-operative stroke and/or cognitive dysfunction have also been reported[1, 2, 3, 4, 5]. Hyperkalemic cardioplegia has been associated with post-operative contractile dysfunction especially when it is associated with hypothermia[6, 7]. At the subcellular level, hyperkalemic cardioplegic solutions alter the affinity of myofibrils for calcium, thus compromising cardiac output immediately after removal of the aortic crossclamp in procedures involving CPB[8, 9, 10]. In patients with any degree of renal insufficiency, clearance of potassium from the circulation may be difficult and the patient may require longer periods of bypass and/or inotropic support, either pharmacological or mechanical or additional procedures, such as hemofiltration[11, 12, 337, 338]. All these potential complications occuring in any given patient may not necessarily translate into an increased mortality rate, however the patient will consume up to 3 to 5 times the resources of uncomplicated cases. In a comprehensive analysis on patient outcome and hospital cost it has been determined that the greatest costs (approximately US$200,000 per patient) were among patients who did not survive the operation. In this series of 1221 consecutive operations, the second most costly group was the one in which nonfatal morbid complications (10% of the patients, up to US$130,000 per patient) were seen. Further, the authors determined that the significant independent risks for increased hospital cost were: preoperative congestive heart failure which was in first place, kidney dysfunction ranked second, whereas reoperation, operative priority and sex were ranked in sixth, seventh and eighth position respectively. In conclusion, the high-risk patient profile can serve as a target for pre- and intra-operative cost-reduction strategies[486].

In this study, we proposed the use of esmolol as an alternative to potassium to induce cardiac arrest in the classical bypass setting. Esmolol is already being used in

some situations to reduce heart rate and motion and its dose titrated to a level at which the surgeon is comfortable. A number of different variations in the use of esmolol during cardiac procedures have been proposed in the past 5 to 7 years[21-27]. With the advent of minimally-invasive procedures, surgeons have developed, in a somewhat independent fashion, their own cardioplegic strategies based on personal experience. This has allowed variations within the same framework and is largely driven by the therapeutic flexibility characteristic of esmolol. For more complex cases that require classical bypass techniques (longer crossclamp times, reoperations, multiple grafts, associated procedures), the strategy of a "one-drug-blood-solution" has the potential of becoming easier and safer to use.

➢ *Choice of models and techniques*

The experimental models were chosen according to the hypotheses to be tested. The isolated rat heart (Langendorff) is a classical model readily available and praised for its cost-effectiveness and suitability for initial screening studies. Additional work on the rabbit heart was proposed to address interspecies differences. The *in vivo* porcine model under extracorporeal circulation was used to simulate as closely as possible the clinical situation.

Techniques such as magnetic resonance spectroscopy and infrared spectroscopy were used because of their non-invasive nature. MR also allowed assessment of intracellular high-energy phosphates levels and the measurement of intracellular pH. Changes in intracellular concentrations of calcium can also be detected by NMR with the use of fluorine-containing indicators[487, 488]. Despite its proven feasibility[489,490,491,492], ^{19}F

(Ca^{++}) MRS is still problematic[493]. Despite the development of better indicators (with a lower K_D [494, 495, 496]), we judged the technique to be poorly suited for use in our experiments where the intention was to produce cardiac arrest and evaluate functional recovery. The use of indicators that bind intracellular calcium introduces experimental bias that would have altered the interpretation of the effect(s) of esmolol in producing cardiac arrest. The fluorine indicator needed for the NMR studies of calcium would bind significant amount of intracellular calcium even before the infusion of esmolol. This would have reduced the dose of esmolol required to induce cardiac arrest and some of the possible effects of esmolol would not be observed in the presence of the lower (but effective) concentrations of esmolol. Instead, isolated cell preparation and fluorescence microscopy were used to evaluate the effect of esmolol on Ca^{++} levels in myocytes. Infrared spectroscopy provided continuous measurements of methanol with a reagentless approach. A specific sample-holder was developed and adapted to the bypass circuit, which may find use in the assessment of other compounds in the circulating blood during CPB.

The objective of this thesis was to assess potential alternatives to K^+ for inducing cardiac arrest or for reducing cardiac motion to allow better visualization and easier surgical manipulation of the heart. The work was divided into 3 phases to address 3 practical questions:

- Can esmolol produce prompt, titrable, and fully reversible cardiac arrest?
- Does the fact that one of the subproducts of esmolol is methanol preclude its use as a cardioplegic agent?

- Is beta-blockade the only mechanism of action of esmolol when used as a cardioplegic agent?

➢ *Can esmolol produce prompt, titrable, and fully reversible cardiac arrest?*

Esmolol can induce and maintain cardiac arrest for periods of at least 120 minutes with nearly full recovery of contractile values and within clinically relevant time frames. The increase in end-diastolic pressure, was reversible, returning to prearrest when drug infusion was stopped.

A large species variation was observed in the sensitivity to esmolol. Among the species normally used in experimental cardiology, the rat seems to have the most highly developed adrenal system and the highest β–adrenoceptor density. Thus, the response of this species to agonists is also much greater than in rabbits or pigs. Conversely, the amount of antagonist required to produce any given effect should also be higher. Our findings support this hypothesis. In general, pig and rabbit myocardia are considered more similar to the human myocardium than the rat myocardium in terms of receptor density, structure and function of sarcoplasmatic reticulum and sarcolemma[497], as well as in conformation of the action potential and conduction patterns. Among mammalian hearts, the rat heart is considered to belong to a separate category.

Esmolol administered at the concentrations described in the *in vivo* pig experiments did not abolish cardiac electrical activity, although it maintained continuous mechanical, mainly ventricular, arrest. Based on our observations, the sinus node maintains its pacing activity (denoted by the P waves in the ECG) without any ventricular response. The atria showed some motion. In one experiment, the entire heart maintained electrical activity. The ECG showed P waves followed by high-amplitude QRS

complexes; however, no ventricular movement was observed and no significant pressure wave was registered.

The cardioselectivity and activity of the esmolol metabolites produced at the doses proposed in this study can be questioned. In the bypass model, there was an apparent increase in pulmonary arterial pressure. Weaning from bypass had to be done more carefully in the esmolol group than in the potassium group. Esmolol-perfused hearts tolerated volume reinfusion poorly during the process of interrupting cardiopulmonary bypass, and volume had to be given very slowly, off bypass, through the aortic line. In spite of this, no inotropic support was required and the hearts resumed their initial performance, responding to slow infusion through the aortic cannula of blood accumulated in the reservoir. The hypothesis is that the selectivity of esmolol for various receptors (like other β–blockers) may decrease at high doses. The β–1/β–2 ratio for esmolol is 35 at the pharmacologic concentrations proposed by the manufacturer. At these concentrations, esmolol may be considered cardioselective. However, at the concentrations used to produce arrest, esmolol may also interact with β–2 receptors, which may cause the ratio to decrease.

- *Does the fact that one of the by-products of esmolol metabolism is methanol preclude its use as a cardioplegic agent?*

Our theoretical calculations and initial assessments using infrared spectroscopy and gas chromatography indicate, at least in an estimative basis, that the use of esmolol in the pig under bypass at the concentrations we report does not pose any risks of toxicity. Recent publications on the use of esmolol during bypass in humans undergoing cardiac surgery have not addressed toxicity, and the excellent patient outcome reported has eliminated most of the concern. At the time experiments were being carried out in our pigs, we wished to address the issue of methanol toxicity at least on an experimental basis, although theoretical calculations indicated that esmolol at the concentrations we proposed to use would produce methanol at levels at least an order of magnitude below its toxic level in humans, assuming no losses of methanol.

Infrared spectroscopy was chosen because of its non-invasive nature and the task seemed relatively simple compared to other on-line approaches, such as NMR spectroscopy. IR spectroscopy was seen as the technique of choice for continuous measurements in the bypass blood, with the only requirement of developing a suitable sample holder that would fit easily into the bypass circuit. Gas chromatography, the gold-standard for measuring alcohols in blood, was chosen as the validation technique.

Our data suggest that the amount of methanol produced during the experiments was below the 1 mM detection limit of infrared spectroscopy for methanol. The overlap of the esmolol and methanol bands with sugar groups, presumably due to mannitol present in the priming solution, rendered the analysis more difficult, but not impossible. If the threshold level for detection of methanol had been reached, changes in the bands

located at 1080 and 1020 cm^{-1} would reveal the presence and amount of methanol with a simultaneous decrease in esmolol concentration. The gas chromatography results supported the IR data, indicating a maximum level of methanol of 325 μM at the end of 1h of cardioplegic arrest. The methanol peak could not be detected in any of the chromatograms obtained from pigs in the potassium control group. Peaks attributed to isoflurane were present in both groups. Based on these initial observations, the concentrations of esmolol used in our studies did not produce high levels of methanol. Our measurements did not show the theoretical yield of methanol in either blood or gas samples. A possible explanation for this could be the dilutional effect induced proposedly by the high output of the bypass centrifugal pump (systemic flow was kept above 3.0 L/min) and/or the rapid metabolism of methanol into further metabolites such as formaldehyde and formic acid.

Despite its pitfalls, this series of experiments provides a basis for further studies of the metabolism of esmolol used as a cardioplegic agent. Gas chromatography of blood samples collected from patients undergoing surgery and esmolol cardioplegia could be used to analyze all the products of esmolol metabolism. The on-line IR data may also provide information on hemodilution, plasma components and levels of anesthetic drugs, which were not explored in this study.

- *Is β–blockade the sole mechanism of action of esmolol when used as a cardioplegic agent?*

The work performed using magnetic resonance spectroscopy was designed to assess the effects of esmolol on K^+ and Na^+ kinetics across the cell membrane. We have evidence suggesting that esmolol when used to induce cardiac arrest produces effects other than beta-blockade. Inhibition of the efflux of Li^+ and Rb^+ suggests an effect on Na^+ and K^+ channels, respectively. ^{31}P MR spectroscopy showed an increase in energy expenditure during the arrest period, as demonstrated by an increase in the rate of decay of the PCr peak in the ^{31}P spectra relative to controls and to potassium-arrested hearts. Fluorescence microscopy of intracellular Ca^{++} transients in isolated myocytes demonstrated that esmolol, in contrast to potassium, does not lead to an increase in intracellular $[Ca^{++}]$. The data, however, did not provide any evidence of a direct effect on Ca^{++} channels that could not be separated from the suggested effect on Na^+ channels. Thus, effects on cellular structures other than β–adrenergic receptors could be documented, when esmolol was used to induce and maintain cardiac arrest in isolated, buffer-perfused rat hearts.

- *Effects on K^+ Kinetics*

In our experiments, Rb^+ uptake by the myocardial cell was not altered relative to controls using linear and exponential association functions as strategies for mathematically modeling the data. No differences were found between esmolol and the control group using either model. In physiological terms, the bulk inward transport of K^+ is mediated by Na^+/K^+ ATPase, the function of which is to pump K^+ into the cell against strong electrochemical and concentration gradients. During the action potential itself, the

kinetics of K^+ movement involve mainly outward currents, however small inward currents have been described (see Background, item 2.1.1.1, Action potential generation).

As discussed previously, Rb^+ replaces K^+ in Na^+/K^+ ATPase as well as in potassium channels and the $Na^+/K^+/2Cl^-$ contransporter for the inward flow of K^+ ions. Previous studies with ^{133}Cs NMR spectroscopy have shown that ouabain reduced inward Cs^+ kinetics by 85-90%, suggesting that the bulk of Cs^+ transport occurs through the Na^+/K^+ pump[498]. Cesium, like rubidium, is a K^+ congener and is nearly 100% MR visible. It has proven useful in assessing function of the Na^+/K^+ ATPase but its permeability through membrane K^+ channels is on the order of 0.1-.0.2 relative to K^+, whereas Rb^+ permeability is ~ 0.8, rendering Rb^+ a better tracer for the study of membrane channel kinetics. Previous work from our laboratory has suggested that in beating rat hearts, Na^+/K^+ ATPase is responsible for ~ 85% of the total Rb^+ uptake. Perfusion with specific inhibitors of the $Na^+/K^+/2Cl^-$ co-transporter (bumetanide) and K^+ channel blockers (4-aminopyridine) reduced Rb^+ uptake marginally (~ 10%). Ouabain, on the other hand, despite functional collateral effects (arrhythmias, contracture, and reduction in coronary flow), reduced Rb^+ influx by ~ 75%, indicating that the uptake of Rb^+ depends on function of $Na^+/K^+/ATPase$. In these studies energy levels were monitored by ^{31}P MR spectroscopy and revealed no dramatic changes in the energy state or intracellular pH during treatment with these specific inhibitors[486,487]. Most of the Rb^+ that enters the cell during the loading period will do so via the Na^+/K^+ pump, whereas the contribution of the $Na^+/K^+/2Cl^-$ co-transporter and K^+ channels to Rb^+ influx is small[486]. Because there were no differences in Rb^+ uptake between the esmolol and control groups, it is reasonable to conclude that esmolol at the concentrations used in this thesis does not

alter function of the Na^+/K^+ pump. Experimentally, this hypothesis could be easily verified by measuring Rb^+ inward kinetics in the presence of esmolol and ouabain relative to esmolol alone and/or to ouabain alone and control. In the absence of interactions or incompatibilities between esmolol and ouabain, Rb^+ uptake would possibly be inhibited in the presence of pharmacological concentrations of ouabain.

Our data show a 30-40 % inhibition of Rb^+ efflux during the washout period in esmolol-arrested hearts relative to controls, suggesting a significant effect of esmolol mainly on K^+ channels. Potassium efflux takes place mainly during phases 3 and 4 of the action potential and is responsible for inducing repolarization of the cell. In many species, including humans, the K^+ current that passes through the cardiac delayed-rectifyer channels corresponds to the sum of two distinct currents: a rapidly activating current I_{Kr}, and a slowly activating current, I_{Ks}. These two currents play a major role in the physiological control of heart rate and are subjected to strict control. Dysfunction of these channels is associated with a variety of clinical entities such as the Long-QT syndrome. Long-QT syndrome is known to increase predisposition to serious arrhythmias ("torsade-de-pointes") that may be followed by death. The underlying mechanism is that due to the increased cycle length and increased repolarization time, the ventricles are subjected to a longer relative refractory period, therefore are more prone to an "R-on-T phenomenon" that can trigger ventricular fibrillation. During ventricular fibrillation, the chaotic rhythm prevents any effective pumping activity and cardiac output is negligible. If the patient is not defibrillated, death ensues within minutes. The faster the SA node firing rate, the higher the probability that the AP will encounter ventricular (and atrial) myocytes still in their relative refractory period and trigger an "R-on-T".

Faster hearts such as the rat heart, are thus very prone to arrhythmias. Indeed, in our experiments we observed EAD's (early after depolarizations) and triggered activity in the initial minutes after interrupting infusion of esmolol. Greenspun in 1988[499] described this effect as a "rebound phenomenon", particular to the use of esmolol, in contrast with other intravenous beta-blockers. He reported overshoot of sinus node function parameters and AV nodal refractoriness (sinus cycle length, sinus node recovery time, atrial-Hiss intervals in sinus rhythm and at paced cycle length) in humans within the first 5 minutes after abrupt interruption of infusion that lasted up to 30 minutes or three half-lives of the drug. In our experiments in the pig, we did not observe any arrhythmias that precluded interruption of extracorporeal circulation or maintenance of cardiac output after 20-30 minutes of recovery from arrest. Triggered activity was observed and extrasystoles were recorded but mainly immediately after interrupting arrest. Thus, esmolol also prolongs the AP, typical of class III drugs that are known to affect K^+ homeostasis non-specifically. Recent work has now identified and cloned the genetic loci for I_{Kr} and I_{Ks}. The I_{Kr} voltage-gated K^+ channel is the product of the HERG gene. The new results show that the association of two structurally different membrane proteins, K_VLQT1 and IsK reconstitutes the cardiac slow delayed-rectifier I_{Ks} current. The expression of K_VLQT1 alone induces a voltage-dependent K^+ outward current that has very different biophysical properties from the native K^+ currents recorded in ventricular cells. K_VLQT1 kinetics are much faster than those of I_{Ks} and, in contrast to I_{Kr}, no inward rectification is present at positive potentials. The expression of IsK alone does not produce detectable K^+-channel activity in transfected cells. The co-expression of IsK and K_VLQT1 formed a channel that induced a K^+ current having similar gating kinetics to the native I_{Ks} but with a much

higher amplitude than with K_VLQT1 alone, rendering the channel more effective[500,501]. The clinical implications of these findings can be important if by better identification of the molecular structure of these channels drug design can be improved, by affecting specific channels or currents, and possibly, selective blockade of either component. Single channel studies would be interesting if carried out in the presence of esmolol or similar drugs (such as sotalol) that share properties of classes II and III anti-arrhythmic drugs. Clearly, questions remain regarding the mechanisms by which I_{Ks} contribute to the efficiency of the K^+ channel and how could this be exploited clinically. Identification of the domains through which IsK and K_VLQT1 interact with each other and that are affected by drugs such as esmolol, sotalol and bretylium are just a few investigations that could be undertaken.

➢ *Effects on Na^+ Kinetics*

Sodium transport across cardiac membranes is subject to a delicate balance regulated by the interactions of several membrane structures, mainly Na^+/K^+ ATPase and voltage-dependent Na^+ channels. Na^+ exchangers (Na^+/Ca^{++}, and Na^+/H^+) and co-transporters ($Na^+/K^+/2Cl^-$ and Na^+/HCO_3^-) may operate in both directions depending on ion concentrations and membrane potential[502,503,504]. In addition, Na^+ and K^+ fluxes across the sarcolemma are tightly coupled. Previous work has indicated that Rb^+ uptake can serve as an index of Na^+ influx rate and intensity of ionic homeostasis[486]. A decrease in Na^+ entry through Na^+ channels (induced by application of procaine or lidocaine) or specific blockade of the Na^+/H^+ exchanger (using dimethylamiloride) resulted in a decrease in Rb^+ uptake. Conversely, an increase in Na^+ entry (by means of the Na^+

ionophore, monensin) stimulated Rb^+ uptake. These observations confirm that, under normal conditions, Na^+/K^+ ATPase is the major pathway of Rb^+ and K^+ entry into cardiomyocytes and this same enzyme is a major pathway of Na^+ extrusion[486]. Lithium is a congener of Na^+, and it replaces Na^+ in the fast Na^+ channels, the Na^+/H^+ exchanger and in the $Na^+/K^+/Cl^-$ co-transporter, but not in Na^+/K^+ ATPase or in the Na^+/Ca^{++} exchanger. Nevertheless, lithium is considered useful in evaluating Na^+ channel kinetics, and ^7Li MRS, an effective technique to assess the effects of pharmaceutical agents that target Na^+ channels. As described in the Methods section, we used a moderate (15 mM) concentration of LiCl as a tracer and the MR data acquisition parameters were set to enhance the NMR signal contribution from intracellular Li^+ ($\sim 0.7 < T_1 < 7.0$ s, pulse length 60° and repetition time 2.2 s) rather than extracellular and bath signals ($T_1 > 15$ s). Experiments could then be performed without the use of shift-reagents however only one peak (other than the reference) was obtained in the spectrum. This procedure is acceptable to evaluate the kinetics of Li^+ efflux from the intracellular compartment through Na^+ channels. Any contribution from extracellular Li^+ was washed out by the superfusion flow, which was set at ~ 5 times the coronary flow. After 3-5 minutes contributions to the Li^+ MR signal from the extracellular compartment are considered to be minimal. Data processing did not include the 1st data point of any curve. This procedure allowed the assessment of only intracellular Li^+ efflux. It was not possible to assess Li^+ influx due to the high background signal coming from Li^+ in the surrounding organ bath.

The rate constants of Li^+ efflux from hearts arrested with esmolol were strongly (~ 60%) inhibited relative to controls. Hyperkalemic (KCl, 25 mM) conditions also caused

a similar degree of inhibition of lithium efflux. Generally speaking, Li^+ efflux kinetics depend on the $[Li^+]_i/[Na^+]_i$ ratio (because Li^+ and Na^+ compete for the same transport mechanism, i.e., the Na^+ channel), the driving force (eletrochemical gradient across the membrane), the number of channels available and their kinetics and operational states (function of the *m* and *h* gates), and the rate of cycling, that is the heart rate. A direct blocking effect of esmolol on Na^+ channels would easily explain the inhibition in Li^+ efflux. Hyperkalemic arrest also produced a similar ($P = 0.32$) effect, however the effect was mediated by a different mechanism (i.e., a change in membrane potential, inactivation of the Na^+ channels and cardiac arrest). The "quinidine-like" (or "lidocaine-like") effect of propanolol has been well described. It is not unlikely that esmolol, another β–blocker with a similar structure, would produce a similar effect through direct blockade of Na^+ channels at the myocyte level. However, based only on our Li^+ MRS data, it is not possible to assess the extent to which the reduction in heart rate *per se* accounts for the inhibition of lithium efflux from the myocyte. The best hypothesis is probably a mixture of both effects. If esmolol did not have any effect on sarcolemmal Na^+ channels, then the observed inhibition of Li^+ efflux would be secondary to a direct effect on the SA node (similar to carbachol, a cholinomimetic that affects pacemaker activity by binding muscarinic receptors in the SA node cells. In the case of esmolol, however, one could also hypothesize effects on T-type calcium channels) or on the AV node cells and conduction time (through its effect on K^+ channels and prolongation of the AP duration). We have shown that esmolol is able to produce mechanical arrest with subsequent cessation of electrical activity. We have also demonstrated a dissociation of electrical and mechanical activity. A suitable interpretation for this effect is that, in

conjunction with β–blockade, esmolol increasingly inactivates sarcolemmal Na^+ channels, reducing Ca^{++} availability for contraction and therefore explaining the initial effects seen on contractility. At higher concentrations, the increasing blockade of membrane Na^+ channels would lead to a virtual unavailability of Ca^{++} (possibly due to reduced local $[Ca^{++}]_i$ pool and stimulation of fewer ryanodine receptors, or possible exhaustion of sarcoplasmatic Ca^{++} over time, because less Ca^{++} from the extracellular medium is entering the cell to replenish SR stores) for contraction up to a point that all sodium channels are blocked and electrical activity of the myocyte is completely interrupted, independently of effects on AP duration and on SA node cells. A similar effect was seen in experiments performed with isolated myocytes and Ca^{++} fluorescence microscopy (discussed below). Single channel preparations would be suitable for studying a direct effect of esmolol on Na^+ channels, including cloning and insertion in bilayers, and performing measurements of different gating constants. Using the same experimental settings as in our experiments, however, pacing would reveal if there is a direct effect on Na^+ channels or if the action of esmolol is restricted to the SA node. If, in the presence of concentrations of esmolol that maintain arrest (i.e., ~ 500 μM), pacing restored the initial heart rate values (say 250 bpm), and concomitantly restore Li^+ kinetics to control values, it would be reasonable to conclude that esmolol affects mainly SA node cells and does not interact (or interacts to a lesser extent) with sarcolemmal Na^+ channels.

➢ *Effects on $[Ca^{++}]_i$ transients*

Pacing in the presence of increasing concentrations of esmolol did not produce contraction at esmolol concentrations > 1.7 mM in isolated myocytes, in agreement with

our initial dose-response curve experiments. The absence of myocyte contraction and lower intracellular Ca^{++} transients in the presence of esmolol at increasing concentrations upon field stimulation, suggests that smaller currents pass through the Na^{+} channels further reducing the entrance of Ca^{++} through sarcolemmal L-type channels (voltage-gated) inducing the release of smaller amounts of Ca^{++} from the sarcoplasmmatic reticulum up to a point that when all Na^{+} channels are blocked by esmolol (@ 1.7 mM), no further depolarization can be achieved and no further intracellular Ca^{++} transients can be detected. This seems a rather plausible explanation but a direct effect on Ca^{++} channels cannot be discarded. Based on lipophilicity characteristics and membrane diffusion coefficients, and its longer ½-life, it is plausible that propranolol could affect the activity of sarcolemmal Ca^{++} channels at high concentrations even more efficiently than esmolol.

➢ *Effects on High-energy Phosphates and Intracellular pH*

Among the parameters measured in both series of experiments, PCr showed the most dramatic changes during cardiac arrest and recovery. Data obtained during heart arrest period in both series of experiments revealed not only that PCr levels of esmolol-arrested hearts were lower but also that the rate of decay during the 60-minute arrest period was much greater than in potassium-treated or control hearts. A comparison of the slopes showed statistically significant differences in the rate of consumption of PCr relative to control (beating) and potassium arrested hearts. Whereas in the esmolol-arrested hearts the slope of the PCr curve was negative and steep during the arrest period, in the K^+ group, the slope was slightly positive. This suggests a sparing effect on PCr during arrest in the K^+ arrested hearts, which is consistent with the fact that in an arrested heart, much less energy is consumed. In the esmolol-arrested hearts energy requirements seem increased, although the β–ATP levels were no different in the esmolol, control and potassium arrested hearts. It is possible that ATP levels are maintained at the cost of PCr.

In the heart, high rates of myocardial energy production are required to maintain the constant ATP demand of the working heart. ATP levels are maintained through the buffering action of PCr, which according the several authors, acts as an energy reservoir. Under stress, it has been suggested that the levels of PCr decline first in order to maintain appropriate levels of ATP to support cell function. In the presence of low-flow hypoxic ischemia, glycolysis is accelerated (the so-called Pasteur Effect) mainly in zones of moderate ischemia. The rate of ATP production derived by this mechanism is small relative to the rate of ATP produced by uptake of residual oxygen. Nevertheless,

glycolysis may be the last mechanism by which the cell can generate ATP to reduce the rate of enzyme release; prevent reperfusion arrhythmias; maintain action potential duration and ionic homeostasis, and prevent ischemic contracture[505]. Experiments using glycolytic inhibition during ischemia produced increased structural damage relative to ischemia under normal conditions. As a result, a glycolytic-sarcoplasmatic reticulum complex has been proposed in which the calcium-accumulating system is in physical association with a series of glycogenolytic enzymes. The postulated mechanism suggests that Ca^{++} arriving into the SR stimulates glycogenolysis and glycolysis and produces more glycolytic ATP. An alternative interpretation has been proposed which suggests that glycolysis has a rate-limiting role for Ca^{++} uptake and therefore indirectly regulates the process of relaxation[498,506].

The classical hypothesis that ATP is the immediate source of energy for contraction and other processes while PCr is kept as a "reservoir" has been enlarged with the additional (but not exclusive) role for PCr as a transport molecule. As ATP is exported from the mitochondria, it is proposed that ATP is immediately converted to PCr by a mitochondrial creatine kinase (analogous to the cytoplasmatic creatine phosphokinase) isoenzyme located between the two layers of the mitochondrial double membrane. Phosphocreatine is then presumably transported throughout the cytoplasm, following a probable downhill concentration gradient to a cytosolic site of utilization of energy where a cytosolic creatine phosphokinase isoenzyme will liberate the ATP required for energetic purposes. During a sustained and severe hypoxic stimulus, ATP will eventually fall, following the initial decrease in PCr levels. However, under conditions such as increased cardiac work requiring increased metabolic activity, PCr will

be restored as the oxygen uptake rises, such that overall tissue levels of ATP are little changed despite a doubling of the cytosolic ratio of ATP/ADP. The currently most favoured view however is that of ATP compartmentalization, not only between the mitochondria and cytosol, but also as a result of the activity of cytosolic creatine kinase isoenzymes.

Assuming that esmolol actually affects HEP metabolism directly, it implies that esmolol must traverse the membrane and enter the cell. Esmolol is a beta-receptor blocker, designed to act on the external side of the membrane. Nevertheless, its ability to cross cell membranes depends on several factors, including its concentration, lipophilicity and charge. Esmolol, despite its hydrochloride (ionized) formulation, has a relatively high pKa = 9.5. At pH 7.4, and at concentrations used to produce arrest (~ 500 μM), one can estimate that approximately 1% (or 5 μM) could accumulate in the intracellular compartment over the 1h arrest period used in our studies. The esterase responsible for the metabolism of esmolol in red blood cells has been described, however even before the identification of this enzyme it was known that non-specific esterases could also cleave the molecule. It may be reasonable to deduce that at least part of the apparent increase in metabolic activity (and the decrease in PCr levels) could be due to this intracellular enzymatic activity. The energy requirement for the proposed activity of the esterases may be considered rather high relative to the controls, that consisted of beating hearts. These were not working models but hearts beating empty, which should be taken into consideration. It has long been demonstrated that energetic requirements under such conditions are substantially less relative to a working model. In spite of the observed effects on PCr, the overall levels of ATP did not change, as is usually the case when a

serious stress (such as long-term hypoxia/ischemia) is imposed. The observed changes may indicate only that esmolol arrest does not lead to the same energy sparing effect as observed in potassium-arrested hearts. It may be the case that the energy spared by inducing arrest is redirected into fueling the enzymatic breakdown of esmolol. It is important to note that 30 minutes after recovery from arrest the overall content of PCr in the esmolol group was only slightly different from that of the potassium group ($P = 0.044$), while the ATP levels were not different ($P = 0.09$). Over a 110-minute recovery period, the rate of decay of PCr in esmolol-treated hearts became much less steep, and no difference was found between the potassium- and esmolol-arrested hearts relative to the control group or to each other. Our observations suggest that regardless the mechanism that uses up the energy spared by arresting contraction, it does not lead to severe ATP depletion, and that in the long-run, under the described experimental conditions, the levels of myocardial energetic reserve are similar in esmolol and potassium arrested hearts. The next step is to verify the presence of this effect of esmolol on PCr levels in the blood-perfused (isolated or *in vivo*) pig heart.

Measurements of intracellular pH in esmolol-arrested hearts were performed prior to arrest, during arrest and recovery. Intracellular pH of esmolol-arrested hearts was somewhat higher than in control hearts, but did not differ from the potassium-treated group ($P = 0.053$). The slight increase in pH immediately upon inducing arrest has been documented[507]. The mechanism proposed by the authors is based on an acute reduction in the production of CO_2 immediately after induction of cardiac arrest. Hyperkalemic arrest induced in isolated rabbit hearts resulted in a slight increase (~ 7.2) in intracellular pH, within the same range as the values obtained in the present series.

CHAPTER V - CONCLUSIONS

- Esmolol can match the ability of hyperkalemic cardioplegic solutions in producing reversible cardiac arrest with the advantage that its arresting properties are easily titrable. Its metabolic characteristics are independent of the patient's kidney or liver function.

- Esmolol under the conditions described in this study and at the stated concentrations is at least one order of magnitude below the level at which its metabolites become toxic after one hour of cardioplegic arrest.

- Esmolol at the concentrations stated in this thesis exerts effects other than classical beta-blocking. It may act by blocking Na^+ and K^+ channels. A direct effect on Ca^{++} channels cannot be excluded. The levels of phosphocreatine are reduced in esmolol-arrested hearts but the ATP pool is not altered, indicating no significant effect of esmolol on the overall balance of high-energy compounds in the cell.

- Esmolol may be useful and safe for use as a cardioplegic agent especially for patients with compromised kidney or liver function who have difficulties eliminating the high load of K^+ administered during traditional hyperkalemic cardioplegia.

- Esmolol may also be useful in the minimally invasive setting, to reduce the beating rate and motion of the heart.

- Esmolol has non-specific effects on Na^+ and K^+ channels that may explain the arrhythmogenic effects it produces immediately after interrupting its infusion. Further investigation is required to identify specific subtypes of ion channels and currents or cell structures that may be affected by esmolol.

- The work presented in this thesis outlines efforts towards the development of better techniques and strategies of myocardial protection. Alternative pharmaceutical and surgical approaches are essential elements in any cardioplegic strategy. This work is expected to trigger research for the development of new agents with more targeted effects.

REFERENCES

[1] Toner I, Taylor KM, Lockwood G, Newman S, Smith PLC. EEG changes during cardiopulmonary bypass surgery and postoperative neuropsychological deficit: the effect of bubble and membrane oxygenators. Eur J Cardiothorac Surg 1997;11:312-319.

[2] Waldenberger FR, Hotz H, Haisjackl M, Konertz W. Chrurgische koronarrevaskularisation am schlagenden Herzen. Z Kardiol 1996;85(4):35-41.

[3] Greenspun HG, Adourian AU, Fonger JD, Fan JS. Minimally Invasive Direct Coronary Artery Bypass (MIDCAB): Surgical techniques and anesthetic considerations. J Cardiothorac Vasc Anesth 1996;10(4):507-509.

[4] Kurth CD, Steven JM, Nicolson SC, Jacobs MLJ. Cerebral oxygenation during cardiopulmonary bypass in children. J Thorac Cardiovasc Surg 1997;113:71-79.

[5] Vingerhoets G, Van Nooten G, Vermassen F, De Soete G, Jannes C. Short-term and long-term neuropsichologycal consequences of cardiac surgery with extracorporeal circulation. Eur J Cardiothorac Surg 1997;11:424-431.

[6] Kurpriyanov VV, Xiang B, Butler KW, St-Jean M, Deslauriers R. Contractile dysfunction caused by normothermic ischemia and KCl arrest in the isolated pig heart: A 31P NMR study. J Mol Cell Cardiol 1995;27:1715-1730.

[7] Damiano R, Cohen N. Hiperpolarized arrest attenuates myocardial stunning following global surgical ischemia. J Card Surg 1994;9:515-525.

[8] Cavallo MJ, Dorman BH, Spinale FG, Roy RC. Myocyte contractile responsiveness after hypothermic, hyperkalemic cardioplegic arrest. Disparity between exogenous calcium and β–adrenergic stimulation. Anesthesiology 1995;82:926-939.

[9] Roberts AJ, Spies SM, Sanders JH, Moran JM, Wilkinson CJ, Lichtenthal PR, White RL, Michaelis LL. Serial assessment of left ventricular performance following coronary artery bypass grafting. J Thorac Cardiovasc Surg 1981;81:69-84.

[10] Phillips HR, Carter JE, Okada RD, Levine FH, Boucher CA, Osbakken M, Lappas D, Buckley MJ, Pohost GM. Serial changes in left ventricular ejection fraction in the early hours after aortocoronary bypass grafting. Chest 1983;83:28-34.

[11] Ede M, Lessana A, Lehouerou D et al. "Acquisitions récentes en Cardioplégie Normothermique: Contrôle de la Kaliémie et de l'Hémodiluiton". L'Information Cardiologique 1993;16:125-132.

[12] Ede, M., Ye, J., Gregorash, L., Summers, R., Pargaonkar, S., LeHouerou, D., Lessana, A., Salerno, T.A. and Deslauriers, R. Beyond hyperkalemia: β–blocker-induced cardiac arrest for normothermic cardiac operations. Ann Thorac Surg 1997;63: 721-727.

[13] Robinson MC, Gross DR, Zeman W. A minimally invasive surgical method for coronary revascularization--preliminary experience in five patients. Abstract. 1995 Annual Meeting of the American Heart Association. Circulation 1995;92(8).

[14] Cosgrove DM III, Sabik JF. Minimally Invasive approach for aortic valve operations. Ann Thorac Surg 1996;62:596-7.

[15] Kolessov VL. Mammary artery-coronary artery anastomosis as method of treatment for angina pectoris. J Thorac Cardiovasc Surg 1967;54:535-44.

[16] Favaloro RG. Saphenous vein autograft replacement of severe segmental coronary artery occlusion. Ann Thorac Surg 1968;5:334-9.

[17] Garret HE, Dennid EW, DeBakey ME. Aorto-coronary bypass with saphenous vein graft. Seven-year follow-up. JAMA 1973;223:792-4.

[18] Trapp WG, Bisarya R. Placement of coronary artery bypass graft without pump-oxygenator. Ann Thorac Surg 1975;19:1-9.

[19] Ankeney JL. To use or not to use the pump oxygenator in coronary bypass operations. Ann Thorac Surg 1975;19:108-9.

[20] Buffolo E, Andrade JCS, Branco JNR, Teles CA, Aguiar LF, Gomes WJ. Coronary artery bypass grafting without cardiopulmonary bypass. Ann Thorac Surg 1996;61:63-6.

[21] Sweeney MS, Frazier OH. Device-supported myocardial revascularization: safe help for sick hearts. Ann Thorac Surg 1992;54:1065-70.
[22] Laub GW, Muralidharan S, Reibman J, Fernandez J, Anderson WA, Gu J, Daloisio C, McGrath LB, Mulligan LJ. Esmolol and percutaneous cardiopulmonary bypass enhance myocardial salvage during ischemia in a dog model. J Thorac Cardiovasc Surg 1996;111:1085-91.
[23] Lonn U, Peterzen B, Granfeldt H, Casimir-Ahn H. Coronary artery operation with support of the Hemopump Cardiac Assist System. Ann Thorac Surg 1994;58:519-23.
[24] Matsuda H, Fukushima N, Kadoba K, Sawa Y, Nomura F, Kume Y, Miyagawa S, Shimazaki Y. Application of ultra-short acting beta-blockade in pediatric open heart surgery: A trial in total anomalus pulmonary venous return. JCard Surg 1996;11:411-415.
[25] Schaff HV. New surgical techniques: Implications for the cardiac anesthesiologist: Mini-thoracotomy for coronary revascularization without cardiopulmonary bypass. J Cardiothorac Vasc Anesth 1997;11(2):6-9.
[26] Melhorn U, Allen SJ, Adams DL, Davis KL, Gogola GR, Warters RD. Cardiac surgical conditions induced by β–blockade: Effect on myocardial fluid balance. Ann Thor Surg 1996;62:143-50.
[27] Ingwall JS. Measuring sodium movements across the myocardial cell wall using 23Na NMR Spectroscopy and shift reagents.
[28] Deslauriers R, Kozlowski P, Stewart LC, Smith ICP. Spectroscopy: Princilples and additional instrumentation.
[29] Ugurbil K and From AHL. Nuclear magnetic resonance studies of kinetics and regulation of oxidative ATP synthesis in the myocardium.
[30] Zeipes DP. Genesis of cardiac arrhythmias: Electrophysiological considerations. In : Braunwald E. (ed.) Heart Disease :588-627. McGraw-Hill (1993).
[31] Biggeri JT. Electrical activity of the heart. In: Hurst EM (ed.) The Heart. Wilkams and Williams (1993).
[32] Coraboeuf E, Escande D. Ionic currents in the human myocardium. New in Physiol Sciences 1990;5:28.
[33] Escande D, Coulombe A, Fairre JF. Two types of transient outward currents in adult human atrial cells. Am J Physiol 1987;21:H142.
[34] Bahinski A, Nairn AC, Greengard P, Gadsby DC. Chloride conductance regulated by cyclic AMP-dependent protein kinase in cardiac myocytes. Nature 1989;340:718.
[35] Harvey RD, Hume JR. Autonomic activation of a chloride current in the heart. Science 1989;244:983.
[36] Harvey RD, Hume JR. Histamine activates the chloride current in cardiac ventricular myocytes. J Cardiovasc Electrophysiol 1990;1:309.
[37] Mc Allister RE, Noble D, Tsien RW. Reconstruction of the electrical activity of cardiac Purkinje fibers. J Physiol 1975;251:1-59.
[38] Noble D. Initiation of the heartbeat. London, Oxford University Press, 1979.
[39] Rozanski, GJ. Electrophysiological properties of automatic fibers in rabbit atrioventricular valves. Am J Physiol 1987;253:H720.
[40] Kirchhof CJ, Bonke FI, Allessie MA. Evidence for the presence of electronic depression of pacemakers in the rabbit atrioventricular node. The effects of uncoupling from the surrounding myocardium. Basic Res Cardiol 1988; 83:190.
[41] Atkins DL, Marvin WJ Jr. Chronotropic responsiveness of developing sinoatrial and ventricular rat myocytes to autonomic agonists following adrenergic and cholinergic innervation in vitro. Circ Res 1989;64:1051.
[42] James TN, Sherf L, Fine G, Morales AR. Comparative ultrastructure of the sinus node in man and in dog. Circulation 1966;34:139-163.
[43] James TN. The connecting pathways between thesinus node and the AV node and between the reght and left atrium in the human heart. Am Heart J 1963;66:498-508.
[44] James TN, Sherf L. Specialized tissues and preferential conduction in the atria of the heart. Am J Cardiol 1971;28:414-427.
[45] Weidmann S. Effect of current flow on the membrane potential of cardiac muscle. J Physiol 1951;115:227-236.
[46] Vassale M. An analysis of cardiac pacemaker potential by means of a voltage clamp technique. Am J Physiol 1966;210:1335-1341.
[47] Noble D, Tsien RW. The kinetics and rectifier properties of the slow potassium current in cardiac Purkinje fibers. J Physiol 1968; 195:185-214.

[48] Di Francesco D. The cardiac hyperpolarizing current I_f. Origins and development. Prog Biophys Mol Biol 1985;46:163.

[49] Gilmour RF, Zipes DP. Abnormal automaticity and related phenomena . In Fozzard HM et al. (eds.) The heart and cardiovascular system. New York, Raven Press (2nd ed), 1986:1239.

[50] Jalife J, Moe GK. Effect of electrotonic potentials on pacemaker activity of canine Purkinje fibers in relation to parasystole. Circ Res 1976;39:801-808.

[51] Callewert G, Carmeliet E, Vereecke I. Single cardiac Purkinje cells: general physiology and voltage clamp analysis of the pace-maker current. J Physiol (Lond.) 1984;349:643-661.

[52] Di Francesco D, Ferroni A, Mazzanti M, Tromba C. Properties of the hyperpolarizing -activated current (I_f) in cells isolated from the rabbit sino-atrial node. J Physiol (Lond.) 1986; 377:61-88.

[53] Yatani A, Brown AM. Regulation of cardiac pacemaker current I_f in excised membranes from sinoatrial node cells. Am J Physiol 1990;258:H1947-H1951.

[54] Chang F, Gao J, Tromba C, Cohen J, DiFrancesco D. Acetylcholine reverses the effects of β–agonists on pacemaker current in canine cardiac Purkinje fibers but has no direct action. A difference between primary and secondary pacemakers. Circ Res 1990;66:633-636.

[55] Campbell GD, Edwards FR, Hirst GDS, O'Shea JE. Effects of vagal stimulation and applied acetylcholine on pacemaker potentials in guinea pig heart. J Physiol (Lond.) 1989;415:57-68.

[56] Brywater RAR, Campbell G, Edwards FR, Hirst GDS, O'Shea JE. The effects of vagal stimulation and applied acetylcholine on the sinus venosus of the toad. J Physiol (Lond.) 1989;415:35-56.

[57] Baumgarten CM, Fozzard HA. Cardiac resting and pacemaker potentials. In: Fozzard HA, et al. (eds.) The heart and Cardiovascular System 2nd ed. Raven Press NY. 1992:963-1001.

[58] Hodgkin HA, Rushton WAH. The electrical constants of a crustacean nerve fibre. Proc R Soc Lond (Biol), 1946; 133:444-479.

[59] Weidmann S. The electrical constants of Purkinje fibres. J Physiol (Lond) 1952;118:348-360.

[60] Jack JJB, Noble D, Tsien RW. Electric current flow in excitable cells. Clarendon Press, Oxford.

[61] Fozzard HA. Conduction of the action potential. In: Handbook of Physiology , vol. I The Heart American Physiological Society 1979:335-356.

[62] Goldstein SS, Rall W. Changes in action potential shape and velocity for changing core conductor geometry. Biophys J 1974; 14:731-757.

[63] Spach MS, Miller WT, Dolber PC, Kootsey JM, Sommer JR, Mosher CE Jr. The functional role of structural complexities in propagation of depolarization in the atrium of the dog. Cardiac conduction disturbances due to discontinuities of effective axial resistivity. Circ Res 1982;50:175-191.

[64] Fozzard HA, Arnsdorf MF. Cardiac electrophysiology In: Fozzard HA et al. (eds.) The Heart and Cardiovascular System. 2nd ed., Raven Press New York, 1992:63-98.

[65] Carafoli E. Intracellular calcium homeostasis. Annu Rev Biochem 1987;56:375.

[66] Rappaport L, Samuel JL. Microtubules in cardiac myocytes. Int Rev Cytol 1988;113:101.

[67] Fabiato A, Fabiato F. Calcium and cardiac excitation muscle. Mayo Clin Proc 1982;57(suppl):6.

[68] Shuba LM, McDonald TF. Excitation-contraction coupling: relationship of calcium currents to contraction. In Sperelakis N (ed.) Physiology and pathophysiology of the heart. 3rd ed., Kluwer, Boston, 1995:269.

[69] Bassingthwaighte JB, Reuter H. Calcium movements and excitation-contraction coupling in cardiac cells. In: de Mello (ed.) Electrical phenomena in the heart. New York, Academic Press, 1972 pp. 353-393.

[70] Chapmann RA. Control of cardiac contractility at the cellular level. Am J Physiol 1983;245:H535-H552.

[71] Fabiato A, Fabiato F. Calcium and cardiac excitation-contraction coupling. Annu Rev Physiol 1979;41:473-484.

[72] Wier WG. Cytoplasmic $[Ca^{2+}]_i$ in mammalian ventricle: Dynamic control by cellular processes. Annu Rev Physiol 1990;52:467-485

[73] Wier WG. $[Ca^{2+}]_i$ transients during excitation-contraction coupling of mammalian heart. In: Fozzard et al. (eds.) The heart and cardiovascular system, 2nd ed., New York, Raven Press, 1992, pp.1223-1248.

[74] Morad M, Cleerman L. Role of Ca^{2+} channel in development of tension in heart muscle. J Mol Cell Cardiol 1987;19:527-553.

[75] Beuckmann DJ, Weir WG. Mechanism of release of calcium from sarcoplasmic reticulum of guinea-pig cardiac cells. J Physiol 1988;404:233.

[76] Fabiato A. Simulated calcium current can both cause calcium loading and trigger calcium relese from the sarcoplasmic reticulum of a skinned canine cardiac Purkinje cell. J Gen Physiol 1985;85:291.

[77] Lee KS, Tsien RW. High selectivity of calcium channels in single dialysed heart cells of the guinea-pig. J Physiol (Lond.) 1984;354:253-272.

[78] McDonald TF. The slow calcium current in the heart. Annu Rev Physiol 1982;44:425-434.

[79] McDonald TF. Cavalié A, Trautwein W, Pelzer D. Voltage-dependent properties of macroscopic and elementary calcium channels currents in guinea pig ventricular myocytes. Pfluger Arch 1986;406:437-488.

[80] Bean BP. Two kinds of calcium channels in canine atrial cells. Differences in kinetics, selectivity, and pharmacology. J Gen Physiol 1985;86:1-30.

[81] Mitra R, Morad M. Two types of calcium channels in guinea pig ventricular myocytes. Proc Natl Acad Sci USA 1986;83:5340-5344.

[82] Nilius B, Hess P, Lansman JB, Tsein RW. A novel type of cardiac calcium channel in ventricular cells. Nature 1985;316:443-446.

[83] Balke CW, Rose WC, Marban E, Wier WG. Macroscopic and unitary properties of physiological ion flux through T-type Ca^{2+} channels in guinea-pig heart cells. J Physiol (Lond.) 1992;456:247-265.

[84] Bers DM. Early transient depletion of extracellular Ca during individual cardiac muscle contractions. Am J Physiol 1983;244:H462-H468.

[85] Dixon IMC, Afzal N, Takeda N, Nagano, Dhalla NS. Remodeling of cardiac membranes during the development of congestive heart failure due to myocardial infarction. In: Dhalla NS, Beamish RE, Takeda N and Nagano M (eds.) The Failing Heart Lippincont Raven, Philadelphia 1995;217.

[86] Niggli E, Lederer WJ. Voltage-independent calcium release in heart muscle. Science 1990;250:565-568.

[87] Gibbons WR. Cellular control of cardiac contraction. In Fozzard et al (eds.) The heart and cardiovascular system, New York, Haven Press 1986; pp.747-778

[88] Gibbons WR. Zygmunt AC. Excitation-contraction coupling in heart. In: In Fozzard et al. (eds.) The heart and cardiovascular system, 2nd ed. New York, Raven Press 1992; pp.1249-1279.

[89] Gilman AG. Guanine nucleotide-binding regulatory proteins and dual control of adenlylate cyclase. J Clin Invest 1984;73:1.

[90] Gilman AG. G proteins: Transducers of receptor-generated signals. Annu Rev Biochem 1987;56:615.

[91] Alvarez JL, Vassort G. Properties of the low threshold Ca current in single frog atrial cardiomyocytes. A comparison with the high threshold Ca current. J Gen Physiol 1992;100:519-545.

[92] LeGrand B, Deroubais E, Coulombe A, Caraboeuf E. Stimulatory effects of ouabain on T- and L-type calcium currents in guinea pig cardiac myocytes. Am J Physiol 1990;258:H1620-H1623.

[93] Johnson EA. Force-interval relationship of cardiac muscle. In Berne RM (ed.) Handbook of Physiology, section 2, The cardiovascular system, Vol. 1 The Heart. Bethesda, American Physiology Society, 1979:475-496.

[94] Chapmann RA. Sodium/calcium exchange and intracellular calcium buffering in ferret myocardium. An ion-sensitive micro-electrode study. J Physiol 1986;373:163-179.

[95] Hinglemann DW. Numerical approximations of the sodium-calcium exchange. Prog Biophys Mol Biol 1988;51:1-45.

[96] Reeves JP, Hale CC. The stoichiometry of the cardiac sodium-calcium exchange system. J Biol Chem 1984;259:7733-7739.

[97] Lytton J, MacLennan DH. Sarcoplasmic reticulum. In: Fozzard et al. (eds.) The heart and cardiovascular system, New York, Raven Press 2nd ed. 1992; pp. 1203-1222.

[98] Williams AJ. Ion conduction and discrimination in the sarcoplasmic reticulum ryanodine receptor/calcium-release channel. J Muscle Res Cell Motility 1992;13:7-26.

[99] Otsu K, Willard HF, Khanna VK, Zorzato F, Green NM, MacLennan DH. Molecular cloning of cDNA encoding the Ca^{2+} release channel (ryanodine receptor) of rabbit cardiac muscle sarcoplasmic reticulum. J Biol Chem 1990;265:13472-13483.

[100] Takasago T, Imagawa T, Shigekawa M. Phosphorylation of the cardiac ryanodine receptor by cAMP-dependent protein kinase. J Biochem (Tokyo) 1989;106:872-877.

[101] Witcher DR, Kovacs RJ, Schulmann H, Cefali DC, Jones LR. Unique phosphorylation site on the cardiac ryanodine receptor regulates calcium channel activity. J Biol Chem 1991;266:11144-11152.

[102] Meissner G, Darling E, Eveleth J. Kinetics of rapid Ca^{2+} release by sarcoplasmic reticulum. Effects of Ca^{2+}, Mg^{2+}, and adenine nucleotides. Biochemistry 1986;25:236-244.

[103] Meissner G, Henderson JS. Rapid calcium release from cardiac sarcoplasmic reticulum vesicles is dependent on Ca^{2+} and is modulated by Mg^{2+}, adenine nucleotide, and calmodulin. J Biol Chem 1987;262:3065-3073.

[104] Isenber G. Cardiac excitation-contraction coupling: from global to microscopic models. In: Sperelakis N (ed.) Physiology and pathophysiology of the heart. 3rd ed. Kluwer Academic Press, Boston 1995:289.

[105] Williams AJ. Ion conduction and discrimination in the sarcoplasmic reticulum ryonodine receptor/calcium-release channel. J Muscle Res Cell Motility 1992;13:7-26.

[106] Bers DM, Bridge JHB. Relaxation of rabbit ventricular muscle by Na-Ca exchange and saroplasmic reticulum calcium pump. Ryanodine and voltage sensitivity. Circ Res 1989;65:334-342.

[107] Bridge JHB, Spitzer KW, Ershler PR. Relaxation of isolated ventricular cardiomyocytes by a voltage-gated process. Science 1988;241:823-825.

[108] Bers DM, Lederer WJ, Berlin JR. Intracellular Ca transients in rat cardiac myocytes: role of Na-Ca exchange in excitation-contraction coupling. Am J Physiol 1990;258:C944-C954.

[109] Yatani A, Brown AM. Rapid β–adrenergic modulation of cardiac calcium channel currents by a fast G protein pathway. Science 1989;245:71.

[110] Hicks MJ, Shigekawa M, Katz AM. Mechanism by which cyclic adenosine 3',5'-monophosphate-dependent protein kinase stimulates calcium transport in cardiac sarcoplasmic reticulum. Circ Res 1979;44:384.

[111] Winegrad S, McClellan G, Horowitz R. Regulation of cardiac contractile proteins by phosphorylation. Fed Proc 1983;42:39.

[112] Trautwein W, Cavalie A. Cardiac calcium channels and their control by neurotransmitters and drugs. J Am Coll Cardiol 1985;6:1409.

[113] Catterall WA. Molecular properties of voltage-gated ion channels in the heart. In: Fozzard HA et al.The heart and cardiovascular system 2nd ed., Raven Press, New York 1992;945.

[114] Noda A, Shimizu T, Tanabe T, et al. Primary structure of *Electrophorus electricus* sodium channel deduced from cDNA sequence. Nature 1984;312:121-127.

[115] Catterall W. Neurotoxins that act on voltage-sensitive sodium channels. Annu Rev Pharmacol Toxicol 1980;20:15-43.

[116] Gordon D, Merrick D, Wollner DA, Catterall WA. Biochemical properties of sodium channels in a wide range of excitable tissues studied with site-directed antibodies. Biochemistry 1988;27:7032-7038.

[117] Bean BP. Classes of calcium channels in vertebrate cells. Annu Rev Physiol 1989;51:367-389.

[118] Campbell KP, Leung AT, Sharp AH. The biochemistry and molecular biology of the dihydropyridine-sensitive calcium channel. Trends Neurosci. 1988;11:425-430.

[119] Flockerzi V, Hofmann F. Molecular structure of the cardiac calcium channel. In: Sperelakis N (ed.) Physiology and pathophysiology of the heart. 3rd ed. Kluwer Academic Publishers, Boston 1995;91.

[120] Heinmann SH, Stuhmer W. Molecular structure of potassium and sodium channels and their structure-function correlation. In: Sperelakis N (ed.) Physiology and pathophysiology of the heart. 3rd ed. Kluwer Academic Publishers, Boston 1995;101

[121] Jan LY, Jan YN. Voltage-sensitive ion channels. Cell 1989;56-13-25.

[122] Guy HR, Seetharamulu P. Molecular model of the action potential sodium channel. Proc Natl Acad Sci USA 1986;83:508-512.

[123] Stuhmer W, Conti F, Suzuki H, Wang X, Noda M, Yahagi N, Kubo H, Numa S. Structural parts involved in activation and inactivation of the sodium channel. Nature 1989;339:597-603.

[124] Heinemann SH, Terlau H, Stuhmer W, Imoto K, Numa S. Calcium channel characteristics conferred on the sodium channels by single mutations. Nature 1992;356:441-443.

[125] MacKinnon R, Yellen G. Mutations affecting TEA blockade and ion permeation in voltage-activated K^+ channels. Science 1990;250276-279.

[126] Heginbotham L, Abramson T, MacKinnon R. A functional connection between the pores of distantly related ion channels as revealed by mutant K^+ channels. Science 1992;258:1152-1155.

[127] Hodgkin AL, Huxley AF. Current carried by sodium and potassium ions through the membrane of the giant axon of *Loligo*. J Physiol 1952;116:449-472.

[128] Hodgkin AL, Huxley AF. A quantitative description of membrane current and its application to conduction and excitation in nerve. J Physiol 1952;117:500-544.
[129] Armstrong CM, Gilly WF. Fast and slow steps in the activation of sodium channels. J Gen Physiol 1979;74:691-711.
[130] Armstrong CM. Sodium channels and gating currents. Physiol Rev 1981;61:644-683.
[131] Kirsch GE, Brown AM. Cardiac sodium channels. In: Zipes DF and Jalife J (eds.) Cardiac Physiology. From Cell to Bedside. Philadelphia, W.B. Saunders Company, 1990:1.
[132] Hess P. Cardiac calcium channels In: Zipes DF and Jalife J (eds.) Cardiac Physiology. From Cell to Bedside. Philadelphia, W.B. Saunders Company, 1990:10.
[133] Pelzer D, Pelzer S, McDonald TF. Calcium channels in the heart. In: Fozzard HA et al.The heart and cardiovascular system 2nd ed., Raven Press, New York 1992;1049.
[134] Cohen NM, and Lederer WJ. Calcium current in isolated neonatal rat ventricular myocytes. J Physiol (Lond.) 1987;391-169-171.
[135] Kass RS, Sanguinetti MC. Inactivation of calcium channel current in the calf cardiac Purkinje fiber. Evidence for voltage- and calcium-mediated mechanisms. J Gen Physiol 1984;84:705-726.
[136] Hirano Y, Fozzard HA, January CT. Characteristics of L-type and T-type Ca^{2+} currents in canine cardiac Purkinje cells. Am J Physiol 1989;256:H1478-H1492.
[137] Hess P, Lansman JB, Tsien RW. Different modes of Ca channel gating behaviour favoured by dihydropyridine Ca agonists and antagonists. Nature 1984;311:538-544.
[138] Yue DT, Herzig S, Marban E. β–adrenergic stimulation of calcium channels occurs by potentiation of high activity gating modes. Proc Natl Acad Sci USA. 1990;87:735-757.
[139] Cavalié A, Pelzer D, Trautwein W. Fast and slow gating behaviour of single calcium channels in cardiac cells. Relation to activation and inactivation of calcium-channel current. Pflugers Arch 1986;406:241-258.
[140] Kawashima Y, Ochi R. Voltage-dependent decrease in the availability of single calcium channels by nitrendipine in guinea pig ventricular cells. J Physiol (Lond.) 1988;402:219-235.
[141] Ochi R, Kawashima Y. Modulation of slow gating process of calcium channels by isoprenaline in guinea pig ventricular cells. J Physiol (Lond,) 1990;424:187-204.
[142] Droogmans G, Nilius B. Kinetic properties of the cardiac T-type calcium channel in the guinea pig. J Physiol (Lond.) 1989;419:627-650.
[143] Guy HR. A model relating the structure of the sodium channel to its function. In: Agnew W et al. (eds.) Molecular Biology of Ion Channels: Current Topic in Membrane Transport. Academic Press, New York, 1989.
[144] Catterall WA. Molecular pharmacology of voltage-sensitive sodium channels . ISI Atlas Science: Pharmacol 1988:190-195.
[145] Rossie S, Catterall WA. Regulation of ion channels In: Boyer P et al. (eds.) Enzyme control by protein phosphorylation.: The enzymes. vol XVIII. Academic Press, New York, 1987:335-358.
[146] Trautwein W, Heschler J. Regulation of cardiac L-type calcium current by phosphorylation and G proteins Annu Rev Physiol 1990;52:257-274.
[147] Schubert B, VanDongen AMJ, Kirsch GE, Brown AM. β–adrenergic inhibition of cardiac sodium channels by dual G-protein pathways. Science 1989;245:516-519.
[148] Numann R, Catterral W, Scheuer T. Functional modulation of brain sodium channels by protein kinase C phosphorylation. Science 1991;254:115-118.
[149] Ruppersberg JP. Stocker M, Pongs O, Heinemann SH, Frank R, Koenen M. Regulation of fast inactivation of cloned mammalian IK(A) channels by cysteine oxidation. Nature 1991;352:711-714.
[150] Pardo LA, Heinemann SH. Terlau, Ludewig U, Lorra C, Prongs O, Stuhmer W. Extracellular K^+ specifically modulates a rat brain potassium channel. Proc Natl Acad Sci USA 1992;89:2466-2470.
[151] Shine KI. Myocardial effects of magnesium. Am J Physiol 1979;237:H413-H423.
[152] Hasselbach W, Fassold E, Migala A, Rauch B: Magnesium dependence of sarcoplasmic reticulum calcium transport. Fed Proc 1981;40:2657-2661
[153] Bretschneider HJ, Gebhard MM, Preusse CJ. Reviewing the pros and cons of myocardial preservation within cardiac surgery. In: Longmore DB (ed.) Towards Safer Cardiac Surgery. Lancaster:MTP, 1981:21-53.

[154] Gebhard MM, Bretschneider HJ, Schnabel PA. Cardioplegia principles and problems In: Sperelakis N (ed.) Physiology and Pathophysiology of the Heart, 3rd edition, Kluwer Academic Publishers 1995:731.
[155] Berne RM, Levy MN. Regulation of the heartbeat. In: Physiology 3rd edition, 1993:417.
[156] Stiles GL. Structure and function of cardiovascular membranes, channels and receptors. In Hurst's The Heart. Eighth ed., edited by Schlant RC and Alexander RW et. al. Mc Graw-Hill 1994.
[157] Raymond JR, Hnatovich M, Lefkowitz RJ, Caron MG. Adrenergic receptors: models for regulation of signal transduction processes. Hypertension 1990;15:119-131.
[158] Krief S, Lonqvist F, Raimbault S, Baude B, Van Spronsen A, Arner P, Strosber AD, Ricquer D, Emorine LJ. Tissue distribution of β3–adrenergic receptor in mRNA in man. J Clin Invest 1993;91:344-349.
[159] Hancock AA, DeLean AL, Lefkowitz RJ. Quantitative resolution of β–adrenergic receptor subtypes by selective ligand binding. Application of a computerized model fitting technique. Mol Pharmacol 1980;16:1-9.
[160] Carlsson E, Dahlof C, Hedberg A, Tangstrand B. Differentiation of cardiac chronotropic and inotropic of β–adrenoceptor agonists. Naunyn-Schmiedebergs Arch Pharmacol 1977;300:101-105.
[161] Levitski A. β–adrenergic receptors and their mode of coupling to adenylyl cyclase. Physiol Rev 1986;66:819-854.
[162] Schwinn DA, Caron MC and Lefkowitz RJ. The beta-adrenergic receptor as a model for molecular structure-function relationships in G-protein-coupled receptors. In The Heart and the Cardiovascular System, edited by Fozzard HA et. al. Raven Press, 2nd ed., 1657-84 (1992).
[163] Holmer SR, Homey CJ. G proteins in the heart: A redundant and diverse transmembrane signaling network. Circulation 1991;84:1891-1902.
[164] Watanabe AM, Mc Connaughey MM, Strawbridge RA, Fleming JW, Jones LR, Besch HR,Jr. Muscarinic cholinergic receptor modulation of β–adrenergic receptor affinity for catecholamines. J Biol Chem 1978;253:4833-4836
[165] Gilman AG. G proteins and regulation of adenylyl cyclase. JAMA 1989;262:1819-1825.
[166] Birnbaumer L. G proteins in signal transduction. Annu Rev Pharmacol Toxicol 1990;30:675-705.
[167] Robinshaw J, Foster KA. Role of G proteins in the regulation of the cardiovascular system. Annu Rev Physiol 1989;51:73-100.
[168] Ueda K, Hayaishi O. ADP-rybosilation. Annu Rev Biochem 1985;54:73-100.
[169] Fleming JW, Wisler PL, Watanabe AM. Signal transduction by G proteins in cardiac tissues. Circulation 1992;85:420-433.
[170] Cerlone RA, Staniszcwski C, Gierschich P, Codina J, Somers RL, Birnbaumer L, Spiegel AM, Caron MG Lefkowitz RJ. Mechanism of guanine nucleotide regulatory protein-mediated inhibition of adnylyl cyclase. J Biol Chem 1986;261:9514-9520.
[171] Robertson SP, Johnson JD, Holroyde MJ, Kranias EG, Potter JD, Solaro RJ. The effect of troponin I phosphorylation in the Ca^{2+}-binding properties of the Ca^{2+}-regulatory site of bovine cardiac troponin. J Biol Chem 1980;257:260-263.
[172] Hartzel HC, Titus L. Effects of cholinergic and adrenergic agonists on phosphorylation of a 165,000-Dalton myofibrillar protein in intact cardiac muscle. J Biol Chem 1980;257:2111-2120.
[173] Hartzel HC, Glass DB. Phosphorylation of purified cardiac muscle C-protein by purified cAMP-dependent protein kinase and endogenous Ca^{2+}-calmodulin-dependent protein kinases. J Biol Chem 1984;259:15587-15596.
[174] Winegrad S, Wisberg A, Lin LE, McClellan G. Adrenergic regulation of myosin adenosine triphosphatase activity. Circ Res 1986;58:83-95.
[175] Tada M, Katz AM. Phosphorylation fo the sarcoplasmic reticulum and sarcolemma. Annu Rev Physiol 1982;44: 401-423.
[176] Fujii J, Ueno A, Katsuhiko K, Tanaka S, Kadoma M, Tada M. Complete complementary DNA-derived amino-acid sequence of canine cardiac phospholamban. J Clin Invest 1987;79:301-304.
[177] Kovacs RJ, Nelson MT, Simmerman HKB, Jones LR. Phospholamban forms Ca^{2+}-selective channels in lipid bilayers. J Biol Chem 1988;263:18364-18368.
[178] Kranias EG, Solaro RJ. Phosphorylation of troponin I and phospholamban during catecholamine stimulation of rabbit heart. Nature 1982;298:182-184.

[179] Wegener AD, Simmerman HKB, Lindermann JP, Jones LR. Phospholamban phosphorylation in intact ventricles. Phosphorylation of serine 16 and threonine 17 in response to β–adrenergic stimulation. J Biol Chem 1989;264:11468-11474.

[180] Lokuta AJ, Rogers TB, Lederer WJ, Valdivia HH. Modulation of cardiac ryanodine receptors of swine and rabbit by a phosphorylation-dephosphorylation mechanism. J Physiol (Lond.) 1995;487:609-622.

[181] Smith JS, Rousseau E, Meissner G. Calmodulin modulation of single sarcoplasmic reticulum Ca^{2+}-release channels from cardiac and skeletal muscle. Circ Res 1989;64:352-359.

[182] Guerrini RP, Menegazzi P, Anacardio R, Marastoni M, Tomatis R, Zorzato F, Treves S. Calmodulin binding sites of the skeletal, cardiac, and brain ryanodine receptor Ca^{2+} channels: modulation by the catalytic subunit of cAMP-dependent protein kinase? Biochemistry 1995;34:5120-5129.

[183] Hain J, Onoue H, Mayrleitner M, Fleischer S, Schindler H. Phosphorylation modulates the function of the calcium release channel of sarcoplasmic reticulum from cardiac muscle. J Biol Chem 1995;270:2074-2081.

[184] Hohenegger M, Suko J. Phosphorylation of the purified cardiac ryanodine receptor by exogenous and endogenous protein kinases. Biochem J. 1993;296:303-308.

[185] Wang J, Best PM. Inactivation of the sarcoplasmic reticulum calcium channel by protein kinase. Nature 1992; 359:739-741.

[186] Franzini-Armstrong C, Protasi F. Ryanodine receptors of striated muscles: A complex channel capable of multiple interactions. Physiol Rev 1997;699-729.

[187] Reuter H. Calcium channel modulation by neurotransmitters, enzymes and drugs. Nature 1983;301:569-574.

[188] Palmer CJ, Scott BT, Jones LR. Purification and complete sequence determination of the major plasma membrane substrate for cAMP-dependent protein kinase and protein kinase C in myocardium. J Biol Chem 1991;266: 11126-11130.

[189] Moorman JR, Palmer CJ., John JE III, Durieux ME, Jones LR. Phospholemman expression induces a hyperpolarization-activated chloride current in Xenopus oocytes. J Biol Chem 1992;267:14551-14554.

[190] Stiles GL. "A riddle wrapped in a mystery inside an enigma. Circulation 1995;92:1678-9.

[191] Ferguson DW, Berg WJ, Roach PJ, Oren MR, Mark AL. Effects of heart failure on baroreflex control of sympathetic neural activity. Am J Cardiol 1992; 69:523-531.

[192] Thames MD, Kinugawa T, Smith ML, Dibner-Dunlap ME. Abnormalities of baroreflex control in heart failure. J Am Coll Cardiol 1993; 22(suppl.A): 56A-60A.

[193] Brodde OE, Hilleman S, Kunde K, Vogelsang M and Zerkowski HR. Receptor systems affecting force of contraction in the human heart and their alterations in chronic heart failure. J Heart Lung Transplant 1992; 11:S164-74.

[194] Gilbert EM, Olsen SL, Renlund DG, Bristow MR. Beta-adrenergic receptor regulation and left ventricular function in idiopathic dilated cardiomyopathy. Am J Cardiol 1993; 71:23C-29C.

[195] Altschuld RA, Starling RC, Hamlin RL, Billman GE, Hensley J, Castillo L, Fertel RH, Hohl CM, Robitaille PML, Jones LR, Xiao RP and Lakatta EG. Response to failing canine and human heart cells to beta-2-adrenergic stimulation. Circulation 1995; 92:1612-18.

[196] Galinier M, Senard JM, Srour A, Ligou V, Valet P, Glock Y, Massabuau P, Roux D, Monastruc JL and Bounhoure JP. Modifications des récepteurs bêta-adrénergiques myocardiques au cours de l'hypertrophie ventriculaire gauche des surcharges barométriques et volumétriques. Arch Mal Coeur 1994; 87:1015-8.

[197] Atkins FL, Bing OHL, DiMauro PG, Conrad CH, Robinson KG and Brooks WW. Modulation of left and right ventricular beta-adrenergic receptors from spontaneously hypertensive rats with left ventricular hypertrophy and failure. Hypertension 1995; 26:78-82.

[198] Mukherjee A, Wong TM, Buja LM. Beta adrenergic and muscarinic cholinergic receptors in canine myocardial: Effects of ischemia. J Clin Invest 1979;64:1423.

[199] Buja LM, Eigenbrodt ML, Eigenbrodt EH. Apoptosis and coagulation necrosis: Basic types and mechanisms of cell death. Arch Pathol Lab Med 1993;117:1208-1214.

[200] Buja LM. Lipid abnormalities in myocardial cell injury. Trends Cardiovasc Med 1991;1:40-45.

[201] Chien KR, Sen A, Buja LM, Willemson JT. Accumulation of unesterified arachidonic acid in ischemic canine myocardium. Cycle and depletion of membrane phospholipids. Circ Res 1984;54:313-322.

[202] Morris AC, Hagler HK, Willerson JT, Buja LM. Relationship between calcium loading and impaired energy metabolism during Na+/K+ pump inhibition and metabolic inhibition in cultured neonatal rat cardiac myocytes. J Clin Invest 1989;83:1876-1887.

[203] Armstrong SC, Ganote CE. Flow cytometric analysis of isolated adult cardiomyocytes: Vinculin and tubulin fluorescence during metabolic inhibition and ischemia. J Mol Cell Cardiol 1992;24:149-162.

[204] Farber JL, Kyle ME, Coleman JB. Biology of disease. The mechanisms of cell injury by activated oxygen species. Lab Invest 1990;62:670-679.

[205] Mukherjee A, Bush LR, McCoy KE, Duke RJ, Hugler H, Buja LM, Witterson JT. Relationship between β–adrenergic receptor numbers and physiological responses during experimental canine myocardial ischemia. Circ Res 1982;50:735-741.

[206] Thandroyen PT, Muntz KH, Buja LM, Witterson JT. Alteration in β–adrenergic receptors, adenylate cyclase, and cyclic AMP concentrations during acute myocardial ischemia and reperfusion. Circulation 1990;82(suppl. II):II30-II37.

[207] Rosendorff C, Susanni E, Hurwitz ML, Ross FP. Adrenergic receptors in hypertension: Radio ligand binding studies. J Hypertens 1985;3:571.

[208] Simpson P, McGrath A. Norepinephrine-stimulated hypertrophy of cultured rat myocardial cells is an α1–adrenergic response. J Clin Invest 1983;72:732-738.

[209] Simpson P. Stimulation of hypertrophy of culture neonatal rat heart cells through an α1–adrenergic receptor and induction of beating through an α1 and β1–adrenergic receptor interaction. Evidence for independent regulation of growth and beating. Circ Res 1985;56:884-894.

[210] Simpson P, Bishopric N, Coughlin S, Karliner S, Ordahl C, Starksen N, Tsao T, White N, Williams L. Dual trophic effects of the alpha-1-adrenergic receptor in cultured neonatal rat heart muscle cells. J Mol Cell Cardiol 1986;18(suppl. 5):45-48.

[211] Dhalla NS, Dixon IMC, Suzuki S, Kaneko M, Kobayashi A and Beamish RE. Changes in adrenergic receptors during the development of heart failure. Mol Cell Biochem 1992;114:91-95.

[212] Benfey RG. Function of myocardial α–adrenoceptors. Life Sci 1990;46:743-757.

[213] Minneman KP. α–1 adrenergic subtypes, inositol phosphates, and sources of cell Ca^{2+}. Pharmacol Rev 1988;40: 87-119.

[214] Heschler J, Trautwein W. Modulation of calcium currents of ventricular cells. In: Piper HM, Isenberg G (eds.) Isolated Cardiac Myocytes, Vol. II, Electrophysiology and contractile function. Boca Raton FL, CRC Press, 1989: 129-154.

[215] Otani H, Das DK. α1–adrenoceptor-mediated phosphoinositide breakdown and inotropic response in rat left ventricular papillary muscles. Circ Res 1988;62:8-17.

[216] Ravens U, Wang XL, Wettwer E. Alpha-adrenoceptor stimulation reduces outward currents in rat ventricular myocytes. J Pharmacol Exp Ther 1989;250:364-370

[217] Shah A, Cohen IS, Rosen MR. Stimulation of cardiac alpha receptors increases Na/K pump current and decreases gK via a pertussis toxin-sensitive pathway. Biophys J 1988;54:219-225.

[218] Keely SL, Corbin JD, Lincoln T. Alpha-adrenergic involvement in heart metabolism: Effects on adenosine cyclic 3'-5'monophosphate, adenosine cyclic 3'-5'-monophosphate dependent protein kinase , guanosine cyclic 3'-5' monophsophate and glucose transport. Mol Pharmacol 1977;13:965-975.

[219] Steinberg SF, Druggee ED, Bilezikian JP, Robinson RB. Acquisition by innervated cardiac myocytes of a pertussis toxin-specific regulatory protein linked to the α1-receptor. Science 1985;230:186-188.

[220] Tajima T, Tsuji Y, Brown JH, Pappano AJ: Pertussis toxin-insensitive phosphoinositide hydrolysis, membrane depolarization, and positive inotropic effect of carbachol in chick atria. Circ Res 1987;61:436-445.

[221] Del Bazo U, Rosen MR, Malfatto G, Kaplan LM, Steinberg SF. Specific α–adrenergic recptor subtypes modulate catecholamine-induced increases and decreases in ventricular automaticity. Circ Res 1990;67:1535-1551.

[222] Berridge MJ, Inositol triphosphate and diacylglycerol: Two interacting second messengers. Annu Rev Biochem 1988;56:159-193.

[223] Nosek TM, Williams MF, Zeigler ST, Godt RE. Inositol triphosphate enhances calcium release in skinned cardiac and skeletal muscle. Am J Physiol 1986;250:C807-C811.

[224] Parker JD, Newton GE, Landzberg JS, Floras JS, Colucci WS. Functional significance of presynaptic alpha-adrenergic receptors in failing and nonfailing human left ventricle. Circulation 1995;92:1793-1800.

[225] Manalan AS, Werth DK, Jones LR, Watanabe AM. Enrichment, solubilization, and partial characterization of digitonin solubilized muscarinic receptors derived from canine ventricular myocardum. Circ Res 1983;52:664-676.

[226] Kurose K, Katada T, Haga T, Haga K, Ichiyama A, Ui M. Functional interaction of purified muscarinic receptors with purified inhibitory guanine nucleotide regulatory proteins reconstituted in phospholipid vesicles. J Biol Chem 1986;261:6423-6428.

[227] Inoue D, Hachisu M, Pappano AJ. Acetylcholine increases resting membrane potassium conductance in atrial but not in ventricular muscle during muscarinic inhibition of Ca^{2+}-dependent action potentials in chick heart. Circ Res 1983;53:158-167.

[228] Yatani A, Codina J, Brown AM, Birnbauner L: Direct activation of mammalian atrial muscarinic potassium channels by GTP regulatory protein G_k. Science 1987;235:207-211.

[229] Logothetis DE, Kurachi Y, Galper J, Neer EJ, Clapham DE. The βγ subunits of GTP-binding proteins activate the muscarinic K^+ channel in heart. Nature 1987;325:321-326.

[230] Goldberg ND, Haddox MK. Cyclic GMP metabolism and involvement in biological regulation. Annu Rev Biochem 1977;46:823-896.

[231] Linden J, Brooker G. The questionable role of cyclic guanosine 3'-5'-monophosphate in heart. Biochem Pharmacol 1979;28:3360-1979.

[232] Lincoln TM, Keeney SL. Regulation of the cardiac cyclic GMP-dependent protein kinase. Biochem Biophys Acta 1981;676:230-244.

[233] Revtyak G, Jones LR, Watanabe AM, Besch HR Jr. Canine myocardial guanylate cyclase: Differential activation of sarcolemmal and cytoplasmic forms. Pharmacologist 1978;20:147.

[234] Brown SL, Brown JH. Muscarinic stimulation of phosphotidylinositol metabolism in atria. Mol Pharmacol 1983;24:351-356

[235] La Raia PJ, Sonnenblick EH. Autonomic control of cardiac cAMP. Circ Res 1971;28:377-384.

[236] Lindemann JP, Watanabe AM. Mechanisms of adrenergic and cholinergic regulation of myocardial contractility. In: Sperelakis N (ed.) Physiology and Pathophysiology of the Heart, 3rd ed., Kluwer Academic Publishers 1995:467.

[237] England PJ. Studies on the phosphorylation of the inhibitory subunit of troponin during modification of contraction in perfused rat heart. Biochem J 1976;160:295-304.

[238] Lindenmann JP, Watanabe AM. Muscarinic cholinergic inhibition of β–adrenergic stimulation of phospholamban phosphorylation and Ca^{2+} transport in guinea pig ventricles. J Biol Chem 1985;258:4571-4575.

[239] Ahlquist RP. Study of adrenotropic receptors. Am J Physiol 1948;153:586-600.

[240] Lands AM, Arnold A, McAuliff JP, Cudena FP, Brown TG. Differentiation of receptors systems by sympathomimetic amines. Nature London 1967;214:597-598.

[241] Carlsson E, Ablad B, Brandstrom A, Carlsson B. Differentiated blockade of the chronotropic effects of various adrenergic stimuli in the cat heart. Life Sci 1972;11:953-958.

[242] Liggett SB. Functional properties of the rat and human beta-3 adrenergic receptors: Differential agonist activation of recombinant receptors in Chinese hamster ovary cells. Mol Pharmacol 1992;42:634.

[243] Arch JRS, Kaumann AJ. β_3 and atypical β–adrenoceptors. Med Rev 1993;13:1.

[244] Fitzgerald JD, Singh BN. β–adrenergic receptor blocking drugs. In: Singh BM et al. (eds.) Cardiovascular Pharmacology and Therapeutics, Churchill Livingstone 1994:85.

[245] Reybrouck T, Amery A, Billet L. Haemodynamic response to graded exercise after chronic beta-adrenergic blockade. J Appl Physiol 1977;42:133.

[246] Persson H, Erhardt L. Beta-receptor antagonists in the treatment of heart failure. Cardiovasc Drugs Ther 1991;5:58.

[247] Levenson JA, Simon AC, Zabludowski JE, Safar ME. Effects of beta-adrenergic blockade on the arterial vasculature in essential hypertension. Am J Nephrol 1986;6:88.

[248] Young MA, Knight DR, Vatner SF. Autonomic control of large coronary arteries and resistance vessels. Prog Cardiovasc Dis 1987;30:211.

[249] Nies AS, Evans GH, Shand DG. Regional haemodynamic effects of beta adrenergic blockade with propranolol in the unanesthetized primate. Am Heart J 1973;83:97.
[250] Mackay AD, Gribbin HR, Baldwin CJ, Tattersfield AE. Assessment of bronchial beta blockade after oral benvantolol. Clin Pharmacol Ther 1981;29:1
[251] Smith HJ, Halliday SE, Earl DCN, Stribling D. Effects of selective (beta-1 and beta-2) and non-selective beta adrenoceptor antagonists on the cardiovascular and metabolic responses to isoproterenol: Comparisons with ICI141-292. J Pharmacol Exp Ther 1983;266:211.
[252] Granneman JG, Lahners KA. Different adrenergic regulation of beta-1 and beta-3 adrenoceptor messenger ribonucleic acids in adipose tissues. Endocrinology 1992;130:109.
[253] Dzau VJ, Sacks FM. Regulation of lipoprotein metabolism by adrenergic mechanisms. J Cardiovasc Pharmacol 1987;10:2
[254] Byington RP, Worthy J, Craven T, Furberg CD. Propranolol induced changes and their prognostic significance after a myocardial infarction: The beta-blocker heart attack trial experience. Am J Cardiol 1990;65:1287.
[255] Avorn J, Everitt DE, Weiss S. Increased anti-depressant use in patients prescribed beta blockers. JAMA 1986; 255:357
[256] Lichter I, Richardson PJ, Wike NA. Differential effects of atenolol and enalapril on memory during treatment ofr essential hypertension. Br J Clin Pharmacol 1986;21:641.
[257] Broadhurst AD. The effect of propranolol on human psychomotor performance. Aviat Environ Med 1980;51:176.
[258] Vaughan-Williams EM. The mode of action of beta-receptor antagonists on cardiac muscle. Am J Cardiol 1966;18:399.
[259] Cruickshank JM. The clinical importance of cardioselectivity and lipophilicity in beta-blockers. Am Heart J 1980;100:160.
[260] Lee-YC. Effects of carvedilol on systolic and diastolic left ventricular performance in idiopathic dilated cardiomyopathy or ischemic cardiomyopathy [letter]. Am-J-Cardiol. 1997 Apr 1; 79(7): 1001.
[261] Doughty RN, Sharpe N. Beta-adrenergic blocking agents in the treatment of congestive heart failure: mechanisms and clinical results. Annu-Rev-Med. 1997; 48: 103-14
[262] Ruffolo RR Jr, Feuerstein GZ. Pharmacology of carvedilol: rationale for use in hypertension, coronary artery disease, and congestive heart failure. Cardiovasc-Drugs-Ther. 1997 May; 11 Suppl 1: 247-56
[263] Frey MV, Gruber M. Untersuchyngen uber den Stoffwechsel isolierter Organe: Ein Respirations-Apparat fur isolierte Organe. Arch F Physiol 1885; 9:519.
[264] Gibbon JH Jr. Application of a mechanical heart and lung apparatus to cardiac surgery. Minn Med 1954; 37:171.
[265] Bjork VO. Brain perfusion in dogs with artificially oxygenated blood. Acta Chir Scand 1948; 96 (suppl):137.
[266] Senning A. Ventricular fibrillation during extracorporeal circulation: Used as a method to prevent air-embolism and to facilitate intracardiac operations. Acta Schir Scand 1952; 171(suppl):1.
[267] Crafoord C, Norberg B, Senning A. Clinical studies in extracorporeal circulation with a heart-lung machine. Acta Chir Scand 1957; 112:200.
[268] Andreasen AT, Watson F. Experimental cardiovascular surgery: "The azygos factor". Br J Surg 1952; 39:548.
[269] Cohen M, Lillehei CW. A quantitative study of the "azygos factor" during vena cava occlusion in the dog. Surg Gynecol Obstet 1954; 98:255.
[270] Kirklin JW, DuShane JW, Patrick RT, Donald DE, Hetzel PS, Harshbarger HG, Wood EH. Intracardiac surgery with the aid of a mechanical pump-oxygenator system (Gibbon type): report of eight cases. Mayo Clin Proc 1955; 30:201.
[271] Currie J. Appendix on the treatment of shipwrecked mariners. The effects of water cold and warm, as a remedy in fever. Liverpool, UK 1798.
[272] Bigelow WG, Lindsey WK, Greenwood WF. Hypothermia: Its possible role in cardiac surgery. Ann Surg 1950; 132:849-56.
[273] Shumway NE, Lower RR. Topical hypothermia for extended periods of anoxic arrest. Surg Forum 1959; 10:563-6.

[274] Griepp RB, Stinson EB, Shumway NE. Profound local hypothermia for myocardial protection during open heart surgery. J Thorac Cardiovasc Surg 1973; 66:731-7.

[275] Reitz BA, Stinson EB. Profound local hypothermia for myocardial protection. In: Myocardial Protection for Cardiovascular Surgery edited by Isselhard W. Koln Pharmazeutische Verlagsgesellschaft, 1980; 373-82.

[276] Boncheck LI, Burlingame MW, Vazales BE, Lundy EF, Gassman CJ. Applicability of non-cardioplegic coronary bypass to high-risk patients. J Thorac Cardiovasc Surg 1992; 103:203-7.

[277] Miller DW Jr, Hessel EA, Winterschied LC, Merendino KA, Dillard DH. Current practice of coronary artery bypass surgery. J Thorac Cardiovasc Surg 1977; 73:75-83.

[278] Miller DW Jr, Ivey TD, Bailey WW, Hessel EA. The practice of coronary bypass surgery in 1980. J Thorac Cardiovasc Surg 1981; 81: 423-9.

[279] Akins CW. Non-cardioplegic myocardial preservation for coronary revascularization. J Thorac Cardiovasc Surg. 1984; 88: 174-80.

[280] Shargge BW, Digerness SB, Blackstone EH. Complete recovery of myocardial function following cold exposure. Circulation 1978; 56(2):97-103.

[281] Hearse DJ, Stewart DA, Chain EB. Recovery from cardiac bypass and elective cardiac arrest. Circ Res 1974; 74:284-9

[282] Hearse DJ, Stewart DA, Baimbridge MV. Cellular protection during myocardial ischemia: The development and utilization of a procedure for the induction of reversible ischemic arrest. Circulation 1976; 54:193-202.

[283] Tyers GFO, Williams EH, Hughes HC, Todd GJ. Effects of perfusate temperature on myocardial protection from ischemia. J Thorac Cardiovasc Surg 1977; 73:766-71.

[284] Flaherty JT, Schaff HV, Goldman RA, Gott VI. Metabolic and functional effects of progressive degrees of hypothermia during global ischemia Am J Physiol 1979; 236:H839-H845.

[285] Melrose DG, Dreyer B, Bentall HH, Baker JDE. Elective Cardiac Arrest. Lancet 1955: 2:21-2.

[286] William VL, Cooper T, Zafiracopoulous P, Hanlon CR. Depression of ventricular function following elective cardiac arrest with potassium citrate. Surgery 1959; 46:792-6.

[287] Waldhausen JA, Braunwald NS, Bloodwell RD, Cornell WP, Morrow AG. Left ventricular function following elective cardiac arrest. J Thorac Cardiovasc Surg 1960; 39:799-807.

[288] Bjork VO, Fors B. Induced cardiac arrest. Surgery 1961; 41:387-94.

[289] Hoelscher B, Just OH, Merker HJ. Studies by electron microscope on various forms of induced cardiac arrest in dog and rabbit. Surgery 1961; 49:492-9.

[290] Hoelscher B. Studies by electron microscopy on the effects of magnesium chlroide-procaine amide or potassium citrate on the myocardium in induced cardiac arrest. J Cardiovasc Surg (Torino) 1967; 8:163-6.

[291] Bretschneider HJ. Uberlenszeit und, Weiderbelebungszeit des, Herzens bei Normo- und Hypothermie. Verh Dtsch Ges Kriesl-Forsch 1964; 30:11-34.

[292] Bretschneider HJ, Habner G, Knoll D, Lohr B, Nordbeck H, Spiekermann PG. Myocardial resistance and tolerance to ischemia: Physiological and biochemical basis. J Cardiovasc Surg (Torino) 1975; 16:241-60.

[293] Sodergaard T, Berg E, Staffeldt I, Szcezepanski K. Cardioplegia cardiac arrest in aortic surgery. J Cardiovasc Surg (Torino) 1975; 16:228-90.

[294] Gebhard MM, Bretschneider HJ, Preusse CJ. Cardioplegia: Principles and problems. In: Physiology and Pathophysiology of the Heart edited by Sperlakis N. Boston-The Hague: Martinus Nijhoff, 1984; 605-16.

[295] Bretschneider HJ, Gebhard MM, Preusse CJ. Reviewing the pros and cons of myocardial preservation within cardiac surgery. Lancaster, England: MTP Press, 1981:21-53.

[296] Kirsch U, Rodewald G, Kalmar P. Induced cardiac arrest: Clinical experience with cardioplegia and open-heart surgery. J Thorac Cardiovasc Surg 1972; 63:121-30.

[297] Holland CE Jr., Olson RE. Prevention by hypothermia of paradoxical calcium necrosis in cardiac muscle. J Moll Cell Cardiol 1975; 2:917-28.

[298] Bleeze N, Doring V, Kalmar P, Pokar H, Polonius MJ, Steiner D, Rodewald G. Intraoperative myocardial protection by cardioplegia in hypothermia. Clinical findings. J Thorac Cardiovasc Surg 1978; 75:405-18.

[299] Gay WA Jr., Ebert PA. Functional, metabolic and morphologic effects of potassium -induced cardioplegia. Surgery 1973; 74:284-9.

[300] Hearse DJ, Stewart DA, Chain EB. Recovery from cardiac bypass and elective cardiac arrest. Circ Res 1974; 35:448-56.

[301] Hearse DJ, Stewart DA, Baimbridge MV. Cellular protection during myocardial ischemia: The development and utilization of a procedure for the induction of reversible ischemic arrest. Circulation 1976; 54: 193-202.

[302] Baimbridge MV, Chayen J, Bitensky L, Hearse DJ, Jynge P, Cankovic-Darracott S. Cold cardioplegia or continuous coronary perfusion? J Thorac Cardiovasc Surg 1977; 74:900-6.

[303] Hearse DJ, Stewart DA, Braimbridge MV. Hypothermic arrest and potassium arrest. Metabolic and myocardial protection during elective cardiac arrest. Circ Res 1975; 36: 481-9.

[304] Ledingham SJN, Baimbridge MV, Hearse DJ. The St. Thomas' Hospital cardioplegic solution: A comparison of the efficacy of the two formulations. J Thorac Cardiovasc Surg 1987; 93:240-6.

[305] Follette DM, Mulder DG, Maloney JV, Buckberg GD. Advantages of blood cardioplegia over continuous perfusion or intermittent ischemia. J Thorac Cardiovasc Surg 1978; 76:604-17.

[306] Barner HB, Laks H, Codd JE, Standeven J, Pennington DG, Hahn JAW, Willman VL. Cold blood as the vehicle for potassium cardioplegia. Ann Thorac Surg 1979; 28:509-16.

[307] Barner HB, Kaiser GC, Tyras DH, Pennington DG, Lakas H, Willman VL. Blood as the vehicle for hypothermic potassium cardioplegia. Ann Thorac Surg 1980; 29:224-30.

[308] Barner HB. Blood cardioplegia: A review and comparison with crystalloid cardioplegia. Ann Thorac Surg 1991; 52: 1354-67.

[309] Rosenkranz ER, Vinten-Johansen J, Buckberg GD, Okamoto F, Edwards H, Bugyi H. Benefits of normothermic induction of blood cardioplegia in energy-depleted hearts with maintenance of arrest with multi-dose blood cardioplegic infusions. J Thorac Cardiovasc Surg 1982; 84:667-77.

[310] Follette D, Steed D, Foglia R, Frey K, Buckberg GD. Reduction of post-ischemic myocardial damage by maintaining arrest during initial reperfusion. Surg Forum 1977; 28:281-3.

[311] Teoh KH, Christakis GT, Weisel RD. Accelerated myocardial metabolic recovery with terminal warm blood cardioplegia (hot shot). J Thorac Cardiovasc Surg 1986; 91:888-95.

[312] Rosenkranz ER, Okamoto F, Buckberg GD, Vinten-Johansen J, Robertson JM, Bugyi HI. The safety of prolonged aortic clamping with blood cardioplegia. II. Glutamte enrichment in energy depleted hearts. J Thorac Cardiovasc Surg 1983; 86:507-18.

[313] Rosenkranz ER, Buckberg GD, Laks H, Mulder DG. Warm induction of cardioplegia with glutamte enriched blood in coronary patients with cardiogenic shock who are dependent on inotropic drugs and intraaortic balloon support. J Thorac Cardiovasc Surg 1983; 86: 507-18.

[314] Ghomeshi HR, Tian GH, Ye J, Sun JK, Hoffenberg EF, Salerno T, Deslauriers R. Aspartate/Glutamate enriched blood does not improve myocardial energy metabolism during ischemia-reperfusion: A ^{31}P Magnetic resonance spectroscopy study in isolated pig hearts. J Thorac Cardiovasc Surg *In Press* 1996.

[315] Gott VL, Gonzalez JL, Paneth M, Varco RL, Sellers RD, Lillehei CW. Cardiac retroperfusion with induced asystole for open surgery upon the aortic valve or coronary arteries. Proc Soc Exp Biol Med 1957; 94(4):689-92.

[316] Gott VL, Gonzalez JL, Zuhdi MN, Varco RL, Lillehei CW. Retrograde perfusion of the coronary sinus for direct vision aortic surgery. Sug Gynecol Obstet 1957; 104:319-328.

[317] Ringer S, Morshead EA. On the effect of the chlorides, bromides, and iodides of potassium on frogs. J Anat Physiol 1878; 12:73-84.

[318] Ringer S, Murrell W. Concerning the effects on frogs of arrest of the circulation, and an explanation of the action of potash salts on the animal body. J Physiol (Lond) 1878-9; 1:72-95.

[319] Ringer S, Regarding the action of hydrate of soda, hydrate of ammonia, and hydrate of potash. J Physiol (Lond) 1880-82, 3:195-202.

[320] Greene CW. On the relation of the inorganic salts of blood to the automatic activity of a strip of ventricular muscle. Am J Physiol 1898-9; 2:82-126.

[321] Howell WH. On the relation of the blood to the automacity and sequence of the heartbeat. Am J Physiol 1898-9; 2: 47-81.

[322] Lingle DJ. The action of certain ions on ventricular muscle. Am J Physiol 1900; 4: 265-282.

[323] Zwikster GH, Boyd JE. Reversible loss of all or none response in cold blooded hearts treated with excess potassium. Am J Physiol 1935; 113:356-67.

[324] Buckberg GD, Brazier JR, Nelson RL, Goldstein SM, McConnell DH, Cooper N. Studies of the effects of hypothermia on regional myocardial blood flow and metabolism during cardiopulmonary bypass. J Thorac Cardiovasc Surg 1977; 73-87-94.

[325] Landymore R, Marble A. Effect of hypothermia and cardioplegia on intra-myocardial voltage and myocardial oxygen consumption. Can J Surg 1989; 32:452-5.

[326] Yau TM, Weisel RD, Mickle DAG. Optimal delivery of blood cardioplegia. Circulation 1991; 84(III):380-8.

[327] Yau TM, Ikonomidis JS, Weisel RD, Mickle DAG, Ivanov J, Mohabeer MK, Tumiati L, Carson S, Liu P. Ventricular function after normothermic versus hypothermic cardioplegia. J Thorac Cardiovasc Surg 1993; 105:833-44.

[328] Panos A, Abel J, Slutsky AS, Salerno TA, Liechtenstein SV. Warm aerobic arrest: a new approach to myocardial protection. J Mol Cell Cardiol 1990; 22(V):S31.

[329] Salerno TA. Continuous blood cardioplegia: option for the future or return to the past? J Mol Cell Cardiol 1990; 22(V):S49.

[330] Bernhard WF, Schwarz HF, Malick NP. Selective hypothermic cardiac arrest in normothermic animals. Ann Surg 1961; 153:43-51.

[331] Leaf A. Cell Swelling: a factor in ischemic tissue injury. Circulation 1973; 48:455-458.

[332] McMurchie EJ, Raison JK, Cairncross KD. Temperature-induced phase changes in membranes of heart: a contrast between the thermal response of poikilotherms and homeotherms. Comp Biochem Physiol 1973; 44B:1017-1026.

[333] Fukomoto K, Takenaka H, Onitsuka T. Effect of hypothermic ischemia and reperfusion on calcium transport by myocardial sarcolemma and sarcoplasmatic reticulum. J Mol Cell Cardiol 1991; 23:525-35.

[334] Kayser L, Jansen E, Schmidt W, Bomfim V. Myocardial energy depletion during profound hypothermic cardioplegia for cardiac operations. J Thorac Cardiovasc Surg 1985; 90:896-900.

[335] Weisel RD, Mickle DAG, Finkle CD. Delayed myocardial metabolic recovery after blood cardioplegia. Ann Thorac Surg 1989; 48:503-507.

[336] Christakis GT, Weisel RD, Mickle DAG. Right ventricular function and metabolism. Circulation 1990; 82(IV):332-340.

[337] LeHouerou D, Singh A, Romano M, Lessana A. Minimal hemodilution and optimal potassium use during normothermic aerobic arrest. Ann Thorac Surg 1992; 54:809-16.

[338] Lessana A, Romano M, Singh AL, LeHouerou D. Chirurgie cardiaque en normothermie et aerobiose: a propôs de 530 patients. Arch Mal Coeur 1992; 85:1545-50.

[339] Gates RN, Laks H, Drinkwater DC. Gross and microvascular distribution of retrograde cardioplegia in explanted human hearts. Ann Thorac Surg 1993; 56(3):410-16.

[340] Caldarone CA, Kruenkamp IB, Misare BD, Levitsky S. Perfusion deficits with retrograde warm cardioplegia. Ann Thorac Surg 1994; 57(2):403-406.

[341] Partington MT, Acar C, Buckberg GD, Julia P, Kofsky ER, Bugyi HI. Studies of retrograde cardioplegia: I. Capillary blood flow distribution to myocardium supplied by open and occluded arteries. J Thorac Cardiovasc Surg 1989; 97(4):605-612.

[342] Le Boutiller M, Grossi E, Steinberg B, Nguyen H, Galloway A, Colvin S. Effect of retrograde warm continuous cardioplegia on right ventricular function. Circulation 1993; 88(4 part 2):I-288.

[343] Ali IS, Al-Nowaiser O, Barrozo CAM, Panos AL, Salerno TA. Retrograde continuous normothermic blood cardioplegia. In: Cardioplegia: Current concepts and Controversies edited by Chiu RC-J. Austin TX: RG Landes, 1993:72-91.

[344] Menasché P, Fleury JP, Droc L, N'Guyen A, Piwnica A, Bloch G. Metabolic and functional evidence that retrograde warm blood cardioplegia does not injure the right ventricle in human beings. Circulation 1993; 88 (4 part 2): I-288.

[345] Gundry SR, Wang N, Sciolaro CM, Eke CC, Bailey LL. Warning! In human hypertrophied heart and/or redos, warm cardioplegia may not be so hot! Circulation. 1992; 84(I):102.

[346] Tian G, Chen J, Deslauriers R. Unpublished data. Institute for Biodiagnostics, National Research Council of Canada, Winnipeg, Manitoba. 1996.

[347] Panos AL, Ali IS, Birnbaum PL, Barrozo CAM, Al-Nowaiser O, Salerno TA. Coronary sinus injuries during retrograde continuous normothermic blood cardioplegia. Ann Thorac Surg 1992; 54(6):1137-1138.

[348] Nader J, Bogousslavsky J. Complications Cérébrovasculaires de la Chirurgie Cardiaque. Schweiz Rundsch Med Prax (1992); 81(51):1543-7.

[349] Hornick P, Smith PL and Taylor KM. Cerebral Complications After Cardiopulmonary Bypass Grafting. Current Opinion in Cardiology(1994); 9:670-679.

[350] Liechtenstein SV, Salerno TA, Slutsky AS. Warm continuous cardioplegia versus intermittent hypothermic cardioplegia for myocardial protection during cardiopulmonary bypass: pros and cons. J Cardiothorac Anesth. 1990;4:279-283.

[351] Levitsky S, Wright RN, Rao KS, Holland C, Roper K, Engelman R, Feinberg H. Does intermittent coronary perfusion offer greater myocardial protection than continuous aortic cross clamping? Surgery 1977; 82:51-59.

[352] Hilton CJ, Teubl W, Acker M. Inadequate cardioplegic protection with obstructed coronary arteries. Ann Thorac Surg 1979; 28:323-34.

[353] Bolling SF, Flaherty JT, Bulkley BH, Gott VL, Gardner TJ. Improved myocardial preservation during global ischemia by continuous retrograde coronary sinus perfusion. J Thorac Cardiovasc Surg 1983; 86: 659-66.

[354] Bhayana JN, Kalmabach T, Booth FV, Mentzer RM Jr., Schimert G. Combined antegrade/retrograde cardioplegia for myocardial protection: a clinical trial. J Thorac Cardiovasc Surg 1989;98:956-60.

[355] Shiki M, Masuka M, Yonenaga K. Myocardial distribution of retrograde flow through the coronary sinus of the excised normal canine heart. Ann Thorac Surg 1986; 41:265-71.

[356] Partington MT, Acar C, Buckberg GD, Julia PL, Kofsky ER, Bugyi HT. Studies of retrograde cardioplegia. II. Advantages of antegrade/retrograde cardioplegia to optimize distribution in jeopardized myocardium. J Thorac Cardiovasc Surg 1989;97:613-22.

[357] Buckberg GD. Antegrade/retrograde blood cardioplegia to ensure cardioplegic distribution: operative techniques and objectives. J Cardio Surg 1989;4:216-38.

[358] Menasche P, Subayi JB, Piwnica A. Retrograde coronary sinus cardioplegia for aortic valve operations: a clinical report on 500 patients. Ann Thorac Surg 1990; 49:556-64.

[359] Diehl JT, Kaplan E, Dresdale AR, Kreis A, Konstan MA, Ross IM, Connoly RJ, Pandian NG, Aronovitz M, Payne DD. Effects of atrial cardioplegia on the ischemic right ventricle after acute coronary artery occlusion and reperfusion. Ann Thorac Surg 1989;48:829-34.

[360] Fabiani JN, Swanson J, Deloche A, Carpentier AF. Right atrial cardioplegia. In: Roberts AJ (ed.) Myocardial Protection in Cardiac Surgery. Boston: Dekker, 1986;505.

[361] Christakis GT, Salerno TA. Normothermic continuous retrograde blood cardioplegia for coronary artery bypass surgery. J Cardiac Surg 1991;5:359-372.

[362] Ali S, Al-Nowaiser O, Barrozo CAM, Panos AL, Salerno TA. Retrograde continuous normothermic blood cardioplegia. In: Chiu RCJ (ed.) Cardioplegia Current Concepts and Controversies. RG Landes Co., Austin 1993:72-91.

[363] Greeley WJ, Ungerleider RM, Smith R et al. The effects of deep hypothermic cardiopulmonary bypass and total circulatory arrest on cerebral blood flow in infants and children. J Thorac Cardiovasc Surg 1989;97:737-45.

[364] Kuluz JW, Gregory GA, Yu ACH, Chang Y. Selective brain cooling during and after prolonged global ischemia reduces cortical damage in rats. Stroke 1992;23:1792-7.

[365] Greeley, WJ, Kern FH, Meliones JN, Ungerleider RM. Effect of deep hypothermia and circulatory arrest on cerebral blood flow. Ann Thorac Surg 1993;56:1464-6.

[366] Guillmet D, Bachet J, Goudot B, Dreyfus G, Martinelli GL. Aortic dissection: anatomic types and surgical approaches. J Cardiovasc Surg 1993; 34:23-32.

[367] Azariades M, Firmin F, Lincoln C, Lennox S. The effect of propranolol on the cerebral electrical response to deep hypothermia and total circulatory arrest in lambs. J Thorac Cardiovasc Surg 1990; 99: 1030-7.

[368] Filgueiras CL, Winsborrow B, Ye J et al. Brain protection during circulatory arrest. Surg Forum 1994;45:263-5.

[369] Sueda T, Hayashi S, Nominura T, et al. Retrograde cerebral and coronary perfusion for acute dissection of Stanford type A with dissection of the right coronary ostia. Hiroshima J Med Sci 1993; 42:117-9.

[370] Kazui T, Kimura N, Yamada O, Komatsu S. Surgical outcome of aortic arch aneurysms using selective cerebral perfusion. Ann Thorac Surg 1994;57:904-11.

[371] Svenson LG, Crawford ES, Hess KR, Coselli JS, Raskin S, Safi HJ. Deep hypothermia with circulatory arrest. J Thorac Cardiovasc Surg 1993; 106:19-31.

[372] Henriksen L, Hjelms E, Linderburgh T. Brain hyperperfusion during cardiac operations. J Thorac Cardiovasc Surg 1983;86:202-8.

[373] Hickey PR, Andersen NP. Deep hypothermic circulatory arrest: a review of pathophysiology and clinical experience as a basis for anesthetic management. J Cardiothorac Anesth 1987;1:137-55.

[374] Kil HY, Zhang J, Piantadose CA. Brain temperature alters hydroxyl radical production during cerebral ischemia/reperfusion in rats. J Cereb Blood Flow Metab 1996;16:100-6.

[375] Crittenden MD, Roberts CS, Rosa L, et al. Brain protection during circulatory arrest. Ann Thorac Surg 1991; 51:942-7.

[376] Ikonomidis JS, Yau TM, Weisel RD. Optimal flow rate for retrograde warm cardioplegia. Circulation 1992; 86:449-59.

[377] Rubanyi GM, Vanhoutte PM. Potassium-induced release of endothelium derived relaxing factor from canine femoral arteries. Circ Res 1988; 62: 1098-1103.

[378] Camus F. Facteurs determinants de l'oxygenation tissulaire. Reanimation et médécine d'urgence. Paris: Masson, 1991; 305-16.

[379] Yau TM, Weisel RD, Mickle DA. Optimal delivery of blood cardioplegia. Circulation 1991; 84(III):380-8.

[380] Christakis GT, Koch JP, Deemar KA. A randomized study of the systemic effects of warm heart surgery. Ann Thorac Surg 1992; 54:449-59.

[381] LeHouerou D, Singh A, Romano M. Minimal hemodilution and optimal potassium use during normothermic aerobic arrest. Ann Thorac Surg 1992; 54:809-16.

[382] Allen BS, Okamoto F, Buckberg GD, et al. Studies of controlled reperfusion after ischemia. XVI. Early recovery of regional wall motion in patients following surgical revascularization after eight hours of acute coronary occlusions. J Thorac Cardiovasc Surg 1986; 92:636-648.

[383] Hearse DJ, Stewart DA, Braimbridge MV. Myocardial protection during ischemic cardiac arrest. The importance of magnesium in cardioplegic infusates. J Thorac Cardiovasc Surg 1978; 75:877-85.

[384] Aglio LS, Stanford GG, Maddi R. Hypomagnesemia is common following cardiac surgery. J Cardioth Vasc Anesth 1991; 5:201-208.

[385] Lichtenstein SV, El Dalati H, Panos A, Slutsky AS. Long cross clamp times with warm heart surgery. Lancet 1989; 1:1443.

[386] Salerno TA, Houck J, Barrozo CAM. Retrograde continuous warm blood cardioplegia: a new concept in myocardial protection. Ann Thorac Surg 1991; 54:245-47.

[387] Sweeney MS, Frazier OH. Device-supported myocardial revascularization: safe help for sick hearts. Ann Thorac Surg 1992; 54:1065-70.

[388] Melhorn U, Davis KL, Burke EJ, Adams D, Laine GA, Allen SJ. Impact of cardiopulmonary bypass and cardioplegic arrest on myocardial lymphatic function. Am J Physiol. 1995;268:H178-H183.

[389] Melhorn U, Allen SJ, Adams DL, et al. Normothermic continuous antegrade blood cardioplegia does not prevent myocardial edema and cardiac dysfunction. Circulation. 1995;92:1940-6.

[390] Ede M, Ye Jian, Filgueiras CL, Salerno TA and Deslauriers RD. An alternative agent to induce cardiac arrest during Warm Heart Surgery. Initial results in isolated rat and rabbit hearts. Abstract. Presented at the XXII Congress of the Brazilian Society of Cardiovascular & Thoracic Surgery. Brasilia, Brazil, March 1995.

[391] Laub GW, Muralidharan S, Reibman J, Fernandez J, Anderson WA, Gu J, Daloisio C, McGrath LB, Mulligan LJ. Esmolol and percutaneous cardiopulmonary bypass enhance myocardial salvage during ischemia in a dog model. J Thorac Cardiovasc Surg 1996;111:1085-91.

[392] Lonn U, Peterzen B, Granfeldt H, Casimir-Ahn H. Coronary artery operation with support of the Hemopump Cardiac Assist System. Ann Thorac Surg 1994;58:519-23.

[393] Schaff HV. New surgical techniques: Implications for the cardiac anesthesiologist: Mini-thoracotomy for coronary revascularization without cardiopulmonary bypass. J Cardiothorac Vasc Anesth 1997;11(2):6-9.

[394] Robinson MC, Gross DR, Zeman W. A minimally invasive surgical method for coronary revascularization--preliminary experience in five patients. Abstract. 1995 Annual Meeting of the American Heart Association. Circulation 1995;92(8).

[395] Cosgrove DM III, Sabik JF. Minimally Invasive approach for aortic valve operations. Ann Thorac Surg 1996;62:596-7.

[396] Gadian DG. Nuclear magnetic resonance and its applications to living systems. Clarendon Press, Oxford, 1982.

[397] Chen C-N and Hoult DI. Biomedical magnetic resonance technology. Adam Hilger, New York, 1989.

[398] Moon RB, Richards JH. Determination of intracellular pH by ^{31}P Magnetic Resonance. J Biol Chem 1973;248:7276.

[399] Hoult DI, Busby SJW, Gadian DG, Radda GK, Richards RE and Seeley PJ. Observation of tissue metabolites using ^{31}P Nuclear Magnetic Resonance. Nature 1974;252:285.

[400] Bezabeh, T., Smith, I.C.P., Krupnik, E., Somorjai, R.L., Kitchen, D.G., Bernstein, C.N., Pettigrew, N.M., Bird, R.P., Lewin, K.J. and Brière, K.M. Diagnostic potential for cancer via ^{1}H magnetic resonance spectroscopy of colon tissue. *Anticancer Res.* 16: 1553-1558, 1996.

[401] Brière, K.M., Kuesel, A.C., Bird, R.P. and Smith, I.C.P. ^{1}H MR visible lipids in colon tissue from normal and carcinogen-treated rats. *NMR Biomed.* 8: 33-40, 1995

[402] Brière, K. and Smith, I.C.P. Magnetic resonance imaging and spectroscopy: Chemistry in vivo. In International Congress of Pharmaceutical Sciences (53rd : 1993 : Tokyo, Japan): Topics in pharmaceutical sciences 1993 : proceedings of the 53rd International Congress of Pharmaceutical Sciences of F.I.P., held in Tokyo, Japan, 5-10 September 1993 (Crommelin, D.J.A., Midha, K.K. and Nagai, T., Eds.) Chapter 18, Stuttgart: Medpharm Scientific Publishers, 1994, 263-277.

[403] Ackerman JH, Grove TH, Wong GG, Gadian DG and Radda GK. Mapping metabolites by ^{31}P NMR usiong surface coils. Nature 1980;283:167.

[404] Evelhoch JL, McCoy CL, Gire BP. A method for direct in vivo measurment of drug concentrations from a single 2H spectrum. Magn Res Med 1989;9:402.

[405] Newmark RD, Taylor SE, Williams PG, Simpson PC, Budinger TF. Taurine enhances metabolism in anoxic neonatal cardiac myocytes monitored with 3H NMR spectroscopy. Abstracts of the Nineth Annual Meeting of the Society of Magnetic Resonance in Medicine 1990:922.

[406] Geissler A, Ross BD, Domenick R, Kanamori K. 15N NMR Spectroscopy in the isolated perfused rat liver. Abstracts of Work in Progress - 10th Annual Scientific Meeting of the Society of Magnetic Resonance in Medicine 1991:1038.

[407] Constantinides I, and Gamcsick MP. Effects of partial ischemia on the production of ammonium in hte RIF-1 tumour. Abstract. 11th Annual Scientific Meeting of the Society of Magnetic Resonance in Medicine 1992:167.

[408] Marban E, Kitakaze M, Koretsune Y, Yue DT, Chacko VP, Pike MM. Quantification of [Ca2+] in perfused hearts. Critical evaluation of 5F-BAPTA and nuclear magnetic resonance method as applied to the study of ischemia and reperfusion. Circ Res 1990;66:1255.

[409] Beech JS and Iles RA. Hepatic intracellular pH in vivo using F-quene 1 and 19F NMR spectroscopy. Magn Res Med 1991;19:386.

[410] Ceckler TL, Gibson SL, Hilf R and Bryant RG. In situ assessment of tumour vascularity using fluorine NMR imaging. Magn Res Med 1990;13:416.

[411] Lewandowski ED. Nuclear magnetic resonance evaluation of metabolic and respiratory support of work load in intact rabbit hearts. Circ Res 1992;70:576.

[412] Jue T, Rothman DL, Tavitian BA, Shulman RG. Natural abundance ^{13}C NMR study of glycogen repletion in human liver and muscle. Proc Natl Acad of Sci USA 1989;86:1439.

[413] Deslauriers R, Kozlowsky P, Stewart LC, Smith ICP. Spectroscopy: Principles and Addtional Instrumentation. In: Sprawls P and Bronskill MJ (eds.) The Physics of MRI – 1992 AAPM Summer School Proceedings. American Institute of Physics, 1993.

[414] Bottomley PA, Weiss RG, Hardy CJ, Gerstenblith.31P NMR stress-testing in patients with coronary disease: evidence for myocardial PCr/Pi changes. Abstract. 10th Annual Meeting of the Society of Magnetic Resonance in Medicine 1991:577.

[415] Ingwall JS. Phosphorus nuclear magnetic resonance spectroscopy of cardiac and skeletal muscles. Am J Physiol 1982;242:H729-H744.

[416] Maris JM, Evans AE, McLaughlin AC, D'Angio GJ, Bolinger L, Manos H, Chance B. ^{31}P MRS investigation of human neuroblastoma in situ. New Engl J Med 1985;312:1500.

[417] Brown MA, Stenzel TT, Ribeiro AA, Drayer BP, Spicer LD. NMR studies of combined lanthanide shift and ralaxation agents for differential characterization of 23Na in a two-compartment model system. Magn Res Med 1986;3: 289-295.

[418] Malloy CR, Buster DG, Castro MMCA, Geraldes CFGC, Jeffrey FMH, Sherry AD. Influence of global ischemia on intracellular sodium in the perfused rat heart. Magn Res Med 1990;15:33-44.

[419] Saier MH, Boyden DA. Mechanism, regulation and physiological significance of the loop diuretic-sensitive NaCl/KCl symport system in animal cells. Mol Cell Biochem. 1984;59:11-32

[420] Eisner DA, Smith TW. The Na-K pump and its effectors in cardiac muscle. In: Fozzard HA, Haber H, Jennings RB, Katz AM, Morgan HE, eds. The Heart and Cardiovascular System. 2nd ed. New York NY: Raven Press Ltd; 1992;1:863-902.

[421] Sheu SS, Blaunstein MP, Sodium/calcium exchange and control of cell calcium and contractility in cardiac and vascular smooth muscles. In: Fozzard HA, Haber H, Jennings RB, Katz AM, Morgan HE, eds. The Heart and Cardiovascular System. 2nd ed. New York NY: Raven Press Ltd; 1992;1:903-943.

[422] Kupriyanov VV, Xiang B, Yang L, Deslauriers R. Lithium ion as a probe of Na^+ channel activity in isolated rat hearts: A multinuclear NMR study. NMR in Biomed 1997; 10:271-275.

[423] Burnstein D, Fossel E. Intracellular sodium and lithium NMR relaxation times in the perfused frog heart. Magn Reson Med 1987;4:261-273.

[424] Keon CA, Nedelec J-FJ, Clarke K, Characteristics of lithium relaxation in the perfused rat heart. (abstract). Society of Magnetic Resonance in Medicine, 11th Annual Meeting, 1992. Abstr. vol 2:2206.

[425] Hodgkin AL, Huxley AF. A quantitative descripton of membrane current and its application to conduction and excitation in nerve. J Physiol 1952;117:500-544.

[426] Love WD, Burch GE. A comparison of potassium^{42}, rubidium^{86} and cesium^{134} as tracers of potassium in the study of cation metabolism of human erythrocytes in vitro. J Lab Clin Med. 1953;41:351-362.

[427] Beauge LA, Ortiz O. Rubidium, sodium and ouabain interactions on the influx of rubidium in rat red blood cells. J Physiol (Lond.) 1970;210:519-532.

[428] Eisner DA, Lederer WJ. The relationship between sodium pump activity and twitch tension in cardiac Purkinje fibres. J Physiol (Lond.) 1980;303:441-474

[429] Eisner DA, Smith TW. The Na-K pump and its effectors in cardiac muscle. In: Fozzard HA, Haber H, Jennings RB, Katz AM, Morgan HE, eds. The Heart and Cardiovascular System. 2nd ed. New York NY: Raven Press Ltd; 1992;1:863-902.

[430] Haworth RA, Goknur AB, Berkoff HA. Inhibition of ATP-sensitive potassium channels of adult rat heart cells by antiarrhythmic drugs. Circ Res. 1989;65:1157-1160.

[431] Ponce-Hornos JE, Marquez MT, Bonazzola P. Influence of extracellular potassium on energetics of resting heart muscle. Am J Physiol. 1992;262:H1081-H1087.

[432] Stemmer P, Akera T. Sodium pump sensitivity and its inhibition by extracellular calcium in cardiac myocytes of guinea pigs. Biochim Biophys Acta 1988;940:188-196.

[433] Allis JL, Snaith CD, Seymour AML, Radda GK. ^{87}Rb NMR studies of the perfused rat heart. FEBS Lett. 1989;12:171-180.

[434] Allis JL, Endre ZH, Radda GK. ^{87}Rb, ^{23}Na and ^{31}P nuclear magnetic resonance spectroscopy of the perfused rat kidney. Renal Physiol Biochem. 1989;12:171-180.

[435] Piwnica-Worms D, Jacob R, Horres CR, Lieberman M. (K^+/Cl^-) cotransport in cultured chick heart cells. Am J Physiol. 1985;249:C337-C334.

[436] Haas M. Properties and diversity of (Na-K-Cl) contransporters. Annu Rev Physiol 1989;51:443-457.

[437] Drewnowska et al., 1991 Drewnowska K, Baumgarten CM. Regulation of cellular volume in rabbit ventricular myocytes: bumetanide, chlorothiazide, and ouabain. Am J Physiol 1991;260:C122-C131.

[438] Palfrey HC, Rao MC. $Na^+/K^+/Cl^-$ cotransport and its regulation. J Exp Biol. 1983:106:43-54.

[439] Saier MH, Boyden DA. Mechanism, regulation and physiological significance of the loop diuretic-sensitive NaCl/KCl symport system in animal cells. Mol Cell Biochem. 1984;59:11-32

[440] Chipperfield AR. The (Na^+-K^+-Cl^-) co-transport system. Clin Sci. 1986;71:465-476.

[441] Campbell ID, Dwek RA. (eds.) Biological Spectroscopy. Benjamin/Cummings Publishing Company, Menlo Park, CA, USA. 1984:37.

[442] Jackson M and Mantsch HH. Biomedical infrared spectroscopy. In: Mantsch HH and Chapman D (eds.) Infrared Spectroscopy of Biomolecules. Wiley-Liss, Toronto, 1996:311

[443] Naumann D, Schultz CP, Helm D. What can infrared spectroscopy tell us about the structure and composition of intact bacterial cells? In: Mantsch HH and Chapman D (eds.) Infrared Spectroscopy of Biomolecules. Wiley-Liss, Toronto, 1996:279.

[444] Pizzi N, Choo LP, Mansfield J, Jackson M, Halliday WC, Mantsch HH, Somorjai RL. Neural network classification of infrared spectra of control and Alzheimer's diseased tissue. Artif Int Med 1995;7:67-79.

[445] C.P. Schultz, K.-Z. Liu, J.B. Johnston & H.H. Mantsch: Study of Chronic Lymphocytic Leukemia Cells by FT-IR Spectroscopy and Cluster Analysis. Leukemia Research, 20:649-55 (1996).

[446] H.H. Eysel, M. Jackson & H.H. Mantsch: Method for Diagnosing Arthritic Disorders by Infrared Spectroscopy. United States Patent, # 5,473,160, issued December 5, 1995.

[447] McCormick PW, Stewart M, Goetting MG, Dujovny M, Lewis G, Ausman JI. Noninvasive cerebral optical spectroscopy for monitoring cerebral oxygen delivery and hemodynamics. Crit Care Med 1991;19: 89-97.

[448] Wiest D. Esmolol - A review of its therapeutic efficacy and pharmacokinetic characteristics. Clin Pharmacokinet 1995;28(3):190-202.

[449] Benfield P and Sorkin EM. Esmolol - A preliminary review of its pharmcodynamic and pharmacokinetic properties, and therapeutic efficacy. Drugs 1987;33:392-413.

[450] Cuneo BF, Zales VR, Blahunka PC, Benson Jr DW. Pharmacodynamics and pharmacokinetics of Esmolol, a short-acting β–blocking agent, in children. Pediatr Cardiol 1994;15:296-301.

[451] Sintetos AL, Hulse J, Pritchett ELC. Pharmacokinetics and pharmacodynamics of Esmolol administered as an intravenous bolus. Clin Pharmacol Ther 1987;41:112-117.

[452] Sum CY, Yacobi A, et al.: Kinetics of Esmolol, an ultra short acting beta blocker, and of its major metabolite. Clin. Pharmacol. Ther. 1983;34:427-434.

[453] Frishmann W, Silverman R: β-adrenergic antagonists: New drugs and new indications. N Engl J Med 1981;305:500-506.

[454] Viray R, Turlapaty P, Laddu A. Esmolol: a short-acting titrable β-blocker in acute myocardial ischemia. Inter J Clin Ther 1988;26(3):153-161.

[455] Greespan AM, Spielman SR, Horowitz LN, Laddu A, Senior S. The electrophysiologic properties of Esmolol, a short acting beta-blocker. Int J Clin Pharm Ther Toxicol 1988;26(4):209-216.

[456] Friedman J, Rosenblum R, Enselberg C, Rosenberg A. Propranolol treatment of chronic, intractrable supraventricular arrhythmia. Am J Cardiol 1968;22:711-717.

[457] Marrot PK, Ruttley MST, Jenkins PM, Muir JR. The electrophysiologic evaluation of intravenous acebutolol, a beta-blocking drug. Eur J Cardiol 1977;6:117-130.

[458] Ward DE, Camm AJ, Spurrel RAJ. The acute cardiac electrophysiologic effects of intravenous sotalol hyodrochloride. Clin Cardiol 1979;2:185-191.

[459] Erzi MD, Marchlinski FE, Buxton AE, Waxman HL, Josephson ME. Electrophysiologic effects of intravenous timolol. Int J Cardiol 1983;3:329-337.

[460] Robinson C, Birkhead J, Crook B, Jennings K, Jewitt D. Clinical electrophyisiological effects of atenolol, a new cardioselective, beta-blocking agent. Br Heart J 1978;40:14-21.

[461] Quon C Y and Stampfli H F: Biochemical properties of blood Esmolol esterase. Drug Metabol Disp 1985;13:420-424.

[462] Quon C Y, Mai K, Patil G and Stampfli H F: Species differences in the stereoselective hydrolysis of Esmolol by blood esterases. Drug Metabol Disp 1988;16(3):425-428.

[463] Elbaum D, Wiedenmann B, Nagel RL. Some properties of the reaction site for the esterase activity of hemoglobin. J Biol Chem 1982;257:8454-8.

[464] Shaw FR, Snyer FN, Tashian RE. New genetically determined molecular forms of erythrocyte esterase in man. Science 1962;138:31-32.

[465] Rollins D. Pharmacokinetics of Esmolol in hepatic disease. Clin Pharmacol Ther 1986;39:224.

[466] Bleske BE. Esmolol. Conn Med 1987;51(10):669-671.

[467] Achari R, Drissel D, Matier WL et al. Metabolism and urinary excretion of Esmolol in humans. J Clin Pharmacol 1986;26:44-7.

[468] Flaherty JF, Wong B, La Follete G, et al. Pharmacokinetics of Esmolol and ASL-8123 in renal failure. Clin Pharmacol Ther 1989;321-27.

[469] Brevibloc® package insert. Ohmeda Corp., Mississaurga, ON, Canada. L5R 1B8.

[470] Lowenthal DT, Porter RS, Saris SD et al. Clinical pharmacology, pharmacodynamics and interactions with Esmolol. Am J Cardiol 1985;56:14F-17F.

[471] Olfert ED, Cross BM, McWilliam AA. Guide to the care and use of experimental animals. Canadian Council on Animal Care. 2nd ed., 1993.

[472] Good PI. Permutation tests: a practical guide to resampling methods for testing hypotheses. New York: Springer-Verlag, 1994.

[473] Achari R, Drissel D, Thomas D, Shin K, Look Z. Analysis of esmolol in human blood by high-performance liquid chromatography and its application to pharmacokinetic studies. J Chromatogr Biomed Appl 1988;424:430-434.

[474] Melendez JA, Stone JG, Delphin E, Quon CY Influence of temperature on in vitro metabolism of esmolol. J Cardiothorac Anesthesia 1990;4:704-706.

[475] W. Frishmann, R. Silverman: Beta-adrenergic antagonists: New drugs and new indications. N Engl J Med 1981;305:500-506.

[476] Wiest D. Esmolol. A review of its therapeutic efficacy and pharmacokinetic characteristics. Clin Pharmacokinet 1995;28(3):190-202.

[477] C.Y. Sum, A. Yacobi, et al.: Kinetics of Esmolol, an ultra short acting beta blocker, and of its major metabolite. Clin. Pharmacol. Ther. 1983;34, 427-434.

[478] Burtis CA, Ashwood ER (*Eds.*). Tietz Textbook of Clinical Chemistry. 2nd ed. W.B. Saunders, 1994.

[479] J. Wang, M. Sowa, H.H. Mantsch, A. Bittner & H.M. Heise: Comparison of Different Infrared Measurement Techniques in the Clinical Analysis of Biofluids. Trends in Analytical Chemistry 15:186-296 (1996).

[480] Sum CY, Yacobi A. Gas chromatographic-mass spectrometric assay for the ultra-short-acting β–blocker Esmolol. J Pharm Sci 1984;73(8):1177-9

[481] Kupriyanov VV, Stewart LC, Xiang B, Kwak J and Deslauriers R. Pathways of Rb^+ influx and their relation to intracellular [Na^+] in the perfused rat heart. A ^{87}Rb and ^{23}Na NMR Study. Circ Res 1995;76:839-851.

[482] Kupriyanov VV, Yang L and Deslauriers R. Cytoplasmic phosphates in Na^+ - K^+ balance in KCN-poisoned rat heart: a ^{87}Rb-, ^{23}Na-, and ^{31}P NMR study. Am J Physiol 1996;270 (Heart Circ. Physiol 39): H1303 – H1311.

[483] Laughlin MH, Schaeffer ME, Sturek M. Effect of exercise training on intracellular free Ca2+ transients in ventricular myocytes of rats. J Appl Physiol 1992; 73(4):1441-1448.

[484] Frangakis-CJ; Bahl-JJ; McDaniel-H; Bressler-R. Tolerance to physiological calcium by isolated myocytes from the adult rat heart; an improved cellular preparation. Life-Sci. 1980; 27(10): 815-25

[485] Grosso-DS; Frangakis-CJ; Carlson-EC; Bressler-R. Isolation and characterization of myocytes from the adult rat heart. Prep-Biochem. 1977; 7(5): 383-401.

[486] Ferraris VA, Ferraris SP, Singh A. Operative outcome and hospital cost. J Thorac Cardiovasc Surg 1998;115:593-603.

[487] Aiken NR, Satterle JD, Galey WR. Measurement of intracellular Ca^{2+} in young and old human erythrocytes using ^{19}F-NMR spectroscopy. Biochimica et Biophysica Acta 1992;1136:155-160.

[488] Harding DP, Smith GA, Metcalfe JC, Morris PG, Kirschenlohr HL. Resting and end-diastolic $[Ca^{2+}]_i$ measurements in the Langendorff-perfused ferret heart loaded with a ^{19}F NMR indicator. Mag Res Med 1993;29:605-615.

[489] Song SK, Hotchkiss RS, Neil J, Morris PE Jr., Hsu CY, Ackerman JJH. Determination of intracellular calcium *in vivo* via fluorine-19 nuclear magnetic resonance spectroscopy. Am J Physiol 1995;269 (Cell Physiol 38): C318-332.

[490] Yanagida, S, Luo CS, Balschi JA, Pohost GM, Pike MM. Simultaneous multicompartment intracellular Ca^{2+} measurements in the perfused heart using 19F NMR spectroscopy. Mag Res Med 1996;35:640-647.

[491] Tymiansky M, Spiegelman I, Zang L, Carlen PL, Tator CH, Charlton MP, Wallace MC. Mechanism of action and persistence of neuroprotection by cell-permeant Ca^{2+} chelators. J Cereb Blood Flow Metab 1994;14:911-923.

[492] Dowd TL, Gupta RK. Multinuclear NMR studies of intracellular cations in the prehypertensive rat kidney. Biochimica et Biophysica Acta 1994;1226:83-88.

[493] Marban E, Kitakaze M, Koretsume Y, Yue DT, Chacko VP, Pike MM. Quantification of $[Ca^{2+}]_i$ in perfused hearts. Critical Evaluation of the 5F-BAPTA and nuclear magnetic resonance method as applied to the study of ischemia and reperfusion. Circ Res 1990;66:1255-1267.

[494] Kirschenlohr, HL, Grace AA, Clarke SD, Shachar-Hill Y, Metcalfe JC, Morris PG, Smith GA. Calcium measurements with a new high-affinity NMR indicator in the isolated perfused rat heart. Biochem J 1996;293:407-411.

[495] Murphy E, Steenbergen C, Levy LA, Gabel S, London RE. Measurement of cytosolic free calcium in perfused rat heart using TF-BAPTA. Am J Physiol 1994;266 (Cell Physiol 35): C1323-C1329.

[496] London RE, Rhee CK, Murphy E, Gabel S, Levy L. NMR-sensitive fluorinated and fluorescent intracellular calcium ion indicators with high dissociation constants. Am J Physiol 1994;266 (Cell Physiol 35): C1313-C1322.

[497] Fabiato A. Calcium release in skinned cardiac cells: variation with species, tissues, and development. Fed Proc 1982;41:2238-44.

[498] Schornack PA, Song SK, Ling CS, Hotchkiss R, Ackerman JJH. Quantification of ion transport in perfused rat heart: $^{133}Cs^+$ as an NMR active K^+ analog. Am J Physiol 1997; 272 (Cell Physiol 41): C1618 – C1634.

[499] Greenspan AM, Speilman SR, Horowitz LN, Laddu A, Senior S. The electrophysiologic properties of Esmolol, a short acting beta-blocker. Int J Clin Pharmacol Ther Toxicol 1988;26(4):209-16.

[500] Barhanin-J; Lesage-F; Guillemare-E; Fink-M; Lazdunski-M; Romey-G $K_{(V)}$LQT1 and IsK (minK) proteins associate to form the $I_{(Ks)}$ cardiac potassium current. Nature.1996 Nov 7; 384(6604): 78-80.

[501] Neyroud-N; Tesson-F; Denjoy-I; Leibovici-M; Donger-C; Barhanin-J; Faure-S; Gary-F; Coumel-P; Petit-C; Schwartz-K; Guicheney-P. A novel mutation in the potassium channel gene K_VLQT1 causes the Jervell and Lange-Nielsencardioauditory syndrome. Nat-Genet.1997 Feb; 15(2): 186-9.

[502] Matsuda T, Takuma K, Baba A. Na^+ -Ca^{2+} Exchanger: Physiology and Pharmacology. Jpn J Pharmacol 1997;74:1-20.

[503] Karmazyn M. The sodium-hydrogen exchange system in the heart: Its role in ischemic reperfusion and reperfusion injury and therapeutic implications. Can J Cardiol 1996;12(10):1074-1082.

[504] Saier MH, Boyden D. Mechanism, regulation and physiological significance of the loop diuretic sensitive NaCl/KCl symport system in animal cells. Mol Cell Biochem 1984;59:11-32.

[505] Opie LH. Substrate and energy etabolism of the heart. In: Sperelakis N (ed.) Physiology and Pathophysiology of the heart 3rd. ed. Kluwer 1995:385.

[506] Nakamura Kazuhiro, Kusuoka H, Ambrosio G, Becker LC. Glycolysis is necessary to preserve myocardial Ca^{2+} homeostasis during β–adrenergic stimulation. Am J Physiol 1993;264 (Heart Circ Physiol 33): H670 – H678.

[507] Heineman FW, Kupriayanov VV, Marshall A, Fralix TA and Balaban RS. Myocardial oxygenation in the isolated working rabbit heart as a function of work. Am J Physiol 1992; 262 (Heart Circ Physiol 31): H255 - H267.

IMAGE EVALUATION
TEST TARGET (QA-3)

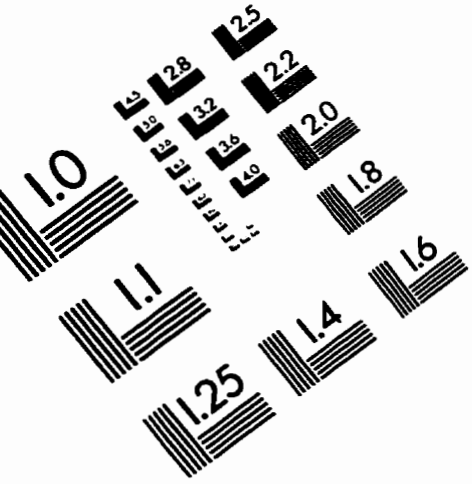

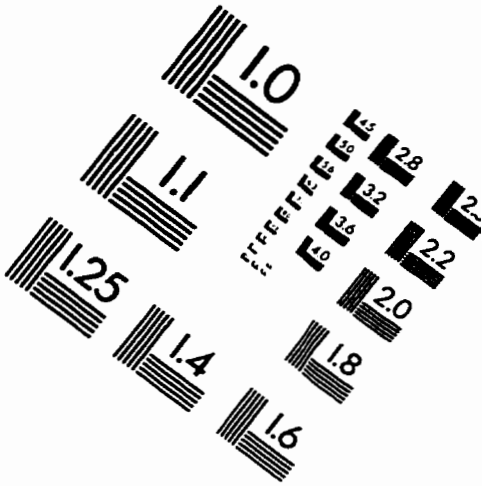

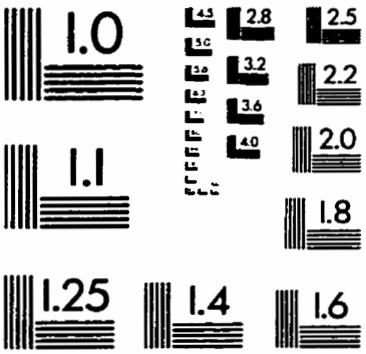

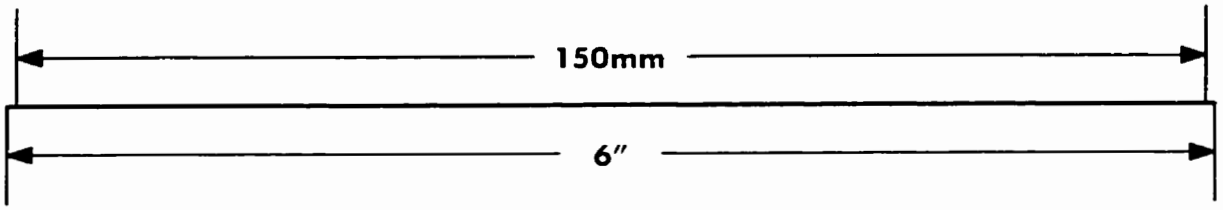

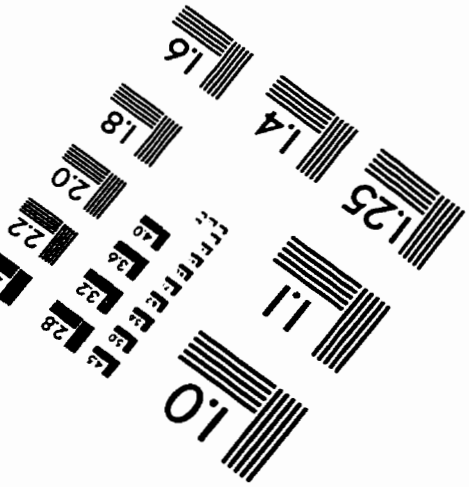

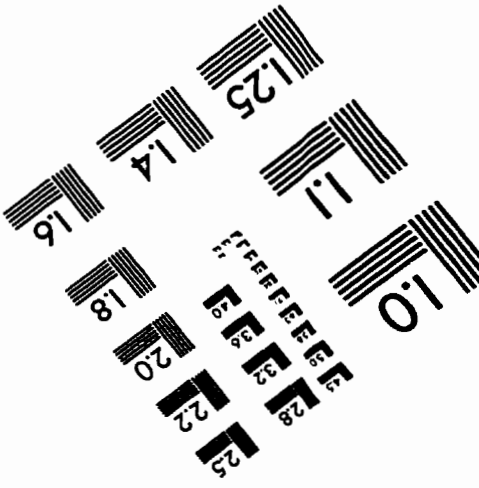

APPLIED IMAGE, Inc
1653 East Main Street
Rochester, NY 14609 USA
Phone: 716/482-0300
Fax: 716/288-5989